Summer 7-31-2019

Development of Novel Zika and Anthrax Viral Nanoparticle Vaccines

Elizabeth Henderson

Development of Novel Zika and Anthrax Viral Nanoparticle Vaccines

By

Elizabeth A. Henderson

A Dissertation submitted to the Faculty of Keck Graduate Institute of Applied Life Sciences in partial fulfillment of the requirements for the degree of Doctor of Philosophy in Applied Life Sciences.

Claremont, California

2019

Approved by:

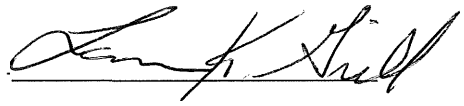

Laurence K. Grill, Dissertation Chair

We, the undersigned, certify that we have read this dissertation of Elizabeth Henderson and approve it as adequate scope and quality for the degree of Doctor of Philosophy.

Dissertation Committee:

_____

Laurence K. Grill, Dissertation Chair

_____

Mikhail Martchenko, Member

_____

Craig W. Adams, Member

_____

Hal Padgett, Member

Dissertation Abstract

Development of Novel Zika and Anthrax Viral Nanoparticle Vaccines

By Elizabeth A. Henderson

Keck Graduate Institute of Applied Life Sciences: 2019

Vaccines protect against numerous infectious diseases and prevent millions of deaths annually, but there are still many infectious diseases for which no licensed vaccine exists. Developing a new vaccine requires balancing safety and efficacy, and viral nanoparticle (VNP) vaccines possess both of these characteristics. The work herein demonstrates how tobacco mosaic virus (TMV) nanoparticles can serve as a platform to create candidate vaccines for Zika virus (ZIKV) and anthrax. In the first study, a ZIKV-specific epitope was genetically fused to TMV to create a safe and inexpensive vaccine that proved highly immunogenic in mice and led to the discovery of ZIKV-specific neutralizing antibodies that may have applications in therapeutics and diagnostics. In the second study, anthrax toxin domains were expressed, purified, and conjugated to the outer surface of modified TMV nanoparticles. These VNPs were readily recognized by anthrax immune serum, but further studies will be necessary to ascertain their ability to induce a protective immune response. As demonstrated in these studies, genetic fusions and chemical conjugations to TMV each have distinct benefits and limitations. However, both methods result in the production of TMV-based VNPs, in which the TMV virion acts as both a scaffold and delivery mechanism, ensuring that the foreign antigens are taken up by DCs, transported to lymph nodes, and stimulate robust, antigen-specific B and T cell responses. In summation, this work shows how TMV VNPs displaying exogenous antigens can be used to create novel vaccines against both viral and bacterial pathogens.

Dedication

To the Edmans, the Hendersons, and the Crapos. Without you I never would have made it this far.

ACKNOWLEDGMENTS

I would first like to thank my supervisors, Dr. Larry Grill, and Dr. Mikhail Martchenko, for their guidance, support, encouragement, and advice. Larry, thank you for allowing me to join your lab, giving me the opportunity to pursue my PhD, and the beautiful trip to Africa. I am grateful to you for giving me the freedom to pursue these projects and for putting up with me for so many years. Mikhail, your expertise in infectious disease proved invaluable, and your passion for science always kept me motivated. Thank you for facilitating intense scientific discussion and for teaching me how to throw spaghetti at the wall.

I would also like to thank my committee members, Dr. Craig Adams and Dr. Hal Padgett, for their support and scientific input. Craig, thank you for sharing your knowledge on expressing and purifying proteins and for letting me conduct some of my work in your lab; it has been a privilege working with you and Jamie Liu. I am also grateful to you for teaching me how to question everything, think outside of the box, and to always err on the side of caution. And to Hal, thank you for letting me visit your facilities and allowing me to work with the Dock-and-Lock system. I sincerely appreciate your continued willingness to help, from sharing vectors to providing business plan ideas, and for allowing me to explore the business side of science.

I couldn't have done this without the training, guidance, and day-to-day input provided by Dr. Ryan McComb, Dr. Kelvin Phiri, and (soon-to-be Dr.) Andrea Gochi. Thank you for your friendship and for putting up with all my idiosyncrasies in the lab.

Many thanks to Dr. Matt McGee of Novici Biotech for providing guidance and technical support; I owe you (and Hal) vast quantities of beer.

Thank you to our collaborators on the Zika project: Luisa W. Chang and Christina C. Tam at the USDA, and Sujan Shresta, Annie Elong Ngono, and Anh-Viet Nguyen at the La Jolla Institute for Allergy and Immunology.

To all of the KGI professors, staff, and students that I have met while on this journey, it has been a pleasure working with you.

Finally, and most importantly, I would like to acknowledge my entire family for their support and love. To my mom, thank you for being my role model; you have taught me how to be strong and independent. I would also like to thank my step-father, Robert O. Crapo, for igniting my passion for science; even though you aren't here to celebrate this milestone, I hope you would have been proud.

TABLE OF CONTENTS

LIST OF ABBREVIATIONS

ADE antibody-dependent enhancement

AIM agroinduction media

APC antigen-presenting cell

AVA anthrax vaccine adsorbed (anthrax vaccine licensed in the United States)

AVP anthrax vaccine precipitated (anthrax vaccine licensed in the United Kingdom)

BARDA Biomedical Advanced Research and Development Authority

BCA bicinchoninic acid

BIDMC Beth Israel Deaconess Medical Center

BME β-mercaptoethanol

bp base pair

BSA bovine serum albumin

cAMP cyclic adenosine monophosphate

CDC Centers for Disease Control and Prevention

cDNA complementary deoxyribonucleic acid

cHM hybridoma medium supplemented with 10% fetal calf serum

CLR C-type lectin receptor

CMG2 capillary morphogenesis gene-2 (receptor)

CNS central nervous system

CP coat protein

CR complement receptor

CTL cytotoxic T lymphocyte

CZS congenital Zika syndrome

DAP diaminopimelic acid

DC dendritic cell

DC-SIGN dendritic cell-specific intercellular adhesion molecule-3-grabbing non-integrin

DENV dengue virus

DF diafiltration

DNA deoxyribonucleic acid

DPI days post-infection

EDE envelope dimer epitope

EDTA ethylenediaminetetraacetic acid

EF edema factor (*Bacillus anthracis*)

EFCA glutamic acid, phenylalanine, cysteine, alanine

ELISA enzyme-linked immunosorbent assay

EME envelope monomer epitope

ER endoplasmic reticulum

ET edema toxin (*Bacillus anthracis*)

FBI Federal Bureau of Investigation

FDA Food and Drug Administration

FL fusion loop of the Zika virus envelope protein

FRNT focus reductions neutralization test

g gravity

GBS Guillain-Barré syndrome

GFP green fluorescent protein

GL glycan loop of the Zika virus envelope protein

GST glutathione S-transferase

HAT hypoxanthine-aminopterin-thymidine (medium)

His histidine

HIV human immunodeficiency virus

HM hybridoma medium

HPV human papillomavirus

hr hour

HRP horseradish peroxidase

HRV human rhinovirus

IC inhibitory concentration

IFN interferon

Ig immunoglobulin

IL interleukin

InaD inactivation-no-after-potential D protein (*Drosophila melanogaster*)

IPTG isopropyl-β-D-1-thiogalactopyranoside

JEV Japanese encephalitis virus

kan kanamycin

kbp kilobase pair

kDa kilodalton

LAV live-attenuated vaccine

LB Luria Broth

LF lethal factor (*Bacillus anthracis*)

LJIAI La Jolla Institute for Allergy and Immunology

LT lethal toxin (*Bacillus anthracis*)

M membrane protein

MϕCM macrophage conditioned medium

mAb monoclonal antibody

MAPKK mitogen-activated protein kinase kinase

MBP maltose-binding protein

MES 2-(N-morpholino)ethanesulfonic acid

MHC major histocompatibility complex

min minute

MWCO molecular weight cut-off

MyD88 myeloid differentiation primary response 88 (protein)

NAb neutralizing antibody

NF-κB nuclear factor kappa-light-chain-enhancer of activated B cells

Ni-NTA nickel-nitrilotriacetic acid

NIAID National Institute of Allergy and Infectious Diseases

NK natural killer (cell)

NLR nucleotide-binding oligomerization domain-like receptor

Nlrp nucleotide-binding oligomerization domain-like receptor protein

NOD nucleotide-binding oligomerization domain (receptor)

NorpA no receptor potential A (*Drosophila melanogaster*)

NP nanoparticle

NS non-structural (protein)

NT neutralization titer

OD optical density

OPD o-Phenylenediamine dihydrochloride

PA protective antigen (toxin from *Bacillus anthracis*)

PAD protective antigen domain

PAMP pathogen-associated molecular pattern

PBS phosphate-buffered saline

PCR polymerase chain reaction

PDZ postsynaptic density protein-95, *Drosophila* disc large tumor suppressor protein, Zonula Occludens-1 protein

PEG polyethylene glycol

PelB pectate lyase B (*Erwinia carotovora*)

PGA poly-ɣ-D-glutamic acid

prM pre-membrane protein

PRNT plaque reduction neutralization test

PRR pattern recognition receptor

rE recombinant envelope protein

RLR retinoic acid-inducible gene-I-like receptor

RNA ribonucleic acid

rPA recombinant protective antigen

rxn reaction

SD standard deviation

SDS-PAGE sodium dodecyl sulfate polyacrylamide gel electrophoresis

TAM Tyro3/Axl/Mer (receptor)

TBEV tick-borne encephalitis virus

TBS Tris-buffered saline

TBST Tris-buffered saline with Tween 20

TEM-8 tumor endothelial marker-8 (receptor)

TGF-β transforming growth factor beta

TIM T cell immunoglobulin mucin domain (receptor)

TLR Toll-like receptor

TMB 3,3',5,5' tetramethylbenzidine

TMV tobacco mosaic virus

TNF tumor necrosis factor

UF ultrafiltration

USDA United States Department of Agriculture

v/v volume per volume

VLP virus-like particle

VNP viral nanoparticle

VNDT valine, asparagine, aspartic acid, threonine

WHO World Health Organization

WNV West Nile virus

WRAIR Walter Reed Army Institute of Research

WT wild type

w/v weight per volume

YFV yellow fever virus

ZIKV Zika virus

OVERVIEW

The purpose of this work was to examine the utility of TMV-based viral nanoparticles as vaccines against infectious diseases. This dissertation is broken down into two chapters that are based on the two different projects that I worked on during my Ph.D. While these projects all fit within the overall theme of plant-produced vaccines, they differ in their aims and methods. Thus, each chapter contains a project-specific introduction, followed by background information, materials and methods, results, and discussion. The following overview lays the groundwork for the subsequent chapters by providing brief introductions to central topics such as the immune system, vaccines, and the plant-based production of biopharmaceuticals.

THE IMMUNE SYSTEM

Innate immunity

The innate immune system is the first line of defense against pathogens and is non-specific. It consists of physical and chemical components, the complement system, and cellular defenses that prevent pathogens from entering and spreading throughout the body. When pathogens enter the body, they are detected by pattern recognition receptors (PRRs), which recognize a vast array of structural motifs on the surface of pathogens, called pathogen-associated molecular patterns (PAMPs). PRRs can either be soluble (i.e., complement proteins), on the surface of host cells (e.g., Toll-like receptors (TLRs), or in the cytoplasm of cells (e.g., NOD-like receptors (NLRs) [1].

Complement is a group of soluble proteins that circulate in the bloodstream and bind to pathogens, which tags the pathogen for destruction by other parts of the immune system. PRRs of the complement system include mannan-binding lectin, C-reactive proteins, ficolins, and C1q. Complement activation can occur via three different proteolytic cascades: the classical pathway, the lectin pathway, or the alternative pathway. The classical pathway is activated when C1q complement proteins bind to

the surface of certain pathogens or when C1q bind to the Fc portion of an antigen-antibody complex on the surface of a pathogen. Because activation can be antibody-dependent, the classical pathway is also considered to be part of the adaptive immune response [2]. The lectin pathway is activated when lectin proteins, such as mannan-binding lectin and ficolin L, bind to carbohydrate or glycoprotein residues on pathogens [3]. Unlike the classical and lectin pathways, activation of the alternative pathway does not require a PRR. Instead, it is activated by the spontaneous cleavage of C3 proteins. C3 is a normal constituent of plasma, and, therefore, this pathway is constitutively active. These three proteolytic cascades all occur on the surface of the pathogen, and converge at the cleavage of C3, which results in four effector functions: 1) a large number of activated complement proteins complement and generated, which bind to pathogens (opsonization) and induce phagocytosis; 2) the formation of membrane attack complexes that lyse cells; 3) the recruitment of inflammatory cells and the secretion of immunoregulatory molecules, which increases vascular permeability and enhances migration of immunoglobulins, phagocytes, and more complement proteins to the infection site; and 4) the solubilization and clearance of immune complexes through the liver and spleen [4].

Transmembrane PRRs, such as TLRs and C-type lectin receptors (CLRs) and cytosolic PRRs, such as NLRs and retinoic acid-inducible like receptors (RLRs) are expressed by phagocytes and leukocytes of the innate immune system including neutrophils, macrophages, DCs, natural killer cells, eosinophils, and basophils [5,6]. When one of these PRRs binds to its cognate PAMP ligand, a signaling cascade is activated, which results in the expression of cytokines. Cytokines are soluble proteins that act as chemical messengers to regulate the innate and adaptive immune responses. There are many types, including interferons (IFNs), tumor necrosis factor-α (TNF-α) and interleukins (ILs); all of them are pleiotropic and redundant [7]. Cytokines that regulate the innate immune system include TNF-α, IL-1, IL-12, chemokines, and type I IFNs. Examples of their effector functions include: TNF-α and IL-1 mediate acute inflammation, IL-12 induces T lymphocytes and NK cells to produce IFN-ɣ, chemokines recruit other

immune cells to the site of inflammation and type I IFNs initiate the antiviral state. Cytokines also activate the adaptive immune response. For example, in addition to mediating the early innate immune response, IL-12 also induces cell-mediated immunity by stimulating the differentiation of naïve $CD4^+$ T lymphocytes [8].

In summation, the innate immune system employs PRRs to recognize pathogens and quickly responds by activating complement, inducing inflammation, and promoting phagocytosis. However, some pathogens have developed methods of evading these innate immune responses. For example, *Mycobacterium tuberculosis* secretes proteins that prevent phagosome maturation [9] and proteins produced by poxviruses bind to and block the activity of chemokines [10]. Thus, the innate immune system in vertebrates can also recruit the appropriate adaptive immune response to help in the fight against pathogens.

Adaptive immunity

When the innate immune system fails to control an infection, a threshold level of antigen is reached, which initiates the adaptive immune response. In contrast to the innate immune system, the adaptive immune responses are specific to particular pathogens and provide long-lived protection. However, activation of the adaptive immune system is a complex process that involves multiple types of cells, extensive intercellular communication, cellular proliferation, and signals from the innate immune system [4]. Consequently, adaptive immune responses occur approximately 3-5 days after exposure to a pathogen, in contrast to the almost immediate response from the innate immune system. The adaptive immune response includes the activation of T cells (i.e., cell-mediated immunity) and the activation of B cells and subsequent production of antibodies (i.e., humoral immunity).

Cell-mediated Immunity

Antigen-presenting cells (APCs), such as macrophages and dendritic cells (DCs), have pattern recognition receptors that recognize pathogen-associated molecular patterns (PAMPs) on different

pathogens. After the pathogen is ingested and degraded, DCs migrate to peripheral lymph nodes and present antigens on a specific cell surface protein called major histocompatibility complex class II (MHC II). Naïve helper T cells, also known as naïve $CD4^+$ T cells, become activated upon binding to antigens presented on MHC II molecules and then proliferate and differentiate into specific types of $CD4^+$ T cells. Differentiation depends on multiple factors, including the concentration of antigens, the type of APC, and the presence of specific cytokines and costimulatory molecules [11]. There are various types of $CD4^+$ T cells, including T_h1, T_h2, T_h3, T_h17, and regulatory $CD4^+$ T cells. Each type expresses distinct cell surface molecules and secretes specific cytokines, which facilitate their various effector functions [12]. This review will focus on T_h1, T_h2, and T_h17, as these $CD4^+$ T cell subsets play the most critical roles in the immune response against pathogens.

DCs produce interleukin-12 (IL-12) in response to intracellular bacteria and viruses, which stimulates the development of T_h1 cells. T_h1 effector functions include: 1) secreting interferon-ɣ (IFN-ɣ), which activates macrophages to phagocytose and kill bacterial pathogens; 2) activating cytotoxic T lymphocytes (CTLs) and natural killer cells (NKs) to kill virus-infected cells and tumors; and 3) contributing to T cell memory by secreting IL-2 [13]. The cytokine released by APCs to induce T_h2 differentiation remains unknown, but IL-2 and IL-4, which are mainly produced by T_h2 cells themselves, are known to drive further T_h2 differentiation [14]. T_h2 cells are responsible for activating and maintaining the antibody-mediated immune response against extracellular parasites, toxins, and bacteria. This is achieved through the production of various cytokines, including 1) IL-4, which is a positive feedback cytokine for T_h2 differentiation and mediates class-switching in B cells; 2) IL-5, which stimulates and recruits specialized immune cells, like eosinophils and basophils, to the site of infection; 3) IL-9, which activates eosinophils, neutrophils, and airway epithelial cells and causes the hypersecretion of mucus; and 4) IL-13, which activates and recruits eosinophils, and defends against parasite infection. Exposure to TGF-β and IL-6 causes naïve $CD4^+$ T cells to differentiate into T_h17 cells, which are mainly found on

mucosal surfaces, like the lining of the gastrointestinal tract and the epithelial barrier [15]. The T_h17 response targets extracellular pathogens and fungi, primarily through the production of IL-17, which recruits and activates neutrophils and promotes the production of antimicrobial peptides, and IL-22, which helps strengthen epithelial barrier functions to prevent pathogen entry and has proinflammatory functions [15]. In summation, there are many subsets of $CD4^+$ T cells, and they various roles in innate immune response, including the recruitment of granulocytes, macrophage induction, providing help to other types of effector cells, and the production of chemokines and cytokines.

In contrast to MHC II, MHC class I molecules are present on most cells types. MHC I molecules present endogenous proteins (i.e., proteins found in the cytoplasm of the cell) to cytotoxic T cell lymphocytes ($CD8^+$ cells). Binding of $CD8^+$ T cells to the antigen-MHC class I complexes on infected or aberrant cells induces apoptosis in a process called T cell-mediated cytotoxicity. All viruses, as well as some bacteria and protozoans, replicate and/or produce proteins in the cytoplasm of host cells, where they are inaccessible to antibodies. Thus, T-cell mediated cytotoxicity is particularly important for the clearance of viruses and other intracellular pathogens [16]. Certain DCs are also capable of loading exogenous particulate antigens onto MHC class I molecule, in a process called cross-presentation [17-19]. This allows exogenous antigens to induce $CD8^+$ T cell responses in the presence of pathogens that do not directly infect APCs.

Armed effector T cells (i.e., $CD8^+$ and $CD4^+$ T_h1 cells) migrate from the lymphatic tissue to the site of infection via endothelium that has already activated by the innate immune system's inflammatory response (e.g., through the production of TNF-α). At the site of infection, only the effector T cells that recognize the invading pathogen carry out their effector function, undergo clonal expansion, and produce more cytokines to recruit more armed effector T cells and non-specific inflammatory cells to the site of infection. In contrast to armed T cells, T_h2 cells interact directly with, or produce cytokines that interact with, B cells to generate the humoral immune response. For example,

activated T_h2 cells produce the cytokine IL-4, which stimulates B cell proliferation, maturation, and class switching [20]. In addition, activated, antigen-specific T_h2 must interact with naïve antigen-binding B cells to initiate the T cell-dependent antibody response.

Thus, in the cell-mediated immune response, APCs migrate to the lymph nodes where they activate T cells. Activated T cells then migrate to the site of infection to perform their effector functions ($CD8^+$ T cells control infection by inducing apoptosis while $CD4^+$ cells secrete cytokines to activate cells of the innate immune system or induce inflammation) or remain in the lymph node to initiate the humoral immune response. In addition, memory T cells can be formed from effector $CD4^+$ or $CD8^+$ T cells that persist in peripheral tissues and in the bloodstream after an infection has been cleared. Memory T cells are rapidly activated to perform their respective effector functions upon re-stimulation by their cognate antigens [21].

Humoral immunity

In humoral immunity, B cells are activated and mature into cells that secrete antibodies. Depending on the nature of the antigen, TLR signals, and cytokine and costimulatory signals, B cells differentiate into plasmablasts, plasma cells, or memory B cells [22]. Membrane-bound immunoglobulins (Ig) on the surface of B cells act as receptors that are capable of recognizing and internalizing a wide range of microbial antigens. Repetitive arrays of antigens lead to cross-linking of multiple B cell receptors, which form aggregates rapidly internalized [23]. The binding of a foreign antigen to B cell receptors provides the first of two signals required for B cell activation. B cell receptors on follicular B cells recognize protein antigens, and the binding of these antigens triggers two processes within the B cell: First, it induces B cells to migrate to secondary lymphoid tissues that are rich in T cells; second, the antigen is internalized, degraded, and displayed on MHC II molecules. $CD4^+$ helper T cells, typically T_h2 cells, displaying the same antigen, although not necessarily the same epitope, that initially activated the B cell, binds to the antigen-MHC complex on the B cell. This triggers T_h2 cells to synthesize effector

molecules, like CD40L and IL-4, which act as a second signal for B cell activation. Activated B cells undergo clonal expansion and somatic hypermutation, and then form germinal centers where they differentiate into either antibody-secreting plasma cells or memory B cells [24]. Plasma cells are short-lived and immediately secrete antibodies, while memory B cells do not secrete antibodies and persist long after the infection has been cleared. Upon re-exposure to their cognate antigen, memory B cells rapidly differentiate into plasma cells that secrete high titers of high-affinity antibodies [25]. Thus, plasma cells secrete antibodies to control the current infection, while memory B cells remain dormant until they are reactivated by subsequent infections by the same pathogen.

B cell receptors on B1 and marginal zone (MZ) B cells recognize carbohydrate and phospholipid antigens. However, such antigens are not good at activating T cells and are called T cell-independent antigens because they do not rely on T cell help to produce antibodies. Instead, TLRs expressed by B1 cells and some MZ B cells allow the second activation signal to come from the binding of TLR ligands. Following antigen and TLR-ligand recognition, these B cells rapidly differentiate into short-lived plasmablasts, which secrete low-affinity IgM, polyreactive IgA, or isotype-switched IgG antibodies to provide immediate protection against pathogens [22,24]. B cells also contribute to cellular immunity in multiple ways. For example, B cells can act as antigen-presenting cells and produce cytokines that contribute to enhanced T cell activation and differentiation [22]. Plasmablasts can also mature in the bone marrow or infected tissues to become long-lived memory plasma cells. Unlike memory B cell, memory plasma cells secrete specific antibodies in the absence of additional antigenic stimulation, and they do so for extended periods without dividing [26].

Antibodies are large, y-shaped, glycoproteins that contain two regions important to their immune functions: the antigen-binding fragment (Fab) recognizes antigens, while the crystallizable fragment (Fc) interacts with other parts of the immune system, such as cell surface receptors and phagocytes. After they are secreted by B cells, antibodies circulate in the bloodstream where they

protect against pathogens in three primary ways: 1) Neutralization, in which antibodies bind to viral particles, toxins, or intracellular bacteria to prevent them from binding to and entering cells; 2) Opsonization, in which antibodies bind to extracellular bacteria and make it easier for macrophages and neutrophils to ingest and destroy them; and 3) Complement activation, in which the Fc region of a pathogen-bound antibodies initiates the complement cascade, which kills the pathogen directly or leads to phagocytosis [27].

Antigens and immunogenicity

While the terms antigen and immunogen tend to be used interchangeably, they are different. Antigens are defined as structures that are recognized by products of an immune response (i.e., T cells, B cells, and antibodies) while immunogens are molecules capable of eliciting an immune response. The term immunogenicity thus refers to the capacity of an antigen to induce an immune response [28], and epitopes are the specific region of an antigen to which an individual antibody, B cell receptor binds, or T cell receptor binds. Antibodies and B cells primarily interact with whole pathogens and intact antigens, so they recognize epitopes in their three-dimensional conformation (i.e., conformational epitopes). On the other hand, T cells recognize antigens that have been processed and presented on APCs, and these are typically short linear peptides (i.e., linear epitopes). Many factors influence the immunogenicity of an antigen, including its size, structure, chemical properties, and degradability [29]. High molecular weight proteins or polysaccharides tend to be highly immunogenic, although lipids, nucleic acids, polypeptides, and other non-infectious and non-replicating antigens can also be immunogenic if they are attached to a carrier protein or used with an adjuvant.

The process of vaccine development involves selecting an antigen that is not homologous to human proteins and is able to elicit the appropriate immune response without being toxic. As discussed in the subsequent section, small antigens that are not inherently immunogenic are sometimes used to create vaccines. Such antigens can be coupled to large protein carriers, such as bacterial toxins,

meningococcal membrane proteins, *H. influenzae* protein D to increase their immunogenicity [30]. Adjuvants can also be used to improve the immunogenicity of an antigen. Adjuvants are molecules that enhance the immunogenicity of an antigen either by acting as PRR ligands to activate the innate immune system or by inducing adaptive immune responses [31]. Adjuvants effect these responses by forming antigen depots, recruiting immune cells, activating the inflammasome, enhancing antigen presentation by MHC molecules, or inducing the production of cytokines [31]. Adjuvants that are currently licensed for use in vaccines include aluminum derivatives, oil-in-water emulsions, virosomes, and monophospholipid A, a bacterial lipopolysaccharide [32,33].

VACCINES

Following exposure to pathogens, our innate immune system quickly mounts a non-specific immune response, followed by a primary adaptive immune response during which the adaptive immune system eliminates the pathogen while also retaining an immunological memory of the pathogen. Upon re-exposure to the same pathogen, a rapid secondary adaptive immune response is generated, which allows the pathogen to be quickly neutralized and/or eliminated. This ability to induce long-lived antigen-specific protection against reinfection is the foundation by which vaccines elicit protective immunity. Vaccines also induce a primary immune response, which leads to the formation of immunological memory, and a rapid secondary response. Unlike a natural infection, vaccination does not typically lead to disease. Thus, vaccines provide a safe way of priming our immune systems. In addition to their use for pre-exposure prophylaxis, vaccines have also be used for post-exposure prophylaxis [34,35] and as cancer treatments [36,37].

The primary objective of vaccination is to induce a long-lasting immune response capable of preventing disease. Most licensed vaccines are thought to prevent disease by generating neutralizing or opsonizing antibodies, and historically vaccine development has focused primarily on B cell responses

[38,39]. However, highly variable pathogens, such as HIV, and pathogens kept in check primarily by T cells, such as tuberculosis, may require a combination of both cellular and humoral immunity to prevent infection [38], and therapeutic vaccines for cancer or chronic infections depend on robust pro-inflammatory $CD8^+$ T cell responses [39]. In addition to ensuring that the appropriate types of responses are induced (i.e., B cell and T cell), the duration of the immune response must be considered. Vaccines that induce short-term protection require that booster immunizations be administered to maintain protective immunity [40]. Such booster requirements decrease patient compliance to immunization regimens and increase both cost and risks associated with vaccination. Therefore, the ideal vaccine induces long-term immunological memory, but the mechanisms required long-lasting immunity are still largely unknown [41]. Under certain conditions, naïve antigen-specific B and T cells become memory B and T cells, which confer long-term immunological memory [42]. This requires multiple processes, like antigen uptake and processing, APC activation, T cell activation, B cell activation, and then the formation of immunological memory. For example, antibody responses are short-lived without helper T cells functions such as class-switching and the generation of long-lived plasma cells [39]. Consequently, both cellular and humoral immune responses are likely required for optimal vaccine efficacy and long-term protection.

Vaccines are one of the greatest public health successes in the last century and have significantly reduced the global burden of infectious diseases [43]. They have also proven to be one of the most cost-effective means of disease prevention, and are estimated to save 2-3 million lives each year [38]. In addition to protecting vaccinated individuals, vaccines can also provide indirect protection to unvaccinated individuals if a large proportion of the population is vaccination, in a process called herd protection [44]. One of the biggest challenges in vaccine development is designing vaccines that are safe but also induce potent and long-lasting immune responses [39]. And, although vaccines have been developed for many infectious diseases, increasing the affordability and accessibility of vaccines is

essential as vaccine-preventable diseases are still a major cause of morbidity and mortality in developing countries [45,46]. In addition, effective vaccines still need to be developed for many widespread diseases, such as dengue, HIV, malaria, and tuberculosis [46]. Historically, vaccine development involved isolating, inactivating, purifying, and then injecting a whole pathogen or parts of a pathogen. Live-attenuated virus vaccines date back to 1796 when Edward Jenner used material from a milkmaid's cowpox pustule to inoculate a boy against smallpox. Since then, a wide array of vaccine production platforms have been developed, each with its own advantages and limitations as discussed below and summarized in Table 1.

Live-attenuated vaccines

The traditional approach to vaccine development utilizes a weakened version of the pathogen that closely resembles the wild-type pathogen, but either does not cause disease or causes a very mild form of the disease. For viral vaccines, attenuation is typically accomplished by passaging the virus multiple times through a non-human host or by selecting a virus that is pathogenic in a different mammalian host (e.g. Jenner's use of cowpox to protect humans from smallpox), but temperature-sensitive strains (i.e., strains that grow poorly at 37°C) have also been used [47]. The most modern method of attenuation uses recombinant DNA technology to modify or delete specific genes responsible for virulence. These attenuated viruses are still capable of replicating, so they provide continual antigenic stimulation to the immune system. However, it can be challenging to find the right balance between immunogenicity and ability to cause disease [48]. Thus, most LAVs cause mild disease but induce strong cellular and humoral immunity. Drawbacks of LAVs include their instability, the need for cold-chain storage, the possibility that the virus could revert to a form capable of causing disease, and the risk that attenuated pathogens could replicate unchecked in immunocompromised individuals resulting in severe illness or death [49]. Thus, LAVs are contraindicated for anyone with an immunodeficiency. In pregnant women, a fetal infection could theoretically lead to congenital diseases, so LAVs are also contraindicated during pregnancy [50]. Furthermore, LAVs are difficult to make for pathogens that cannot

Table 1. Summary of the advantages and disadvantages associated with various types of vaccines.

Vaccine type	Description	Advantages	Disadvantages	Examples
Live-attenuated	Weakened live pathogen	Highly immunogenic; One or few doses required for long-term protection	Risk of reversion; Cold-storage required; Cannot be given to pregnant women or the immunocompromised individuals; increased safety analysis required	Measles, mumps, rubella, chickenpox yellow fever
Inactivated	Killed pathogen	Cannot induce disease; More stable	Weak immune response; Requires large doses or frequent boosters	Polio, flu, hepatitis A, pertussis
Subunit	Specific peptide or carbohydrate antigens from the pathogen	Cannot induce disease; Safer and more stable; Defined composition	Requires knowledge of protective antigens; weak immune response: requires adjuvants and/or boosters; prone to degradation; high cost	Hepatitis B, HPV, whooping cough, shingles, diphtheria, tetanus
Virus-like Particle	Viral structural proteins without genetic material	Cannot induce disease; Immunogenic; Self-adjuvanting; Safe	Production, purification, and analysis can be difficult/costly	HPV, hepatitis B
Nucleic Acid	DNA or RNA encoding antigenic proteins from a pathogen	Low cost; Relatively safe and stable	Challenging to deliver; Limited to protein antigens; Unstable *in vivo* (RNA); weak immune response; Safety risk of exogenous genetic material	Experimental
Viral Vector	Attenuated exogenous virus used to introduce DNA/RNA-encoded antigen from the pathogen	Highly immunogenic, particularly using replicating vectors; Self-adjuvanting	Risk of recombination/reversion; Tumorigenesis risk; Requires knowledge of protective antigens; Pre-existing immunity to carrier virus; Expensive to prepare; only a portion of immune response is toward pathogenic antigen; Safety risk of exogenous genetic material	Experimental
Nanoparticle*	Nanostructures that display or encapsulate antigens	Stability; Immunogenic; Safe; Self-adjuvanting	Expensive; Limited manufacturability; Toxicity; May require boosters and/or adjuvants	Hepatitis A (Epaxal)

* Each kind of nanoparticle has its own advantages and disadvantages, so the listed ones are only potential advantages and disadvantages.

be easily cultured, have latent stages, or have developed effective immune-evasion strategies [33]. Despite these drawbacks, LAVs have proven to be a cost-effective way to produce effective vaccines against viral diseases such as yellow fever [51] and rabies [52]. The production of LAVs for bacterial pathogens has proven more difficult because reversion rates are much higher, but several live-attenuated bacterial vaccines have been licensed including Bacille Calmette-Guerin (BCG) for tuberculosis [53] and oral cholera and typhoid vaccines [54].

Inactivated vaccines

Inactivated vaccines offer increased stability and safety compared to LAVs because the pathogens they contain are inactivated or killed. Inactivated vaccines typically do not require cold storage, and physical and/or chemical inactivation processes, such treatment with heat or formalin, ensure that pathogens cannot replicate or revert to their virulent state. Because these pathogens cannot replicate, inactivated vaccines are safe for immunocompromised individuals, but the inactivation process can destroy key epitopes. Inactivated vaccines must also be administered in larger doses or more frequently to build up and maintain immunity, and the immune response is mainly humoral [47]. In addition, inactivated vaccines are more expensive to produce than LAVs. Both bacterial and viral inactivated vaccines have obtained licensure, including IPV for polio and a whole-cell pertussis vaccine [55].

Subunit vaccines

Like inactivated vaccines, subunit vaccines are considered very safe because they do not contain live pathogenic material. However, instead of utilizing the whole pathogen, subunit vaccines contain only specific antigenic pieces of the pathogen. Designing this type of vaccine thus requires detailed knowledge of which particular parts of the pathogen will adequately stimulate the immune system to produce a protective immune response. These antigens are typically peptides or carbohydrates exposed

on the external surface of the pathogen. Subunit vaccines do not induce immune responses as potently as whole-pathogen vaccines though, so adjuvants and boosters are necessary to ensure long-term protective immunity [56]. Furthermore, peptide and polysaccharide antigens are prone to enzymatic degradation rapid clearance giving them less time to stimulate an immune response [57]. The most common types of subunit vaccines are protein vaccines, toxoid vaccines, conjugate vaccines, and virus-like particles.

Protein vaccines

Immunogenic peptides and proteins can be produced and purified from cultured pathogens that are chemicals broken down (e.g., detergent disrupted viruses), manufactured recombinantly in a heterologous host (e.g., yeast-based expression of hepatitis B antigens), or chemically synthesized [58]. While producing proteins in a heterologous host eliminates the risks involved with using a pathogenic organism for production, recombinant peptides and proteins can fold in a non-native manner and present an antigenic landscape different than that of the native peptide. Furthermore, proteolysis is a common problem when expressing heterologous proteins. The hepatitis B vaccine Heplisav-B™, which is composed of the hepatitis B virus surface antigen, is an example of a licensed purified protein vaccine.

Toxoid vaccines

Some bacterial pathogens, such as *Clostridium tetani,* secrete toxins that are largely responsible for illness. Once inactivated by formalin, toxins can be safely used as a vaccine antigen to elicit humoral immunity. Like subunit vaccines, toxoid vaccines are relatively stable and safe because they cannot cause disease or revert to their virulent form. Examples of licensed toxoid vaccines include the tetanus toxoid vaccine and the diphtheria toxoid vaccine [49]. Many toxins are only weakly immunogenic, which necessitates the use of adjuvants and boosters. However, some toxins are highly immunogenic and are used as adjuvants/carrier proteins in vaccines against heterologous pathogens. An inactive and nontoxic form of the diphtheria toxin, CRM197, has been used for vaccines against *Haemophilus influenza*,

pneumococcus, and meningococcus [59], and the tetanus toxoid possesses multiple $CD4^+$ T cell epitopes and has been used to create the conjugate meningococcal vaccine Nimerix [60].

Polysaccharide vaccines

Many pathogenic bacteria, like *Streptococcus pneumonia*, are coated with capsular polysaccharides that protect them from being phagocytosed by the host macrophages and neutrophils. However, these bacteria can be efficiently phagocytosed if they are covered with antibodies. Thus carbohydrate-based subunit vaccines can be used to induce an antibody response to bacterial capsids. Pure polysaccharide vaccines, such as Pneumovax 23, contain only polysaccharides that are either purified from whole bacteria or synthesized [49]. Such vaccines were shown to be poorly immunogenic in adults and inconsistently immunogenic in young children while providing only short-term protection mediated mostly by an IgM response [61]. Glycoconjugate vaccines, in which polysaccharides are chemically linked to a carrier protein, have proven to be much more immunogenic due to the induction of a T-cell-dependent response (as opposed to the T-cell independent response seen in polysaccharide-only vaccines). However, such conjugate vaccines require complex methods of production and can, therefore, be costly to produce [33]. Examples of licensed polysaccharide vaccines include *Haemophilus influenza* type B polysaccharides conjugated to tetanus toxoids and *Neisseria meningitidis* polysaccharides conjugated to diphtheria toxoids [62].

Virus-like particle vaccines

Virus-like particles (VLPs) are multimeric nanostructures composed of one or more viral structural proteins that self-assemble to mimic the structure of a native virus but do not contain the viral genome. The highly-ordered, repetitive structure of VLPs induces strong cellular and humoral immune responses without the need for adjuvants, and are therefore considered the most effective type of subunit vaccine [63]. While many VLPs can bind to and enter host cells, they cannot replicate, revert, or cause pathogenic infection. Thus, VLPS combine the efficacy of LAVs and the safety of subunit

vaccines [63,64]. Licensed VLP vaccines include human papillomavirus vaccines, such as Cervarix and Gardasil, as well as hepatitis B virus vaccines, such as Recombivax HB [65].

Nucleic acid-based vaccines

For nucleic acid-based vaccines, DNA or RNA encoding antigenic proteins from a pathogen is delivered to host cells for expression. Both DNA and RNA vaccines can be rapidly manufactured for relatively low costs at large scale and can be given to immunocompromised patients [66]. However, both are limited to peptide or protein antigens, lead to a comparatively weak immune response, and can elicit anti-nucleic acid antibodies. For DNA vaccines, plasmid DNA encoding for antigens is delivered into the nuclei of host cells for transcription, and then the antigens are then translated in the cytoplasm and secreted. The secreted antigens provoke an antibody response, and antigen-presenting cells display processed peptides MHC molecules [67]. However, getting the DNA into the host cell nuclei is a challenge; examples of delivery systems include Inovio's electroporation system [68], NIAID's pressure-based delivery system [69], and Pharos' nanoparticle-based delivery system [70]. While several DNA vaccines have been licensed for veterinary use, none are currently licensed for human use mainly due to their inability to generate a protective immune response in clinical trials, even when administered with an alum adjuvant or a genetic adjuvant [70,71]. If they do elicit a protective immune response, at least three doses over 12 weeks are required [72,73]. Additionally, the transfected DNA can integrate into the host cell's genome and cause dysregulated gene expression and mutations [71].

On the other hand, the advantages of RNA vaccines include that they are easy to manufacture and can be transported without a cold-chain [70]. Unlike DNA vaccines, RNA vaccines do not need to enter the nuclei of cells to be effective [70]. Instead, they rely on endogenous expression of antigens in the cytoplasm and thus avoid the risk of introducing genetic material into the hosts' genome [74]. However, the cellular environment contains a multitude of enzymes and effectors of the innate immune system that can degrade the mRNA before it is translated. Strategies for overcoming degradation include using

lipid nanoparticles to deliver mRNA [75], making modifications to the mRNA sequence that increase their stability [76-78], and using self-amplifying RNA replicon particles [79].

Viral vector vaccines

Viral vectors vaccines are essentially a combination of a LAV and a nucleic acid vaccine. Non-pathogenic or attenuated virus, such as adenovirus or pox virus, are recombinantly modified to contain a payload, typically DNA or RNA encoding protein antigens from the pathogen of interest. Thus, viral vector vaccines capitalize many inherent features of viruses, including their natural ability to effectively insert genetic material into host cells, the specificity with which they can deliver genes to particular cells, and the induction of both cellular and humoral immune responses [80]. Both replicating and non-replicating viral vectors have been used, but replicating vectors are more immunogenic as their active invasion and replication in host cells increase the immune response [80]. Viral vector vaccines that contain oncolytic agents or tumor antigens have also been used for cancer immunotherapy [81]. Similar to LAVs, viral vector vaccines carry the risk of recombination or reversion, both of which could lead to pathogenesis. Thus, the optimization of viral vector vaccines involves finding the right balance between immunogenicity and safety. Also, like subunit vaccines, protective antigens from the pathogen of interest much be known to design a viral vector vaccine. Pre-existing vector-specific immunity can impair the ability of these vaccines to elicit a strong immune response against their payload. Thus, multiple vaccinations with one type of viral vector or with a viral vector that the person has already been exposed to naturally would be ineffective. Certain vectors also pose additional safety risks; for example, retroviruses and lentiviruses have the potential for tumorigenesis [82]. While several viral vector vaccines have been licensed for veterinary use, none are currently available for human use likely due to concerns about safety and inefficacy [38].

Nanoparticle vaccines

Nanoparticle (NP) vaccines utilize various materials to create nanostructures capable of either encapsulating vaccine antigens or displaying them on their surface. When used in vaccines, NPs can serve a variety of functions including protecting antigens from proteolytic degradation, stimulating the immune system or increase immunogenicity (i.e., they can be used as an adjuvant), improving antigen delivery to APCs, or ensuring that immune cells have prolonged exposure to the antigen (i.e., the depot effect) [83-86]. NPs can be made from a variety synthetic, inorganic, or organic materials including gold, silica, synthetic polymers (e.g., poly(D,L-lactic-coglycolic acid (PGLA), chitosan, liposomes, and viral particles. Based on the size, shape, composition, and surface chemistry, nanoparticles can activate specific immune responses or be targeted to different tissues [87]. Attaching viral, bacterial, or parasitic antigens to NPs can be achieved by chemical conjugation, encapsulation, adsorption, or translational fusion (in the case of viral nanoparticles) [83]. For example, the licensed liposome-based vaccine against hepatitis A, Epaxal, is composed of inactivated, purified hepatitis A virions absorbed to the surface of a self-assembling bilayer of phospholipids [88]. In summation, NPs can serve as both an adjuvant and a carrier molecule for antigens, and thus can be used to create safe and effective vaccines. However, there can be material-specific drawbacks, such as limited antigen loading, poor targeting to immune cells, limited manufacturability, and accumulation in organs that leads to toxicity [86,87,89,90].

Viral nanoparticle vaccines

While many articles tend not to differentiate viral nanoparticles (VNPs) and VLPs, there are two notable differences [63,83,86]. First, VLPs are typically composed of a subset of viral proteins and don't contain viral genetic material, while VNPs usually consist of whole viruses, including genetic material [91]. Second, viral nanoparticles are typically used to display antigens from a heterologous pathogen, while VLPs typically only display homologous antigens [63]. However, some VLPS have been used to display heterologous antigens. For example, hepatitis B virus and human papillomavirus VLPs displaying HIV

epitopes [92,93] and influenza VLPs displaying Mycobacterium tuberculosis epitopes have been developed [94], but these VLP vaccines do not contain viral genetic material. In contrast, the viral nanoparticle vaccine ALVAC-HIV is composed live-attenuated recombinant canarypox virus expressing HIV-1 epitopes from gp120, gp41, Gag, and Pro and is currently being tested in a phase IIb/III clinical trial [95].

Vaccine development

Even though there are many different types of vaccines, the processes by which they are developed are relatively analogous. Developing an effective vaccine first requires extensive knowledge of the pathogen (e.g., structure, cellular receptors, pathogenesis, etc.) and the demographics of those at risk for infection. Second, a thorough understanding of the interactions between the pathogen and the host immune system is required so that the appropriate antigen can be selected and a vaccine candidate can be properly formulated. Third, preclinical and clinical testing of the vaccine candidate is required to determine its immunogenicity, safety, and efficacy [33]. Once a vaccine is developed, it must gain licensure before it can be deployed. This process includes filing an application with the appropriate agencies, receiving authorization, and beginning post-licensure studies. As shown in Figure 1, this process takes 10-20 years and requires a budget of $138 million to $1.1 billion [96-99].

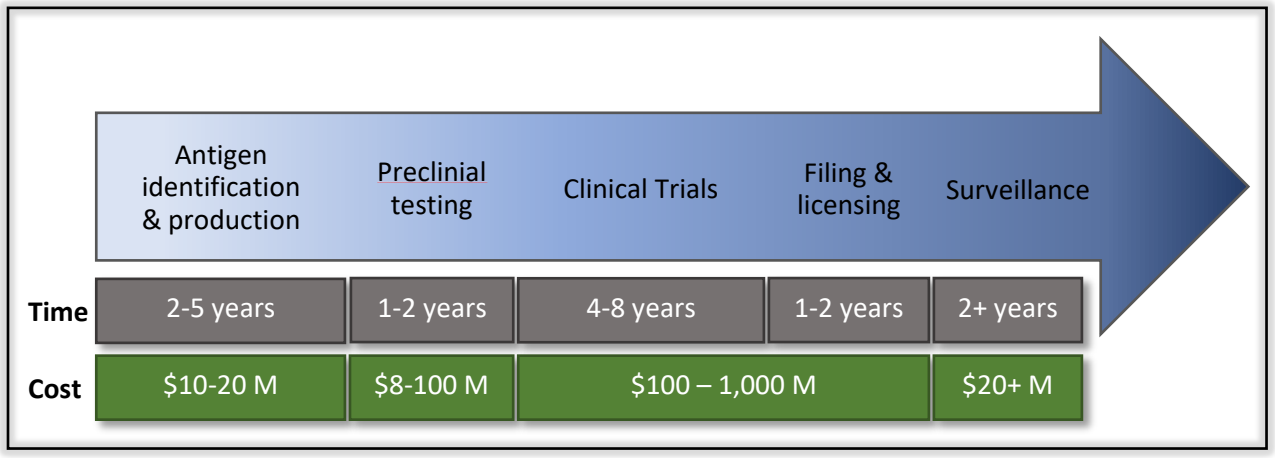

Figure 1. The vaccine development process (adapted from Han [97]).

Developing vaccines also requires walking the fine line between safety and efficacy. In general, immune responses are better if the form of the vaccine is similar to the pathogenic form of the organism, but, as demonstrated by LAVs, this often entails greater safety issues. Thus, each type of vaccine has its own advantages and disadvantages (Table 1), and all must be taken into account during the development process. The technical hurdles are high, but they are not the only ones. The bigger picture includes defining the vaccine's target population and ensuring that the target population has equal access to the vaccine [46]. Data from the World Health Organization suggests that 1.5 million people die annually from vaccine-preventable diseases primarily due to the underuse of vaccines in developing countries [100]. Cost, lack of medical infrastructure, and lack of cold storage facilities all contribute to under-vaccination [43,101-103]. Some of these issues could be addressed by employing a high-yield low-cost production platform to create heat-stable vaccines that can elicit long-term protective immunity after a single dose.

Vaccine manufacturing

Many viral vaccines, including seasonal flu vaccines, are manufactured using fertilized embryonic chicken eggs. Egg-based vaccine production started in the 1940s and has a yield of approximately one vaccine dose for every 1-2 eggs [104]. Disadvantages of this system include 1) egg-based vaccines can induce egg allergies in some people; 2) production is limited by the available supply of eggs [105]; 3) viral mutation can take place during propagation; 4) long lead times of at least 4-6 months make it impractical for pandemic situations [106,107]. To address these shortcomings, cell-based vaccine manufacturing was started in the 1990s. In this process, cultured mammalian cells are infected with the virus, which replicates inside the cells, and can then be harvested. The method takes approximately half the time of the egg-based process, avoids the egg allergy issue, and is amenable to the production of biosafety level 3 viruses. However, cell culture costs are high, the volumetric yield is lower than in eggs, and it requires more capital investment and higher levels of sterility [104]. Bacterial vaccines are typically

much easier to manufacture, as the pathogenic bacteria can be grown directly in culture. This process is amenable to the production of live-attenuated bacterial vaccines, inactivated bacterial vaccines, and bacterial subunit vaccines. Alternatively, both bacterial and viral antigens can be recombinantly produced in a variety of host cells, including mammalian cells, yeast, *E. coli*, transgenic animals, and insect cells [108,109]. However, none of the aforementioned technologies can produce heat-stable vaccines in less than two months at lows costs (i.e., less than $1 per dose) [104]. Most vaccines are inherently unstable, and thus must be stored under controlled conditions until they are administered. Live-attenuated viral vaccines are particularly sensitive to high temperatures and must be stored frozen or at 2-8 °C, and vaccines that utilize aluminum adjuvants lose potency if they are frozen, so they must be kept at 2-8 °C [103].

Irrespective of the type of vaccine being produced or the manufacturing platform used, vaccine production is expensive. Fixed costs, such as construction and maintenance of production facilities, research and development, quality control and quality assurance, as well as storage and distribution, can constitute up to 90% of total cost per dose [110]. Increasing productivity and taking advantage of economies of scale can reduce the cost per dose, but vaccines that rely on recombinant DNA technology or complex manufacturing processes, such as conjugating polysaccharides to protein carriers, are not very amenable to scale-up. In addition to high fixed costs, the high costs and risk associated with vaccine research and development, complex manufacturing processes, and the relatively small market for vaccines create a high barrier to entry for vaccine manufacturers [110,111]. Once a vaccine is manufactured, low profit margins and the relatively small size of the vaccine market make vaccines much less attractive than traditional drugs to pharmaceutical companies that produce them [112]. Thus, there is limited financial incentive for pharmaceutical companies to develop and produce vaccines in general.

PLANT-MADE BIOPHARMACEUTICALS

Many types of pharmaceutical proteins have been recombinantly produced in plants, including antibodies, subunit vaccines, toxins, VLP vaccines, and therapeutic enzymes. Diverse plant species have been used as expression hosts, ranging from leafy crops, like tobacco and lettuce, to fruits, legumes, oil crops and even simple plants like duckweed [113]. The advantages of plant-based production are product and host-species specific, but can include:

1) **Low cost**- plants can be used to produce recombinant proteins at low costs and do not require the same capital-intensive facilities, equipment, and media used for bacterial or mammalian cells cultures [114,115]. Most plant-made biopharmaceuticals can be produced using basic agricultural methods and require only inorganic nutrients, water, carbon dioxide, and sunlight to grow [116]. In fact, Nandi *et al*. showed that plant-based production platforms reduce capital investment and the cost of goods by at least 50% compared to expression in mammalian cells [117].

2) **Shorter lead times-** Vaccine antigens transiently expressed in tobacco plants require only 3-10 days for production once the appropriate vectors have been created [43 115].

3) **Glycosylation-** The majority of biopharmaceuticals are glycosylated, and glycosylation profiles can affect the stability, functionality, and immunogenicity of therapeutic proteins [118]. Mammalian cells are notoriously difficult to work with because they produce a heterogeneous mixture of glycoforms. Conversely, plant glycoforms are largely homogeneous, and thus plant-produced recombinant proteins tend to have better batch consistency [118]. Furthermore, there are only minor differences between plant and mammalian glycans [119]. As in all eukaryotes, the initial stages of N-glycosylation in plants occurs in the endoplasmic reticulum. Glycan processing steps in the Golgi apparatus then lead to high-mannose glycan biosynthesis. In plants, the last stages of the N-glycan maturation process produce β1,2 xylose, α1,3 fucose, and Lewis A-type

structures, as opposed to α1,6-fucose and β1,4 galactose produced in mammalian cells [120]. Despite these differences in N-glycosylation, no allergic or hypersensitive responses to plant-glycosylated therapeutics have been reported in humans [121,122]. Nevertheless, transgenic plants and plant cells capable of producing recombinant proteins with mammalian N- [123] and O-glycosylation [124,125] have been engineered. Thus, the overexpression of mammalian glycosylation enzymes allows plant-based production biopharmaceuticals with better-defined N- and O-glycans.

4) **Proper folding and secretion**- Plants can properly fold and assemble complex proteins, such as homodimeric vascular endothelial growth factor (VEGF) and antibodies [126-128].
5) **Scalability-** Transgenic plants can easily be expanded to agricultural scales; Buyel *et al*. estimate that recombinant proteins could be produced at 100 kg ha^{-1} y^{-1} [115]. Vertical farming could also be used to achieve similar yields if controlled conditions are required. For example, Caliber Biotherapeutics designed a commercial-scale manufacturing facility with the capacity to grow over 4 million plants at a time which can produce at least 150 kg of plant-made products per year [129].
6) **Low risk of adventitious human pathogens-** While human pathogens easily replicate in animal-based expression systems, such as eggs and mammalian cell cultures, they cannot replicate in plants [130]. In addition, there is no risk of prions. Thus, the risk of contamination in plant-produced products is much lower.
7) **High Yields** – Recombinant protein yields of up to 80% of the total soluble protein in a plant have been demonstrated [131,132], although yields ranging from 0.01% to 15% of total soluble protein are more typical [133-135].

8) **Thermo-stability**- Vaccines antigens recombinantly produced in plant seeds remain stable for over 18 months without refrigeration [136], and transgenic rice expressing cholera toxin subunits can be stored for more than three years at ambient temperatures [137].

9) **Reduced ecological footprint**- Waste material from plant-based production is biodegradable, unlike the ~61 kg of plastic required for every 1,000 L cell culture process in which single-use bioreactors are used [115]. Plants also absorb carbon dioxide, which can offset the emissions that are causing global warming, and any residual biomass that remains after the target product is extracted could be used to generate biofuel [115].

Despite these advantages, only a few plant-produced products have been licensed for human use. These include CaroRx™, an anti-caries monoclonal antibody licensed in the European Union, and Taliglucerase™, an enzyme replacement therapy for patients with Gaucher's disease [138]. While the lack of licensed plant-made pharmaceuticals is at least in part due to the resistance of major pharmaceutical companies to switch from established production platforms to a new production platform [139], it can also be attributed to the perceived and actual drawbacks to plant-based production. These include: similar downstream production costs as other recombinant proteins, the presence of plant host-cell proteins and metabolites (e.g., flavonoids, alkaloids, and pigments) that can cause difficulties in downstream processing, yields that are still relatively low compared to other cell culture platforms, the environmental risks of producing transgenic crops, and regulatory uncertainty [140-143 144,145].

Recombinant protein production in plants can be accomplished either through stable transfection or transient transfection technologies. Stable transfection involves inserting foreign genes into the host plant's genome in a way that allows the foreign gene to be retained over multiple generations [43]. For example, the Pharma-Planta Consortium stably expressed an anti-HIV monoclonal antibody for the prevention of HIV transmission in transgenic tobacco plants [146]. However, stably expressing heterologous proteins in plants is an elaborate process that is both time-consuming and

labor-intensive [147]. In contrast, transient expression employs viral or bacterial vectors for the short-term expression of foreign transgenes [43]. Transient expression can be used to quickly produce vaccines during pandemics [148], for emerging infectious diseases [149], or for patient-specific cancer treatments. For example, Large Scale Biology Corporation created a TMV-based transient expression vector for the production of idiotype vaccines (i.e., single-chain antibodies derived from each patient's tumor) for the treatment of non-Hodgkin's lymphoma [150]. The advantage of using plants for this process was that the personalized vaccines could be produced quickly (within weeks of obtaining a biopsy from a patient's tumor). Plant cell cultures can also be used to produce pharmaceutical proteins. For example, Protalix Therapeutics utilizes carrot cell cultures to manufacture β-glucocerebrosidase, a treatment for Gaucher's disease [151]. It should be noted that plant cell culture eliminates some of the cost-savings associated with plant-based production requiring capital-intensive facilities and equipment comparable to mammalian- or yeast-cell production systems [152,153]. In summation, plant-based production has proven to be both scalable and economical with production costs that are far lower than production systems based on *E. coli* or eukaryotic cells and a better safety profile than products produced in mammalian cells [117,147,153-155].

Nicotiana benthamiana

Nicotiana benthamiana belongs to the Solanaceae family and is indigenous to Australia. A close relative of *Nicotiana tabacum* (tobacco), *N. benthamiana* possesses multiple traits that make it an ideal production system, including that it has a fast growth rate [149] and is a non-food, non-feed crop that can easily be cultivated in growth rooms [28]. Because *N. benthamiana* is not grown for food or feed, the risk of transgene spread is low [113,130]. Furthermore, when transient expression is used, transgenes are not stably incorporated into the plant genome, so transgene flow is not a problem [130]. *N. benthamiana* also possesses a mutated RNA-dependent RNA polymerase gene, which reduces gene silencing, thereby making it highly susceptible to the viruses and agrobacterium often used for transient expression [156,157].

In fact, it is widely used to study plant virology and plant host-pathogen interactions because it can be easily infected by a large number of plant viruses and other plant pathogens [157]. For these reasons, *N. benthamiana* is the most routinely used species for transient expression of biopharmaceuticals in plants [149,157].

The anti-Ebola virus antibody cocktail, ZMAPP, is produced in *N. benthamiana* [158], and it is currently in phase II/III clinical trials [159]. Other biopharmaceuticals produced in *N. benthamiana* that have been tested in clinical trials include Medicago's VLP influenza and rotavirus vaccines [160,161] and Icon Genetics' idiotype vaccines for non-Hodgkin's lymphoma [162]. The fast growth rate and high yields associated with *N. benthamiana* are particularly amenable to producing vaccines during pandemics when they can be used to create large amounts of vaccines in a short period of time. For instance, with funding from the Defense Advanced Research Agency (DARPA), Medicago produced 10 million doses of their H1N1 influenza vaccine in just 30 days using *N. benthamiana* [163]. A single plant can produce up to 50 doses of a flu vaccine, and, if scaled-up, a single manufacturer could theoretically produce 1 billion doses per year [164] at a cost of less than $0.12 per dose [129]. A similar egg-based influenza vaccine production facility produces only 100 million doses per year, with a yield of 1-2 doses per egg and a cost of $1.50 per dose [165,166]. Plant-based production of VLP and VNP vaccines has thus proven to be both scalable and economical with production costs are far lower than egg-based or mammalian cell culture-based production systems [43].

Agrobacterium-mediated expression

Agrobacterium tumefaciens is a gram-negative, soil-dwelling bacterium that possesses the ability to transfer DNA sequences (i.e., T-DNA) from its Ti plasmid into the nuclei of plant cells, a trait which usually leads to the formation of crown gall disease [167]. This ability has been exploited to produce exogenous proteins by replacing some of the tumor-inducing genes on the Ti plasmid with DNA encoding proteins of interest [168]. Plants can then be inoculated with modified *Agrobacterium* by

agroinoculation, in which a small amount of bacterial culture is pipetted onto an abraded leaf, or by agroinfiltration, which uses negative pressure to flood the interstitial spaces of plant leaves with *Agrobacterium* culture [169] (Figure 2). After inoculation, the T-DNA region of the modified Ti plasmid can become stably integrated into plant genome to create transgenic plants [170]. Copies of the T-DNA are also transiently transcribed in the nuclei of the plant cells, which leads to transient expression [171]. By co-cultivating *Agrobacterium* with plant calluses, this process can also be used to transiently express proteins in plant cell cultures [172]. Thus, stable and transient expression of recombinant proteins in whole plants and plant cell cultures can be accomplished through *Agrobacterium*-mediated expression.

Figure 2. Agroinfiltration of *Nicotiana benthamiana*. Plants are placed in *Agrobacterium* culture (water is used here for clarity) and a vacuum chamber is used to create negative pressure. Upon releasing the vacuum, the bacterial culture floods the interstitial spaces of plant leaves and leads to *Agrobacterium*-mediated expression.

Plant virus-based expression vectors

A variety of plant virus-based vectors have been used to transiently express proteins in plants, including tobamoviruses, potexviruses, and comoviruses [169]. These plant viral vectors contain full copies of the viral gene into which a foreign gene has been inserted, which are known as full viral vectors, or they can be deconstructed viral vectors [173]. Initially, double-stranded cDNA copies of single-stranded DNA viral genomes were used to mechanically inoculate plant leaves using diatomaceous earth (i.e., rub-inoculation). Similarly, double-stranded cDNA copies of single-stranded RNA viral genomes could be reverse transcribed *in vitro* to make infectious RNA, which could then be used to rub-inoculate plants [174]. Rub-inoculation limits the use of viral vectors because it requires that the virus be mechanically transmitted and is a very inefficient, low-throughput process [169]. Thus, second-generation viral vectors included sequences from the Ti plasmid of *Agrobacterium* and the 35s promoter from cauliflower mosaic virus (CaMV) to create agroinfection-compatible plant-virus expression vectors [175-177]. When used with agroinfiltration, these vectors are delivered to the majority of leaf cells leading to high levels of heterologous protein expression [169].

Such expression vectors can also be used to create VNPs in which a heterologous immunogen is expressed on the surface of plant viruses, such as cowpea mosaic virus (CPMV) or tobacco mosaic virus (TMV). The advantages of plant VNPs over other types of VNPs are that they have a favorable safety profile (i.e., they are unable to replicate in animals [178]) and they can easily be produced and purified at large-scale using low-cost plant hosts. To create plant VNPs, the heterologous immunogen is typically cloned into the viral vector so that it is produced as a translational fusion to the viral coat protein because maximum immunogenicity is achieved when the heterologous peptide is surface exposed [179]. However, these translational fusion restrain the size of the immunogen because large heterologous proteins tend to destabilize viral particles or hinder their assembly [180]. Mammalian viruses, such as adenovirus and poxvirus, can also be used as VNPs, but many people have high levels of antibodies to

these common viruses because of prior exposure [181]. Pre-existing antibodies to these viral scaffolds can neutralize the VNPs before an immune response can be triggered against the heterologous immunogen they carry, leading to low efficacy.

Tobacco mosaic virus

TMV was the first virus to be identified, purified, visualized via electron microscopy, and studied by x-ray crystallography [182,183]. TMV-infected tobacco plants produce TMV in such abundance that viral inclusion bodies can be seen using a light microscopy [184]. Despite its name, TMV is capable of infecting over 150 types of plants, including tobacco, tomatoes, cucumbers, and peppers [185]. TMV-infected plants display symptoms such as flexion of the upper part of the stem, mottled light and dark green leaves (i.e., chlorosis), leaf curling, and stunted growth (Figure 3).

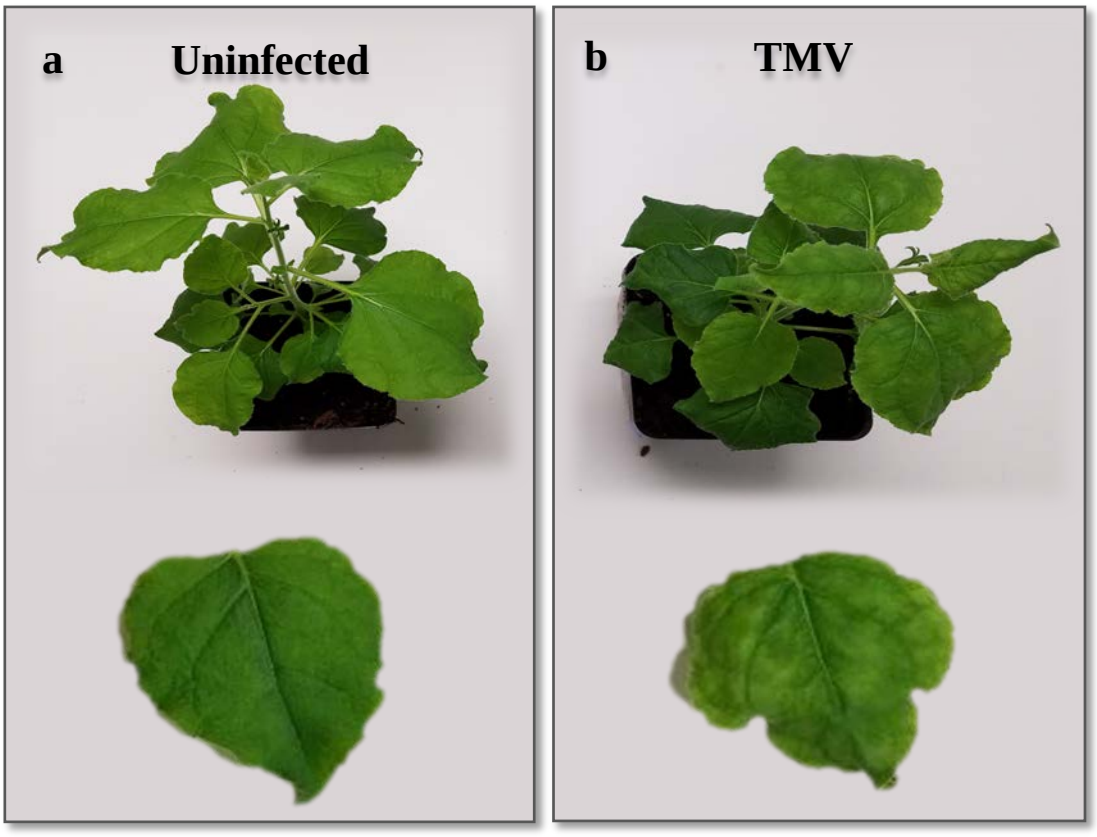

Figure 3. Symptoms of tobacco mosaic virus infection in *Nicotiana benthamiana*. **a)** Uninfected *Nicotiana benthamiana*. **b)** *Nicotiana benthamiana* showing symptoms of TMV infection, including mottled leaves, stunted growth, and leaf curling.

TMV consists of over 2,100 cylindrical coat proteins arranged in a helical manner around a single-stranded, positive-sense RNA genome to form rods approximately 300 nm long and 18 nm wide [182]. Due to the densely packed nature of its coat proteins, TMV is extraordinarily stable and purified virions stored at 5°C remain viable for at least 50 years [182]. This inherent stability of TMV allows it to be used with a wide variety of buffers and even some organic solvents over a pH range of 3.5-9, which allows for chemical surface modifications and electroless deposition of metals [186]. Along with the intrinsic ability of TMV coat proteins to spontaneously assemble *in vitro* [187], this robustness has led to TMV nanoparticles being used in vaccines, imaging reagents, biosensors, battery components, drug delivery, chemical catalysis, and data storage [188].

In addition to robustness, TMV possesses many other properties that make it an ideal scaffold for displaying exogenous epitopes. These include 1) it is composed of a single coat protein, which is easily genetically modified [183]; 2) it is a non-enveloped virus that is flexible in terms of shape and composition [189]; 3) it tolerates insertions at several surface-exposed residues on its coat protein [91,183]; 4) large quantities of virus can easily be purified from infected plants [190]; and 5) the density of epitopes displayed on TMV is unmatched by any other VNP or VLP system (i.e. TMV can display over 2,100 copies of an epitope, compared to CPMV VNPs, which display only 25 copies, and papillomavirus VLPs, which display 420 copies) [191,192]. TMV VNPs can also be thought of as a conjugated subunit vaccine in which TMV serves as a stable adjuvant, which may prove beneficial in resource-poor settings where cold-storage dependent adjuvants are impractical [193]. In addition, when displayed on TMV, weak B cell antigens become high ordered, which leads to effective cross-linking of B cell receptors and elicit a potent antibody response [194]. In fact, the size, particulate nature, and high density of repetitive antigens that can be displayed on TMV VNPs efficiently trigger the innate immune response, allow for efficient uptake by DCs in the lymph nodes, and trigger long-lasting cellular and humoral immune response

[39,181,195,196]. As a result, TMV VNPs have been used to induce humoral and cell-mediated immunity against a variety of pathogens (Table 2).

Table 2. TMV VNPs created as vaccines against viral diseases, bacterial diseases, and parasitic diseases, as well as cancer vaccines and immunotherapies.

	Pathogen	Epitope displayed	Reference
Viral pathogens	HIV	HIV-1 Tat protein	[197]
		Envelope protein gp120	[198]
	Influenza virus	Hemagglutinin glycoprotein	[198]
	Rabies virus	G5-24 glycoprotein peptide	[199]
	Poliovirus	VP1 of poliovirus type 3	[200]
	Foot-and-mouth disease virus	F11 & F14 from the VP1 capsid protein	[201]
Bacterial pathogens	*Pseudomonas aeruginosa*	OMPF peptide	[202]
	Francisella tularensis (tularemia)	OmpA, DnaK, and Tul4	[196]
Parasites	*Plasmodium falciparum* (Malaria)	B cell epitope	[203]
Cancer	-	Mouse tumor T cell epitopes	[204]
	-	Tn (a tumor-associated carbohydrate antigen)	[205]

TMV viral vectors

Most TMV expression vectors contain a T7 promoter which means transcripts can be made *in vitro* and used to rub inoculated plants. However, this process is inefficient, labor-intensive, expensive, and not conducive to scale-up [176]. Agroinfection-compatible TMV expression can be transformed into *A. tumefaciens,* cultured, and then injected or vacuum-infiltrated into the leaves of the plant [206]. The addition of a plant-driven 35S promoter from Cauliflower mosaic virus then allows the viral cDNA to be transcribed into RNA in the nuclei of the plant cells. Once the TMV proteins are transcribed, the recombinant viral particles assemble, spread throughout the plant, and replicate on their own. The coat

protein gene and/or other non-essential viral genes can be removed from TMV vectors to create a "deconstructed" vector into which large genes encoding foreign peptides can be inserted [207]. Because these vectors do not produce viral particles that can assemble, replicate and move to other parts of the plant on their own, vacuum infiltration is required to ensure every cell will produce the protein of interest.

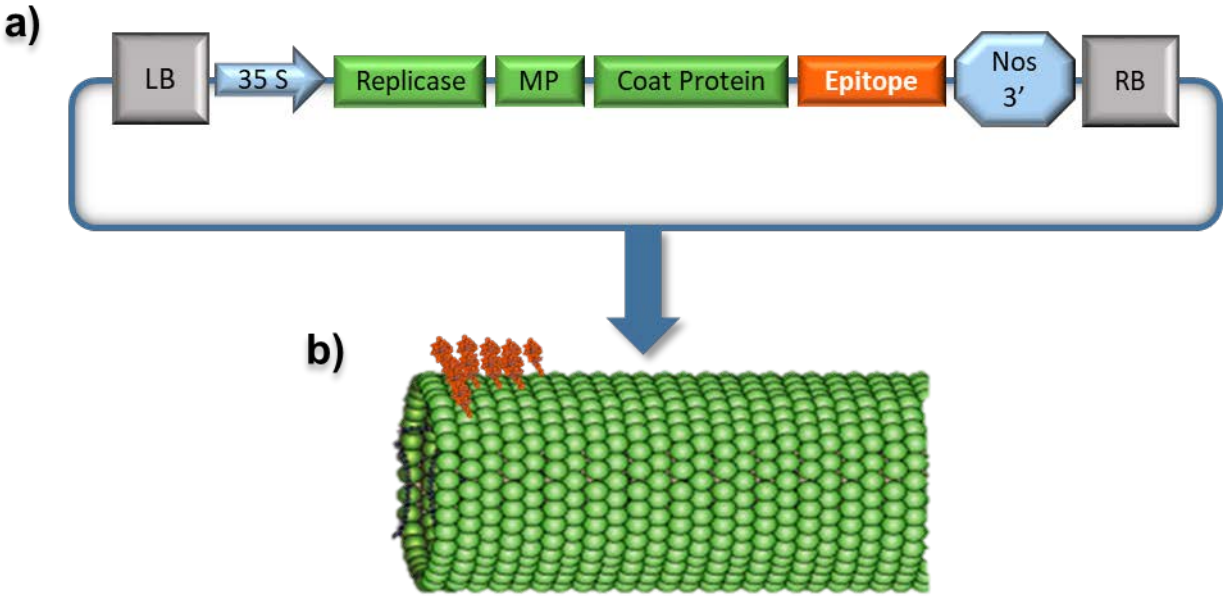

Figure 4. Diagram of an agroinfection-compatible TMV expression vector and a TMV-based viral nanoparticle. **a)** Grey boxes show the left and right border sequences (LB and RB) of the *Agrobacterium* binary plasmid delimit the region of the launch vector that is transferred into plant cells following infiltration of plants. Blue boxes indicate regulatory elements: 35s is a strong constitutive DNA promotor from cauliflower mosaic virus; Nos 3' is the transcriptional terminator of *Agrobacterium* nopaline synthase. Green boxes indicate the TMV genes required for viral replication and movement: replicase is the TMV RNA-dependent RNA polymerase for viral replication; movement protein (MP) allows cell-to-cell movement of TMV through the plasmodesmata of the plant cells; coat proteins self-assemble to form the rod-shaped virions. Orange box indicates the foreign epitope that can be inserted as a translational fusion to the 3' end of the coat protein. **b)** Diagram showing a TMV nanoparticle with foreign epitopes (orange) displayed on the coat protein (green). Note: on a TMV VNP, the foreign epitope would be displayed on every copy of the coat protein.

SUMMARY

The mammalian immune system is complex and multi-faceted, and both T cell and B cell responses are essential for inducing the long-lived protective immunity required by most vaccines. In general, vaccines are composed of whole pathogens that have been attenuated or inactivated or smaller antigenic peptides from the pathogen, but there is always a tradeoff between the immunogenicity and safety. While safe and efficacious vaccines exist for many human pathogens, many people in developing countries do not have access to them. A novel vaccine production platform that produces high yields of vaccine antigens at a low cost could increase access to vaccines in developing countries while also providing a means of developing new vaccines for emerging infectious diseases. Using plants as a host for vaccine production may provide such a solution; it has already proven to be a cost-effective, scalable, and rapid means of producing other pharmaceutical products. The following chapters explore the use of agroinfection-compatible, TMV-based vectors to transiently express viral nanoparticles vaccines in *Nicotiana benthamiana*.

CHAPTER ONE: ZIKA VIRUS

INTRODUCTION

Zika virus (ZIKV) belongs to the *Flavivirus* genus of the *Flaviviridae* family, which is composed of enveloped positive-stranded RNA viruses. The *Flaviviridae* family contains many well-known human pathogens including yellow fever (YFV), dengue (DENV), West Nile (WNV) and hepatitis C. Mosquitoes of the *Aedes* genus transmit the virus to humans [208], but it can also be transmitted from one human to another perinatally, sexually, and through breast milk and blood transfusions [208]. In 1947, the first strain of ZIKV was isolated from sentinel monkeys in Uganda, and the first case in humans was documented in 1952 [209]. There were no significant outbreaks of ZIKV until 2007 when approximately 5,000 cases were recorded on Yap Island in Micronesia [210]. Thereafter, 19,000 cases were documented in 2013 (French Polynesia), and an estimated 440,000 to 1.3 million cases were documented in 2015 (the Americas and Southeast Asia) [211,212]. As a result of these explosive outbreaks, a causal link was established between ZIKV infection and congenital brain abnormalities [213,214]. This prompted the World Health Organization (WHO) to declare ZIKV a Public Health Emergency of International Concern on February 1, 2016 [215].

Most ZIKV infections are asymptomatic, and the 20% [216,217] of cases that are symptomatic typically manifest as a mild, self-limiting, flu-like illness [208]. Recent outbreaks have shown that ZIKV infections are also associated with a variety of severe neurological outcomes, including Guillain–Barré syndrome(GBS) [218] and congenital Zika syndrome (CZS) [219,220]. Congenital Zika syndrome (CZS) encompasses a wide range of abnormalities found in fetuses and infants, including microcephaly, brain atrophy, and macular scarring [221,222]. Risk estimates for CZS range from 6% - 42% based on the geographic area [223-226]. Guillain–Barré syndrome is a group of peripheral nerve disorders characterized by muscle weakness and progressive paralysis, which leads to severe disability in 20% of cases [227]. While the exact etiology of GBS is unknown, it is thought to be an autoimmune disorder in which the immune

system attacks the peripheral nervous system following a bacterial or viral infection. Viral infections that have been shown to trigger GBS include cytomegalovirus and Epstein-Barr virus [228]. The incidence of ZIKV-induced GBS has been estimated to be as low as 0.024 % [218,229] but could be as high as 1.23% [230]. Other complications associated with Zika virus infection include ocular lesions[231], thrombocythemia [232] meningoencephalitis [233], and multiple organ failure [234].

The global burden of ZIKV disease is difficult to determine. Because it typically manifests as a mild disease, most people who are infected do not seek medical care. Even if patients seek medical care, the clinical manifestations of Zika virus infection are very similar to infection by other flaviviruses, like Dengue and Chikungunya [235]. Differential diagnosis requires a serological assay to be performed in which viral RNA is detected by RT PCR [236], but these tests aren't typically available in resource-poor areas. If testing is available, cases are not always reported to public health officials. Given these limitations, estimating the number of people at risk of ZIKV infection is primarily assessed by looking at the geographic distribution of the primary vector, *Aedes* mosquitoes (Figure 5). For example, by taking into account various factors such as temperature, precipitation, vegetation and urbanicity, Messina *et al*. created a model that showed which geographic areas were suitable for *Aedes* mosquitoes [237]. Based on this approach, a predicted 2.2 billion people live in areas that are conducive to ZIKV transmission [237]. Furthermore, this number will likely increase as global warming increases the range of *Aedes* mosquitoes [238].

Currently, there are no therapeutics or vaccines approved to prevent, control, or treat ZIKV infection. Several approaches have been taken to limit the spread of ZIKV, such as vector management and educational programs, but these strategies have proven ineffective [239,240]. Numerous antiviral therapeutics are also being developed, such as the small molecule therapeutic bithionol [241] and monoclonal antibodies [242-244]. While these therapeutics have shown anti-ZIKV activity in cellular and animal models, none have yet been licensed for the prevention or treatment of ZIKV infection.

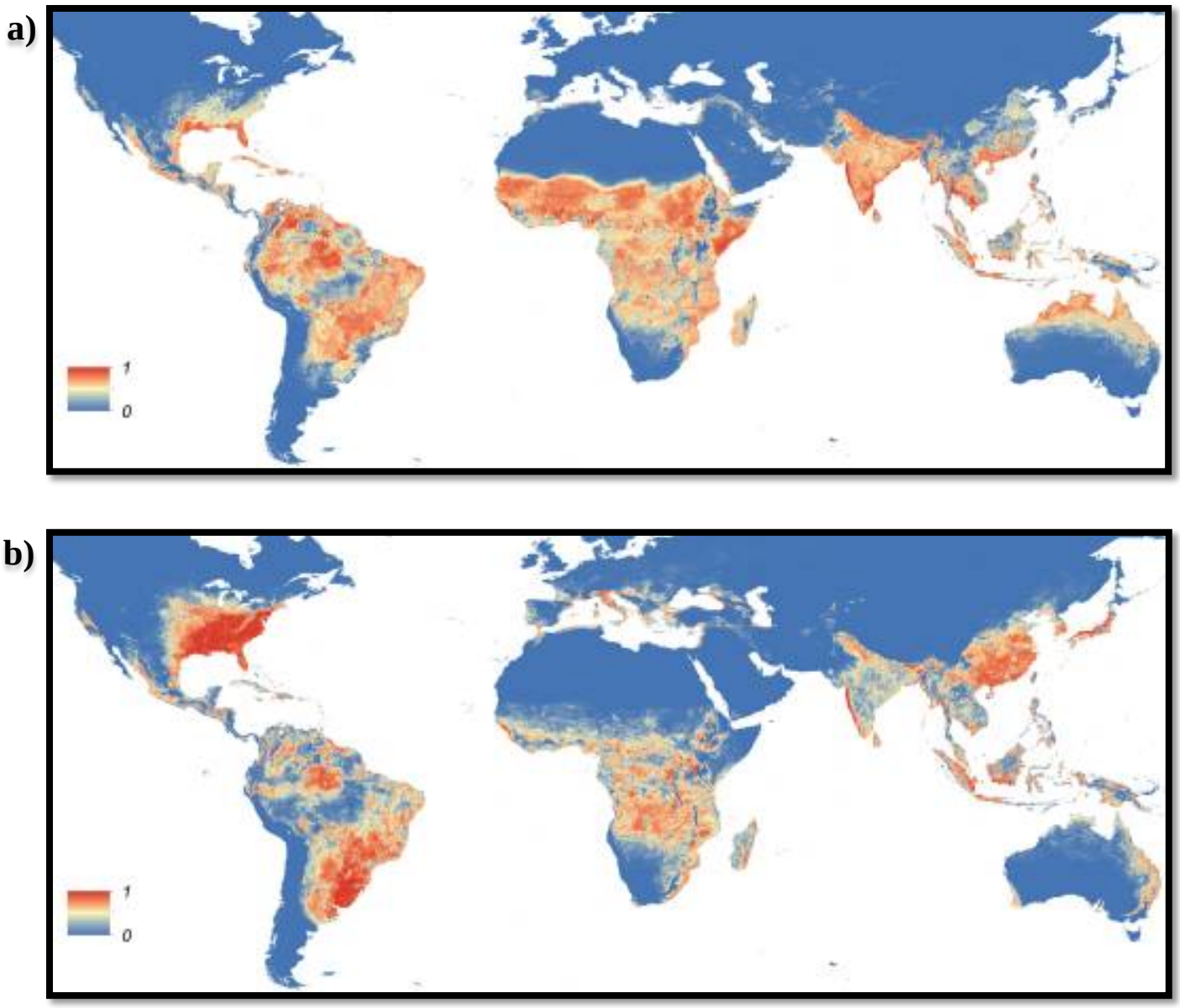

Figure 5. Global maps of the predicted distribution of *Aedes aegypti* **(a)** and *Aedes albopictus* **(b)**. Maps depict the probability of occurrence (from 0 blue to 1 red). Adapted from Kraemer *et al*. [245].

Historically, public health strategies to combat flavivirus infections have relied on vaccines to reduce the burden of disease [246,247]. Numerous factors must be taken into account when developing a safe and efficacious ZIKV vaccine, such as the limited understanding of ZIKV immunity and pathogenesis and the lack of an animal model that accurately mimics ZIKV infection in humans [248]. However, as explained below, antibody-dependent enhancement of disease, vaccinating pregnant women, the homology of

ZIKV strains, and affordability are likely the most critical factors to consider when developing a ZIKV vaccine.

1. **Antibody-dependent enhancement (ADE) of disease** - Researchers have theorized that a ZIKV infection or being immunized with an anti-ZIKV vaccine could generate antibodies that cross-react with other flaviviruses [249]. Upon subsequent infection with another flavivirus, these cross-reactive antibodies might be protective [250,251], but they could also lead to enhancement of disease [252] (the potential mechanisms behind ADE are discussed in the next section). Furthermore, many flaviviruses are transmitted by the same types of mosquitoes and co-circulate in the same geographic areas as ZIKV [253], a situation that is conducive to ADE. The risk posed by vaccine-induced ADE was recently seen in the clinical trials for a DENV vaccine in which children under nine had an increased risk of hospitalization following immunization [254,255]. And, while many *in vitro* and *in vivo* studies have looked at the role DENV antibodies might play in ZIKV pathogenesis, only a few *in vitro* studies have looked at the role that pre-existing ZIKV antibodies might play in ADE of DENV [256]. Even though ZIKV-induced ADE has not been confirmed *in vivo*, ZIKV vaccines should still be designed with this potential safety risk in mind [257].
2. **Vaccination of pregnant women and women of childbearing age** - Health authorities, most notably the WHO, identify the highest risk group to be women of childbearing age and pregnant women due to the severe outcomes associated with CZS. Morabito *et al.* suggest that the best way to protect pregnant women from ZIKV is via a high rate of ZIKV immunity in the general population. Thus, vaccinating all healthy individuals over nine years of age could be the best strategy to decrease the risk of ZIKV transmission to pregnant women [66]. Additionally, due to the disproportional risk to pregnant women, the ideal ZIKV vaccine should be designed with the safety of women of childbearing age and pregnant women in mind [258]. Live virus vaccines are

generally not administered to pregnant women because of the risk to the fetus, so inactivated virus, non-replicating virus-like particles, and subunit vaccines are preferred.

3. **Homology between ZIKV strains**- Different vaccine development strategies are required for single-serotype flaviviruses, such as YFV and JEV, versus multiple serotype flaviviruses like DENV. Developing vaccines for viruses with numerous serotypes is difficult because neutralizing antibodies against one serotype typically do not cross-neutralize other serotypes [259-261]. Thus, multivalent vaccines may be required, and these come with additional technical and regulatory challenges [262,263]. Recently, several studies have shown that only a single serotype of ZIKV exists. For example, Dowd *et al*. utilized sera from patients and mice infected with different strains of ZIKV to show that immune sera from one strain were capable of neutralizing different strains in neutralization assays, suggesting that there is only one serotype of ZIKV [264]. Aliota *et al.* showed that rhesus macaques infected with one strain were completely protected when challenged with a heterologous strain [265]. Furthermore, the limited diversity among ZIKV isolates (approximately 99.2 % sequence similarity [266] and 96% amino acid similarity [267,268]) suggests that a vaccine against one strain will protect against all strains.
4. **Affordability**- Most ZIKV infections occur in developing countries, so a preventative vaccine would have to be both affordable and ideally not require more than one dose [257,269]. Using various models of ZIKV transmission, studies have found that to be cost-effective, a ZIKV vaccine should cost no more than $10 per dose [270,271].

BACKGROUND

The Zika virus has a 10.8 kb positive-stranded RNA genome with a single open reading frame that is translated into one polyprotein [272]. Host and viral proteases cleave the polyprotein into three structural proteins and seven nonstructural proteins. The three structural proteins are the capsid (C)

protein, the precursor membrane (prM) protein (aka the membrane (M) protein in mature viral particles), and the envelope (E) protein, which along with the viral genomic RNA, form Zika virions. The C protein encapsidates the viral genome, the M protein facilitates fusion of the viral envelope with the host cell membrane, and the envelope protein is involved in receptor binding and viral assembly [273].

The seven ZIKV non-structural (NS) proteins are NS1, NS2A, NS2B, NS3, NS4A, NS4B, and NS5. Although functional data for the ZIKV NS is incomplete, their functions are likely similar to those of other flaviviral NS proteins, which play various roles in viral replication and assembly, evading the host's immune response [274], and even enhancing *Ae*. *aegypti* oral susceptibility [275]. For example, NS1 and NS2A are cofactors in the viral replications complex, and NS1 also recruits other NS proteins to membrane vesicles during viral replication [276,277]. Together with NS2B, NS3 functions as a serine protease to cleave the ZIKV polyprotein; NS3 also serves as an RNA helicase and NTPase [278]. NS4A regulates the ATPase activity of the NS3 helicase, and NS4B induces the formation of ER-derived membrane vesicles for viral replication [278]. The role that the ZIKV NS proteins play in immune evasion and pathogenesis will be discussed in subsequent sections.

Knowledge of the specific host cell receptors that facilitate ZIKV binding and entry remains incomplete despite numerous studies on the subject. DC-SIGN (dendritic cell-specific ICAM3-grabbing nonintegrin) receptors mediate antigen uptake and signaling on immune cells, such as macrophages and dendritic cells, and have been shown to facilitate viral entry [279-281]. In other tissues, ZIKV utilizes phosphatidylserine receptors TIM (T cell immunoglobulin mucin domain) and TAM (Tyro3, Axl, and MER) for cellular entry. Lipids on the exposed portions of the viral membrane interact with these receptors in a process called apoptotic mimicry (the normal function of these receptors is to recognize phosphatidylserine on apoptotic cellular debris and trigger phagocytosis) [282,283]. Specifically, TIM1 has been implicated in ZIKV binding to placental cells [284], while TAM receptors have been implicated in skin cells [279], endothelial cells [285], and neural stem cells [286]. However, a recent study showed that there was

no difference in viral replication or symptoms of viremia in mice with homozygous AXL knockout versus mice with a heterozygous AXL knockout [287]. Thus, ZIKV can likely exploit multiple receptors in different tissues types and in different hosts.

Cryo-electron microscopy and X-ray crystallography studies have revealed that the glycoproteins (E & M) undergo conformational changes as they are converted from their immature noninfectious form to their mature infectious form. On the immature virus, 60 heterotrimers of prM/E project outward from the membrane, resulting in a spikey appearance [288] (Figure 6a). In the acidic environment of the trans-Golgi network, the prM/E heterodimers rearrange so that they lie parallel to the membrane (Figure 6b). prM is proteolytically cleaved, and the mature virions are released into the extracellular space. These mature virions have a smooth surface composed of 180 copies of M/E heterodimers embedded in the viral membrane, and the 90 antiparallel E protein homodimers on the surface of the virion form an icosahedral herringbone pattern (Figure 6c) [289,290]. However, inefficient prM cleavage is common [291,292] and can lead to a wide range of partially mature virions that display a variety of conformational epitopes. In addition, flavivirus glycoproteins on partially mature and even fully mature virions are thought to be dynamic and continuously rearranging in a process called "viral breathing" [293,294]. During this process, the viral lipid membrane may be temporarily exposed, which accounts for the TIM & TAM interactions mentioned earlier.

Immune response to ZIKV

ZIKV induces both innate and adaptive immune responses. Minutes to hours after infection, the innate immune response responds to viral infection through the interferon (IFN) system. Type I IFNs are the primary mediator of the innate immune response against ZIKV, but type II and type III IFNs have also been implicated in protection against ZIKV infection [295-298]. Lazear *et al*. demonstrated the importance of type 1 IFN pathway as mice lacking components of this pathway show increased susceptibility to ZIKV

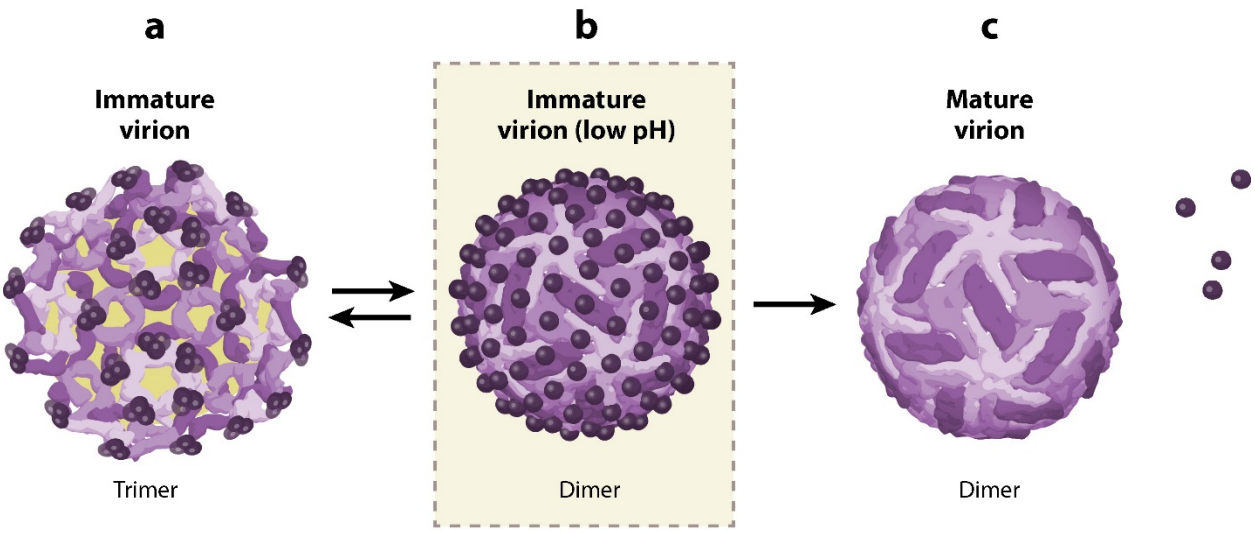

Dowd KA, Pierson TC. 2018. *Annu. Rev. Virol.* 5:185–207

Figure 6. "Flavivirus structures during virion biogenesis. **(a)** The lipid envelope of the immature virus contains 180 copies each of the pre-membrane (prM) and envelope (E) structural proteins. E and prM heterodimers are further arranged into heterotrimeric spikes that project away from the surface of the particle. Immature virions are noninfectious and must undergo a maturation step that involves cleavage of prM by host furin-like serine proteases. **(b)** In the low-pH environment of the trans-Golgi network, E and prM proteins rearrange to form 90 sets of antiparallel E protein homodimers that lie flat against the surface, with the prM proteins situated on top. This conformational change reveals a furin cleavage site in prM, resulting in a short membrane-bound M protein and a cleaved pr portion. The pr peptide remains associated with the virion during viral egress and protects the conserved fusion loop at the distal end of E-DII from prematurely initiating fusion. In the absence of prM cleavage, this conformational change is reversible for dengue virus when pH is returned to neutral; however, this does not appear to be the case for tick-borne encephalitis virus. **(c)** Infectious mature virions are released from cells by exocytosis. In the neutral pH of the extracellular space, the cleaved pr peptide dissociates from the virion, leaving a smooth particle coated by antiparallel E dimers. In all panels, shading of E protein dimers represents the distinct chemical environments present on the mature virion. Dark purple circles represent prM or cleaved pr peptide. Trimer versus dimer designation noted below each panel refers to the arrangement of E proteins." [293]. Annual Review of Virology by Annual Reviews. Reproduced with permission of Annual Reviews in the format Thesis/Dissertation via Copyright Clearance Center.

infection while ZIKV could not replicate efficiently in immunocompetent mice [296]. The type I IFN system is triggered when cellular pattern recognition receptors (PRRs), such as retinoic acid-inducible gene I-like receptors (RLRs) and Toll-like receptors, specifically TRL3 [299] and TRL7, recognize the nucleic acid of flaviviruses. RLRs are present in the cytoplasm of multiple types of cells and recognize viral RNA. TRL3 and TLR7 are expressed in intracellular cytoplasmic vesicles, such as endosomes, and recognize ssRNA and the double-stranded RNA produced during viral replication [300,301]. TLR3 is present in dendritic cells, macrophages, fibroblast, and epithelial cells, while TLR7 is only expressed on plasmacytoid dendritic cells. After these PRRs recognize viral RNA, they activate transcription factors like interferon regulatory factors (IRFs), which induces the production of IFN-α and IFN-β [279,280]. Secreted IFNs then bind to IFNAR

receptors, activating the JAK/STAT signaling pathway and leading to the transcription of interferon-stimulated genes (ISGs). ISGs are translated into proteins that exert a variety of antiviral effector functions. For example, the IFITM3 has been shown to inhibit ZIKV replication and prevent ZIKV-induced cell death [302], CXCL10 recruits natural killer cells to inhibit ZIKV replication [303], and MxA targets ZIKV nucleocapsids [303].

When PRRs recognize viral RNA, the NFκB-induced production of pro-inflammatory cytokines and chemokines also serves to eliminate viruses. During ZIKV infections, pro-inflammatory cytokines such as IL- 1β, IL-4 IL-6, IL-8, and IL-10 have been shown to be upregulated in monocytes [303]. However, the pro-inflammatory immune responses to ZIKV infection are cell-type specific. For example, embryonic neuroprogenitor cells [304] and dendritic cells [305] do not secrete pro-inflammatory cytokines, while cranial neural crest cells secrete multiple pro-inflammatory cytokines, such as LIF, IL-6, PAI-1 [306].

Natural killer (NK) cells are also part of the innate immune response to ZIKV that occurs prior to the adaptive immune response. A recent study showed that sera from ZIKV-infected patients contained high levels of IL-18, TNF-α, and IFN-ɣ, which are all associated with the function of NK cells [307]. CD14+ monocytes, various chemokines (CXCL9, CXCL10, CXCL11, and CCL5), and cytokines, like IL-15, have been shown to activate NK cells during ZIKV infection [308]. Once activated NK cells produce and release cytotoxic molecules that lead to apoptosis of the infected cell, limiting the ability of the virus to replicate and spread to neighboring cells. Another component of innate immunity is autophagy. While the normal function of autophagy to engulf, digest, and recycle macromolecules in the cytosol, this process can also be used to limit viral replication through degradation of viral proteins. This type of autophagy is thought to be induced by TLR7 and the adaptor proteins MyD88 and TRIF [309] and type 1 IFN signaling has been shown to promote autophagy of the viral proteases NS2B and NS3 [310], which are necessary for viral replication.

ZIKV subversion of the innate immune response

The type I IFN system is very effective at halting viral replication. To maintain their ability to replicate and disseminate, flaviviruses have evolved various mechanisms to counteract the antiviral effects of the type I IFN system. To varying degrees, all of the nonstructural proteins suppress IFN-β production by targeting components of the RIG-I pathway. ZIKV uses NS4A and NS5 to inhibit IFR3 and NFkB activation [311,312], while NS1 and NS4B interact with TBK1 to impede activation of IRF3 [310,311]. ZIKV non-structural proteins also antagonize JAK/STAT signaling: NS5 interacts with STAT2 and promotes its degradation [313] and NS2B/NS3 has a similar effect on JAK1 [310]. Additionally, the 5' methylated cap on the ZIKV genome mimics cellular mRNAs, and it is thought that this is used to evade detection by RLRs and other components of the I IFN pathway [314].

Flaviviruses have also evolved pro-viral mechanisms to either subvert or enhance autophagy at different stages of the viral replication cycle. For example, early in infection, the NS4A and NS4B proteins inhibit mTOR activity, thus upregulating non-selective autophagy. This is thought to mobilize the membranes and lipids required for membrane biogenesis during ZIKV replication [315] and also play a role in the maternal-fetal transmission of the virus [316]. Later in infection, the NS3 and NS2B proteins inhibit selective autophagy by cleaving the FAM124B receptor, thereby inactivating ER-phagy. This leads to expansion of the ER and thus increased viral replication [317,318].

Adaptive immune response to ZIKV

If the innate immune response cannot sufficiently stop viral replication, the adaptive immune response is activated. The adaptive immune response includes two class of responses: the cell-mediated response and humoral, or antibody-mediated, response. Evidence suggests that both cellular and humoral responses contribute to controlling ZIKV. The cell-mediated response is carried out by T cells that when activated proliferate and differentiate into effector T cells, of which there are two main types: cytotoxic T cells ($CD8^+$ cells) and helper T cells ($CD4^+$ cells). $CD8^+$ T cells recognize short viral

peptides bound to MHC class I molecules on antigen-presenting cells and destroy infected cells before the virus can proliferate and infect neighboring cells. $CD8^+$ T cells have been shown to mediate viral clearance from tissues in WNV [319] and JEV [320], and numerous studies suggest that $CD8^+$ T cells play a similar role during ZIKV infection [321-324]. Upon recognition of antigens on MHC class II molecules, $CD4^+$ T cells can differentiate into T_h1 cells or T_h2 cells. Cytokines produced during the innate immune response determine which type of $CD4^+$ T cell develops. Tappe *et al*. analyzed sera from ZIKV infected patients and found that levels of cytokines associated with T-cell activation were increased. These included T_h1-promoting cytokines (IL-12 and IFN-ɣ) and T_h2-promoting cytokines (IL-4, IL-13) [325]. T_h1 cells secrete IFN-ɣ and TNF-α, which activate macrophages and dendritic cells to kill phagocytosed viruses. T_h2 cells produce and secrete a variety of interleukins (i.e. IL-4, IL-5, IL-10, and IL-13) with different functions. The most critical antiviral functions are 1) activating B cell proliferation and antibody production, and 2) enhancing the cytotoxic functions of $CD8^+$ T cells and aiding in the survival of memory $CD8^+$ T cells.

ZIKV infection induces both $CD8^+$ and $CD4^+$ effector T cell responses, indicating that T cell epitopes play an important role in the immune response to ZIKV. In this case, T cell epitopes are short sequences of viral peptide sequences presented on the MHC molecules of antigen-presenting cells to stimulate a cellular immune response. Ngono *et al*. mapped ZIKV epitopes that elicited $CD8^+$ T cell responses in mice and found that these responses target all ZIKV proteins except NS1 and NS2B, but preferentially target the structural proteins with the immunodominant epitope being in the E protein [322]. Pardy *et al*. also found a potentially immunodominant $CD8^+$ epitope in the envelope protein [321]. Grifoni *et al*. analyzed peripheral blood mononuclear cells from ZIKV-infected donors and found that ZIKV structural proteins (C, E, and prM) are the primary target for both $CD4^+$ and $CD8^+$ T cells [326]. In a mouse model of DENV, $CD4^+$ T cells were shown to contribute to viral clearance [327]. Ngono *et al*. found that the $CD4^+$ T cell response in mice is directed against the E, NS3, NS4B, and NS5 and this contributed to IgG

response, local control of infection in specific tissues, and viral clearance during primary ZIKV infection [328].

Antibody-mediated protection

As previously mentioned, in the humoral immune response, effector $CD4^+$ T-cells activate B cells to secrete antibodies. Antibodies then circulate in the bloodstream where they bind to cognate antigens on the virus and inactivate them through a variety of mechanisms, including neutralization and opsonization [27]. Neutralization of flaviviruses occurs when antibodies block the virus from binding to host cell receptors, block uptake into cells, or block the membrane fusion process [329-331]. ZIKV induces the production of neutralizing antibodies [332], and numerous studies have shown that neutralizing monoclonal antibodies (mAbs) can fully protect mice from ZIKV infection [242-244,332,333]. Neutralizing antibodies have also been shown to mediate long-term protection from flavivirus infections [334]. Studies of WNV demonstrate that antibody-mediated flavivirus neutralization might be a "multi-hit process in which an individual virion must be bound by a threshold number of antibody molecules to inhibit infection" [293,335,336]. It is thought that two factors play a role in reaching this threshold: antibody affinity and the accessibility of epitopes. Studies of WNV suggest that even high-affinity antibodies require at least 30 accessible epitopes be present on a virion for neutralization to occur [337]. Furthermore, antibody-mediated neutralization is complicated by partially mature virions and viral breathing, both of which lead to different epitopes being displayed on the surface of ZIKV, and therefore different antibody-recognition sites [293].

Antibodies also indirectly contribute to protection through their Fc-mediated functions. When bound to a viral antigen, the Fc portion of the antibody's constant region activates the complement system, which plays a crucial role in protection from flaviviruses. The antiviral mechanisms of the complement system are diverse and include the direct inactivation of virions, recruitment and activation of monocytes, opsonization of viral particles, and the lysis of enveloped viral particles and infected

cells [338]. Evidence suggests that opsonization via the lectin pathway may be the primary mechanism by which the complement system neutralizes flaviviruses [338-340], because the small surface area of flaviviruses may limit the formation of the membrane-attack complexes (MAC) [338]. However, Schiela *et al*. demonstrated that the classical complement pathway reduced ZIKV titers and that this pathway was activated by IgM binding to viral particles or binding of C1q to viral proteins [341]. This would eventually lead to the formation of MACs and lysis of virions, which suggests that complement-mediated lysis is responsible for the reduction in ZIKV viral titers rather than opsonization [341].

Antibody-dependent enhancement of disease

In addition to hijacking the innate immune response for pro-viral purposes, flaviviruses have also been shown to exploit the antibody-mediated complement and FcR pathways. For example, WNV, YFV, and DENV NS1 proteins have been shown to block or attenuate activation of all three complement pathways [340,342]. However, the Fc receptor pathway likely plays a more significant role in ADE. When virus-antibody complexes form, they bind to Fcɣ receptors expressed on monocytes, macrophages, and dendritic cells and are phagocytosed. In DENV infections, primary infection or immunization can elicit an inadequate antibody-mediated response, which leads to severe disease upon subsequent infection with a different serotype of DENV [343,344]. prM-targeting antibodies have been shown to increase the infectivity of immature and partially mature DENV particles by facilitating entry into cells through FcɣII receptors [345]. Once the immature virus is endocytosed, conditions inside the endosome are thought to lead to viral maturation and initiation of membrane fusion [346,347]. Thus, by hijacking antibody-and-Fcɣ-mediated endocytosis, the otherwise uninfectious immature virions can become highly infectious and lead to severe disease [348]. This augmented viron uptake and the subsequent increase in infected cells is termed “extrinsic ADE”. Antibodies-mediated entry into cells can also lead to an increase in the amount of virus produced by each cell through a process called “intrinsic ADE”. This involves the aforementioned suppression of the antiviral type I IFN response, which allows infected cells to survive

longer and thereby increase viral replication [349]. Due to the structural similarities between flaviviruses, antibodies to one flavivirus can also be cross-reactive (i.e., capable of binding to other flaviviruses), which can lead to cross-neutralization [250,350]. Alternatively, if the cross-reactive antibodies have low avidity or are present at sub-neutralizing concentrations, they can increase virus production.

Indeed, *in vitro* and *in vivo* studies have shown that pre-existing DENV-neutralizing antibodies can lead to antibody-dependent enhancement of a ZIKV infection by mediating viral entry into otherwise unsusceptible cells or poorly susceptible cell types [249,351-354]. Additionally, a recent DENV infection, as measured by the level of DENV NS1-specific IgG3 antibodies in a patient's blood, seemed to increase a person's susceptibility to ZIKV infection [355]. Aside from this subset of patients with high levels of DENV NS1 IgG3 antibodies, the same study showed that the overall presence of preexisting DENV NS1-specific IgG antibodies was associated with less risk of ZIKV infection and fewer ZIKV symptoms [355]. However, caution must be used when interpreting this data in an ADE context though, because NS1 proteins are not part of flavivirus virions, and therefore would be incapable of enhancing uptake and binding of ZIKV virions. Furthermore, because ZIKV-induced GBS is relatively rare, a much larger cohort would have been needed to definitively show a correlation between preexisting DENV antibodies and ZIKV-induced GBS. Another study showed that the seroprevalence of neutralizing DENV antibodies was significantly lower in mothers of neonates with CZS than control groups, suggesting that cross-reactive antibodies may play a role in protection rather than enhancement of disease [356]. Thus, further studies are needed to definitively determine the role, if any, that preexisting DENV antibodies and ADE play in CZS and ZIKV-associated GBS. Despite the uncertainty surrounding ADE and ZIKV, ADE activity has been observed in several other viruses [337,357-359], indicating that ADE of ZIKV is a real possibility.

Neutralizing monoclonal antibodies against ZIKV

ZIKV infection leads to the production of both IgM and IgG antibodies. IgM is the first antibody produced in response to viral infections because it does not require isotype switching and can be

produced before B cells undergo somatic hypermutation. However, because of this, most IgM binding sites are low-affinity, and, therefore, IgMs form pentamers that contain ten antigen-binding sites to increase avidity. While the primary effector function of IgM is activating the complement system, IgMs can also neutralize viruses. Ngono *et al*. demonstrated the vital role of IgM plays in the humoral immune response by chemically inactivating IgM in sera from ZIKV-infected *LysMCre*$^{+}$*Ifnar1*$^{fl/fl}$ mice. Sera collected 7 and 10 days after infection was then used in a neutralization assay that showed that IgM was largely responsible for the neutralizing capacity of the sera [328]. Although IgM responses typically peak about one week after infection and disappear within 2-3 weeks, IgM antibodies can persist for 12 weeks or more after a ZIKV infection [360,361]. Even though IgM seems to play a significant role in ZIKV neutralization, no cryo-EM or X-ray crystallography studies have been done to determine the specific ZIKV proteins that neutralizing IgM antibodies bind. However, in an attempt find a ZIKV-specific antibody to serologically discriminate ZIKV infections from other flavivirus infections, Hansen *et al*. created a microarray of overlapping peptides from the entire ZIKV polyprotein, which was then used to screen sera from ZIKV-infected donors. A comprehensive list of linear antibody targets was generated that showed IgM binds to epitopes across the genome polyprotein [362], suggesting that IgMs target all ten ZIKV proteins.

In contrast to IgM, IgG antibodies exist as monomers with only two antigen-binding sites. These sites typically have a higher affinity for antigens, as the B cells that produce them have undergone affinity maturation. The IgG response usually peaks around 12-14 days after infection and persists long after infection. Studies of the antibody kinetics of ZIKV-infected individuals show that anti-ZIKV IgG in sera peaks anywhere between at 9-28 days after infection [361,363] and is maintained at high levels for up to two years [361]. IgGs are especially important for inhibiting viral infections because their primary effector function is neutralization though they also have other effector functions, such as triggering

opsonization and activating the complement system. The majority, if not all of, the neutralizing ZIKV mAbs that have been discovered are thus of the IgG isotype.

As mentioned previously, neutralization occurs when antibodies bind to a virion and prevent attachment, entry, or fusion. These functions are typically mediated by proteins on the surface of the virus, and the surface of ZIKV is comprised mainly of E proteins. Indeed, studies involving other flaviviruses have shown that the E protein is the major target of neutralizing IgG antibodies [251,266,294,334,335,364-366], but antibodies against prM and NS1 can also neutralize flaviviruses [367]. Studies in both mice and humans have revealed neutralizing epitopes within the E protein can include residues on an E monomer from one domain [243,368], the junction between two domains [369], and/or multiple domains [370]. Alternatively, envelope dimer epitopes (EDE) require quaternary structures, such as E dimers [250,370] or a neighboring pair of E dimers [371]. Two subsets of EDE mAbs have been defined: EDE1 and EDE2. EDE1 antibodies bind better in the absence of glycosylation at N154, while EDE2 antibodies bind better in the presence of the glycan [249,250]. Interestingly, EDE mAbs were first presented as potent neutralizers of DENV [249], but subsequent studies have shown that some of them also cross-neutralize ZIKV [250,370].

To date, hundreds of ZIKV E IgG mAbs have been described in literature. Some of these mAbs were discovered by sequencing antigen-specific memory B cells from the blood of ZIKV-infected patients [242,332] or creating human hybridomas [244,251]. Others were discovered by infecting mice with ZIKV [243] or re-screening previously discovered DENV-neutralizing mAbs [250]. The characteristics of 12 E-binding mAbs that inhibit 50% of ZIKV at a concentration of less than 1 μg/mL are summarized in Table 3. These mAbs bind to a variety of epitopes across all three ectodomains of E, have different structural requirements, and some are capable of cross-neutralizing DENV.

Table 3. Monoclonal antibodies against ZIKV envelope protein that are moderately to highly neutralizing (IC_{50}, $PRNT_{50}$, or $FRNT_{50} \leq 1$ µg/mL). IC_{50} = Inhibitory concentration, concentration at which antibody reduces viral replication by 50%. $PRNT_{50}$ = Plaque reduction neutralization test, concentration of antibody at which the number of plaques are reduced by 50% compared to no-antibody control. $FRNT_{50}$ = Focus reduction neutralization test, the same as PRNT, except uses the term foci instead of plaque.

mAb	E Domain Epitopes	E structure	Neutralization	Origin	DENV Cross-Neutralization	Reference(s)
ZIKV-117	DII	Dimer	IC_{50} = 5.4 ng/mL	Human (ZIKV)	None	244,372
Z004	DIII lateral ridge	Monomer	IC_{50} = 0.7-2.2 ng/mL	Human (ZIKV)	DENV-1	332
ZKA190	DI-DIII linker, DIII lateral ridge	Monomer	IC_{50} = 9 ng/mL	Human (ZIKV)	None	251,373
ZV-64	DIII C-C' loop	Monomer	$FRNT_{50}$ = 1-10 µg/mL	Mice (ZIKV)	None	243
SMZAb2	DII fusion loop	Monomer	$FRNT_{50}$ = 120-370 ng/mL	Human (ZIKV)	DENV-1, 2, 3	333
ZIKV-195	DI glycan loop, DII fusion loop	Dimer	IC_{50} = 77-600 ng/mL	Human (ZIKV)	None	244,374
Z3L1	DI, DII, DI-DII hinge	Monomer	IC_{50} = 170 ng/mL	Human (ZIKV)	None	242
Z20	DII	Dimer	IC_{50} = 370 ng/mL	Human (ZIKV)	DENV-1,2,3,4 (weakly)	
Z23	DIII	Neighboring dimers	IC_{50} = 370 ng/mL	Human (ZIKV)	None	
A11	DI glycan loop, DII fusion loop, DIII	Neighboring dimers (EDE2)	$FRNT_{50}$ = 506-904 nM	Human (DENV)	DENV-1,2,3,4	250
C8	DII fusion loop, DIII	Dimer (EDE1)	$FRNT_{50}$ = 15-26 nM	Human (DENV)	DENV-1,2,3,4	250,375
C10	DI, DII fusion loop, DII	Neighboring dimers (EDE1)	$FRNT_{50}$ = 13-63 nM	Human (DENV)	DENV-1,2,3,4	250,371,375
A9E	DIII lateral ridge, DI-DIII linker, DI- glycan loop	Monomer	$FRNT_{50}$ = 3- 17 ng/mL	Human (ZIKV)	None	376
G9E	DII	Monomer	$FRNT_{50}$ = 20-38 ng/mL	Human (ZIVK	None	

Pathology of ZIKV

Some viruses, such as poliovirus and rabies virus, are cytopathic because they interfere with essential cellular processes when they replicate in host cells, leading to cell death. Other viruses, such as HIV and DENV, are considered poorly cytopathic or non-cytopathic because they are capable of replicating in host cells without interfering with essential cellular processes. This suggests it is the host's immune response that is largely responsible for disease [377]. The pathogenicity of ZIKV seems to come from both its cytopathic effects and the immune responses it stimulates. For example, ZIKV-induced cytokines production triggers symptoms typical of flaviviral infection (e.g., fever, muscle pain, headache, joint pain, and rash) [378], while viral replication has been shown to cause cell cycle dysfunction and apoptosis in certain types of cells [379-381]. However, ZIKV is better known for distinctive neurological complications it can cause, specifically congenital Zika syndrome (CZS) and Guillain-Barre syndrome (GBS). While the exact mechanisms behind ZIKV neuropathology have not been fully elucidated, studies have shown a variety of pathways are likely involved. These include the previously mentioned inhibition of the IFN-triggered signaling cascade by ZIKV nonstructural proteins [310], the potential ability of non-neutralizing cross-reactive antibodies to increase viral replication (i.e., ADE) [256], and dysregulation of autophagy has been known to induce myelin injury. Also, human genetic determinants, such as single nucleotide polymorphisms, have been associated with an increased risk of severe flavivirus-related disease [382]. Other mechanisms implicated in ZIKV-associated neurological complications are discussed below.

To cause CZS, ZIKV must cross the placenta. Placenta-specific cells, such as Hofbauer cells (i.e., placental macrophages), trophoblasts, and placental endothelial cells, are targeted by ZIKV, and thus likely play a role in the vertical transmission of ZIKV [216,383]. Once it has crossed the placenta, ZIKV preferentially targets neuronal precursors and immature neuronal cells, such as neural progenitor cells, astrocytes, microglial cells, and pericytes [286,287,384-386]. The neurological symptoms of CZS could be the

result of ZIKV-related phenotypic changes in these cells, such as autophagy, apoptosis, impaired neurodevelopment, and the dysregulation of mitochondria. Investigations using mouse models have demonstrated that genes associated with both autophagy and apoptosis are upregulated in fetal brains [306,387-389], and ZIKV-related upregulation of TLR3 in various tissues [299,385,390] has been shown to deplete neural progenitor cells [390]. Dysregulation of mitochondria has been implicated in the neuropathogenesis of many diseases, and a study by Khaiboullina *et al*. showed that genes related to mitochondrial function are deregulated during ZIKV infection [303]. Bayless *et al.* observed increased secretion of LIF, VEGF, and IL-6 in ZIKV-infected cranial neural crest cells, which could lead to aberrant differentiation or apoptosis of neural progenitor cells [306]. Further studies have also shown that ZIKV infection disrupts neural development in the brains of embryonic and neonatal mice [387,391] as well as human brain organoids [392,393]. This is at least partially due to the action of the ZIKV nonstructural protein NS2A, which has been shown to degrade adherens junction proteins in the cortex of embryonic mice, which leads to reduced proliferation and premature differentiation of radial glial cells, and also disrupts the positioning of neurons [394]. Currently, these are the primary mechanisms thought to lead to microcephaly and other neurological disorders associated with CZS.

One of the main characteristics of ZIKV-induced GBS is the demyelination of cells in the peripheral nervous system (PNS) [395]. A recent study by Cumberworth *et al*. showed that ZIKV infection causes both demyelination (i.e., failure of myelin to form normally) and demyelination (i.e., loss of previously formed myelin) in murine neuronal cell cultures [396]. Myelinating oligodendrocytes and axons in the central nervous system (CNS) were shown to be particularly vulnerable to damage during ZIKV infection. This mirrors Chimelli's postmortem analysis of neonates with CZS, which found that the hemispheric white matter lacked oligodendrocytes and myelin, and axonal changes had occurred in the brainstem and deep grey nuclei [397]. However, unlike CNS cells, peripheral nervous system (PNS) cells were resistant to ZIKV infection [396], suggesting that this demyelination phenomenon is not the direct

cause of ZIKV-associated GBS. Instead, an autoimmune response triggered by a ZIKV infection leads to demyelination in the PNS, and thus GBS is only indirectly caused by ZIKV.

Pathogens are thought to initiate or exacerbate autoimmune response is a variety of ways. One plausible explanation for the induction of autoimmunity is through molecular mimicry, in which the sequence or structure of viral protein antigens mimic self-antigens [398]. In a recent study, Koma *et al*. showed that portions of the ZIKV envelope protein are structurally similar to C1q, a component of the human complement system that is involved in immunity, synaptic organization, and autoimmune disease [399]. They also showed that ZIKV infection induced C1q-specific antibodies, which could contribute to the development of ZIKV- associated GBS, microcephaly, and thrombocythemia [399]. Similarly, Homan *et al.* used computational analysis to compare the amino acids sequences of predicted ZIKV B cell epitopes to human proteins [400]. They found that ZIKV epitopes mimic a variety of human proteins, such as proNPY and NAV2, which are essential for neurological function and embryonic development. By mimicking these proteins, ZIKV could elicit an autoimmune response in human hosts that compromises the function of these proteins. Once these autoantibodies responses are induced, PNS damage may occur in several ways. One current theory on autoimmune demyelination of PNS cells involves the binding of antibodies to epitopes on the outer surface of the myelin sheath, followed by complement activation, and macrophage invasion [228]. Another mechanism for the autoimmune destruction of PNS cells posits that acute motor axonal neuropathy occurs when autoantibodies bind to gangliosides, an important component of peripheral nerve cells, leading to the formation of a membrane-attack complex, which ultimately causes nerve-conduction failure and axonal degradation [228,401]. Thus, while ZIKV neuropathogenesis is still not fully understood, a lot of effort has gone into revealing the numerous potential mechanisms of ZIKV-related neuronal damage.

ZIKV envelope protein

As previously mentioned, mature ZIKV particles contain 90 M protein dimers and 90 E protein dimers that form an icosahedral shell [289,290]. Most of the outer surface of the virion is comprised of E protein dimers, while the M protein dimers form transmembrane domains beneath the E proteins and therefore remain mostly unexposed [288]. The ZIKV E protein mediates binding to host cell receptors and entry into host cells and is the target of many neutralizing antibodies [242,244,372,402]. The most potent ZIKV-neutralizing mAbs are directed against the E protein epitopes [244,251,372].

The E protein contains approximately 500 amino acids organized into four domains: a pair of transmembrane domains and three ectodomains (Figure 7) [289,368]. Domain I (DI) is a β-barrel-shaped domain located in the middle of the E protein that contains the N terminus and a glycosylation site and is involved in envelope structural organization. Domain II (DII) is an elongated finger-like domain that flanks DI and contains the fusion loop, which is involved in the pH-dependent fusion of the virus with host cell membranes [290], and the E-protein dimerization interface. Domain III (DIII) is a C-terminal immunoglobulin-like domain that flanks the other side of DI [403], and likely includes the receptor-binding region that mediates attachment to host cells [250,289,290].

Notable features of the flavivirus envelope protein

The fusion loop (FL) is an internal hydrophobic loop composed of approximately 14 amino acids at the distal end of domain II (Figure 7b) [404]. Conformational changes occur when virions are exposed to low pH conditions (Figure 6), exposing FL and allowing it to interact with the endosomal membrane of the host cell to promote the fusion process and subsequent entry into the cell [290,405]. FL is a dominant antigenic site [406,407] and studies in both mice and humans have shown that FL mAbs make up approximately 50% of all E-binding mAbs elicited by ZIKV [244,251] as well as the E-binding mAbs elicited by other flaviviruses [408,409]. FL mAbs have been shown to neutralize DENV, YFV, and WNV [344,350,368,410,411], and, as shown in Table 3, they also neutralize ZIKV [69,250,412,413]. This cross-neutralization reflects the fact

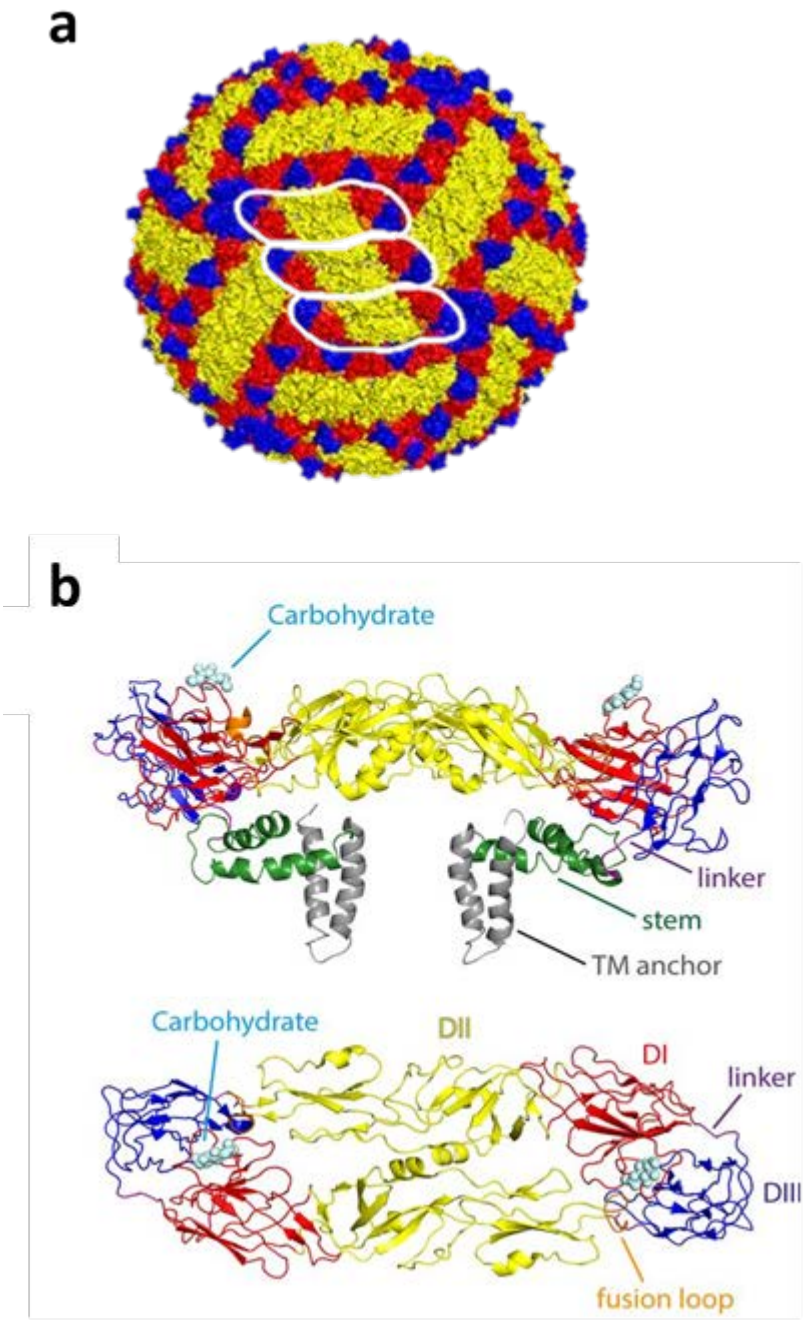

Figure 7. Structure of Zika virus particles and E proteins. **a)** Surface representation of the herringbone arrangement of E dimers at the surface of a mature Zika virus particle. **b)** Ribbon diagrams of the Zika virus E protein dimer in a side and top view, respectively. Asparagine (N)-linked carbohydrates (glycans) are shown as light blue spheres. TM, transmembrane. The three E protein domains are displayed in red (DI), yellow (DII), and blue (DIII), and the DI-DIII as well as DIII-stem linkers are shown in purple. The fusion loop at the tip of domain II is shown in orange [366]. Franz X. Heinz, and Karin Stiasny Microbiol. Mol. Biol. Rev. 2017; doi:10.1128/MMBR.00055-16, Figure 1, E and G. Reproduced and amended with permission from the American Society for Microbiology.

that the fusion loop region is highly conserved among flaviviruses [368] and suggests that FL could be used as an antigen to create a pan-flavivirus vaccine [414].

The glycan loop (GL) is another distinguishing feature of flavivirus envelope proteins [289,290] (Figure 7b). The majority of flaviviruses, including ZIKV, have a single N-linked glycan attached to N153/154 in a looping region of DI. This conserved feature has been shown to play a role in virion assembly [415,416], enhancing transmission in mosquitoes [417], and increased virulence in mammals [418-420]. For example, in DENV-4, removing N153 led to an increase in neurovirulence [421], and ablating both DENV E-protein glycans led to increased infectivity of insect cells, but also led to decreased virion release in both insect and mammalian cells [422]. Furthermore, GL is slightly longer on ZIKV, WNV, and JEV as compared to TBEV, YFV, and DENV, which has been hypothesized to contribute to their neurovirulence [290]. The ZIKV GL contains positively charged amino acids (R138, R164, and K166,) making it hydrophilic and it also contains the only glycosylation site on the ZIKV envelope protein, Asn154 [289,290,368]. In ZIKV envelope protein dimers, the GL of one E monomer interacts with the FL region on the other E monomer, which contributes to the stability of the E dimer [423]. Goo *et al.* demonstrated that GL regulates antigenicity of ZIKV by modulating access to FL epitopes and/or overall E protein conformation [424]. Fontes-Garfias *et al*. also studied the function of ZIKV N-linked glycosylation of residue N154. A mutant virus encoding N154Q, and therefore lacking any glycosylation, showed improved attachment, virion assembly, and infectivity in C6/36 (mosquito) cells [425]. However, in BHK and Vero cells, the mutation did not affect viral replication. Interestingly, the N154Q mutant ZIKV showed less virulence than WT ZIKV in mice but elicited a comparable level of neutralizing antibodies, which protected mice from a subsequent WT ZIKV challenge. The authors noted that similar *in vivo* versus *in vitro* discrepancies were seen in previous flavivirus glycosylation studies, and postulated that this might be due to " lack of cellular factors and complex immune systems in cell lines" [425]. Annamalai *et al*. demonstrated that unglycosylated E displayed attenuated neuroinvasion, possibly because it could not

pass through the blood-brain barrier [426]. However, this glycosylation site is conserved in both neuroinvasive and non-neuroinvasive flaviviruses, indicating that additional elements are also required for neurotropism. In addition, Goo *et al*. showed that non-glycosylated ZIKV particles could still infect Raji cells expressing DC-SIGN receptors, and therefore hypothesized that a glycan on the M protein might be able to facilitate entry of partially mature viral particles [424]. Wen *et al*. suggests that N154 serves to antagonize the vector's immune defense, allowing ZIKV to invade the vector midgut and thereby enhance transmission [427]. In summation, while the exact biological function of the glycosylated N154 on ZIKV E has not yet been fully determined, it likely plays a role in assembly and infectivity [428] and might also be involved in neuroinvasion and vector competence.

ZIKV lineages and polymorphisms

Following the 1947 discovery and isolation of ZIKV in the forests of Uganda, ZIKV circulated for decades in Sub-Saharan African and Southeast Asia only sporadically manifesting as a mild viremia that posed little threat to humans [209,429]. During this time, less than 20 cases of ZIKV were documented [430]. The 2007 Yap Island outbreak marked the first time ZIKV was in the Western hemisphere as well as the first large-scale outbreak of ZIKV ever reported [210,431]. The 2013 outbreak in French Polynesia and the subsequent 2015 outbreak in the Americas demonstrated that ZIKV infection could lead to severe neurological complications [219,229], raising the question of how ZIKV acquired enhanced pathogenicity and increased transmissibility. The answer to this question may lie in the genetic evolution of ZIKV. Phylogenetic and epidemiological data suggest that around 1946 ZIKV diverged into two lineages: the African lineage and the Asian lineage [267,268,432-434]. The African lineage includes the prototype 1947 Ugandan MR 766 strain, as well as strains from Nigeria (IbH 30656), Senegal (ArD 41519), and the Central African Republic collected between 1968 and 2001 [435]. Historically, strains from the African lineage of ZIKV have only been responsible for sporadic infections that resulted in mild febrile symptoms [434]. The Asian lineage includes the prototypic strain (a 1966 isolate from Malaysia), a

Cambodian isolate from 2010, and all contemporary Asian strains [436]. Furthermore, genetic and protein analyses have shown that the strains responsible for the outbreak in French Polynesia and the American epidemic are also part of the Asian lineage of ZIKV [267,268,430,437-439]. Thus, it has been hypothesized that as ZIKV spread eastward from African to Asia, genetic changes occurred and that these genetic changes are responsible for increased host infectivity, enhancement of vector fitness and transmissibility, as well as the increased pathogenicity seen in the recent ZIKV outbreaks [434,440,441].

Various *in vitro*, *ex vivo*, and *in vivo* studies comparing African strains to Asian strains have also provided evidence that the two lineages are phenotypically different, primarily in terms of virulence and pathogenicity [442]. For example, African strains of ZIKV are better at infecting and replicating in cultured human neural stem cells than Asian stains [443], and African strains replicated to higher titers, infected more cells, and induced cell death more frequently than Asian strains in cultured human neural progenitor cells [438]. Comparatively few *in vivo* studies have been done on lineage-specific phenotypic differences, but experiments using various mouse models of ZIKV infection also suggest that African strains are more virulent and pathogenic than Asian strains [296,435,444-446]. Despite this plethora of experimental evidence suggesting that African strains are more pathogenic and more virulent, no epidemics or severe complications have been documented in association with African strains even though seroprevalence data shows that ZIKV is circulating in Africa [447-449]. Alternatively, a handful of studies have demonstrated that Asian-lineage strains are equally or more pathogenic and virulent than African-linage strains. In a study by Vielle *et al*., cultured human monocyte-derived dendritic cells showed similar susceptibility to African and Asian strains and both strains induced similar infection profiles (as measured by IFN-β, IFN-λ, and ISGs) [450], and in a ZIKV infection model of vascular endothelial cells, an Asian strain exhibited higher viral RNA replication rates and induced more cells death than an African strain [285]. Asian strains of ZIKV showed higher infectivity rate and increased cell death compared to African strain MR766 in human primary astrocytes [299], and Asian strains reduced the size of

neurospheres more significantly than African strains, suggesting that Asian strains lead to the death of more neural cells [392].

Moreover, a study by Liu *et al*. revealed that the Asian lineage of ZIKV more effectively infects *Ae. aegypti* mosquitoes [451]. Taken together, these disparate findings indicate that factors other than lineage might play a more significant role in phenotypic differences observed the various ZIKV strains. For example, the differences could be due to strain-specific characteristics, such as the passage history of viral isolates or the type of animal the virus was isolated from (human, mosquito, or non-human primate). This is supported by data showing that even strains that are closely related in a spatiotemporal sense exhibit phenotypic differences [445,452]. Alternatively, the conflicting results of studies on the phenotypic differences between ZIKV lineages have been attributed to the quality of African-lineage ZIKV samples. For example, the prototypic African strain, MR766, was passaged around 150 times in the brains of suckling mice [268,453]. This extensive passaging likely led to mutations that made the MR766 strain progressively more neurovirulent in mice and less pathogenic in humans as this issue has arisen with other flaviviruses [454,455].

Like all RNA viruses, changes are constantly introduced into ZIKV's genome via error-prone replication. The majority of these mutations do not alter viral fitness and are thus removed by purifying selection. However, some of these mutations can increase viral fitness in mosquitoes and/or mammals, and therefore are maintained over time within sublineages. Despite the aforementioned challenges with trying to categorize lineage-specific ZIKV phenotypic differences, amino-acid differences between lineages could hold clues to the cause of the recent ZIKV epidemics. Concerning the phylogenetics of ZIKV, at least 50 lineage-specific amino acid differences have been documented [437,438,445,456], and Tripathi *et al*. found that these differences primarily occur in specific regions of the prM, E, NS2A, or NS5 proteins [435]. Amino acid substitutions within Asian –lineage strains have also been implicated in the increased pathogenicity of ZIKV. Using a neonatal mouse brain infection model, Zhang *et al.* compared

the postnatal effects of infection with a contemporary American strain (VEN/2016) to a pre-epidemic Asian strain from Cambodia (CAM/2010) and showed that the VEN/2016 strain was more effective at infecting murine brain cells and led to more severe microcephaly [391]. A subsequent paper by the same group revealed that an S139N substitution in the prM protein of the VEN/2016 strain substantially increased ZIKV infectivity of human and mouse and neural progenitor cells, and led to a more severe microcephalic phenotype in fetal mice as well as increased mortality rates in neonatal mice [452]. This substitution first emerged in 2013 during the outbreak in French Polynesia and has been stably maintained since then [434,441]. An alanine to valine substitution at position 188 (A188V) of the NS1 has been shown to increase ZIKV infectivity and prevalence in their mosquito hosts, which could have led to the increase in transmission thought to be at least partially responsible for the recent ZIKV epidemics [275]. Xia *et al.* also demonstrated that the A188V mutation led to increased evasion of host interferon induction [311]. With regard to the E protein, Chavez *et al*. documented two mutations in domain III (V603I and D679E) that were not found in pre-epidemic Asian strains, and thus might have contributed to viral fitness that led to the recent ZIKV epidemics [457]. In conclusion, it does appear that mutations might have contributed to increased virulence and transmissibility of ZIKV seen in recent epidemics. However, it is also possible that accumulated mutations did not lead to increased virulence and that all strains have similar virulence. Therefore the only reason severe outcomes were not seen before the 2013 French Polynesian outbreak is that there were not enough cases of ZIKV in previous outbreaks, so the rare severe forms of ZIKV did not manifest. Evidence suggests that the phenotypic differences observed are likely the result of genetic changes as well the greater number of patients observed during the recent ZIKV epidemics [440].

Zika vaccine candidates

The ideal ZIKV vaccine candidate would be safe, affordable, stable, and induce long-lasting immunity that neutralizes the virus, while also taking into account the need to be safe for pregnant

women and their fetuses. And, as previously mentioned, due to the antigenic and structural similarity of flaviviruses, the risk of ADE should also be considered. Historically, flavivirus vaccines have been made using inactivated or live-attenuated viruses, and this approach has yielded effective vaccines against YFV, JEV, and TBEV [51]. Table 4 outlines the ZIKV vaccine candidates that are currently in clinical trials, but there are many other candidates that have not yet reached the clinical trial phase of development [458-460]. Takeda, Valneva, WRAIR, and Bharat Biosciences are taking a traditional approach and have created purified-inactivated ZIKV vaccine candidates. Five nucleic acid vaccine candidates encoding for pre-membrane and envelope protein (prM/E) are also in the pipeline, and each utilizes a different system to deliver the nucleic acid into cells. The two NIAID candidates use a pressure-based delivery system [69], GeneOne Life Sciences uses electroporation [68], and Moderna has a nanoparticle-based delivery system for their mRNA ZIKV vaccine candidate [70]. Themis Biosciences has developed a viral vector-based live-attenuated vaccine candidate using their Themaxyn ® platform, which uses the measles virus vector to express ZIKV prM/E [461]. Similarly, NIAID has created a live-attenuated vaccine using a DENV-4 backbone to express ZIKV prM/E [462]. Since these vaccines are still in clinical trials, it remains to be seen whether any of these approaches will produce an effective, safe, and affordable vaccine against ZIKV.

Table 4. Zika vaccine candidates currently in clinical trials, including the vaccine platform used, the immunogen, and the companies and/or government agencies involved in their development. WRAIR = Walter Reed Army Institute of Research, NIAID = National Institute of Allergy and Infectious Diseases, BIDMC = Beth Israel Deaconess Medical Center, BARDA = Biomedical Advanced Research and Development Authority.

Candidate Vaccine	Platform	Immunogen	Company	Phase	References
ZIKV PIV (ZPIV)	Purified-inactivated virus	Whole virus	WRAIR /NIAID/BIDMC	Phase I	463-465
TAK-426 (PIZV)	Purified-inactivated virus	Whole virus	Takeda, WRAIR, NIAID, BARDA	Phase I	464
VLA1601	Purified-inactivated virus	Whole virus	Valneva, WRAIR, NIAID, BARDA, Emergent Biosolutions	Phase 1	466
BBV121	Purified inactivated virus	Whole virus	Bharat Biotech	Phase I	467
VRC5288	DNA w/ pressure-based delivery	prM/E (codon-modified ZIKV/JEV chimera)	NIAID, BIDMC, WRAIR	Phase I	463,464,468
VRC-ZKADNA090-00-VP*	DNA w/ pressure-based delivery	prM/E	NIAID, EMMES Corporation, Leidos Biomedical Research,	Phase II	464,468
GLS-5700 (INO-4701)	DNA w/ electroporation	prM/E consensus sequence	GeneOne Life Science, Inovio Pharmaceuticals	Phase I	464,469
mRNA-1325	mRNA in lipid nanoparticles	prM/E	Moderna Therapeutics NIAID, GlaxoSmithKline, BARDA	Phase II	463,464,470
MV-ZIKA	Live-attenuated recombinant measles vector	prM/E	Themis Bioscience	Phase I	471-473
rZIKV/D4Δ30-713	Live-attenuated recombinant DENV vector	prM/E	NIAID	Phase I	462

*Includes (VRC705 & VRC320)

MATERIALS AND METHODS

Zika virus epitope selection

The surface of the ZIKV virion is almost completely covered by envelope protein dimers, so most ZIKV-neutralizing mAbs target the E protein. For this reason, almost all ZIKV vaccine candidates contain the E protein or portions of the E protein. We selected two regions of the ZIKV E protein for display on TMV nanoparticles: the fusion loop and the glycan loop (Table 5). The fusion loop is highly conserved region and thus would serve to elicit antibodies that could neutralize multiple flaviviruses. Thus, the fusion loop epitope was chosen because it could potentially serve as a universal flavivirus vaccine. On the other hand, the glycan loop epitope is specific to ZIKV, so the antibodies it elicits should not cross-react with other flaviviruses. This could potentially negate any vaccine-induced ADE. The amino acid sequences are from ZIKV strain BeH823339, an Asian-lineage Brazilian strain collected in 2015 (GenBank accession no. AMK49164.2) [432].

Table 5. Zika virus envelope protein epitopes.

Epitope	ZIKV envelope protein amino acid number	Amino Acid Sequence	Properties (pI/MW) [474]	ZIKV envelope protein domain
Fusion Loop	97-109	VDRGWGNGCGLFG	5.80 / 1.337 kDa	II
Glycan Loop	145-165	GSQHSGMIVNDTGHETDENRA	4.72 / 2.255 kDa	I

Expression vectors and cloning

Two plasmids (pCR2.1) were ordered from Eurofins Genomics: these contained the synthetic gene for the TMV coat protein with each of the ZIKV epitopes (Table 5) genetically fused to the C-terminus. The lyophilized plasmids were resuspended per the manufacturer's instructions and then used as a template for PCR-amplification of the CP-epitope sequences in preparation for NEBuilder HiFi DNA Assembly into pTRBO. The PCR primers include non-priming pTRBO overlaps on the 5' ends (Table

6) and were designed using NEBuilder Assembly Tool and ordered from Integrated DNA Technologies. PCRs were then performed using the appropriate primers and annealing temperatures from Table 6 and Q5® High-Fidelity DNA Polymerase (New England Biolabs) according to the manufacturer's instructions [475]. Each PCR was performed in duplicate 50 µL reactions so that there would be enough DNA for the assembly reactions. Additionally, each set of primers was used to run a no template control in which no template (i.e., plasmid DNA) was included to ensure there were no extraneous nucleic acids contaminating the reaction components. No amplification controls, which contained no DNA polymerase, were also included. Positive controls could not be run because there were no templates that contained both the pTRBO overlaps and the CP-epitope sequences available.

Table 6. Primers used for PCR amplification of CP-GL and CP-FL.

Primer	**Sequence (5' - 3')**[a]	**Annealing Temperature**[b]	**Expected product size**
CP-FL Fwd	ttcttgtcattaattaacggATGTCCTATTCCATAACCAC	59.3 °C	559
CP-FL Rev	ctacctcaagttgcaggaccTTAGCCAAAGAGTCCACAAC		
CP-GL Fwd	ttcttgtcattaattaacggATGAGCTATTCCATAACAAC	57.3 °C	583
CP-GL Rev	ctacctcaagttgcaggaccTTAGGCACGATTCTCATC		

[a] The lowercase portions of the primer sequences are the non-priming pTRBO overlap sequences which are required for HiFi Assembly. The uppercase portions of the primer sequences correspond to the gene-specific sequence of each CP-epitope, which are required for template priming.

[b] Annealing temperatures for primer pairs determined using NEBuilder Assembly Tool [476].

Nucleic acid loading dye was added to the PCR products, which were then run on a 1.4% agarose gel with ethidium bromide for 2 hours at 100 mAmps. To minimize UV damage of any amplified DNA, the UV 365 setting was used while the bands containing the PCR products were excised from the gel. The amplified DNA was then purified from the excised gel bands using the Wizard® SV Gel and PCR Clean-Up System (Promega).

pTRBO in *Escherichia coli* K12 strain DH5α was propagated in LB containing 50 µg/mL of kanamycin at 37°C overnight. Plasmid DNA was isolated per the manufacturer's instructions with the

Monarch Plasmid Miniprep Kit (New England Biolabs). Restriction endonucleases AvrII and NotI (New England Biolabs) were used to double-digest 2 µg of pTRBO (1 µg in two 50 µL digestions) per the manufacturer's instructions. To ensure both endonucleases were functional, 1 µg of pTRBO was digested with AvrII only, and 1 µg of pTRBO was digested with NotI only. Nucleic acid loading dye was added to the digestions, which were then run on a 0.6% agarose gel with ethidium bromide for 82 minutes at 100 mAmps. To minimize UV damage of any amplified DNA, the UV 365 setting was used while an image was taken with the Azure gel imager and the bands containing the PCR products were excised from the gel. The amplified DNA was then purified from the excised gel bands using the Wizard® SV Gel and PCR Clean-Up System (Promega).

Digested pTRBO and the CP-epitope inserts were assembled using the NEBuilder® HiFi DNA Assembly Master Mix (New England Biolabs) per the manufacturer's instructions. The assembly reaction mixtures were then transformed into 10-beta Competent *E. coli* (New England Biolabs) per the manufacturer's instructions, and after 2.5 hours of incubation in SOC media at 37°C, the transformed cells were plated on LB-kan plates. The plates were incubated overnight at 37°C. Insert size was confirmed via colony PCR for eight pTRBO CP-FL colonies using the primers from Table 6. Agarose gel electrophoresis showed that all colonies had the right size insert, so two colonies were chosen from each construct and grown in LB + kan (50 µg/mL) and incubated at 37°C overnight. Plasmid DNA was isolated using the Monarch Plasmid Miniprep Kit (New England Biolabs), and the plasmids were sent with the appropriate primers (Table 7) to Eurofins Genomics for sequencing. Each plasmid was sequenced with three separate primers to ensure the accuracy of sequencing results. Sequences were aligned and confirmed using Serial Cloner.

Table 7. Primers used for sequencing and colony PCR.

Primer	Sequence (5' - 3')	Used to sequence
pTRBO fwd seq	tccatctcagttcgtgttcttg	pTRBO-CP-FL pTRBO-CP-GL
pTRBO rev seq	tgactacctcaagttgcaggac	
Fusion loop rev seq	GCCAAAGAGTCCACAACCAT	pTRBO-CP-FL
Glycan loop for seq	GCCTTAGGCAATCAGTTCCA	pTRBO-CP-GL

Agroinfiltration of plants

The recombinant pTRBO plasmids were transformed into chemically competent *A. tumefaciens* strain GV3101, plated on LB-KGR plates and incubated at 30°C overnight. Single colonies were chosen and cultivated at 30°C in LB containing kanamycin (50 µg/mL), gentamicin (25 µg/mL), and rifampicin (10 µg/mL) to select for recombinant clones. For infiltration, *A. tumefaciens* cultures were expanded in L-MESA to an optical density (OD_{600nm}) of approximately 1.0. The cells were then spun down, resuspended in an equal volume of AIM, and incubated overnight at room temperature. 100 mL of AIM culture was diluted in 1 L of water and then used to vacuum infiltrate *N. benthamiana* plants at -70 kPa for 5 minutes.

Plant growth and incubation

N. benthamiana plants were grown in soil from seeds under controlled conditions (16 hr of light at 24°C and 8 hr of dark at 21°C) for 5-6 weeks prior to infiltration. After infiltration, the plants were incubated for 6-14 days under the same controlled conditions used for pre-infiltration growth. Plants were monitored for signs of WT TMV infection (mosaic patterns on leaves, curling of the upper leaves, and upper stem flexion) or necrotic lesions.

Viral nanoparticle extraction, purification, and characterization

The extraction process is outlined in Figure 8. To extract the viral particles, infected leaves were homogenized in 4 volumes (w/v) of grind buffer (50 mM sodium acetate, 0.1% sodium metabisulfite, 0.01%BME, pH 5), filtered through cheesecloth, and then centrifuged (8,000 x g for 25 min at 4°C). To

precipitate the virus, the resulting supernatant (i.e., green supernatant) was mixed with 40% PEG (v/v) to achieve a final concentration of 4 %, 5 M NaCl was added to achieve a final concentration of 0.68 M, and the solution was incubated on ice for 1 hr. Following centrifugation (15,000 x g for 25 min at 4°C), the pellet (i.e., the PEG pellet) was resuspended in 50 mM phosphate buffer. A clarification step was then performed by centrifuging the resuspended pellet (7,000 x g for 7 min at room temperature) and collecting the supernatant (i.e., the clarification supernatant). This process repeated with leaves from non-infected plants, and these process samples served as negative controls. Process samples were then analyzed by SDS-PAGE and western blot.

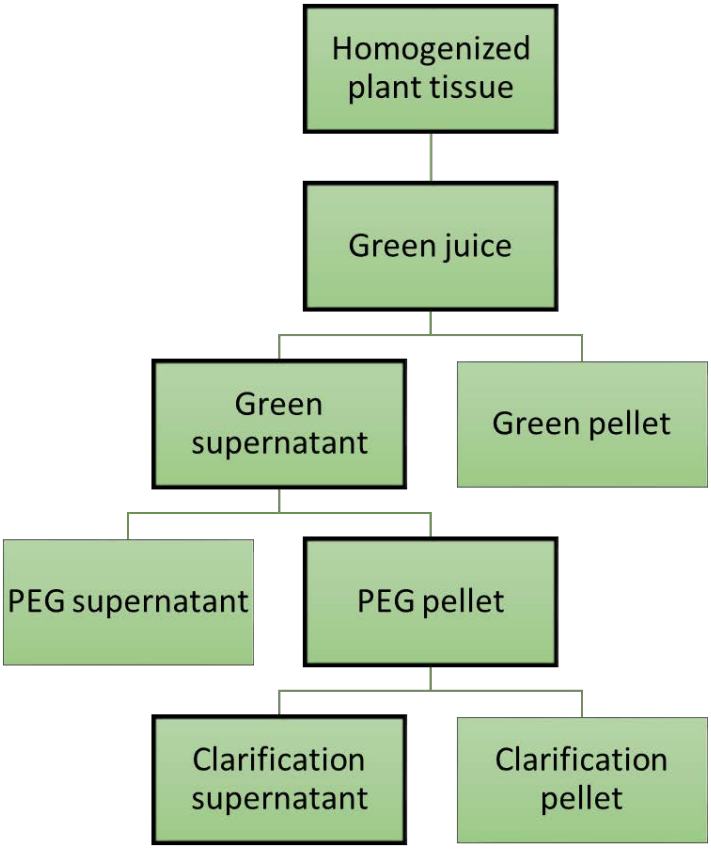

Figure 8. Extraction of TMV from infected plant tissue. Infected plant tissue is homogenized in grind buffer and the filtered through cheesecloth to produce "green juice". The green juice is centrifuged at 8,000 x g for 25 min at 4°C, which separates the "green supernatant" from the "green pellet". PEG and NaCl are added to the green supernatant, followed by incubation on ice for 1 hr. Following centrifugation (15,000 x g for 25 min at 4°C), the PEG pellet is resuspended in phosphate buffer then clarified by low-speed centrifugation (7,000 x g for 7 min at room temperature). The boxes outlined in black indicate the samples that contain the majority of the extracted TMV at each process step.

Sucrose density gradient centrifugation

Sucrose density gradient ultracentrifugation was used to further purify the TMV-GL and WT TMV viral nanoparticles following extraction with PEG-based on a protocol by Bruckman *et al*. [477]. Briefly, viral nanoparticles were loaded on a 10-40% sucrose gradient and ultracentrifuged at 96,000 x g for two hours at 4°C using a Beckman Coulter SW 28 rotor. The light-scattering region (see Figure 14) was collected and diluted in 10 mM phosphate buffer and then ultracentrifuged at 27,000 rpm for 23 hours at 4°C using a Beckman Coulter SW 28 rotor. The supernatant was discarded and the viral pellet resuspended in endotoxin-free PBS by placing it in the 4°C fridge for approximately 18 hours. The resuspended pellet was centrifuged for 15 minutes at 7,500 x g, and the supernatant containing the purified viral nanoparticles was stored at 4°C. Process samples were run on SDS-PAGE as previously described, and percent purity was calculated using AzureSpot software.

SDS-PAGE and western blotting

Laemmli sample buffer was added to the extraction process samples and heated at 95°C for 5 min. Proteins were separated on a 4-20% Tris-Glycine SDS-PAGE gel at 100 volts, followed by staining with Bio-Safe Coomassie (BioRad) or transferred to a nitrocellulose membrane for Western blot analysis. For western blotting, SDS-PAGE gels were transferred onto 0.2 µm nitrocellulose membrane (BioRad) for 90 mins at 400 mAmps. The membrane was blocked with 5% (w/v) nonfat dry milk (First Street) in TBS at room temperature for 1 hour then incubated with a primary antibody in blocking buffer overnight at 4°C. After washing with TBS and TBST, the membrane was incubated with goat anti-rabbit HRP-conjugated secondary antibodies (BioRad) (1:3,000 dilution) for 1.5 hr at room temperature. After another round of washing, a chemiluminescent signal was generated by incubating the membrane for 5 min with Clarity Western ECL Substrate (BioRad) and was documented using the Azure c500 (Azure Biosystems). Three different primary antibodies were used for these western blots were: 1) a 1:2,000 dilution of anti-ZIKV envelope protein polyclonal antibodies (eEnzyme) raised in rabbits immunized with

full-length recombinant envelope protein from the ZIKV strain BeH815744 (a Brazilian strain from the Asian lineage that includes the complete glycan loop) and was produced in mammalian cells (i.e. likely glycosylated at Asn154); 2) a 1:1,000 dilution of anti-ZIKV envelope protein polyclonal antibodies (Abiocode) raised in rabbits immunized with amino acids 140-180 from the MR766 strain (missing VNDT motif in the glycan loop) recombinantly expressed in *E. coli*, and 3) a 1:5,000 dilution of anti-DENV-2 envelope protein polyclonal antibodies (Thermo Fisher Scientific) raised in rabbit immunized with amino acids 1-495 of the DENV type 2 envelope protein recombinantly expressed in *E. coli*. The positive control for all three blots was recombinant full-length ZIKV envelope protein (eEnzyme) from strain a Brazilian strain (BeH815744) that was expressed in *E. coli*. The Pierce™ BCA Protein Assay Kit (Thermo Scientific) was used to estimate the concentration of the TMV-GL viral nanoparticles, and these concentrations were used to calculate yield.

Preparation of TMV-E and rE (Novici Biotech)

Recombinant ZIKV envelope protein (ZIKV-E) (amino acids 291-698, GenBank accession no. AMK49164.2) with an N-terminal extensin secretory signal peptide from *Nicotiana plumbaginifolia* and a C-terminal InaD Pdz domain (amino acids 2-98, GenBank accession no. 1IHJ_A, cys53ala mutation) and 6xHis purification tag were codon-optimized for expression in *Nicotiana* and cloned into a tobamovirus iBioLaunch vector (iBio Inc.). ZIKV-E with the extensin secretory signal peptide and a C-terminal 6xHis purification tag; KDEL was also cloned into an iBioLaunch vector. The plasmids were transformed into *Rhizobium radiobacter* strain GV3101 and transiently expressed in *Nicotiana benthamiana* by vacuum infiltration of GV3101 [478]. 5 or 6 days post-infiltration, plants were ground in 50mM CAPS 10.9, 500mM NaCl, 200mM Sucrose, 40mM Ascorbic Acid, 2mM PMSF. The lysate was filtered through spun-bonded polypropylene fabric, centrifuged at 30,100 x g, acidified with 1 M NaOAc pH 4.5, centrifuged, neutralized with 1 M Tris pH 9.5, centrifuged, and filtered at 0.2 microns. The recombinant protein was

then purified from the lysate by IMAC with Nickel-NTA agarose (Qiagen) or using a 1 ml HisTrap ™ HP (GE Healthcare), dialyzed into PBS, and concentrated with a 10 kDa cutoff spin concentrator.

The TMV-EFCA dock-and-lock virus scaffold was cloned by adding the amino acid sequence "EFCA" from the NorpA protein to the C-terminus of the TMV coat protein in a TMV vector [5]. RNA was transcribed using the Ambion mMESSAGE mMACHINE kit (Invitrogen) and encapsidated with purified TMV U1 capsid protein [6]. The virus was then rub-inoculated onto *N. benthamiana* plants by manual abrasion with diatomaceous earth. Leaf tissue was harvested about 12 days later, and the virus was purified by PEG precipitation [7].

ZIKV-E-TMV VLPs were prepared using the "Dock-and-Lock" method [8] to covalently attach the ZIKV-E-InaD fusion protein to TMV-EFCA virus scaffold. The VLP was then separated from unbound ZIKV-E-InaD by precipitation of the VLP with 0.5 M NaCl/4% PEG. The supernatant was removed, and the VLP resuspended in PBS. Docking was confirmed by Coomassie-stained SDS-PAGE gels of both reduced and non-reduced samples (Figure 9).

Immunization of mice and generation of hybridomas (USDA)

SP2/0 mouse myeloma cells and all hybridoma cells were maintained in hybridoma medium (HM), consisting of Iscove's modified Dulbecco's Minimal Medium (Sigma #I-7633) containing $NaHCO_3$ (36 mM) and glutamine (2 mM)] supplemented with 10% fetal calf serum (cHM). Hybridomas were selected following cell fusion using HAT selection medium prepared by adding Sigma 50 x stock HAT media supplement to 1x hypoxanthine (5 µM), aminopterin (0.2 µM), and thymidine (0.8 µM) to cHM. Macrophage conditioned medium (MϕCM) was prepared as described in Sugasawara *et al.* [479]. A mixture of 40% cHM and MϕCM was used for all cell-cloning procedures [480].

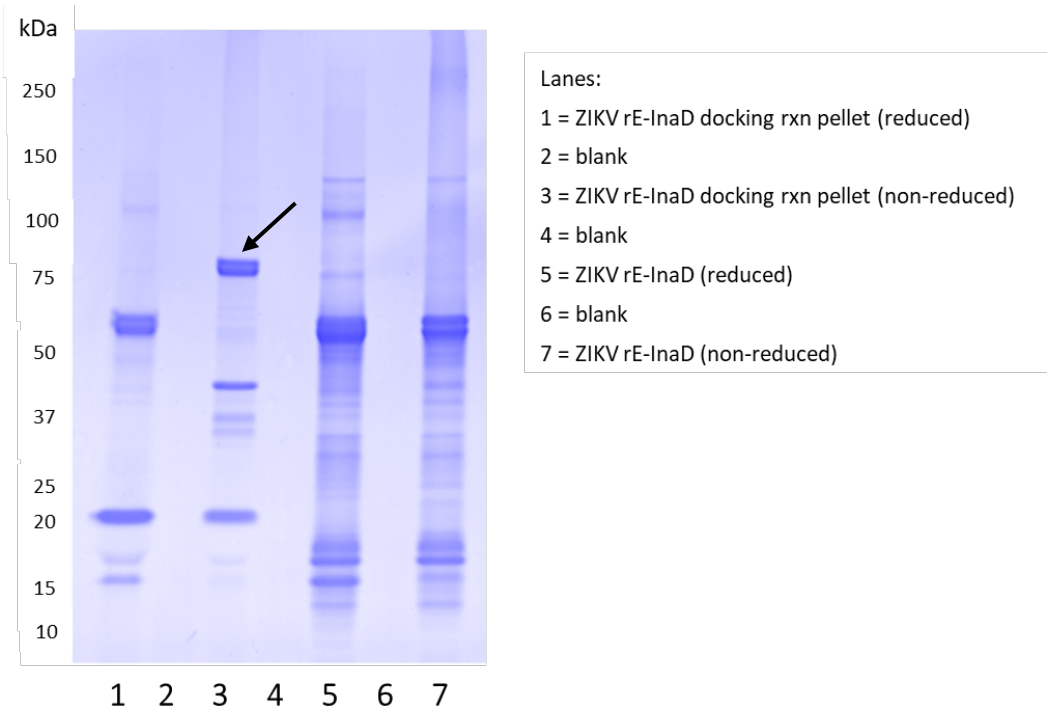

Figure 9. SDS-PAGE of ZIKV rE-InaD fusion protein docked to TMV-EFCA virus scaffold. ZIKV rE-InaD runs at approximately 58 kDa (lanes 5 and 7). When docked to a TMV coat protein, ZIKV rE-InaD runs at approximately 80 kDa (lane 3, band indicated by black arrow). Under reducing conditions, docked rE-InaD runs as its constituent parts (i.e., rE-InaD at 58 kDa, and TMV-EFCA at 20 kDa). Gel image kindly provided by Novici Biotech. Additional information about the "Dock-and-Lock" method can be found in chapter 2.

Five groups of three-month-old female BALB/c mice (Simonsen Labs) were intraperitoneally immunized with 25 µg of antigen: TMV-GL, TMV-E, rE, or a control (TMV or sterile PBS) and adjuvant (Sigma Adjuvant System, Sigma-Aldrich). Boosters were given approximately every 3 weeks for 4 rounds. Sera were obtained and evaluated for reactivity to the various target antigen using a direct-binding ELISA format. Black Nunc Maxisorp 96-well flat-bottom plates were coated with antigen at 30 µL/well of a 1.0 µg mL^{-1} in 0.05 M sodium carbonate buffer, pH 9.6 overnight at 4 °C. The coating solution was aspirated and non-coated sites blocked by adding 300 µL $well^{-1}$ of 3% non-fat dry milk in Tris-buffered saline containing 0.05% Tween-20 (NFDM-TBST) and the plates were incubated for 1 h at 37 °C. The plates were then washed 3 times with Tris-buffered saline containing 0.05% Tween-20 (TBST). Next, sera were added (30 µL $well^{-1}$) and the plates were incubated at 37 °C for 1 hr. Plates were again washed 3x and 30 µL $well^{-1}$ of a 1/5000 dilution of peroxidase-conjugated goat anti-mouse sera

(Sigma, St. Louis, Mo) was added and the plates incubated for 1 h at 37 °C. The plates were then washed 3x with TBST. Freshly prepared luminescence substrate (SuperSignal West Pico chemiluminescence) was added (30 µL/well) according to the manufacturer's recommendation. The plates were incubated for 3 min at room temperature and luminescent counts recorded using the Victor 3 (Perkin Elmer). All protocols were approved by the Western Regional Research Center Institutional Animal Care and Use Committee (Protocol # 16-1).

Mice that were positive for reactivity to antigen were immunized once more three days before the start of cell fusion. Mice were euthanized, and their splenocytes were fused with SP2/0 myeloma cells using polyethylene glycol as previously described in [481]. Following cell fusion, the cells were suspended in 100 mL of HAT selection medium supplemented with 10% fetal calf serum and 10% MϕCM, dispensed into ten, 96-well tissue culture plates, and incubated for 10 to 14 days at 37 °C in 5% CO_2 before screening for antibody production.

Supernatants from cell fusion plates were screened using a direct-binding ELISA. Clear Nunc Maxisorp microtiter plates were rinsed with distilled water and coated by incubating 100 µL/well of a 1.0 µg /mL rE (ZIKV) in 0.05 M sodium carbonate buffer, pH 9.6 overnight at 4 °C. The coating solution was aspirated and non-coated sites blocked by adding 300 µL $well^{-1}$ of 3% non-fat dry milk in Tris-buffered saline containing 0.05% Tween-20 and the plates were incubated for 1 h at 37 °C. The plates were then washed 3 times with Tris-buffered saline containing 0.05% Tween-20. Next, cell culture supernatants were added (100 µL per well) and the plates were incubated at 37 °C for 1 h. Plates were again washed 3x and 100 µL well per well of a 1/1000 dilution of peroxidase-conjugated goat anti-mouse sera (Sigma) was added and the plates incubated for 1 h at 37 °C. The plates were then washed 3x with TBST. 150 µL well per well of K-Blue® enhanced substrate (TMB) (Neogen) was added to each of the 10-96 well plates until color development was sufficient. The signal was read at 650 nm on the VersaMax (Molecular Dynamics). Cells from the wells giving positive signals for antibody production were cloned

by limiting dilution (3x) with screening using direct ELISA [480]. The 26 hybridomas that were created are outlined in Table 8.

Table 8. Hybridomas created from TMV-GL, TMV-E, and rE-vaccinated mice.

Hybridoma #	Vaccine Candidate
1	TMV-GL
2	TMV-GL
3	rE
4	TMV-GL
5	TMV-GL
6	TMV-GL
7	rE
8	TMV-GL
9	TMV-GL

Hybridoma #	Vaccine Candidate
10	rE
11	rE
12	rE
13	TMV-GL
14	TMV-GL
15	rE
16	TMV-GL
17	TMV-GL
18	TMV-GL

Hybridoma #	Vaccine Candidate
19	TMV-GL
20	TMV-GL
21	Non-specific antigen
22	TMV-E
23	TMV-E
24	TMV-E
25	TMV-E
26	TMV-E
27	TMV-E

Evaluation of serum antibody levels by ELISA (USDA)

Mouse sera were analyzed for glycan loop-specific antibody responses by ELISA. Briefly, 96-well plates were coated with antigen in carbonate buffer (0.03 M Na_2CO_3/0.07 M $NaHCO_3$, pH 9.6), incubated overnight at 4°C, and then blocked with 5% BSA for 1 hour at room temperature. Pooled or unpooled serially diluted mouse sera were added to the plates and then incubated overnight at 4°C. Following three washes with PBS, the plates were incubated with HRP-conjugated goat anti-mouse IgG (1:2000, BioRad) for 1 hr at room temperature then washed three times with PBS. OPD substrate (Sigma) was added, and the absorbance at 450nm was measured on a SpectraMax Plus plate reader (Molecular Devices). The antibody endpoint titers were defined as the reciprocal of the highest serum dilution that gave a reading above the cutoff. Cutoff values were determined for each dilution of the pooled adjuvant only serum as described in Frey *et al.* [482].

Flow cytometry-based neutralization assays (LJIAI)

A flow cytometry-based assay was used to measure the capacity of the mouse sera and the hybridoma supernatants to neutralize ZIKV (strain SD001) in U937+DC-SIGN cells as previously described

by de Alwis *et al.* [483]. Briefly, ZIKV and sera or hybridoma supernatants were incubated for 1 hour at 37 °C, followed by addition to U937+ DC-SIGN cells and 2 hr of incubation at 37 °C. Cells were washed twice with infection media, incubated for an additional 22 hr at 37 °C, then fixed and permeabilized. FITC-conjugated 2H2 was used to detect ZIKV, while a phycoerythrin-conjugated anti-CD209 antibody was used to assess DC-SIGN expression. Percentage of infected cells was determined using flow cytometry, and Prism software (GraphPad Software, Inc.) was used to calculate and plot percent neutralization values against Log (1/dilution).

Human serum samples

Four human serum samples from ZIKV-positive patients were purchased from Antibody Systems, and their reciprocal 90% neutralization titers (NT_{90}) were published by Lynch *et al.* [484]. Details of these samples are provided in Table 9.

Table 9. Details of human serum samples from Columbian ZIKV patients. Days after onset of symptoms indicates the number of days that passed between the onset of symptoms of ZIKV and when the serum sample was taken. ZIKV NT_{90} indicates reciprocal dilution at which the serum neutralized 90% of virions from ZIKV strain HF/PF/2013, which was isolated during the outbreak in French Polynesia. Mild symptoms of ZIKV infection include fever, skin rash, joint pain, myalgia, ocular pain, cephalgia, and conjunctivitis.

ID	Age	Gender	Days after onset of symptoms	ZIKV NT_{90}	Mild symptoms	Guillain-Barré Syndrome
ARSZ16308	46	F	51	128,080	Yes	No
ARSZGB16015	40	F	14	15,150	Yes	Yes
ARSZGB16031	48	M	30	25,425	Yes	Yes
ARSZ16467	44	F	37	20,211	Yes	No

Dot blot and ELISA analysis of Z3L1 binding

TMV-GL, unglycosylated rE (eEnzyme), or plant-glycosylated rE were diluted in TBS spotted onto nitrocellulose membrane and allowed to air-dry. The membranes were blocked for 1 hour in 10% NF

milk in TBS, followed by incubation with the Z3L1 mAb diluted 1:1,000 in blocking buffer and incubated overnight at 4 °C. The membranes were washed three times with TBST, followed by one wash with TBS. The blots were incubated for 1 hr at room temperature with 1:2,000 dilution of secondary antibody (goat anti-human IgG – peroxidase (Sigma)) followed by the addition of Clarity Western ECL Substrate (BioRad) and visualization of chemiluminescence using an Azure Biosystems C500 imager with an exposure time of five min.

The binding of human mAb Z3L1 to unglycosylated GL, plant-glycosylated rE, and unglycosylated rE (eEnzyme) was analyzed by ELISA in triplicate wells. Briefly, 96-well plates were coated with protein antigens diluted to 10 ng/µL in carbonate buffer, incubated overnight at 4 °C, and then blocked with 5% non-fat milk in TBS for 1 hr at room temperature. Z3L1 diluted to 10 ng/µL in blocking buffer was added to the plates and then incubated at room temperature for 2 hr. Following two washes with PBST and one wash with PBS, the plates were incubated with a 1:2,000 dilution of secondary antibody (goat anti-human IgG – peroxidase (Sigma)) for 1 hour at room temperature then washed as above. OPD substrate (Sigma) was added, and the absorbance at 450 nm was measured on a SpectraMax Plus plate reader (Molecular Devices). The background was measured as above, except blocking buffer was used instead of antigen. For the unglycosylated rE antigen, anti-ZIKV rE (eEnzyme) was used as a positive control with a goat anti-rabbit HRP-conjugated secondary antibody (BioRad).

Dot blots with mouse sera, human sera, or hybridoma supernatants

TMV-GL, WT TMV, or rE (*E. coli*) were diluted in TBS, spotted onto nitrocellulose membrane, and allowed to air-dry. The membranes were blocked for 1 hour in 10% NF milk in TBS followed by incubation with a 1:500 dilution of human serum/ mouse serum/ hybridoma supernatant in blocking buffer overnight at 4°C. The membranes were washed 3 times with TBST, followed by one wash with TBS and then incubated for 1 hr at room temperature with 1:2,000 dilution of secondary antibody (goat anti-human IgG – peroxidase (Sigma) or goat anti-human IgM- HRP(Novex), followed by the addition of

Clarity Western ECL Substrate (BioRad) and visualization of chemiluminescence using Azure imager. ImageJ software was used to digitally quantify the mean inverted pixels of the signal and corrected by that of the background. Normalized fold changes were subsequently calculated by dividing the corrected mean pixels of the signal of TMV-GL by that of TMV.

RESULTS

TMV-FL and TMV-GL were cloned into pTRBO

Constructs from Eurofins were successfully PCR amplified and then gel purified, cloning into pTRBO, and transformed into *E. coli*. Colony PCR (Figure 10) and/or sequencing (Figure 11) were used to confirm the plasmid sequences were correct prior to transforming into Agrobacterium and then vacuum-agroinfiltrating *Nicotiana benthamiana* plants.

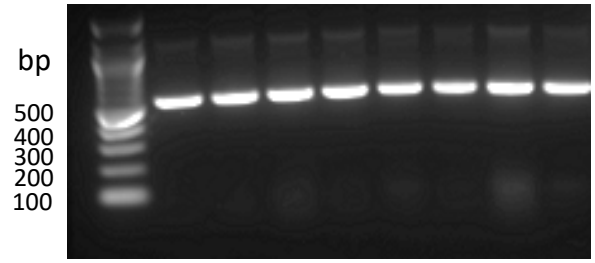

Figure 10. Colony PCR of eight pTRBO-FL colonies.

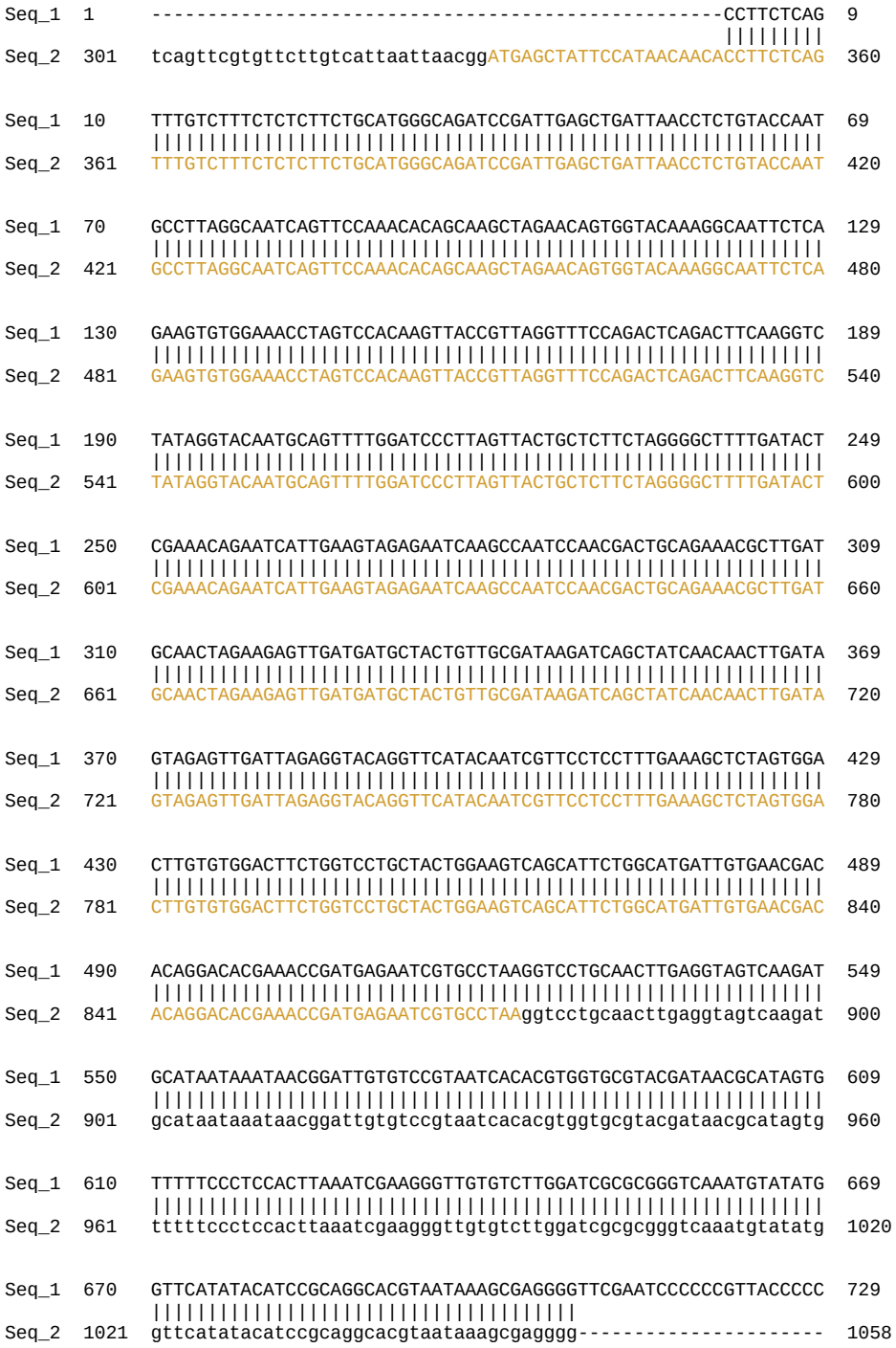

Figure 11. Example of a sequence alignment to check the sequencing results mini-prepped plasmid DNA from a pTRBO-CP-GL colony. Sequence 1 shows the sequencing results from, while sequence 2 shows the expected sequence of the TMV coat protein with the ZIKV glycan loop genetically fused to the 3' end (indicated by the brown letters). Sequences aligned using Serial Cloner software.

Expression of ZIKV epitopes on TMV nanoparticles in *Nicotiana benthamiana*

At 6 days post-infection (DPI), the plants infiltrated with TMV-FL formed necrotic lesions, and the leaves were harvested and frozen to prevent further tissue death (Figure 12b). Following PEG-precipitation, SDS-PAGE analysis revealed that the clarification pellet contained bands of approximately the right size, although the band seemed to have a molecular weight very similar to the wild-type TMV coat protein (Figure 13a). To increase the concentration of TMV-FL and further remove some of the host-cell proteins, and an additional round of PEG-precipitation and clarification were performed. Subsequent western blot analysis demonstrated that polyclonal anti-ZIKV envelope protein antibodies did not recognize the TMV-FL construct (Figure 13c), suggesting that the FL epitope was not being displayed on TMV. Despite multiple further attempts, expression of TMV-FL was not successful, as the coat proteins of the TMV-FL construct seemed to always revert to wild-type coat protein (data not shown). This could be because the fusion loop is hydrophobic [485,486], and thus, TMV doesn't tolerate having it on a solvent-exposed surface. FL also contains positively charged amino acids, which have been shown to alter the isoelectric point of the TMV coat protein to the point that stable viral particles are unable to form [199].

At 14 DPI, the leaves of plants infiltrated with TMV-GL showed classical symptoms of TMV infections (i.e., mosaic patterns on the leaves and curling of the upper leaves) (Figure 12b), as compared to uninfected *N. benthamiana* (Figure 12a). Following PEG-precipitation, SDS-PAGE analysis revealed that the majority of TMV-GL was found in the clarification supernatant and that it appeared to have a higher molecular weight than the wild-type TMV coat protein (Figure 13b). Subsequent western blot analysis showed that the TMV-GL construct did indeed contain an epitope recognized by polyclonal anti-ZIKV envelope protein antibodies (Figure 13c).

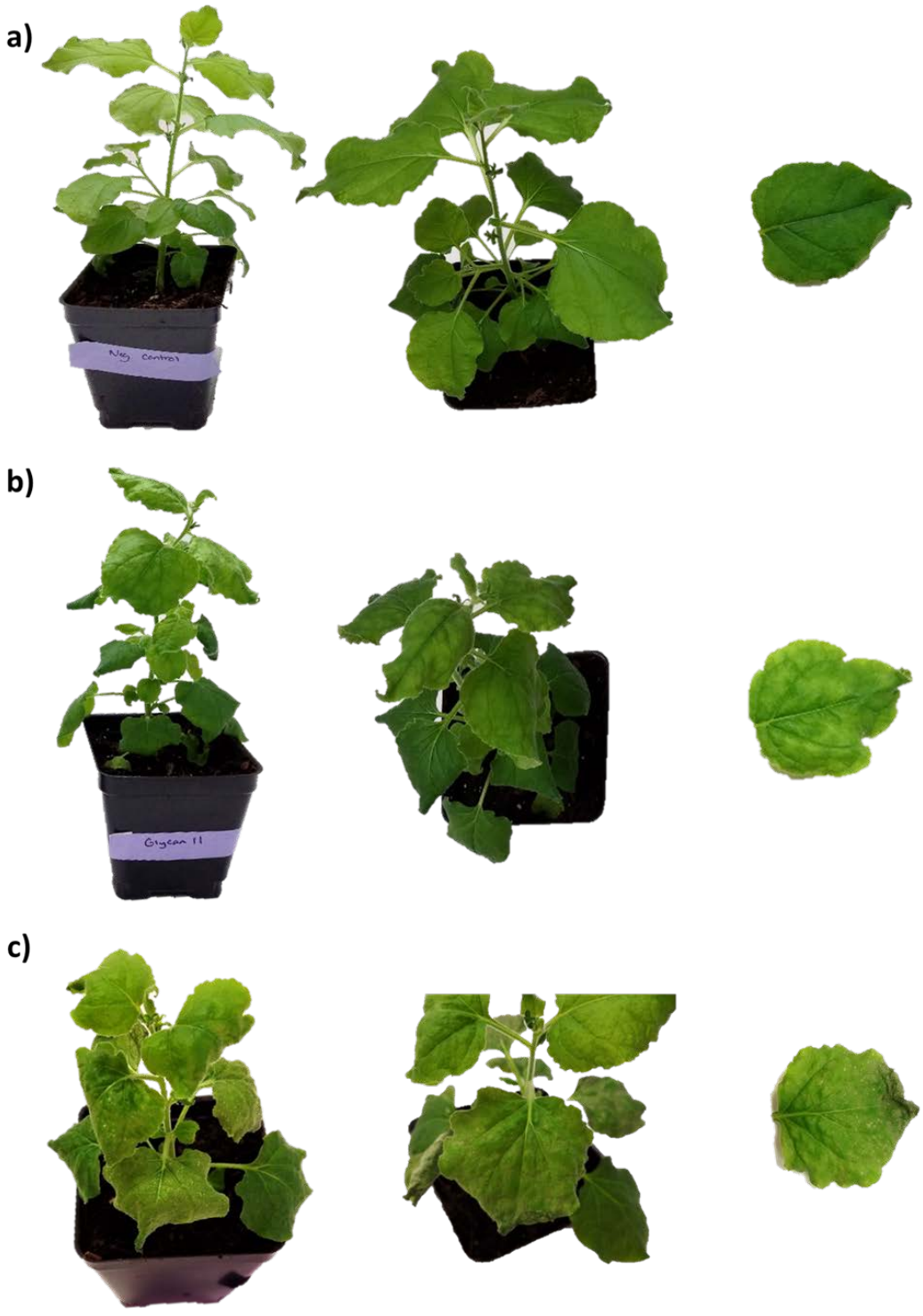

Figure 12. Viral nanoparticle production in *Nicotiana benthamiana.* **a)** Uninfected *N. benthamiana.* **b)** *N. benthamiana* infected by TMV-GL at 14 DPI. **c)** *N. benthamiana* infected by TMV-FL at 6 DPI.

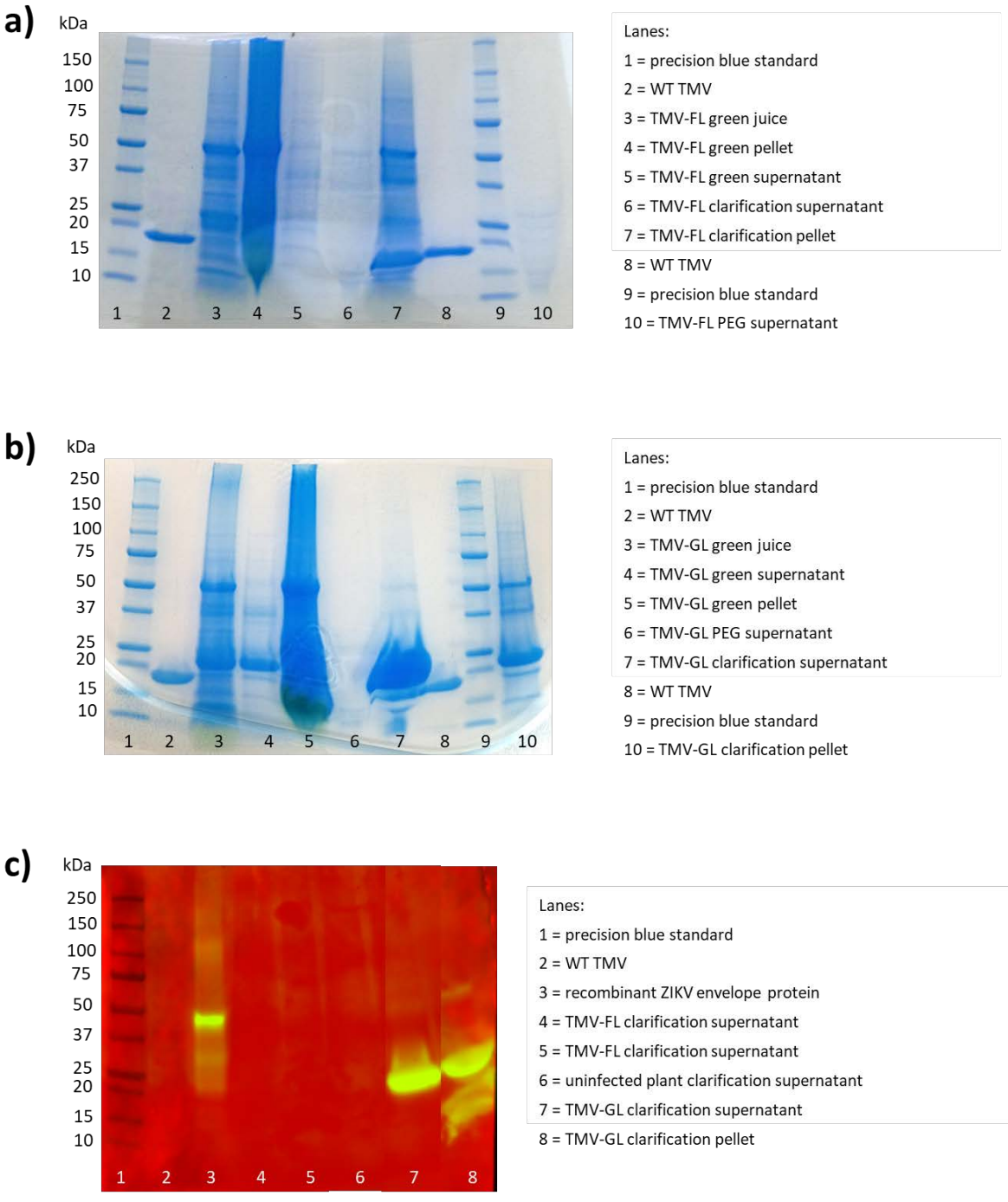

Figure 13. SDS-PAGE and western blot analysis of viral nanoparticle extraction from *N. benthamiana* plants. **a)** Coomassie blue-stained gel of TMV-FL extraction process samples. TMV-FL coat proteins have an expected molecular weight of 18.9 kDa. Wild type (WT) TMV coat proteins have an expected molecular weight of 17.6 kDa. **b)** Coomassie blue-stained gel of TMV-GL extraction process samples. TMV-GL coat proteins have an expected molecular weight of 19.8 kDa. **c)** Western blot analysis of TMV-FL and TMV-GL using polyclonal anti-ZIKV envelope protein antibody. The recombinant ZIKV envelope protein has an expected molecular weight of 55 kDa.

Purification of TMV-GL and WT TMV

Sucrose gradient ultracentrifugation was used to further purify the TMV-GL PEG-precipitation clarification supernatant, as well as the wild-type TMV that would serve as a negative control when immunizing mice (Figure 14). Figure 15 demonstrates the final products of this process: viral nanoparticles free from any visible protein contaminants. The TMV-GL sucrose-purified clarification supernatant showed two bands; the higher molecular weight band (approximately 23 kDa) corresponds with the expected molecular weight of the TMV coat protein plus the ZIKV glycan loop (20 kDa) and accounts for approximately 87% of the protein, and the smaller band at approximately 18 kDa corresponds with the estimated molecular weight of the TMV coat protein alone (17.6 kDa). The sucrose-purified wild-type (WT) TMV was in the sucrose clarification supernatant, as was the majority of TMV-GL VNPs (Figure 15) as expected, and this was used for the subsequent animal studies. Thus, both clarification supernatants were used in subsequent experiments in which human sera were screened for GL-binding antibodies and to determine if GL is capable of eliciting a neutralizing antibody response in mice. Based on a BCA assay of the clarification supernatants, the calculated yield of purified TMV-GL viral particles was approximately 0.42 mg/g of leaf tissue, and the yield of WT TMV was approximately 0.11 mg/g of leaf tissue.

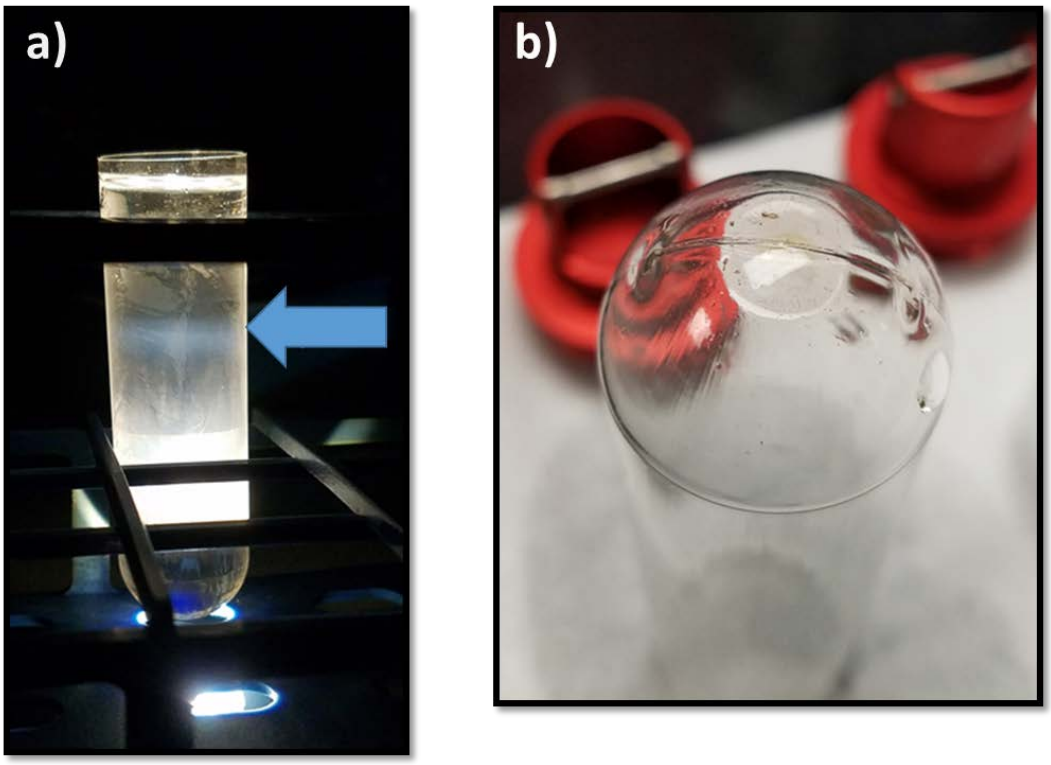

Figure 14. Purification of TMV nanoparticles by sucrose density gradient ultracentrifugation. **a)** Blue arrow indicates the light-scattering region of an ultracentrifuged sucrose density gradient that contains WT TMV. **b)** Viral pellet from the ultracentrifugation of WT TMV.

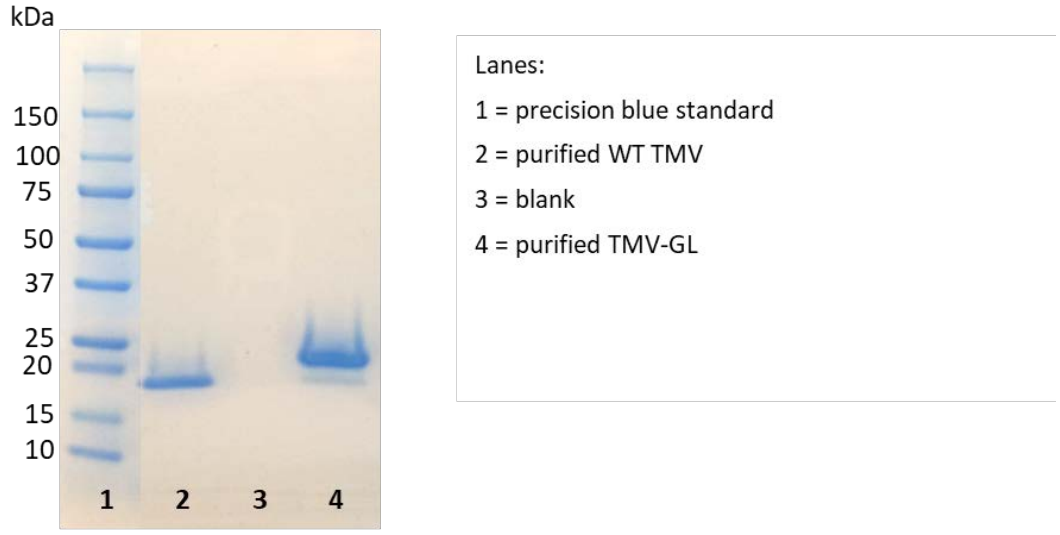

Figure 15. SDS-PAGE of sucrose density gradient purified TMV-GL and wild-type TMV. Coomassie blue-stained gel showing TMV-GL and WT TMV following sucrose density gradient purification, ultracentrifugation, and clarification.

Binding characteristics of commercial anti-E antibodies to the unglycosylated GL epitope

To investigate whether a commercially available polyclonal Ab raised against E of a Brazilian strain of ZIKV recognized unglycosylated GL displayed on TMV, we performed Western blot analysis. The E protein used as a positive control in this experiment was a 55-kDa full-length recombinant E from ZIKV strain BeH815744 expressed in *Escherichia coli*, and, therefore, was unglycosylated. Rabbit polyclonal antibodies raised against a glycosylated ZIKV E protein bound to TMV-GL and to E, but did not bind to the unmodified TMV (Figure 16a). This data demonstrates that antibodies raised against glycosylated E were able to recognize unglycosylated GL displayed on TMV.

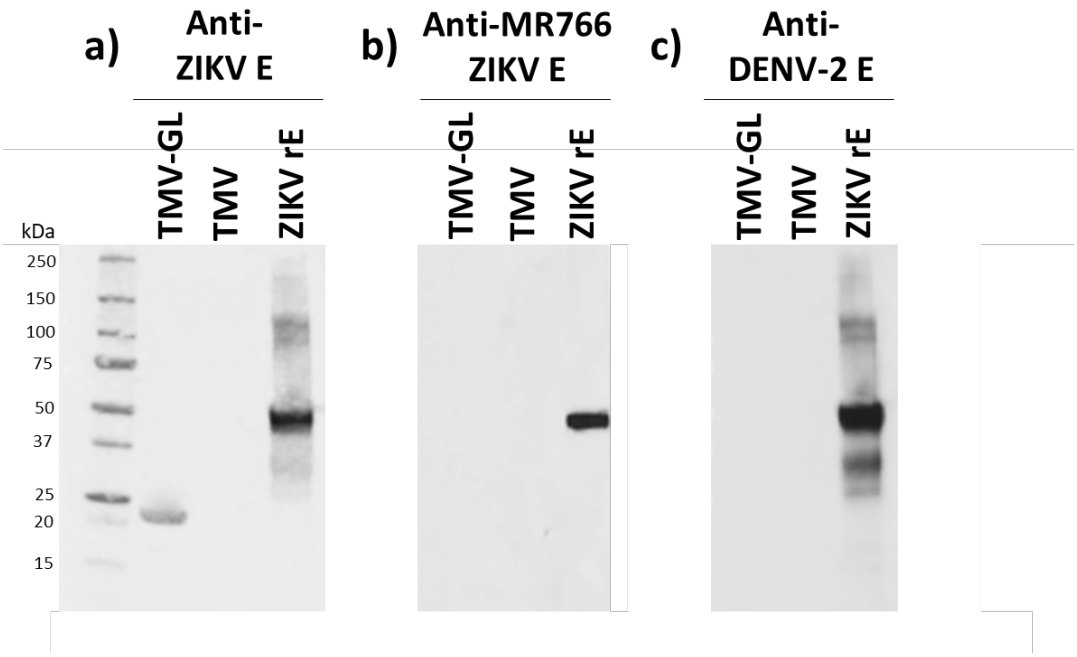

Figure 16. Characterization of plant-expressed TMV-GL by western blot analysis. TMV-GL, TMV, and ZIKV envelope protein recombinantly expressed in *E. coli* were separated on a 4-20% SDS-PAGE gel under reducing conditions and then blotted onto a nitrocellulose membrane. The membrane was then incubated with polyclonal anti-ZIKV envelope protein antibodies **(a)**, polyclonal anti-ZIKV (strain MR766) envelope protein antibodies **(b)**, or polyclonal anti-DENV-2 envelope protein antibody **(c)**.

The Uganda MR766 strain of ZIKV does not contain N154 and three of the surrounding amino acids (i.e. VNDT), and therefore, is not glycosylated (Figure 17). A rabbit polyclonal Ab raised against amino acids 140-180 of the MR766 E protein reacted with the full-length recombinant ZIKV E from strain

BeH815744 but did not react with TMV-GL (Figure 16b). This suggests that antibodies raised against the E protein of the Uganda MR766 strain, as well as antibodies raised against other strains of ZIKV that lack the VNDT amino acid motif in the GL region, would not recognize the GL region of E proteins from the majority of ZIKV strains from the Asian lineage, which includes the strains responsible for recent outbreaks.

While there is a relatively high degree of homology between the ZIKV E protein and the E proteins of other flaviviruses, there is poor homology in the GL region (Figure 17). Thus, we theorized that antibodies raised against other flavivirus E proteins would not bind to TMV-GL, but would be able to bind to the full-length E protein. We tested the ability of an anti-DENV-2 E polyclonal antibody raised in rabbits immunized with full-length DENV-2 E for its ability to bind to TMV-GL and the previously-mentioned recombinant ZIKV E. The anti-DENV-2 E antibody bound to the recombinant ZIKV E protein (Figure 16c), which shows that there is indeed significant homology between the DENV-2 and ZIKV envelope proteins. The anti-DENV-2 antibody did not bind to TMV-GL, suggesting that the glycan loop region is unique to Zika and does not cross-react with DENV antibodies.

```
                 145                    165
ZIKV|ASIAN|        GSQHSGMIVNDTGHETDENRA
ZIKV|MR766|        GSQHSGMI----GYETDEDRA
WNV                GPTTVESHGNYSTQVGATQAG
JEV                GTTTSENHGNYSAQVGASQAA
TBEV               TGDYV-A-ANETH----SGRK
YFV                VGAKQ-ENWN-T------DIK
DENV1              TGDQH-QVGNEST----EHGT
DENV2              SGEE-HAVGNDTG----KHGK
DENV3              TGDQH-QVGNET-----QGV
DENV4              NGDTH-AVGNDTS----SHGV
```

Figure 17. Sequence alignment of the glycan loop regions of various pathogenic flaviviruses, including the Asian (H/PF/2013) and African (MR766) strains of ZIKV. The numbers at the top indicate the position of the amino acids in the ZIKV envelope protein reference sequence (i.e., glycine (G) is at position 145 within the ZIKV (Asian strain) envelope protein amino acid sequence and alanine (A) is at position 165). The asparagine (N) residues in red indicate conserved glycosylation sites.

Collectively, these data demonstrate that commercially available antibodies raised against glycosylated recombinant E protein from a Brazilian strain of ZIKV are capable of binding to unglycosylated GL but that the VDNT amino acid motif is likely an important component of the immune response to this region. If antibodies to the GL region are an essential part of the immune response to ZIKV amino acids variations in GL region of ZIKV strains would elicit strain-specific antibodies that might be incapable of recognizing other strains of ZIKV. Furthermore, DENV-2, which is glycosylated at N153, but contains a GNDT amino acid motif, is not capable of binding to the ZIKV GL (Figure 15d). This data prompted us to investigate whether ZIKV infection leads to the production of antibodies capable of recognizing unglycosylated GL.

To confirm that host cell proteins (i.e. proteins from *N. benthamiana*) were not responsible for the binding of the anti-ZIKV envelope protein antibodies to TMV-GL (Figure 16a), the viral extraction process was performed on uninfected plant material. Samples from the final stage of the extraction process were analyzed by Western blot using the aforementioned anti-ZIKV envelope protein antibody (Brazilian). The ZIKV E antibody does not bind to *N. benthamiana* proteins in the extraction process samples, but it was reconfirmed that it does bind to both ZIKV rE and the TMV-GL construct (Figure 18).

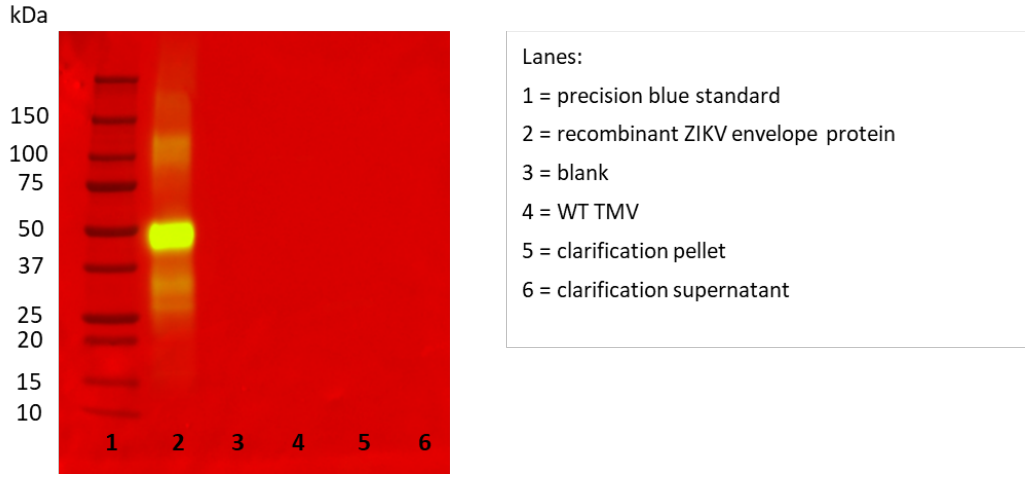

Figure 18. Western blot analysis of extracts from uninfected *N. benthamiana*. Extraction process samples from uninfected *N. benthamiana* plants were separated on a 4-20% SDS-PAGE gel under reducing conditions, blotted onto a nitrocellulose membrane, probed with a polyclonal anti-ZIKV envelope protein antibody (Brazilian strain), and visualized using a chemiluminescent substrate.

To our knowledge, Z3L1 is the only reported ZIKV-neutralizing human antibody with a footprint on monomeric E that includes contacts within GL (i.e., T156, H158, E159) [242]. The binding of Z3L1 to unglycosylated GL displayed on TMV, monomeric unglycosylated rE, and plant-glycosylated rE was analyzed via dot blot and ELISA. Z3L1 did not bind to unglycosylated GL, plant-glycosylated rE, or monomeric unglycosylated rE in the dot blots (Figure 18a). The ELISA showed similar results: Z3L1 did not bind to unglycosylated GL, plant-glycosylated rE, or monomeric unglycosylated rE to any significant degree above background levels (Figure 18b), even though Wang *et al*. showed that Z3L1 does bind to monomeric unglycosylated rE [242]. Thus, the three contacts within the GL region do not seem to be sufficient for Z3L1 to bind to unglycosylated GL on TMV.

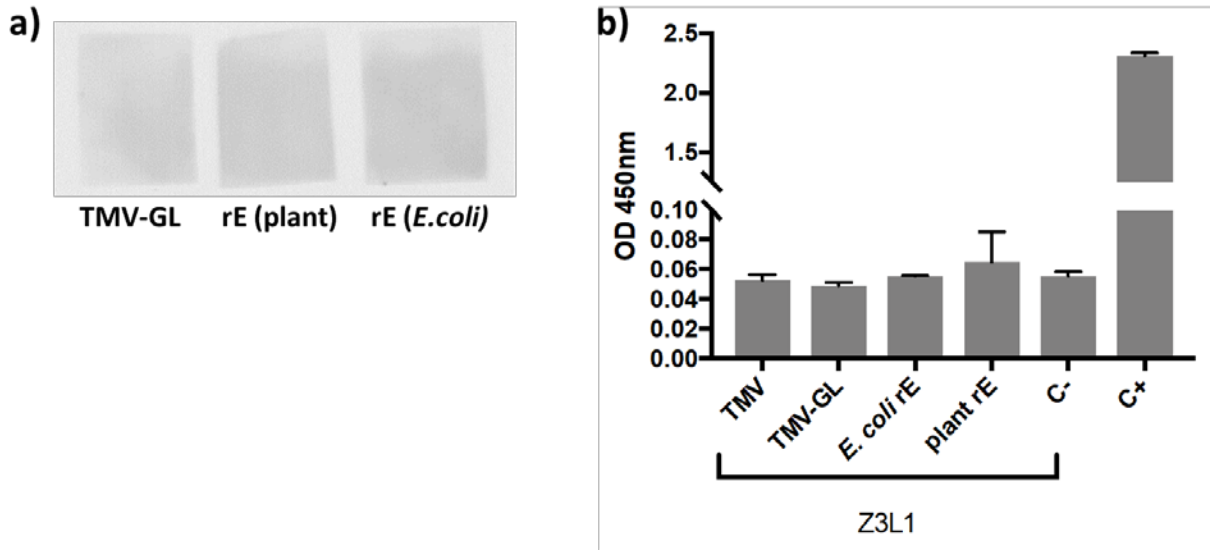

Figure 19. Binding characterization of Z3L1 by dot blot and ELISA. **a)** TMV-GL, ZIKV rE made in *N. benthamiana* plants, or *E. coli*-made ZIKV rE were dotted onto nitrocellulose, blocked, and then incubated with the human anti-ZIKV mAb Z3L1. A peroxidase-conjugated anti-human IgG secondary antibody and a chemiluminescent substrate were then used to detect any Z3L1 binding. **b)** TMV, TMV-GL, plant-made ZIKV rE and *E. coli*-made ZIKV rE were used to coat a 96-well plate. The Z3L1 mAb or an anti-ZIKV rE serum (C+) were added, followed by incubation with HRP-conjugated secondary antibodies and addition of OPD substrate. The data depicted are the mean absorbance at 450 nm $\pm$ SD of triplicate wells. The labels on the x-axis indicate the antigen that was plated. C- indicates that blocking buffer was used to coat the wells instead of an antigen, thus measuring the background noise from Z3L1 antibody binding directly to the blocked plate. C+ indicates the use of an anti-ZIKV rE antibody as a positive control with plated *E. coli*-made rE.

IgM and IgG antibodies in the sera of ZIKV patients react to TMV-GL

In a recent study, sera from fifty-one Zika-infected individuals from Colombia were analyzed for their ability to neutralize ZIKV *in vitro* [487]. We selected four serum samples from this group of individuals based on the ability of the serum to neutralize 90% of Zika strain H/PF/2013 viral particles at low concentrations (i.e., high reciprocal neutralizing titers (Table 9). All four patients exhibited clinical symptoms of ZIKV infection, ZIKV was serologically confirmed, and serum samples were collected 14-51 days after the onset of symptoms [487]. IgMs develop as an immediate response to viruses, but they typically disappear within 2-3 weeks of production, by which time IgGs have developed (although ZIKV infections have been known to cause prolonged IgM responses of up to 4 months [488]). Since the serum samples were collected at different time points after the onset of symptoms, we tested for both IgM and IgG antibodies that recognize unglycosylated GL. Using dot blots, we determined that sera from patients ARSZGB16031 and ARSZ16467 contained IgM and IgG antibodies that bind to unglycosylated GL at levels higher than antibodies recognizing TMV (Figure 20 a, c). The presence of antibodies recognizing TMV could be due to prior exposure to TMV [185] or non-specific binding. Moreover, while all four serum samples appear to have similar levels of anti-rE IgM and IgG antibodies (Figure 20b), GL-binding IgMs constitute a small but significant portion of the total anti-rE IgM response, and IgGs recognizing unglycosylated GL represent an even smaller fraction of total anti-E IgG antibodies. Since these data show that natural ZIKV infections elicit GL-specific antibodies in some patients, we investigated whether some of these antibodies bind to monomeric or dimeric E proteins and whether those antibodies are neutralizing.

TMV-GL is immunogenic in mice

While Wang *et al*. demonstrated that NAbs that recognize monomeric E and GL exist [242], we investigated whether we could find more of such antibodies. Immunocompetent female BALB/c mice were given intraperitoneal injections of 50 μg TMV, TMV-GL, rE, TMV-E in PBS with an adjuvant or PBS +

adjuvant only. Mice were boosted approximately every three weeks thereafter, with a final boost given 3 days prior to final bleeds and harvesting of spleens for cells fusions. The route of administration and the schedule of the immunization was comparable to previously published studies [489]. TMV-GL was used to determine if the unglycosylated GL was immunogenic. Glycosylated TMV-E and rE were included to investigate whether any of the antibodies generated in response to glycosylated rE and capable of binding to unglycosylated GL. Soluble rE that lacks the transmembrane region has been shown to be monomeric under physiological conditions and to crystallize as a dimer [242,250,368]. To further ensure the monomeric state of rE, a TMV-E construct was produced, where rE was displayed as a monomer on the surface TMV. Also, one group of mice received wild-type TMV in order to control for and exclude any immune response to the scaffold virus.

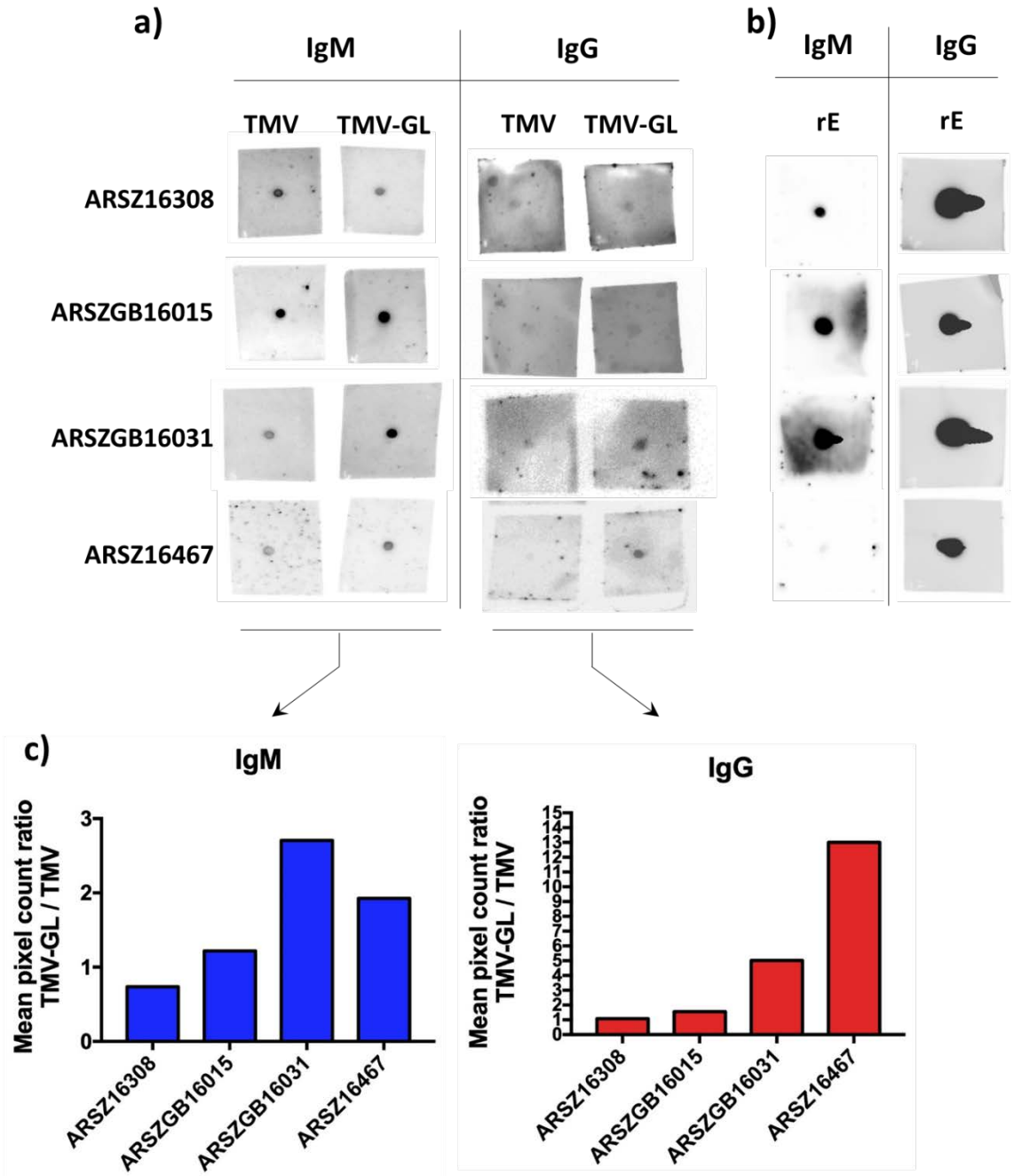

Figure 20. Dot blot analysis of sera from ZIKV-infected patients. **a)** Purified antigen (either TMV or TMV-GL) was spotted onto each square of nitrocellulose, dried, blocked, and then incubated with a 1:500 dilution of the indicated human serum in blocking buffer. After washing, antibody bound to the membrane was detected using horseradish-peroxidase-conjugated secondary antibodies and Clarity Western Substrate. **b)** Dot blot analysis of human sera to detect IgM and IgG responses to ZIKV E recombinantly expressed in plants. **c)** Digital quantification of the magnitude of dot blot assays using ImageJ software. The y-axis represents the mean pixel count ratio of the TMV-GL signal divided by the TMV signal.

While immunized mice possessed detectable levels of IgM antibodies (Figure 21b), we proceeded to study the IgG response, as these antibodies provide long-term immunity. We measured TMV-GL specific

IgG responses of individual mice by ELISA and determined the endpoint titers (Figure 22a). Endpoint titers were defined as the reciprocal serum dilution at which the absorbance at 450 nm (A450) was higher than the A450 signal of the pooled serum of the control mice (i.e., those injected with PBS + adjuvant). We observed that mice immunized with TMV-GL produced the highest levels of IgG against TMV-GL. Importantly, the serum of mice immunized with rE reacted with TMV-GL, which strongly suggests that the immune response to monomeric glycosylated E includes antibodies that recognize GL independently of the glycan. Similarly, serum from mice immunized with either TMV-E or TMV reacted with TMV-GL, likely because antibodies recognize either the TMV or GL portions of the construct. These data show that unglycosylated GL is immunogenic in mice and that some of the antibodies raised against monomeric glycosylated E recognize GL in a glycan-independent manner. Pooled sera from each group of mice were also analyzed by ELISA to determine the relative antigenicity and immunogenicity of each construct (Figure 22b). All four proteins were antigenic, and, as shown in red, TMV, TMV-GL, and the plant-made rE were also immunogenic. We next looked at the ability of the mouse sera to inhibit ZIKV infection in cellular assays.

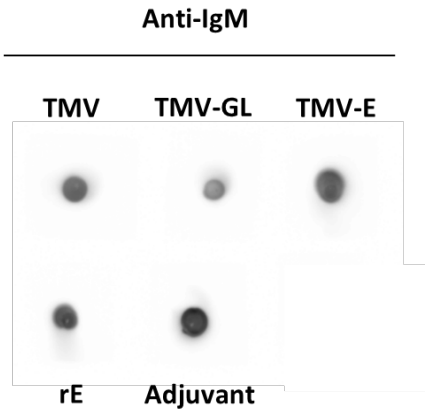

Figure 21. Detection of IgM antibodies in mouse sera. Pooled sera from each of the 5 groups of immunized mice (TMV, TMV-GL, TMV-E, rE, and adjuvant only) was dotted onto nitrocellulose followed by incubation with a goat anti-mouse IgM HRP-conjugated secondary antibody and detection using Clarity Western Substrate.

a)

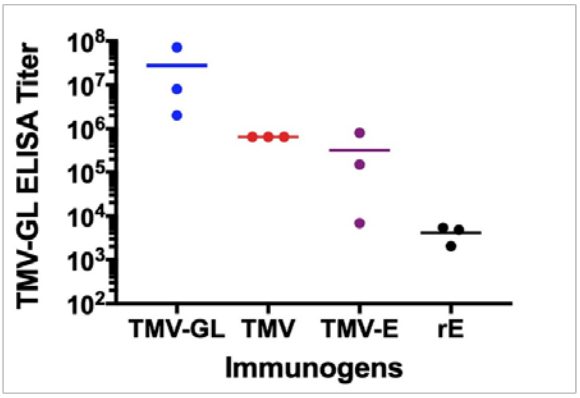

b)

Serum from mice immunized with:	Plated antigen: TMV	TMV-GL	rE (plant)*	rE (*E.coli*)
TMV	4×10^6	7×10^5	10^2	<100
TMV-GL	4×10^6	7×10^7	4×10^5	10^6
rE (plant)*	<100	7×10^4	4×10^9	7×10^5
TMV-E (plant)*	7×10^5	10^7	7×10^7	4×10^6

Figure 22. ELISA endpoint titers using sera from immunized mice. Balb/c mice were immunized with five doses TMV, TMV-GL, rE, or TMV-E. Assay cutoffs were calculated as described by Frey *et al*. [482] using pooled adjuvant-only sera. **a)** Sera from each mouse was serially diluted and endpoint titers against TMV-GL were determined by ELISA. Individual serum samples were assayed in 5 wells and the average A450 of these wells was then used to determine the endpoint titer. Each dot on the graph represents the endpoint titer of the serum from one mouse and the bars indicate the average endpoint titer for each group. **b)** Pooled sera from each group of mice were serially diluted and endpoint titers against TMV, TMV-GL, plant-made rE, and *E. coli*-made rE were determined by ELISA. The numbers shown are the average endpoint titer from three sets of ELISAs. The endpoint titers in red represent immunogenicity, as the plated antigen was the same as the antigen used to immunize the mice in that group. * indicates constructs that were presumably glycosylated.

Sera from immunized mice neutralize ZIKV *in vitro*

Flow cytometry-based neutralization assays were performed to determine if sera from immunized mice could protect U937+DC-SIGN cells against ZIKV infection (strain SD001[490]). As shown in Figure 23, sera from mice immunized with TMV + adjuvant or adjuvant alone provided no protection. In contrast, at a 1:50 dilution, TMV-GL sera had a mean neutralization of 23%, rE sera neutralized at 75%,

and TMV-E sera neutralized 94%. However, 50% neutralization is required for serum to be considered protective, and only the TMV-E and rE constructs met this requirement. These data show that unglycosylated GL in the absence of other E regions is not sufficient to generate a neutralizing antibody response against ZIKV, but that rE is sufficient. This is not surprising, as the ability of rE-based vaccine candidates to elicit ZIKV-neutralizing antibodies has been demonstrated by other groups.

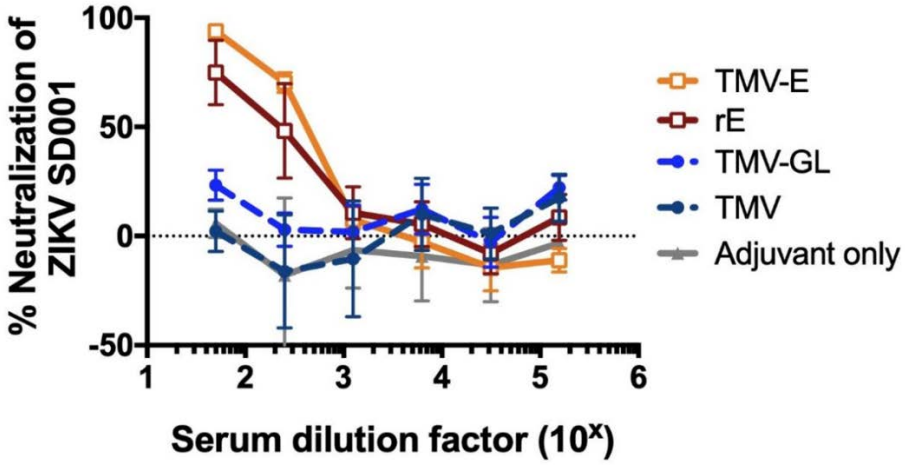

Figure 23. Analysis of mouse sera using a flow cytometry-based ZIKV neutralization assay. Individual serum samples from five groups of immunized mice were assessed for their ability to neutralize ZIKV (strain SD001) using a U937 DC-SIGN flow cytometry-based neutralization assay. The sera were serially diluted two-fold starting at a 50x dilution. Each point represents the mean percent neutralization of the three mice in the group, and the error bars depict the standard deviations.

ZIKV-neutralizing monoclonal antibodies bind to unglycosylated glycan loop

To determine whether any of the NAbs from TMV-E and rE immunized mice were directed towards GL, monoclonal antibodies (mAbs) were made from mice immunized with TMV-E and rE. Hybridomas were also produced from a TMV-GL immunized mouse. All hybridoma supernatants were screened for mAbs capable of binding to plant-produced glycosylated rE, and the 26 clones that bound to rE were cultured further (Table 8). As with the mouse sera, the ability of the mAb-containing hybridoma supernatants to neutralize ZIKV was examined using a flow-cytometry based neutralization assay. Four out of the six hybridoma supernatants from a TMV-E immunized mouse moderately neutralization of ZIKV (Figure 24a, c), and five out of the six hybridoma supernatants from an rE-

immunized mouse strongly neutralized the virus while one (#24) was moderately neutralizing (Figure 24b). None of the TMV-GL hybridoma supernatants were neutralizing (Figure 24c).

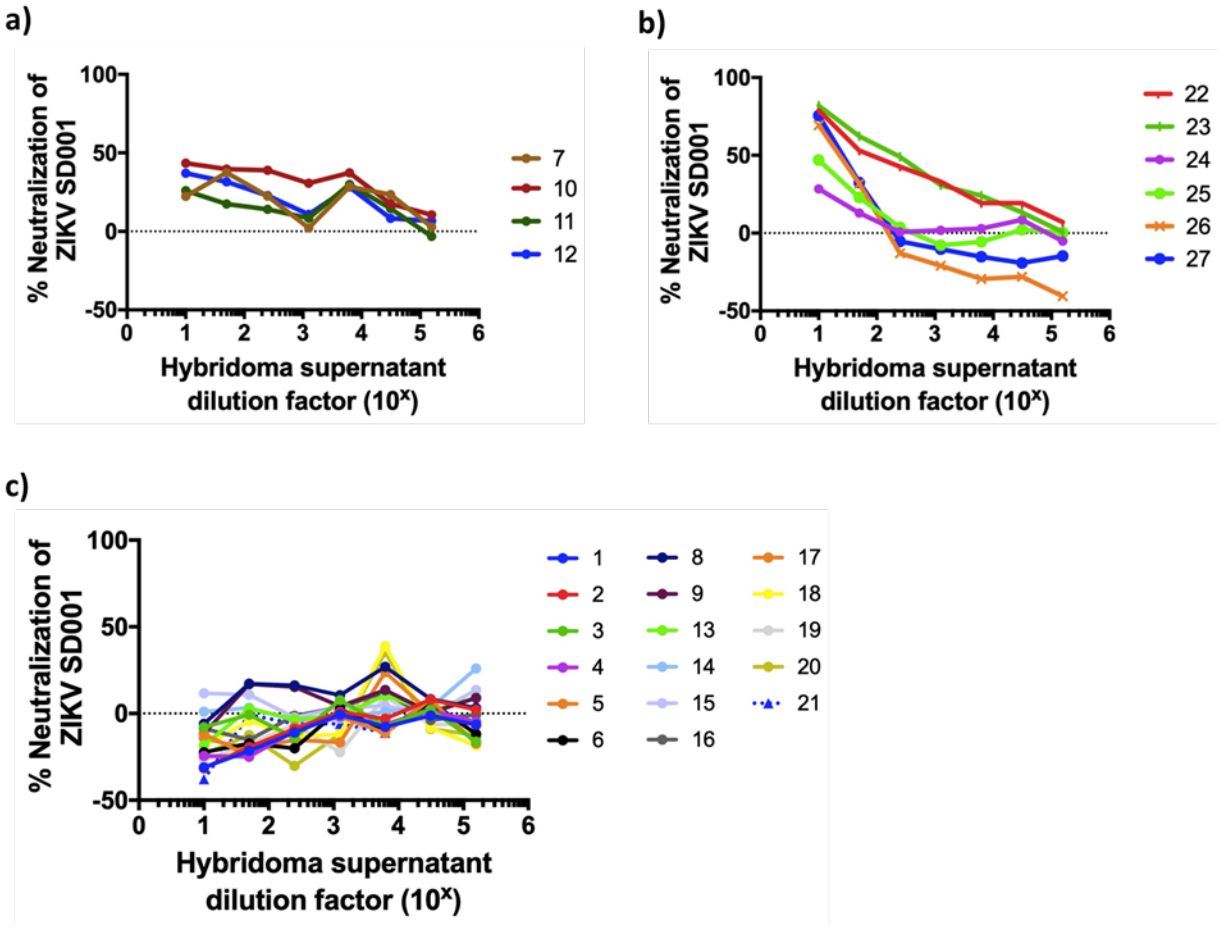

Figure 24. Neutralization of ZIKV by monoclonal-antibody containing hybridoma supernatants. Hybridomas were created from TMV-GL, TMV-E, and rE-immunized mice. Hybridoma supernatants were assessed for their ability to neutralize ZIKV (strain SD001) using a U937 DC-SIGN flow cytometry-based neutralization assay. The supernatants were serially diluted two-fold starting at a 10x dilution. **a)** Neutralizing hybridoma supernatants from a TMV-E -immunized mouse. **b)** Neutralizing hybridoma supernatants from an rE-immunized mouse. **c)** Non-neutralizing hybridoma supernatants from a TMV-GL immunized mouse (#1, 2, 4-6, 8, 9, 13, 14, and 16-20), a TMV-E immunized mouse (#3 and 15), and a control hybridoma supernatant raised from a mouse immunized with a non-specific antigen (#21).

The ten hybridoma supernatants that contain ZIKV-neutralizing mAbs were then analyzed via dot blot for their ability to bind to unglycosylated TMV-GL. All four of the neutralizing mAbs from TMV-E bound to the unglycosylated glycan loop (Figure 25a), while none of the neutralizing mAbs from rE bound to the unglycosylated glycan loop (Figure 25b). Additional immunoblotting revealed that the GL-binding antibodies(e.g., mAb #12) did not recognize the envelope proteins of other flaviviruses (DENV-2

and TBEV), and preferentially bound to unglycosylated rE (expressed in *E. coli*) over plant-glycosylated rE (Figure 26a). In contrast, mAb #26 cross-reacted with the DENV-2 recombinant envelope protein and preferentially bound to plant-glycosylated ZIKV rE compared to unglycosylated rE expressed in *E. coli* (Figure 26b).

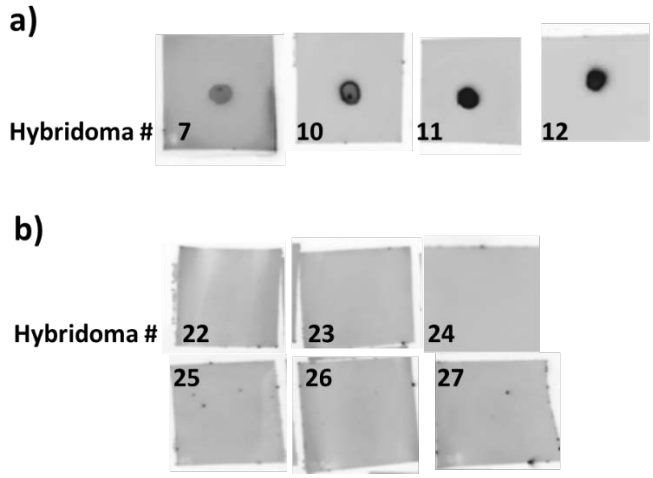

Figure 25. ZIKV-neutralizing mAbs bind to the glycan loop. TMV-GL was spotted onto squares of nitrocellulose, blocked, and then incubated with diluted hybridoma culture supernatants from either a TMV-E immunized mouse **(a)** or an rE immunized mouse **(b)**, followed by incubation with a goat anti-mouse IgG HRP-conjugated secondary antibody and detection using Clarity Western Substrate.

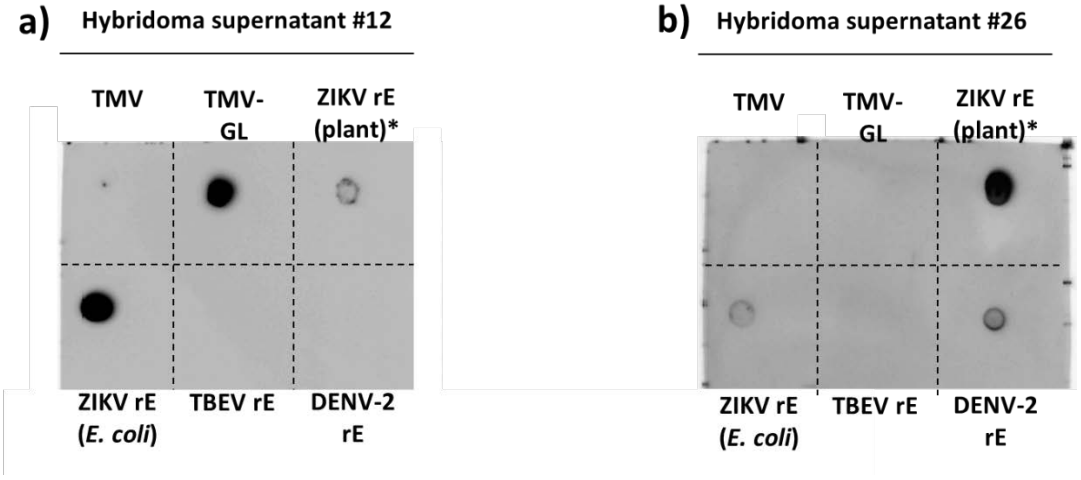

Figure 26. Further characterization of ZIKV-neutralizing mAbs. The indicated antigens were spotted onto squares of nitrocellulose, blocked, and then incubated with either hybridoma culture supernatant #12, from a TMV-E immunized mouse **(a)**, or #26, from a rE-immunized mouse **(b)**, followed by incubation with a goat anti-mouse IgG HRP-conjugated secondary antibody and detection using Clarity Western Substrate. *Indicates the only antigen that was presumably glycosylated.

DISCUSSION

Recent epidemics revealed that the supposedly-innocuous Zika virus can cause serious neurological and developmental complications and led the WHO to declare ZIKV a Public Health Emergency of International Concern in 2016. The scientific community responded vigorously, and hundreds of monoclonal antibodies, antivirals, diagnostics, and vaccines are currently being developed. Because ZIKV induces only mild symptoms in the majority of infected patients, the most pressing need is for a vaccine that could be given to pregnant women and women of childbearing age during outbreaks to mitigate the threat of CZS. However, to prevent endemic transmission of ZIKV, mass vaccination campaigns would be necessary.

Given that an estimated 2 billion people are currently at risk of developing ZIKV, the ideal vaccine candidate would be affordable. Additionally, antibodies elicited by a prior flavivirus infection or vaccine can cross-react with ZIKV, or vice versa, which would hypothetically lead to antibody-dependent enhancement (ADE) of disease. Several studies have attempted to assess the risk of ADE, particularly between ZIKV and DENV due to their antigenic similarity, but whether or not ADE might actually occur between ZIKV and DENV remains to be seen. The WHO recently summarized the ideal characteristics of a ZIKV vaccine as follows: "high-quality, safe and effective ZIKV vaccines that prevent serious ZIKV-associated clinical complications, and ensure availability and affordability for use in countries were ZIKV circulates" [269].

A variety of candidate ZIKV vaccines are currently in clinical trials including inactivated virus, attenuated virus, nucleic acid vaccines, and recombinant viral vectors. Despite the different vaccine platforms being utilized, all of these vaccines have one common characteristic: they all contain the envelope protein (E). Previous studies have highlighted some of the unique structural features of ZIKV E [289,290], including the fusion loop and glycan loop regions. Functional epitopes with high sequence conservation among ZIKV strains are the most likely to induce protective immunity. Thus, when

developing a vaccine or immunotherapies for ZIKV, it is important to utilize such epitopes. With this in mind, we created two TMV-based viral nanoparticle vaccines with ZIKV envelope protein epitopes: one displaying the fusion loop (FL), the other displaying the glycan loop (GL).

Fusion loop construct

The fusion loop mediates the fusion of ZIKV with the host cell's endosomal membrane, which allows the virus to enter the cell. Studies have confirmed that FL is an immunodominant epitope capable of eliciting neutralizing antibodies and is highly conserved across flaviviruses. Thus, we sought to create a TMV-FL vaccine candidate that could potentially be used as a universal flavivirus vaccine. However, the TMV-FL construct seemed to cause necrotic lesion to form on the leaves of the agroinfiltrated *N. benthamiana*, which resembled those seen during the hypersensitive response in TMV-resistant tobacco species [491]. In tobacco plants that contain the *N* gene, the hypersensitive response causes cell death at the site of infection, which prevents viral particles from infecting the rest of the plant [492]. While the process of agroinfiltration has been shown to lead to this type of hypersensitive response in some plant species [493], the fact that necrotic lesions did not appear in the TMV-GL plants that were agroinfiltrated concurrently suggests that it was the construct itself rather than agroinfiltration. Necrotic lesions limited the yield of TMV-FL, but another issue arose with this construct as well. Most, if not all, of the TMV-FL VNPs seemed to revert to wild type TMV, indicating that the TMV particles were not able to correctly assemble with ZIKV FL transcriptionally fused to the TMV coat protein, causing the FL sequence to be "kicked out" of the viral genome. This is likely due to the hydrophobic nature of FL and how they change the isoelectric point of the TMV coat protein [183]. Furthermore, due to their high thermal stability [290], ZIKV virions purportedly undergo less viral breathing than other flaviviruses, meaning that that FL might be less accessible on ZIKV and therefore a poor epitope. Nevertheless, FL-targeting antibodies have been shown to neutralize ZIKV and protect animals from ZIKV infection [333,368,371,374], but they also increase the risk of ADE [244,249,251,407,494].

Glycan loop construct

With the risk of ADE in mind, we chose a region of the ZIKV envelope protein that showed little homology to other flaviviruses: the glycan loop. While the exact biological function of the ZIKV GL remains to be determined, it is thought that the glycosylation on N154 plays a role in assembly, infectivity, vector competence, and neuroinvasion. Unlike the TMV-FL construct, our TMV-GL construct assembled properly and was expressed at high levels in *N. benthamiana*. Subsequent western blot analysis demonstrated that anti-ZIKV E antibodies recognize the unglycosylated GL on TMV, while DENV-2 antibodies do not. Furthermore, IgM antibodies in convalescent sera from patients ARSZGB16031 and ARSZ16467 bound to GL displayed on TMV. Blood samples were collected from these patients 30 and 37 days after the onset of ZIKV symptoms, respectively, which fits with the known pattern of the IgM response peaking earlier in infection. While the primary effector function of IgM is activating the complement system, IgMs have also been shown to neutralize ZIKV, especially during the early stages of an infection [328]. Sera from the same patients (i.e., ARSZGB16031 and ARSZ16467) also showed positive results on IgG dot blots against TMV-GL. However, immune responses are influenced by a variety of host and pathogen-specific factors [376], and antibodies are not always produced against the same epitopes, which may explain why patients ARSZ16308 and ARSZGB16015 showed no IgM or IgG response to GL.

The four human sera analyzed for their ability to bind to GL were selected primarily based on their high neutralizing titers that inhibit 90% of the virus NT_{90} titers. Despite these high NT_{90} titers, all four of these donors experienced clinical symptoms of ZIKV infection, ranging from flu-like symptoms to Guillain-Barré syndrome. This suggests that *in vitro* neutralization might not necessarily be a good predictor of *in vivo* neutralization and that by utilizing sera from patients exhibiting ZIKV symptoms, we might have unintentionally tested sera with poor *in vivo* neutralization. All 51 of the ZIKV-positive serum donors described in Lynch *et al*. were referred to the study based on their clinical manifestations of ZIKV

infection, so serum samples for asymptomatic ZIKV-infected donors were not available [487]. Thus, the presence of GL-binding antibodies in the sera of some patients could reflect exposure to ZIKV instead of functional protection.

TMV-GL as a vaccine candidate

The majority of vaccines effect protection by inducing antibodies that prevent viremia and/or prevent viruses from reaching their target organs, and the laboratory measurement that most frequently correlated with vaccine-induced protection is antibody titer. In the vaccine industry, neutralizing antibody titers, measured via plaque-reduction neutralization tests or other types of viral neutralization assays, are often used as surrogate markers of seroprotection. Vaccine-induced production of neutralizing antibodies has been shown to correlate well with protection for vaccines against YFV and WNV [495,496], but no such correlate of protection has been established for ZIKV. For licensed flavivirus vaccines, a neutralization titer of 1:10 (i.e., at a dilution of 1:10 or greater, the serum is capable of neutralizing at least 50% of the virus) has been established as a surrogate for protective immunity [497,498]. However, several studies have suggested that higher levels of neutralizing antibodies may be required to protect against ZIKV infection and have suggested neutralization titers of 1:50 or 1:100 may be a more appropriate surrogate marker for ZIKV protection [69,412,413,499]. A neutralizing titer (NT_{50}) of 100 has been shown to correlate with protection against viremia in mice and non-human primates challenged with ZIKV [413,465,500,501], but neutralizing titers may vary based on assay type, virus strain, cell type, etc. Even when the same assay type is used, neutralization titers may not be able to be directly compared to one another. For example, flow-based cytometry neutralization assay can have high inter-assay variability, especially with samples tested on different days [502]. Thus, while the TMV-E and rE constructs did elicit neutralizing antibodies based on what has been seen in other studies (i.e., an NT_{50} of 100), we won't know if our constructs, including TMV-GL, truly protect against viremia until we conduct animal challenge studies.

Although an immune correlate of protection has not been established for ZIKV, data from neutralization assay should still be considered when determining the efficacy of a vaccine. Neutralization assays revealed that TMV-GL was unable to elicit neutralizing antibodies in mice, leading us to suspect that either GL antibodies were poorly neutralizing in general, or that our TMV-GL construct was not ideal. Poorly neutralizing antibodies are thought to be elicited, at least in part, by epitopes infrequently displayed on the surface of mature virions [293]. However, cryo-electron microscopy structural studies suggest that GL is a prominent feature of the ZIKV surface [289,290]. As far as our TMV-GL construct not being ideal, there were three potential issues: 1) conformationally, GL was not displayed correctly on TMV, 2) the GL epitope we chose was missing adjacent amino acids critical for the induction of neutralizing antibodies, or 3) TMV proteins are not glycosylated, and the N154 glycosylation on GL was necessary. In an attempt to address all three of these issues, the glycosylated ZIKV E was recombinantly expressed in *N. benthamiana,* and used either or its own (i.e., rE) or docked to TMV (i.e., TMV-E) to immunize mice. Monoclonal antibody-secreting hybridomas were then made from the spleens of the immunized mice and then were screened for their ability to bind to rE and neutralize ZIKV *in vitro*. Out of the ten neutralizing mAbs, four bound to TMV-GL, demonstrating that neutralizing GL-binding mAbs are capable of recognizing the GL epitope we displayed on TMV and bind in the presence or absence of glycosylation at N154. Thus, we suspect that our TMV-GL construct failed to elicit neutralizing antibodies because the epitope we chose was incomplete. Epitope mapping studies using the GL-binding mAbs we discovered would help us determine which critical amino acids are missing in our TMV-GL constructs and hopefully lead to a redesigned GL-based construct capable of eliciting a neutralizing antibody response.

Antibody isotypes and T cell epitopes

To develop a safe and effective ZIKV vaccine, understanding the mechanisms of antibody-mediated protection against ZIKV is crucial. Following an infection or immunization, IgM is the first

antibody isotype produced. IgM-mediated phagocytic clearance and destruction of viruses occur in the early stages of the adaptive immune response while the IgG response is still developing, and several studies have indicated that the IgM response is critical for full protection against ZIKV [341], JEV [503], and other viral infections [504-506]. Clusters of specially-glycosylated IgG antibodies are also able to recruit complement, but the main protective role of IgGs lies in their long-term ability to neutralize viruses. Interestingly, in addition to enhancing phagocytosis, activating complement, and priming the adaptive immune response, IgMs have also been shown to neutralize viruses [506-508]. Furthermore, in one study, ZIKV-specific IgM antibodies cross-reacted weakly with DENV, while IgG antibodies strongly cross-reacted with DENV [361]. Since both IgM and IgG seem to play critical roles in antibody-mediated protection against ZIKV, vaccines may need to effectively induce both isotypes.

Consistent with results from Hansen *et al.*, we observed that peptides within the GL region were recognized by IgM antibodies sera collected within 30 days of the onset of ZIKV symptoms [362]. Sera ARSZGB16015 and ARSZGB16031 were collected in this period, and ARSZGB16031 showed positive results on the IgM dot blot (Figure 20a). An IgM response to GL was also noted for ARSZ16467, and while this serum was taken at 37 days, extended IgM responses have been observed with ZIKV infections [360,361]. Although IgMs are typically less neutralizing than IgGs, and the relative contribution of IgMs and IgGs to neutralization varies by individual [507], IgMs may play an essential role in neutralization early in the course of viral infections. Exploring the contribution of IgMs to protection from infection in a murine WNV model, Diamond *et al.* demonstrated that the delayed development of neutralizing anti-WNV IgMs is likely to be an independent risk factor for morbidity and mortality (i.e., severe WNV infection) [506]. This suggests that vaccine strategies capable of inducing an IgM response could be utilized for both pre- and post-exposure prophylaxis.

In testing the four samples from ZIKV-infected patients, we observed that there was a marked difference in IgM vs IgG binding to GL, as IgM binding led to a stronger signal. While this could be

related to the different secondary antibodies that were used or the inherent differences between IgMs and IgGs, it might also be a characteristic of the GL epitope. Repetitive surface proteins, such as GL displayed on TMV, efficiently crosslink B cell receptors and trigger them to proliferate and produce IgM. However, only a portion of early B cells undergo class-switching and become long-lived memory B cells that produce IgG [509]. Class switching is induced by various stimuli, including signaling by multiple cytokines (e.g., IL-10 and IFN-ɣ) [510], the presence of $CD4^+$ T cells [511], and the affinity of early primary IgM [512]. $CD4^+$ T cells promote affinity maturation and the development of memory B cells. These $CD4^+$ helper T cells are activated by APCs that present MHCII peptides from the proteolytic processing of viral structural proteins. However, only certain peptides induce this T cell response, and the factors that influence which epitopes are immunodominant are not wholly understood [513].

Cell-mediated immune responses play an integral role in controlling and preventing intracellular infections, and both $CD8^+$ and $CD4^+$ T cells have been shown to play important roles in protection against ZIKV [321-323,328,514-516]. Although we did not test the T cell responses of the mice we immunized, previous studies in humans or transgenic mice expressing human HLA proteins have shown that multiple T cell epitopes lie within, or close to, the GL region of the ZIKV envelope protein [513,516-519]. For example, Reynolds *et al*. mapped immunodominant $CD4^+$ T cell ZIKV epitopes in transgenic mice and showed that p14, a peptide that corresponds to amino acids 131-150 in the E protein, is a positive epitope in mice with HLA-DR4 and HLA-DR1. In fact, p14 bound strongly or moderately to almost all the HLA-class II molecules tested and no cross-reactive T cell epitope recognition was seen with the other flaviviruses tested (WNV, YFV, and DENV1-4). [517]. An additional study by Koblischke *et al.* analyzed the $CD4^+$ T cell response of 13 ZIKV patients and identified five peptides entirely or partially composed of GL residues as $CD4^+$ T cell epitopes. Although none of these peptides was considered "immunodominant" as only 10% of the patients recognized each peptide (rather than the 20% recognition that was deemed to be dominant) [513].

The importance of vaccine-induced T cell responses was recently demonstrated by the low efficacy of Dengvaxia, a tetravalent, live-attenuated DENV vaccine. It has been theorized that the low efficacy may be due to the inability of Dengvaxia to stimulate a DENV-specific T cell response, as it contains an NS protein from YFV rather than a DENV NS protein [520]. Along with our observations that more IgM antibodies in human sera bind to TMV-GL than IgG antibodies, these data suggest that if our GL construct contains a $CD4^+$ T cell epitope, this epitope may not be sufficient to effectively induce IgM to IgG class-switching. Furthermore, because the TMV-E construct was able to induce neutralizing, GL-binding mAbs and the TMV-GL constructs did not, perhaps only a portion of the GL immunodominant $CD4^+$ T cell epitope was contained in our TMV-GL construct. Thus, to further develop TMV-GL as a vaccine candidate, T cell responses should be evaluated for all three constructs, and if TMV-GL does not contain an immunodominant $CD4^+$ T cell epitope, then a new iteration of TMV-GL should be created.

Viral nanoparticle vaccines

TMV nanoparticles were chosen to display the ZIKV glycan loop epitope due to their ability to present multiple copies of a foreign epitope on its surface, its favorable safety profile, and the inexpensive production process. However, like other carrier molecules, antibody responses can also be induced to the TMV scaffold itself. It is unclear whether or not this would a negative impact on the immunogenicity of the foreign epitope being displayed, and the presence of carrier-specific antibodies in populations with prior exposure to TMV (e.g., from smoking or previous TMV-based vaccines) may preclude the use of a TMV-based ZIKV vaccine [185]. However, studies have shown that pre-existing immunity to TMV does not lead to loss of immune activation from subsequent injection with the same or different TMV VNPs, and, in the case of booster shots, that this occurs even when levels of anti-TMV antibodies are higher than the level of antibodies to the epitope [193].

Aside from producing an effective vaccine candidate, this project also aimed to create a vaccine candidate that was both affordable and avoided ADE-related safety issues. Based on the results of the

serum neutralization assay (Figure 23), the rE and TMV-E constructs are better at inducing ZIKV-neutralizing antibodies and could, therefore, be considered better candidate vaccines than TMV-GL. However, the sheer number of people at risk for contracting ZIKV necessitates the use of a platform that can produce affordable vaccines at a large scale, and both of these vaccine candidates require the production and purification of a recombinant protein, which increases the cost of manufacturing significantly. Furthermore, many envelope protein-based vaccines are already in clinical trials, which would make further development of the rE and TMV-E constructs redundant, and because the geographical distribution of ZIKV and DENV overlap, minimizing the risk of ADE is an important consideration. Thus, in addition to increased production costs, neither the rE or TMV-E constructs presented here address the issue of ADE. While TMV-GL was designed with the ADE risk in mind, further *in vitro* and *in vivo* tests would be required to determine if TMV-GL induces antibodies that could lead to ADE.

Monoclonal antibodies

The glycosylation site at N154 is a conserved feature of flaviviruses that may be important for infectivity and viral assembly [422,521,522], but the extended loop surrounding it is unique to neuroinvasive flaviviruses (i.e., WNV, JEV, and ZIKV). The extended ZIKV GL shares minimal sequence identity with the WNV and JEV, making it a promising antigen for eliciting ZIKV-specific antibody response. Furthermore, computational approaches have predicted multiple B cell epitopes in the GL region [400,523], and Xu *et al.* showed that the GL region of ZIKV has low sequence identity to other flaviviruses and high surface accessibility [523]. We sought to explore the antibody-mediated immune response to the ZIKV-specific glycan loop.

To focus exclusively on the GL region without the rest of the E protein, we utilized TMV viral nanoparticles to display unglycosylated GL from a Brazilian strain of ZIKV. We confirmed that antibodies raised against ZIKV rE were able to recognize the GL region on our TMV-GL construct. Although

antibodies raised against the GL region of the Uganda MR766 strain of ZIKV recognized rE, they did not recognize the GL portion of our construct. The Uganda MR766 strain lacks the GL "VNDT motif" and is therefore unglycosylated. However, rather than being a natural mutation, this deletion is thought to be the result of the virus adapting to mouse brain cells, as this strain was passaged over 150 times in brains of suckling mice [209,268,453]. Thus, our MR766 western blot data suggests that to elicit antibodies capable of binding to the GL region, the antigen must contain the VNDT motif. And, because the majority of ZIKV strains associated with the recent outbreaks contain the VNDT motif [426], antibodies to this region are particularly relevant. The inability of the anti-DENV-2 envelope protein antibody to bind to our unglycosylated GL construct confirms that the GL region is unique to ZIKV, even though the DENV-2 antibodies cross-reacted with the full ZIKV E protein.

Although we confirmed that antibodies raised against recombinant ZIKV envelope protein recognized our TMV-displayed GL, rE likely presents a slightly different antigenic landscape than the natural Zika virus. Thus, our next step was to determine if antibodies from individuals naturally infected with ZIKV bound to GL. Consistent with observations made by Hansen *et al.* [362], we observed that IgM antibodies in convalescent sera bound the best to the GL region. Serum samples from two patients, ARSZGB16031 and ARSZ16467, showed IgM binding to GL, and these samples were collected from these patients 30 and 37 days after the onset of ZIKV symptoms, respectively. Although the IgM response typically peaks about one week after infection and disappear within 2-3 weeks, IgM antibodies can persist for 12 weeks or more after ZIKV infection [360,361]. Serum samples ARSZGB16031 and ARSZ16467 also showed positive results on the IgG dot blots against GL, suggesting that at least some class switching from IgM to IgG did occur. Because serum sample ARSZ16308 was collected 51 days after the onset of symptoms, the negative results seen for IgM and IgG against GL could be due to the natural disappearance of IgM coupled with no class-switching to IgG. However, this is unlikely as there was still significant levels of rE-binding IgM in the sample and that class switching seems to have occurred in

ARSZGB16031 and ARSZ16467. The negative results from the ARSZGB16015 dots blots could be attributed to the time at which the sample was taken, but, again, the rE blots show that both an IgM and IgG response to ZIKV was present. Thus, the negative results are more likely due to the fact that immune responses vary by individual and antibodies are not always produced against the same epitopes. Taken together, these data suggest that natural ZIKV infection can elicit an antibody response to the GL region, but that the response varies by individual. It should also be noted that despite having high NT_{90} titers, all four serum donors experienced clinical symptoms of ZIKV infection, ranging from flu-like symptoms to Guillain-Barré syndrome. This suggests that *in vitro* neutralization might not necessarily be a good predictor of *in vivo* neutralization and that by utilizing sera from patients exhibiting ZIKV symptoms, we might have unintentionally tested sera with poor *in vivo* neutralization. All 51 of the ZIKV-positive serum donors described in Lynch *et al*. were referred to the study because they manifested clinical symptoms of ZIKV infection, so serum samples for asymptomatic ZIKV-infected donors were not available [487].

In this study, we immunized mice with rE and TMV-E and isolated NAbs that either recognize unglycosylated GL or require glycan for their efficient binding to monomeric E. Based on the existing nomenclature of EDE mAbs, our group proposes a new classification for Abs that bind to E monomer epitopes (EME). We consider NAbs 22-27 EME1 because they bind to envelope protein monomers better in the presence of glycosylation at N154 (Figure 26b). On the other hand, NAbs 7, 10, 11, and 12 are EME2 because they bind to E monomers regardless of the presence or absence of glycosylation at N154, although plant-glycosylation does seem to decrease their binding somewhat (Figure 26a) and rE with mammalian glycosylation was not available for testing. Given their binding characteristics, it seems likely that the group of NAbs that we are calling EME1 are clonal, and the same is true of the EME2 NAbs. Sequencing the variable regions of these NAbs would allow us to determine how many ZIKV-neutralizing mAbs we have discovered, which could be as little as 2 or as many as 10.

Numerous ZIKV-neutralizing mAbs that bind to envelope protein epitopes have been described [242-244,251,332,333,524], including several EDE NAbs isolated from DENV patients [250,370,375,407], as well as both EDE and EME NAbs from ZIKV-infected patients and mice. Of the many EME NAbs described thus far in the literature, only one has been shown to have contacts within the GL region: Z3L1 [242]. Because Z3L1 was commercially available, the ability of Z3L1 to recognize TMV-GL was tested, and the results suggested that the 3 contacts that Z3L1 makes within the GL region are not sufficient for Z3L1 to bind to unglycosylated GL on TMV (Figure 18). Furthermore, although Wang *et al.* suggest that Z3L1 binds to unglycosylated monomeric rE, we were unable to confirm this, as Z3L1 did not bind to unglycosylated monomeric rE in a dot blot or ELISA (Figure 18). These data suggest that our EME2 NAbs likely have more than three contact points in the GL region and that these NAbs are currently the only known GL-binding EME NAbs. Of course, validating these claims would require further work, including epitope mapping studies.

Monoclonal antibodies that bind to the E protein neutralize ZIKV by blocking attachment factors, obstructing binding to entry receptors, or hindering the membrane fusion process. Many cellular receptors, including AXL, Tryo3, DC-SIGN and TIM-1 [279], have been implicated in ZIKV binding and entry. Lectin-type receptors, including DC-SIGN, recognize viral glycoproteins, so any glycans present on the ZIKV E-protein could play a role in viral entry [366,372]. The fact that the N154 glycosylation site remains highly conserved among flaviviruses suggests it has a vital function, such as a binding site for viral entry. However, ZIKV particles lacking the E protein glycan were capable of infecting Raji cells expressing the lectin DC-SIGN, so the prM glycan on partially mature particles may also be able to facilitate entry [424]. Additional studies demonstrate that ZIKV utilizes different host cell receptors in different tissues [274], and each receptor could bind to a different part of the E and/or prM proteins.

Consequently, an antibody that blocks a single binding site may only neutralize ZIKV in specific tissues, and thus may only have limited therapeutic potential. EDE-binding mAbs tend to neutralize by

locking the envelope protein in its dimeric conformation, which prevents membrane fusion. By their nature, EME mAbs cannot lock envelope dimers, but they may still impede the fusion process by sterically hindering the change from the dimeric form to the trimeric form during membrane fusion. GL has been shown to at least partially cover the FL on ZIKV [289] and blocks neutralization by FL-binding mAbs [424], so EME1 could hinder fusion by blocking FL and preventing membrane fusion.

For DENV, strongly neutralizing antibodies frequently target quaternary E epitopes, rather than those displayed on E monomers [365,525,526]. Given that DENV and ZIKV are structurally similar, it has been hypothesized that the same is likely true for ZIKV. Recently, Collins *et al*. observed that the neutralization capacity of sera from ZIKV-infected donors can primarily be attributed to antibodies that target quaternary E epitopes [376]. However, they do concede that in 2 out of the 4 serum samples they tested, antibodies to "simple" epitopes also contributed to neutralization. Other studies have also shown that antibodies targeting recombinant monomeric E protein epitopes are neutralizing [242,243,251,332,527], and some of the most potently neutralizing ZIKV mAbs bind to E monomers (Table 3).

Nevertheless, to be protective *in vivo*, neutralizing antibodies must recognize epitopes on oligomeric ZIKV E proteins in their native state, and these epitopes are often conformational and quaternary [528]. By immunizing mice with monomeric ZIKV E protein, we may have inadvertently selected for moderately or poorly neutralizing antibodies. Determining how effective the EME1 and EME2 mAbs are at neutralizing ZIKV will require additional culturing of the hybridomas, purification and quantification of the mAbs, and another round of neutralization assays. The IC_{50} or $FRNT_{50}$ concentrations could then be compared to other mAbs, such as those found in Table 3, to determine their relative ability to neutralize ZIKV. Further *in vitro* assays and/or *in vivo* studies could also help determine the suitability of these mAbs for use as ZIKV therapeutics or diagnostics.

Passive immunotherapy

Therapeutic antibodies, in the form of pooled sera or recombinant mAbs, can be used to prevent or treat infectious diseases, and post-exposure passive immunotherapy has been shown to prevent congenital disabilities caused by cytomegalovirus [529] and the rubella virus [530]. Thus, as an alternative to vaccination, administering ZIKV-neutralizing mAbs to pregnant women may prevent congenital Zika syndrome (CSZ) [333]. Passive immunotherapy still carries the risk of ADE if the concentration of antibodies is sub-neutralizing or the antibodies cross-react with other flaviviruses. To avoid ADE, a therapeutic ZIKV mAb would have to be given at the proper dose and be ZIKV-specific. The latter of these requirements could be filled by our GL-binding mAbs (EME2). Alternatively, or perhaps additionally, ADE could be avoided by LALA mutations (i.e., mutating the Fc portion of the antibody to abolish its Fc activities) [531]. However, ablating the Fc-mediated effector functions of a ZIKV therapeutic mAb may make it less effective, as this would abrogate its cellular and complement-mediated immune functions [532], but the mAb would still retain its ability to neutralize ZIKV. The passive immunotherapy approach to ZIKV poses more problems than just the risk of ADE. For one, ZIKV has a short incubation period, so treatments utilizing immune sera or mAbs would only be effective if given within a narrow window of time. Second, because many ZIKV-endemic regions are in low-income countries, the availability and cost of immunotherapeutics could prove prohibitive. For example, even using local manufacturers to produce biosimilars, therapeutic mAbs are predicted to cost at least $500 per dose [533]. In conclusion, with further testing and optimization, our EME2 mAbs could potentially be used as a therapeutic. However, due to the high cost of mAb production, it is unlikely that such a therapeutic would be available to those who need it most.

Diagnostics

There is a moderate, but significant, degree of homology between flavivirus envelope proteins (37 to 59%), particularly between DENV and ZIKV (54-59%) [251,290]. DENV is endemic in many of the same

areas as ZIKV outbreaks, which makes serological differentiation difficult [362] and also introduces the possibility of antibody-dependent enhancement (ADE) of disease [242]. Our results indicate that GL may be an important part of the ZIKV-specific adaptive immune response and that DENV2 antibodies cannot bind to this region. The high sequence conservation of the envelope protein across ZIKV strains (94% or greater [251]) holds a promise that an antibody specific to the ZIKV envelope protein would likely work for the majority of ZIKV serotypes.

Furthermore, most of the recent ZIKV outbreaks, in which CZS and GBS were seen, have been attributed to the Asian lineage of ZIKV [437,438], in which there is only a 2% variation in the amino acid sequences of the E protein [366]. An analysis of the protein evolution of ZIKV by Ramaiah *et al*. demonstrated that the GL region contains 2 of the 3 negatively-selected amino acid sites in the E protein so any substitutions in this area may prevent ZIKV from replicating [439]. Together with evidence presented by Faye *et al.* that acquisition of the N154 glycosylation site is a recurrent event in the history of ZIKV [430] and the theory that the N154 was only lost because of serial passage in mice, these data suggest that the residues of the GL region are less likely to change than other areas of the E protein. Our results suggest that GL plays an important part in the B cell response to ZIKV and that DENV2 antibodies cannot bind to this region. Thus, the TMV-GL VNPs could potentially be used to create a ZIKV-specific diagnostic that detects GL-binding antibodies in human serum samples. Alternatively, the GL-binding EME2 mAb could be used to detect Zika virions in various types of human samples.

CONCLUSION

Vaccine-induced antibody-dependent enhancement of disease is a very real possibility when it comes to flavivirus vaccines, particularly in areas where ZIKV and DENV co-circulate. Developing a safe and effective ZIKV vaccine may, therefore, necessitate the use of ZIKV-specific antigens, and we determined that the glycan loop region of the ZIKV envelope protein is not recognized by antibodies

against other flaviviruses. Subsequently, we created TMV viral nanoparticles displaying the ZIKV glycan loop and discovered that sera from ZIKV-infected patients contain antibodies to the GL region. TMV-GL also proved to be highly immunogenic in mice, but neutralization assays demonstrated that this response was not neutralizing. To better elucidate the role the GL plays in the ZIKV immune response, we immunized mice with TMV-E, and rE and analyzed their immune response. Both constructs induced a neutralizing immune response, and the subsequent creation of mAb-expressing hybridomas led to the discovery of 10 NAbs that were categorized into two groups: EME1 and EME2.

Interestingly, the EME2 group of NAbs recognized the glycan loop region displayed on TMV-GL, suggesting that the glycan loop region does contain a neutralizing epitope, but that our TMV-GL construct may not include the entire epitope. Thus, with modifications, our TMV-GL constructs could prove to be a safe, effective, and economical ZIKV vaccine candidate. The discovery of GL-binding NAbs also has significant implications for the development of ZIKV therapeutics and diagnostics, as ZIKV-specific antibodies could prove useful in both of these fields. Although further studies are needed, our data suggest that EME2 Nabs do not bind to other flaviviruses, which may prove advantageous for both therapeutic and diagnostic applications. Thus, future work on this project can include modifying and retesting the TMV-GL vaccine candidate, or further characterization and development of the EME2 NAbs for use as a therapeutic or diagnostic.

CHAPTER TWO: ANTHRAX

INTRODUCTION

Bacillus anthracis, the causative agent of anthrax, is a toxin-producing, Gram-positive bacterium. Spores, the dormant form of the bacteria, naturally dwell in soil and can be found across the world [534]. Primarily a zoonotic disease, domestic and wild animals become infected when they ingest anthrax spores while grazing [535]. Humans can then be infected when they come into contact with infected animals or animal products. Once inside the body, anthrax spores germinate into their vegetative form and start producing toxins. These toxins act synergistically to cause tissue necrosis and edema, and can ultimately lead to cardiopulmonary shock and meningitis, which are lethal if left untreated [535]. Naturally occurring cases of anthrax in humans are extremely rare; in the U.S., only a few cases are reported every year [536]. Globally, an estimated 1,000-2,000 people die per year as a result of anthrax infections [537].

The U.S. government has classified *B. anthracis* as a Category A Priority Pathogen because anthrax spores can be easily acquired and dispersed, which can lead to mass casualties [538,539]. Inhaling as little at 0.01 micrograms of spores can lead to inhalational anthrax, the most severe type of anthrax infection [540]. Symptoms of inhalational anthrax, such a fever and muscle aches, manifest within 1-7 days of exposure, and over 92% of untreated patients die within 48 hours of the onset of symptoms [535]. Exposure to spores can also lead to cutaneous or gastrointestinal anthrax, but the untreated mortality rates, 20% and 25-60%, respectively, are much lower than the inhalational form [541]. Recently, injectional anthrax has been observed among heroin users in Europe, and studies have shown that *Bacillus* species are frequent contaminants of heroin in the United States [541].

Anthrax infections are primarily treated with oral antibiotics, and in the case of cutaneous or injectional anthrax may include surgical debridement and/or adjunctive glucocorticoid therapy [542]. Due to the high mortality rates associated with inhalational anthrax, the existing standard of care for suspected and confirmed cases includes intravenous administration of antibiotics and an antitoxin [539].

Antibiotics, such as ciprofloxacin or levofloxacin, block bacterial growth, while an antitoxin, such as raxibacumab, counteracts the effects of the toxins. However, there are situations in which the standard of care cannot be followed. For example, patients could be allergic to ciprofloxacin or have other contraindications to first-line treatments. Additionally, the Department of Homeland Security announced that antibiotic-resistant strains of anthrax pose a genuine threat to society [543,544]. Multiple studies have been published on antibiotic- and antitoxin-resistant strains of anthrax and terrorist could easily create multi-drug resistant weaponized strain, as this "involves relatively straightforward methodology that does not require a high level of microbiologic knowledge" [544-547]. Delaying treatment, even for a few hours, to test for drug resistance could significantly reduce survival, and in the event of a large-scale attack, this delay could lead to thousands of deaths [548].

BACKGROUND

Anthrax virulence factors and their biological effects

The virulence genes of *B. anthracis* are located on two plasmids, pXO1 and pXO2. The pXO1 plasmid encodes for toxins, while pXO2 encodes for the biosynthetic machinery that produces the bacterium's poly-ɣ-D-glutamyl (PGA) capsule, which allows the bacilli to avoid phagocytosis and the complement system [549]. Anthrax bacterium produce and secrete a tripartite AB toxin composed of a receptor-binding subunit, protective antigen (PA), and two enzymatic subunits, lethal factor (LF) and edema factor (EF) [550]. As outlined in, these subunits work together to gain entry into host cells where they exert their toxic effects (Figure 27). PA is an 83-kDa protein that binds to host-cell receptors and is processed by furin-like proteases into its 63-kDa form (PA_{63}). This process exposes the EF and LF binding sites as well as a heptamerization site. Subsequently, multiple PA_{63} proteins form a heptamer, which binds to EF or LF and is internalized into an endosome by clathrin-mediated endocytosis [551].

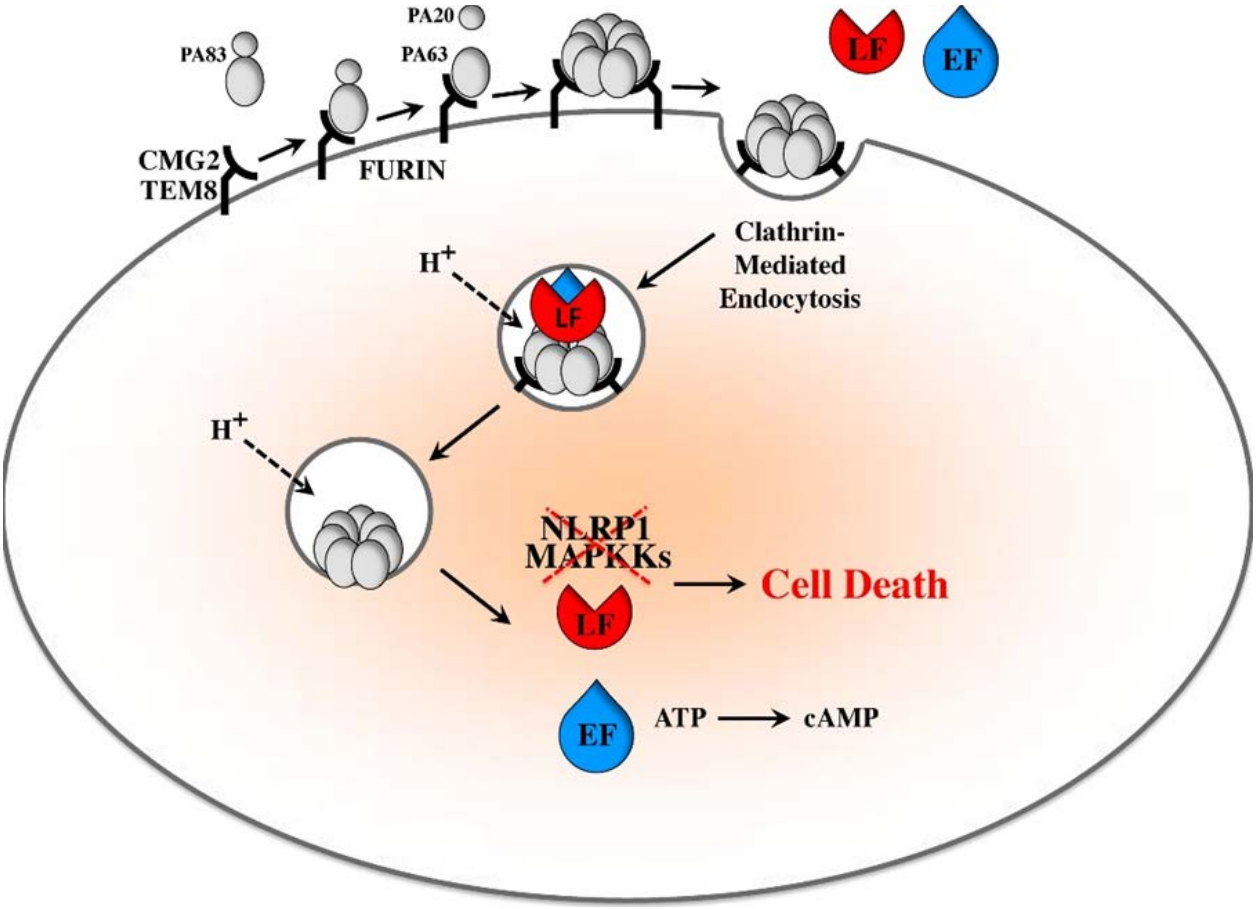

Figure 27. Cellular entry of anthrax toxins; PA_{83} or PA_{63} binds to cell surface receptors CMG2 and TEM8. PA_{83} undergoes cleavage by cellular furin releasing the 20 kDa fragment (PA_{20}). PA_{63} monomers bound to cellular receptors form an oligomer that is capable of binding to three LF or EF molecules. Endocytosis of the PA_{63} oligomer bound to LF or EF and acidification of the endosome result in translocation of LF or EF to the cytosol. LF cleaves and inactivates MAPKKs and Nlrp1, which causes cell death, while EF increases intracellular cAMP levels, leading to edema. Adapted from McComb *et al.* [552]. Reproduced with permission.

The combination of LF and PA is called lethal toxin (LT), while the combination of EF and PA is called edema toxin (ET). After endocytosis, the PA heptamer forms a pore in the endosomal membrane allowing EF and LF to escape into the cytoplasm [553]. LF, a zinc metalloproteinase, cleaves and inactivates members of the MAP kinase kinase family (MAPKK), which causes apoptosis [554]. LF has also been shown to cleave NOD-like receptor protein 1 (Nlrp1) on macrophages, which increases their sensitivity to LF-mediated apoptosis [555]. In animal models, administering LT alone was toxic and led to hypoxic liver failure [556-558]. EF, a calmodulin-dependent adenylate cyclase, converts ATP molecules to cAMP, and the increased intracellular cAMP levels impair homeostasis and cause edema [559,560].

In addition to the two major virulence factors (i.e., toxins and PGA), *B. anthracis* produces a variety of proteases that degrade host tissues. Metalloproteases secreted by *B. anthracis* have been shown to digest casein and gelatin *in vitro* and cause hemorrhage *in vivo* [561]. In addition, these proteases degrade components of the extracellular matrix, such as fibronectin, laminin, and collagen, which leads to tissue damage [562]. It has also been suggested that the proteases may use host plasmin for fibrinolysis and invasion. *B. anthracis* also expresses anthrolysin O, a cholesterol-binding pore-forming toxin, and anthrolysin B, a sphingomyelienase, which have been shown to have hemolytic effects [563,564]. Thus, vegetative bacilli coated in PGA escape the innate immune response and propagate, the virulence factors they secrete accumulate in the blood leading to vascular permeability and decreased function of target organs (e.g., heart, spleen, kidney, and brain). Although both septicemia and toxemia contribute to the pathological features of anthrax, the exotoxins produced by the bacilli are ultimately responsible for anthrax-related mortality in humans [565,566]. Fatal outcomes of anthrax toxemia include hypotension, tachycardia, hemoconcentration, coagulopathy, anoxia, cardiac failure, and meningitis [567].

Immune response to *B. anthracis*

Because cases of anthrax infection are rare, limited data on the human immune response to *B. anthracis* are available [568]. The majority of the available data comes from animal models, *in vitro* assays, studies of vaccinees, or experiments using other members of the *Bacillaceae* family, none of which accurately or fully recapitulate anthrax in humans. In addition, the immune response may vary based on the mode of infection (i.e., cutaneous, gastrointestinal, inhalation, or injectional). The following paragraphs summarize what is known about the innate and adaptive immune response to *B. anthracis* infections.

Infections are initiated when spores enter the host via the epidermis, the gastrointestinal tract, or the respiratory system. While the complete mechanism for the binding and uptake of *B. anthracis*

spores by phagocytes is not entirely understood, several groups have demonstrated that spores can activate the classical complement pathway and then undergo CR3-mediated phagocytosis by macrophages, dendritic cells, and epithelial cells [569-571]. The fate of phagocytosed spores is also unclear. Some studies suggest that once inside these phagocytes, the spores germinate and are subsequently killed in the phagolysosomes [572-574]. Other studies suggest that *B. anthracis* can hijack the phagocytes and use them to disseminate locally or throughout the entire body [575-577]. In the case of inhalational anthrax, *B. anthracis* bacilli can escape from the lysosomes of alveolar macrophages and replicate intracellularly, followed by cell lysis and the release of vegetative bacilli into the extracellular environment where they spread throughout the lymphatic system [576]. These two opposing observations might both be accurate though, as a study by Ross *et al.* demonstrated that in a guinea pig model of inhalation anthrax, some phagocytosed spores are digested and killed, while others germinate and are released into the lymphatic system [578]. Dendritic cells can also internalize spores through coiling phagocytosis, but their internal environment is thought to be even more conducive to vegetative growth and subsequent spread through the lymphatic system than that of macrophages [579-581].

Spores and vegetative *B. anthracis* also activate MyD88-dependent receptors, which triggers the production of inflammatory cytokines [582,583]. One of these cytokines, IL-12, activates natural killer cells (NK cells) to produce IFN-ɣ and cytotoxic granule proteins, which have antibacterial activity. Murine and human NK cells have been shown to mediate the killing of intracellular and extracellular *B. anthracis* [584]. As part of the early innate immune response, neutrophils are also recruited to the site of infection where they can engulf and kill bacterial pathogens. Unlike dendritic cells, and possibly macrophages, neutrophils are capable of efficiently killing *B. anthracis* [585,586]. A study by Mayer-Scholl *et al.* demonstrated that human neutrophils engulf anthrax spores, induce them to germinate, and then kill the vegetative bacteria using α-defensins [587]. However, it was noted that this response likely only pertains to cutaneous anthrax infections, as neutrophil infiltration is rarely seen in the lungs following an

anthrax infection [587,588]. This may also at least partially explain why inhalational anthrax infections do not resolve on their own like cutaneous anthrax infections.

B. anthracis possesses a unique cell wall structure that includes a thick layer of DAP-type peptidoglycan, a proteinaceous S-layer, and a poly-γ-D-glutamic acid capsule [589]. In the case of extracellular vegetative cells, the PGA capsule is thought to protect the bacterium from phagocytosis so that the bacilli can survive in the host as an extracellular pathogen [535]. Even though the peptidoglycan layer of the cell wall is shielded from the immune system by the PGA capsule of B*. anthracis*, studies have shown that peptidoglycan is shed by *Bacillus* species during the logarithmic growth phase and is thus bioavailable to the host [590,591]. Although the extracellular receptor that recognizes peptidoglycan from *B. anthracis* is unknown, Iyer *et al*. demonstrated that the peptidoglycan is internalized and degraded, and can thereby trigger the production of proinflammatory cytokines and chemokines [590]. Additionally, intracellular NOD2 receptors have been shown to recognize degraded *B. anthracis* peptidoglycans and induce caspase-1-mediated secretion of IL-1β and activate NF-κB signaling, which drives the innate inflammatory response [592,593]. Disseminated infections and the subsequent systemic proinflammatory response can lead to sepsis and death [590,594,595].

Bacterial infections are also kept in check by the adaptive immune system. The cellular immune response to bacterial agents includes $CD8^+$ T cells recognizing and destroying host cells infected with intracellular bacteria, T_h1 cells secreting IFN-γ and other cytokines that contribute to antimicrobial defenses, and T_h2 cells regulating the humoral immune response. As for the humoral response, antibodies can neutralize extracellular bacteria, and antibody effector functions can lead to opsonization of bacteria or antibody-dependent cell-mediated cytotoxicity. Because *B. anthracis* bacilli are encapsulated by polysaccharides, they do not tend to elicit a robust adaptive immune response. The capsular polysaccharides of *B. anthracis*, PGA, can elicit a T cell-independent humoral response, but without T cell involvement these types of antigens do not induce immunological memory, and avidity

maturation and isotype switching do not occur [596,597]. PGA is resistant to proteolysis in antigen-presenting cells, making it a weak antigen [598]. Thus, most of the protective adaptive immune response to *B. anthracis* appears to be directed against peptide antigens found on EF, LF, and PA. Laws *et al*. demonstrated that natural anthrax infections lead to the production of PA-, LF-, and EF-specific IFN-ɣ production by T cells, as well as an antibody response to PA and LF [599]. LF and EF antibodies do not provide robust protection against infection, but antibodies to LF may contribute to toxin neutralization [600]. In contrast, multiple studies using a variety of animal models have shown that anti-PA antibodies are sufficient to protect against infection [601-605]. Additionally, Quinn *et al.* established that inhalational anthrax in humans leads to the production of anti-PA IgGs and PA-specific IgG memory B cells and that there is a strong positive correlation between serum levels of anti-PA IgG and *in vitro* serum antitoxin activity [568].

Interestingly, the toxins secreted by vegetative bacilli interact with components of both the innate and adaptive immune system. At the site of infection, low levels of germination allow for the production of toxins that subvert the innate immune response, primarily by effecting phagocytes. This includes inhibiting macrophage activation, promoting apoptosis of macrophages and DCs, suppressing NK cell expression of IFN-γ, delaying apoptosis, inducing migration of monocytes, altering cytokine production in human monocytes, and inhibiting the phagocytic activity of human neutrophils [584,606-609]. The subsequent impairment of proinflammatory activities and reduced recruitment of phagocytes from the bloodstream lead to delayed bacterial clearance [607]. Toxins produced by vegetative bacteria that make it to the regional lymph nodes can also suppress the adaptive immune response. This includes impairing DC maturation and function, blocking T cell activation and proliferation, and inhibiting B cell proliferation and antibody production [610-612]. These effects are exerted at different stages of infection, creating an environment that allows *B. anthracis* to effectively establish an infection and propagate within the host. For example, during the initial stages of infection, LT induces apoptosis of

macrophages, but EF delays their cell death and promotes their migration to lymph nodes so that the bacteria can disseminate through the bloodstream to various organs and tissues [567]. During the second phase of anthrax, i.e., the fulminant stage, LT and ET disrupt vascular tissues to allow bacteria to disseminate throughout organs.

The immunosuppressive effects of LT and ET are not absolute. For instance, in an aerosolized spore infection model, Pickering *et al*. showed that mice are capable of producing proinflammatory cytokines following an anthrax infection [613]. In other studies, it has been demonstrated that anthrax survivors mount potent adaptive immune responses [568,599,614]. However, in cases where large amounts of spores enter the body, such as in inhalational anthrax, patients were given antibiotics, which likely helped keep the vegetative bacteria in check in the absence of an inefficient innate immune response. Without antibiotics and an efficient innate immune response, anthrax bacilli multiply unchecked and disseminate into the blood where they produce increased levels of toxins before an adaptive immune response can be mounted. Thus, without treatment, inhalational anthrax victims typically die within a week or two from toxemia, and even with treatment death can occur within a few days if a large number of spores are inhaled [615-617].

Anthrax vaccines

In 1881, Pasteur created an anthrax vaccine for cattle by using a heat-attenuated strain of *B. anthracis,* even today live-spore vaccines based on the attenuated strains of *B. anthracis* are still used in China, Russia, and in veterinary medicine [565]. Currently, there is only one anthrax vaccine licensed in the United States, anthrax vaccine adsorbed (AVA), also known as BioThrax ®. Developed in the 1950s and licensed in the 1970s, AVA is a subunit vaccine composed of a partially-purified anthrax PA toxin from an avirulent, non-encapsidated strain of *B. anthracis* [618]. Various characteristics make AVA a suboptimal vaccine. These include undefined components, high production expenses, lot-to-lot variability, a complicated initial immunization schedule, temporary protection so an annual booster is required, and

the fact that it contains cellular elements, which can lead to local and systemic reactions [534,605,619,620]. AVA is prepared by adsorbing filtered culture supernatants from an attenuated strain of *B. anthracis* to an alhydrogel adjuvant [621]. Although PA is the principal antigen component of AVA, it also contains EF, LF, and other cellular impurities, which can contribute to side effects. Furthermore, AVA is administered as a series of 6 doses: subcutaneous injections are given at 0, 2, and 4 weeks, followed by boosters at 12 months and 18, and annual boosters are required to maintain protection [621]. In 1997, U.S. Secretary of Defense William Cohen mandated that all active military personnel be vaccinated against anthrax [622]. In accordance with this order, BioThrax ® has been administered to millions of military personnel. However, numerous articles have questioned the safety, practicality, and long-term efficacy of the AVA vaccine [621-623], and it has not been approved as a pre-exposure prophylactic for the general public [624].

Following the terrorist attacks of September 11, 2001, anonymous letters containing anthrax spores were sent to congressional offices and media companies. This led to 21 confirmed or suspected cases of anthrax, including 5 deaths from inhalational anthrax, and more than 10,000 people were given oral antibiotics for post-exposure prophylaxis [625]. Laboratory tests, treatments, decontamination, and the ensuing investigations by the FBI and CDC, as well as state and local authorities, is estimated to have cost billions of dollars [625]. Since this attack there has been increasing concern about anthrax spores being used was as a weapon of bioterrorism against the general population [619], and it is suspected that biological weapons programs in Iraq and Russia have developed technology capable of releasing large amounts of aerosolized spores on urban populations [626,627]. Responding to such widespread exposure would be problematic: local hospitals do not have the resources or infrastructure to provide intravenous antibiotics and antitoxins to thousands of people simultaneously [628], so only those with confirmed cases of anthrax get these treatments, and many suspected exposure cases would only receive oral antibiotics. However, in the wake of the 2001 Postal attacks, it was noted that only 42% of those

exposed to anthrax adhered to the recommended oral antibiotic regimen [629]. Therefore, the CDC now recommends that post-exposure prophylactic treatment include the administration of an anthrax vaccine [629]. Following this recommendation will require the development of a safe and efficacious anthrax vaccine, and such a vaccine would constitute a cost-effective means of countering the threat of weaponized anthrax spores [565].

Previous studies have established that protective immunity against anthrax is primarily mediated by antibodies that bind to PA [603,630-632]. To address the safety issues and lot-to-lot variability of AVA, several candidate anthrax vaccines contain recombinant PA (rPA) [633,634]. Candidate rPA vaccines formulated with an alum adjuvant were shown to induce levels of neutralizing antibodies comparable to AVA and also required annual boosters to maintain protective immunity [552,635,636]. To elicit a longer-lasting immune response and reduce the number immunizations needed, alternative adjuvants and carrier proteins have also been used to create new candidate rPA vaccines [637-640]. Although several of these rPA-based vaccines have made it into clinical trials, none have yet obtained licensure from the FDA [641-645]. The aim of this project was to develop an improved anthrax vaccine candidate using TMV nanoparticles.

Translational fusions to TMV coat protein

As discussed in the previous chapter, neutralizing antibodies primarily recognize conformational epitopes and inducing neutralizing antibodies may, therefore, require conformational antigens. Many neutralizing PA epitopes are known, including two linear epitopes in domain 4 that block the ability of PA to bind to receptors [646,647]. Genetically fusing foreign peptides to the TMV coat protein tends to be the easiest and least expensive method of creating VNP vaccine candidates, but this approach is typically limited to smaller epitopes. Previous work by McComb *et al*. demonstrated that vaccines produced by genetically fusing small, linear PA epitopes to the TMV coat protein failed to protect mice challenged with *B. anthracis* spores [648]. This approach might have proven more successful if multiple linear

epitopes were displayed simultaneously, either by creating multiple monovalent VNPs and combining them or by increasing the size of the translational fusion so that multiple linear epitopes are displayed on a single TMV particle. Thus, PA domains might serve as better antigens.

PA domains

As outlined in Figure 27, PA is an 83-kDa protein that binds to host cellular receptors and facilitates the cellular internalization of EF and LF. PA consists of four domains, each contributing to its role in facilitating the cellular internalization of EF and LF (Table 10). Mutational analysis and crystal structure mapping have revealed residues in all four domains that are essential for PA function [552,649,650]. Additionally, Crowe *et al.* used sera from AVA-vaccinees to map the PA domains that contained neutralizing epitopes and found thirteen antigenic regions that spanned all four domains [651]. Based on this evidence, we included PAD1, PAD1', PAD2, PAD3, and PAD4 in this work.

Table 10. PA domains and their function(s).

Domain		Amino Acids [652]	Function
1	**PA_{20}**	1-167	Furin cleavage site[653,654]
	1'	168-258	Hepatmerization [652] LF & EF binding sites [654,655]
2		259-487	Heptamerization [652] Membrane insertion / Pore formation [656,657] LF & EF translocation [658]
3		488-595	Heptamerization [659]
4		596-735	Binding to cellular receptor [660-662]

The Dock-and-Lock system

VNPs created by genetically fusing foreign epitopes to the coat protein of TMV have several limitations. First, the biophysical properties of certain epitopes elicit necrotic lesions, leading to reduced yields or reversion to wild-type TMV, as was the case for the fusion loop epitope of ZIKV. Second, while most pathogen-neutralizing epitopes are conformational, typically only short linear epitopes of

approximately 20 amino acids can be genetically fused to the TMV coat protein without affecting viral replication and assembly [183] (although some groups have been able to display larger proteins with the use of a linker peptide [663]). These limitations were addressed using an alternative approach that involves expressing and purifying the TMV scaffold and heterologous protein antigen separately, then conjugating the antigen to the surface of TMV.

The Dock-and-Lock system allows large protein antigens to be covalently attached to the TMV nanoparticles. This system utilizes two components of the *Drosophila* phototransduction system: 1) the C-terminal residues of the NorpA protein (EFCA) added to the C-terminus of the TMV coat protein, and 2) the PDZ1 domain of InaD translationally fused to the C-terminus of a recombinant protein antigen (hereafter referred to as an InaD fusion protein) [664,665]. The EFCA sequence and the InaD domain both contain cysteine residues with free thiol groups that can form a disulfide bond, which allows multiple copies of the fusion protein to be covalently attached to the surface of TMV. TMV VNPs displaying PA domains were created by expressing and purifying PAD-InaD fusion proteins and TMV-EFCA separately, followed by conjugation.

MATERIALS AND METHODS

Generation of TMV-EFCA

Purified TMV viral particles with an EFCA sequence genetically fused to the C-terminus of the coat protein (TMV-EFCA) was kindly provided by Novici Biotech. To create a working stock of TMV-EFCA, the leaves of *N. benthamiana* plants were first dusted with diatomaceous earth (Celite® 545, Acros Organics). The TMV-EFCA sample provided by Novici was diluted in PBS, 5 µL of the suspension was pipetted onto the dusted leaves, and the leaves were rub-inoculated with sterile cotton swabs. Infected leaf tissue was harvested 14 days later, and the virions were purified by PEG precipitation [7]. The purified

TMV-EFCA particles were analyzed by SDS-PAGE and used in docking reactions to confirm the presence of the EFCA amino acids to the C-terminus of the coat protein.

Cloning, expression, and purification of PA domain fusion proteins in *Nicotiana benthamiana*

DL24, a TMV launch vector provided by Novici Biotech containing InaD (amino acids 2-98, GenBank accession no. 1IHJ_A, cys53ala mutation) was digested using PacI and XhoI to remove the InaD insert and prepare the vector for HiFi assembly. InaD with a C-terminal poly-histidine affinity purification tag (6xHis) was PCR amplified from the DL24 vector using primers with the appropriate PAD and DL24 overhangs. The PA domains were PCR amplified from vectors created by Ryan McComb using primers with the appropriate InaD and DL24 overhangs. The PCR products were analyzed on agarose gels and then purified using the Wizard ® SV Gel and PCR Clean-Up System (Promega). Digested DL24, PCR-amplified PA domain, and PCR-amplified InaD were then assembled and transformed into 5-α competent *E. coli* using the NEBuilder® HiFi DNA Assembly Cloning Kit (New England Biolabs). Plasmids were extracted from *E. coli* cultures using a Zymo Plasmid Miniprep Kit (Zymo Research), and sequences were confirmed by PCR and sequencing. The plasmids were then transformed into electro-competent *Agrobacterium tumefaciens* (strain GV3101), grown in L-MESA and then AIM, followed by vacuum infiltration into *N. benthamiana.* To isolate the fusion proteins, agroinfected leaves were homogenized in grind buffer (100 mM Tris, 2 mM PMSF, 5 mM imidazole, 500 mM NaCl, 0.005% BME, pH 8) using a mortar and pestle. The lysate was then strained through cheesecloth, centrifuged at 14 k x g for 15 min at 4°C, followed by re-centrifuging the supernatant at 14 k x g for 1 hr at 4°C. The lysate supernatant was filtered through 0.22 µm vaccine filter (Corning), purified on a HisTrap™ HP column (GE Healthcare) following the manufacturer's recommendations [666].

Expression of PA domain fusion proteins in *Escherichia coli*

Cloning and production in Escherichia coli

The nucleic acid sequences for each PA domain fusion protein were codon-optimized for expression in *E. coli* using GENEius (Eurofins Genomics) and then ordered as GeneStrands from Eurofins Genomics. The GeneStrands were designed to include a PA domain, a C-terminal InaD PDZ domain (amino acids 2-98, GenBank accession no. 1IHJ_A, cys53ala mutation), a C-terminal 6xHis purification tag, and 3' and 5' overlaps for insertion into the pSX2 expression vector (Scarab Genomics). The gene strands were cloned into KpnI and SacI-digested pSX2 using the NEBuilder® HiFi DNA Assembly Cloning Kit (New England Biolabs), followed by transformation into 5-alpha competent *E. coli.* The sequence of each plasmid was verified by PCR and sequencing before it was cloned into chemically competent MDS42 *E. coli* (Scarab Genomics). One liter flasks of Terrific Broth containing kanamycin (50 µg/mL) were seeded with 10 mL of the transformed MDS42 *E. coli* grown overnight in the same culture. The bacteria were grown at 37°C to an OD_{600} of approximately 1.0, and PAD fusion protein expression was induced by adding isopropyl-1-thio-β-D-galactopyranoside (IPTG) (Sigma-Aldrich) to a final concentration of 1 mM, and left to grow at either 30°C or 37°C (optimal post-induction temperatures and incubation times were determined for each construct using SDS-PAGE analysis).

Harvesting and lysis of bacterial cells

After induction, *E. coli* cells were separated from the culture media by centrifugation at 10,000 x g for 10 min at 4°C. The supernatant was discarded, and the pelleted cells were washed with cold wash buffer (50 mM Tris, 300 mM NaCl, 20 mM BME, 0.2% Tween, pH 7.5), and centrifuged again at 5,000 x g for 20 min at 4°C. The cell pellet was washed again and centrifuged at 3,000 rpm for 25 min at 4°C. The cell pellet was resuspended in lysis buffer (10 mM Tris, pH 8, 0.1 M NaCl, 1 mM PMSF) plus 1 µg/mL lysozyme (Thermo Scientific) and incubated for 20 min at 37°C to digest the cell wall, followed by

sonication on ice to degrade DNA. The resulting lysate was centrifuged at 14,000 x g for 5 min at 4°C, and the lysate pellet and supernatant were analyzed by SDS-PAGE and western blot.

Purification of His-tagged PA domain fusion proteins

The majority of the his-tagged PA domain fusion proteins were found in the lysate pellet, and thus were solubilized in binding buffer with urea (6 M urea, 20 mM Tris, 0.5 M NaCl, 1 mM BME, 5 mM imidazole) prior to refolding on a HisTrap ™ HP column (GE Healthcare) using a 6-0 M urea step gradient followed by elution with a imidazole gradient [666]. Purification was monitored by SDS-PAGE and/or western blotting. Dialysis was performed on the pooled elution fractions that contained the PAD fusion protein using either SnakeSkin™ Dialysis Tubing (Thermo Scientific) or a Float-A-Lyzer (Spectrum Labs) with a MWCO of 10 kDa and then concentrated using Vivaspin® Centrifugal Concentrators (Sartorius). For soluble fusion proteins, the lysis supernatants were clarified by ammonium sulfate fractionation and membrane filtration prior to purification on HisTrap ™ HP columns (GE Healthcare) per the manufacturer's recommendations [667]. Protein concentrations were determined using the Pierce BCA Protein Assay Kit (Thermo Scientific) with BSA (BioRad) as the standard.

Addition of a PelB leader sequence and secretion into the periplasmic space

Additional *E. coli* expression vectors for PAD1 and PAD1' were designed and cloned as above, except with a PelB leader sequence added to the N-terminal end of the GeneStrands ordered from Eurofins Genomics. Cultures were grown and induced as above, followed by harvesting of the periplasmic proteins by selective disruption of the outer membrane and peptidoglycan layer as described in Wingfield *et al.* [668,669]. Subsequent purification and analyses were performed as above.

Addition of MBP fusion protein partner

The sequences for the His-tagged PAD1 and PAD1'-InaD fusion proteins were PCR amplified with vector overlaps to IPTG-inducible expression vector containing maltose-binding protein (MBP) with a C-terminal PreScission protease cleavage site (pET His6 MBP prescission LIC cloning vector (HMPKS), a gift

from Scott Gradia, Addgene plasmid # 29721). The vector was digested using XhoI and SspI, and the PCR-amplified inserts were cloned in using the NEBuilder® HiFi DNA Assembly Cloning Kit (New England Biolabs), followed by transformation into competent DH5α *E. coli*. After confirming the correct insertion of the PAD-InaD sequences by colony PCR, the plasmids were transformed into chemically-competent T7 Express *E. coli* (New England Biolabs) for MBP-PAD-InaD fusion protein expression.

One liter flasks rich media (10 g/L tryptone, 5 g/L yeast extract, and 5 g/L NaCl) containing kanamycin (50 μg/mL) and glucose (2 g/L) were seeded with 5 mL of overnight cultures, followed by incubation at 37°C until an optical density of 0.5 at 600 nm (OD_{600} of 0.5) was reached. Expression was induced with 1 mM IPTG for 3 hr at 37°C, the cultures were centrifuged at 4,000 x g for 20 min at 4°C, and the cell pellets were resuspended in lysis buffer (20 mM Tris, pH 8, 100 mM NaCl, 1 mM EDTA). Lysis, sonication, and analysis were performed as above, followed by solubilization, purification, and refolding on Ni-NTA resin as above. MBP was cleaved from the MBP-PAD-InaD fusion proteins in solution using the Pierce ™ HRV 3C Protease Kit (Thermo Scientific) following the manufacturer's recommendations [670]. The HRV3C protease was removed using Pierce® Glutathione Agarose (Thermo Scientific) and Pierce™ Centrifuge Columns (Thermo Scientific) per the manufacturer's recommendations [671]. MBP was removed using amylose resin (New England Biolabs) as described in the manufacturer's instructions [672], followed by dialysis and concentration of the PAD-InaD fusion proteins using Vivaspin® Centrifugal Concentrators (Sartorius).

Analysis by SDS-PAGE and western blotting

The different stages of purification of all fusion proteins (e.g. metal ion affinity chromatography using Ni-NTA resin) were monitored by SDS-PAGE and western blot. Some samples were concentrated by acetone precipitation prior to analysis, as described in Fic *et al*. [673]. Protein process samples were diluted with Laemmli Sample Buffer (BioRad) containing 355 mM BME, followed by heating at 100°C for 5 min. Prepared samples and Precision Plus Protein ™ All Blue Prestained Protein Standards (BioRad)

were loaded into 4-20% Mini-PROTEAN® TGX™ Precast Gels (BioRad), ran at 100 volts for 75-90 min, then either stained with Bio-Safe™ Coomassie Stain (BioRad) or transferred to a nitrocellulose membrane for western blotting.

SDS-PAGE gels were transferred to 0.2 µm or 0.45 µm Nitrocellulose Membrane (BioRad) for 2 hr at 150 mAmps, followed by blocking with 5% (w/v) non-fat milk in TBS for 1 hr at room temperature and incubation with primary antibody diluted in blocking buffer overnight at 4°C. After washing the membranes three times with TBST and one time with TBS, the appropriate secondary antibody diluted in blocking buffer was added, and the membrane was incubated 1-2 hr at room temperature. Following an additional round of washing, the membrane was incubated with either a chromogenic or chemiluminescent HRP substrate. Membranes were incubated with a mixture of hydrogen peroxide and a 4-Chloro-1-Naphthol solution (Opti-4CN™ Substrate Kit, BioRad) at room temperature until the desired color was obtained, and then rinsed with water to stop the reaction. Alternatively, Clarity™ Western ECL Substrate (BioRad) was added, the membrane was incubated for 5 min at room temperature, and the resulting chemiluminescent signals were documented using the Azure c500 (Azure Biosystems, Dublin, CA). The primary antibodies used for western blotting were polyclonal goat anti-PA_{83} (List Biological Laboratories) and monoclonal mouse anti-MBP (New England Biolabs); the secondary antibodies used were rabbit anti-goat IgG (Invitrogen) and goat anti-mouse IgG (BioRad), respectively. PA_{83} (recombinant anthrax protective antigen, List Biological Laboratories) was used as a positive control for the anti-PA_{83} blots.

Analysis by ELISA

Endpoint titers to the PAD-InaD fusion proteins were determined using goat polyclonal antibody from List Biologics (product #771B). Briefly, 96-well half area plates (Corning) were coated with PAD-InaD fusion proteins diluted in carbonate buffer (0.03 M Na_2CO_3/0.07 M $NaHCO_3$, pH 9.6) to 10 µg/mL, incubated overnight at 4°C. Plates were blocked with 5% BSA for 1 hr at room temperature, followed by

incubation with serially diluted polyclonal goat anti-PA_{83} diluted in blocking buffer overnight at 4°C. Following three washes with PBS, the plates were incubated with HRP-conjugated rabbit anti-goat IgG (1:2,000, Invitrogen) for 1.5 hr at room temperature then washed three times with PBS. OPD substrate (Sigma) was added and the absorbance at 450nm was measured on a SpectraMax Plus plate reader (Molecular Devices). Endpoint titers were defined as the reciprocal of the highest antibody dilution that gave a reading above the cutoff. Cutoff values were determined for each fusion protein, and each antibody dilution using Normal Goat Serum (Calbiochem) as described in Frey *et al.* [482].

Docking reactions to create TMV-PAD viral nanoparticles

VNPs were prepared using the Dock-and-Lock method to covalently attach the PA-InaD fusion proteins to the TMV-EFCA scaffold [664]. The purified PAD-InaD fusion protein was diluted in 2x reaction buffer (100 mM Tris, pH 8, 0.008% BME), mixed with purified TMV-EFCA, and incubated at room temperature for 30 min. VNPs were then separated from unbound PAD-InaD by precipitation of the virions with 0.5 M NaCl/4% PEG, incubation on ice for 1 hr, and centrifugation at 10,000 x g for 15 min at 4°C. The supernatant was removed, and the virus-containing pellet was resuspended in PBS. Docking was confirmed on SDS-PAGE gels using both reduced and non-reduced samples. Purified green fluorescent protein (GFP)-InaD fusion protein (provided by Novici Biotech) used as a positive control for docking reactions.

RESULTS

Expression of PA domain fusion proteins in *Nicotiana benthamiana*

The five PAD-InaD constructs were successfully cloned into the DL24 expression vector and transformed into 5-α competent *E. coli*. The PAD1' and PAD1 fusion protein expression vectors were transformed into *A. tumefaciens,* and agrobacterium cultures were used to agroinfiltrate *N. benthamiana* plants. Plant leaves were harvested five days post-infection (DPI) and ground with a

mortar and pestle to lyse the cells. The cell lysate was clarified by centrifugation and filtration, and the His-tagged PAD fusion proteins were purified using affinity chromatography. SDS-PAGE analysis of the lysate and column chromatography samples for PAD1'-InaD did not reveal any significant bands that ran at the estimated molecular weight of PAD1'-InaD (22 kDa) (Figure 28a), but western blotting with an anti-PA_{83} antibody did show a band with an apparent molecular weight of 25 KDa of in the column elution fractions (Figure 28b). A smaller band, with an apparent molecular weight of 16 kDa, also appeared on the western blot in the elution column fractions (Figure 28a, b); this may have been a partially degraded or truncated form of the PAD1' fusion protein. In an attempt to minimize *in planta* and *ex planta* degradation, leaf punch samples or agroinfiltrated leaves were harvested at various DPIs and the pH and the composition of the grind buffer, including the addition of various protease inhibitors, was investigated. However, none of these changes led to any significant improvement in yield (data not shown), suggesting that the PAD1' fusion protein was not being expressed at high levels in *N. benthamiana.* Furthermore, while the western blot showed that the highest concentration of the PAD1' fusion protein was in 75 mM imidazole and 100 mM imidazole elution fractions, the SDS-PAGE gel showed that these elution fractions also contained high levels of impurities (i.e., co-purifying host-cell proteins). The yield of "purified" PAD1'-InaD was estimated to be 24 ng of protein per gram of leaf tissue.

The expression of PAD1-InaD proved to have similar issues. SDS-PAGE (Figure 29a) and western blot analysis (Figure 29b) demonstrated that PAD1-InaD was expressed at very low levels and, after affinity chromatography, it migrated mostly as a single band with an apparent molecular weight of 42 kDa (although several degradation products appear to be present in some of the elution fractions). While the PAD1-InaD elution fractions do not contain as many co-purifying host-cell proteins as the PAD1' fusion protein, they are still present at moderate levels (Figure 29a). The yield of "purified" PAD1-InaD was estimated to be 95 ng of protein per gram of leaf tissue.

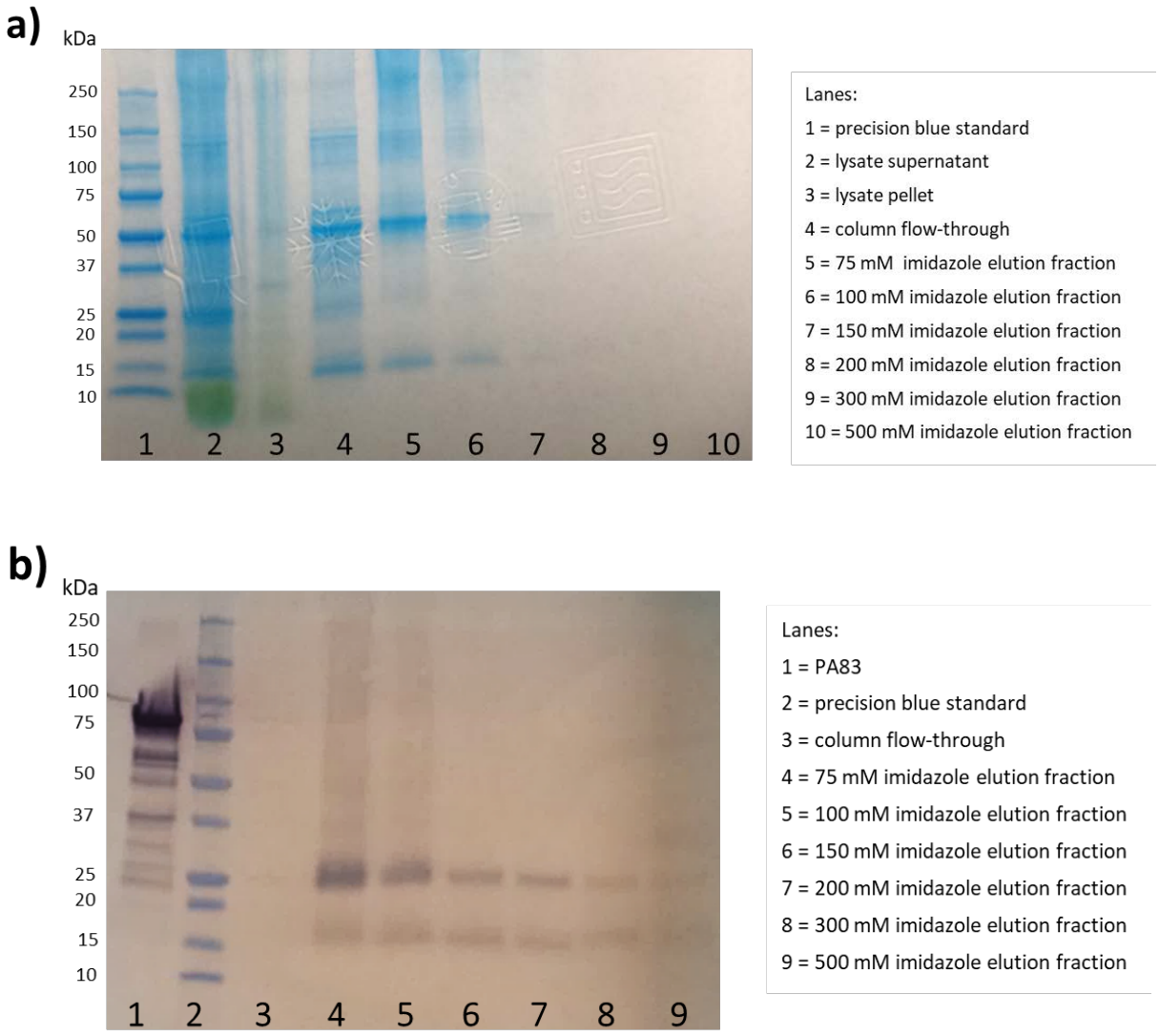

Figure 28. SDS-PAGE and western blot analysis of purified PAD1'-InaD expressed in *Nicotiana benthamiana*. **a)** SDS-PAGE analysis of crude cell lysates and affinity chromatography process samples. **b)** Western blot analysis of affinity chromatography process samples using an anti-PA_{83} primary antibody, followed by a HRP-conjugated secondary antibody and chromogenic substrate.

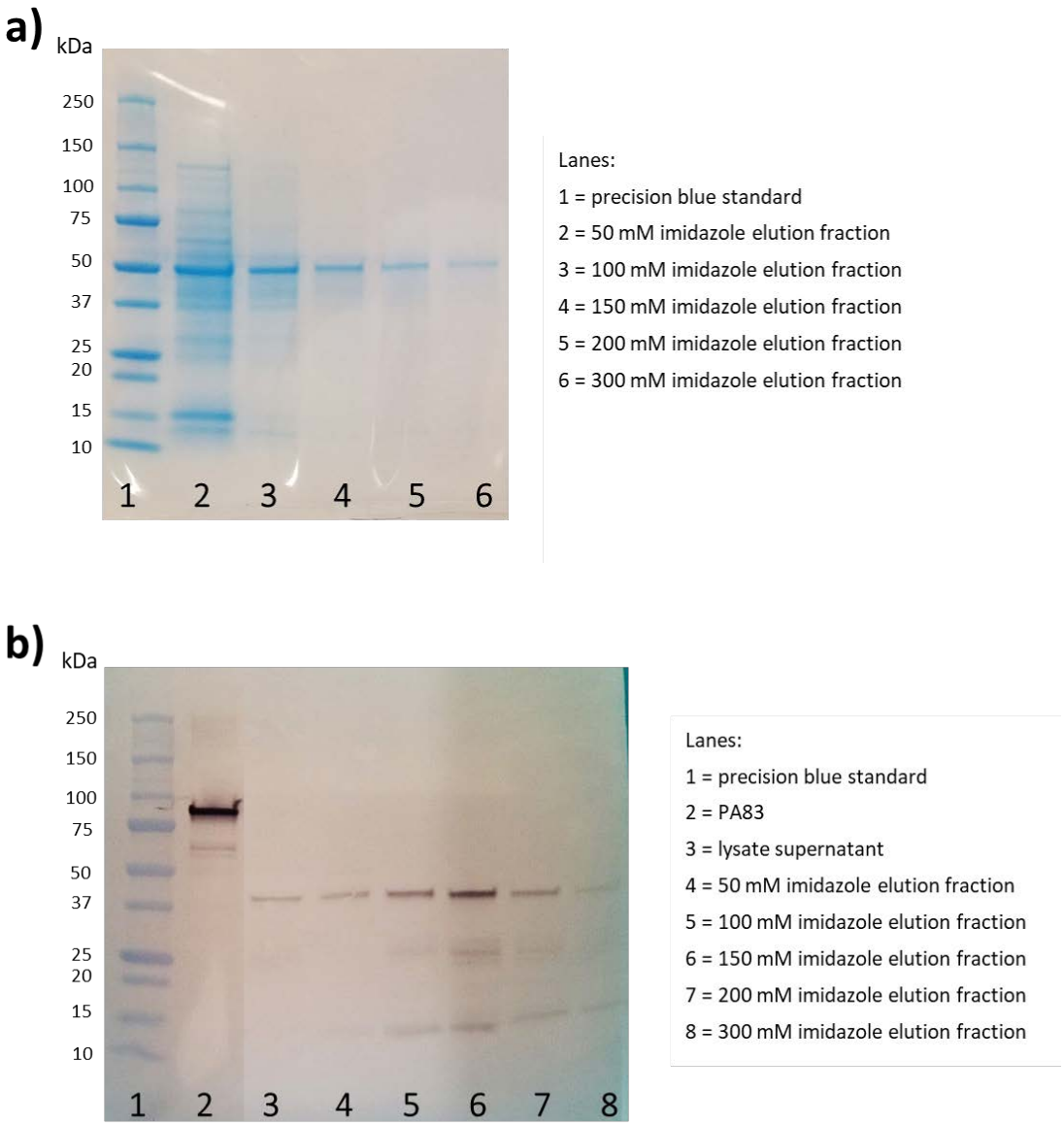

Figure 29. SDS-PAGE and western blot analysis of purified PAD1-InaD expressed in *Nicotiana benthamiana*. **a)** SDS-PAGE analysis of affinity chromatography process samples. **b)** Western blot analysis of clarified cell lysate and affinity chromatography process samples using an anti-PA_{83} primary antibody, followed by a HRP-conjugated secondary antibody and chromogenic substrate.

Expression and purification of PA domain fusion proteins in *E. coli*

All five PAD-InaD constructs were successfully cloned into the pSX2 expression vector and transformed into MDS42 *E. coli* for expression. Following cell lysis, the crude cell lysate was centrifuged to separate the soluble proteins (i.e., the proteins present in the supernatant) and insoluble proteins (i.e., the proteins present in the pellet). SDS-PAGE and/or western blot analysis of the crude cell lysates

confirmed that the PAD2, PAD3, and PAD4 fusion proteins were being expressed at relatively high levels as insoluble proteins, while PAD1' and PAD1 were expressed at low levels as partially soluble proteins. As an example, Figure 30a demonstrates that PAD3-InaD and PAD4-InaD end up in the cell lysate pellets with molecular weights of 25 kDa and 28 kDa, respectively. Both of these fusion proteins can easily be seen on a Coomassie-stained SDS-PAGE gel, indicating that they are being expressed at relatively high levels. In contrast, PAD1'-InaD, with an apparent molecular weight of 25 kDa, was not made as an inclusion body (Figure 30a) and ended up mostly in the cell lysate supernatant and was expressed at very low levels (Figure 30b).

The insoluble fusion proteins that ended up in the lysate pellets (i.e., PAD2, PAD3, and PAD4) were solubilized upon resuspension in buffer containing 6 M urea, refolded on a Ni-NTA column using a 6-0 M urea step gradient, and then eluted with an imidazole gradient. The refolded and purified fusion proteins were then dialyzed to remove the imidazole, concentrated with ultrafiltration centrifugal devices (data not shown). SDS-PAGE analysis of the purified and concentrated PAD2-InaD, PAD3-InaD and PAD4-InaD shows that they are present at high concentrations with almost no contaminating host-cell proteins and run at 36 kDa, 25 kDa, and 28 kDa, respectively (Figure 31a). Subsequent western blot analysis demonstrated that all three fusion proteins were detected by the anti-PA_{83} antibody at their respective molecular weights, and while there were no apparent degradation products, the fusion proteins did appear to be former dimers, as shown by the bands that ran at twice their respective molecular weights (Figure 31b). The concentrations of the purified PAD2-InaD, PAD3-InaD, and PAD4-InaD proteins were calculated using a BCA assay, and final product yields were estimated at 62, 30, and 85 milligrams of protein per liter of cell culture, respectively.

The initially soluble but poorly expressed fusion proteins that ended up in the lysate supernatant (i.e. PAD1' and PAD1) were purified on Ni-NTA columns followed by dialysis and concentration. After concentration, visible particulates formed in the PAD1' and PAD1 fusion protein

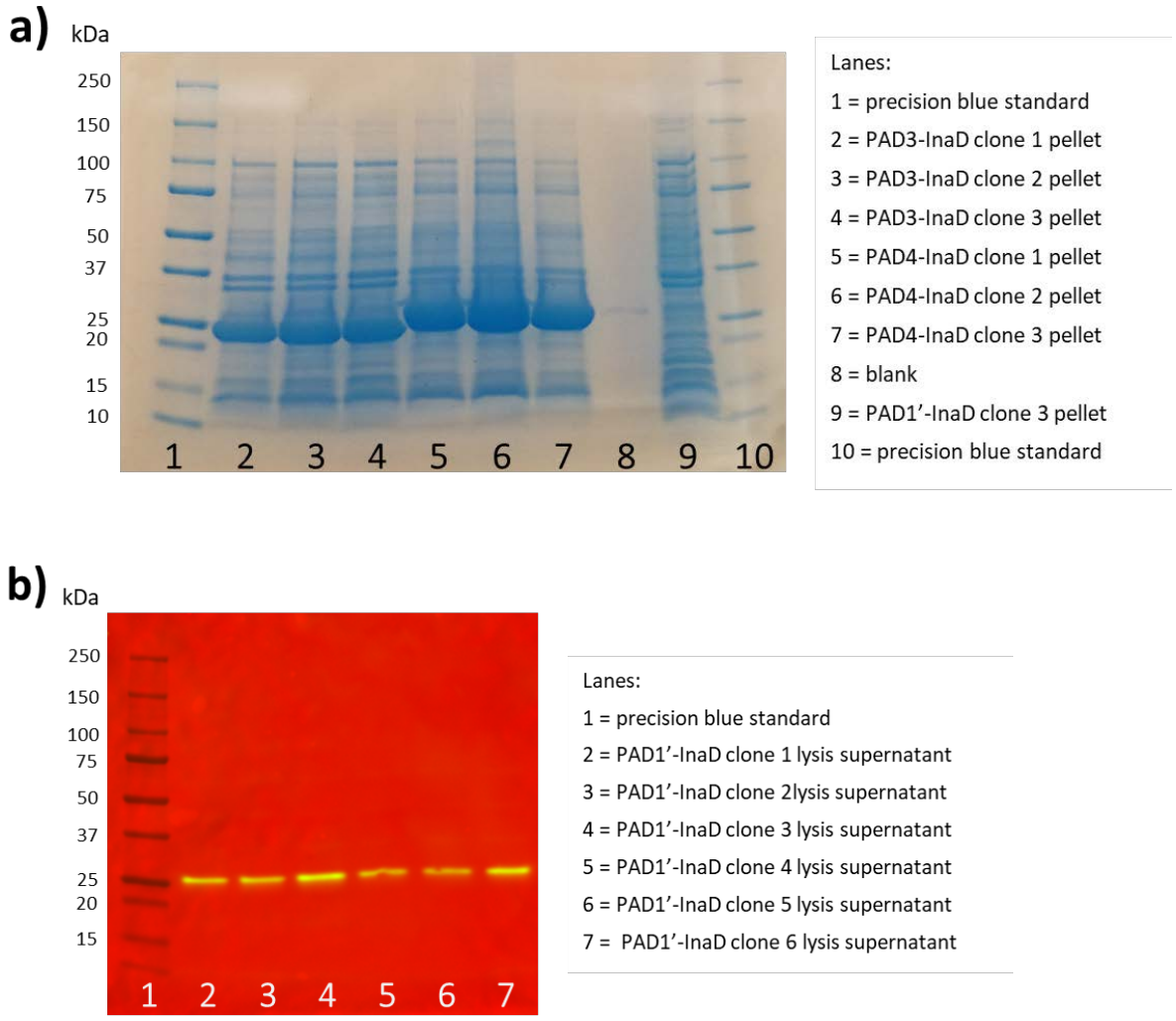

Figure 30. SDS-PAGE and western blot analysis of crude cell lysates for PAD1', PAD2, and PAD4 fusion proteins expressed in *E. coli*. **a)** SDS-PAGE analysis of crude cell lysate pellets from clones expressing PAD3-InaD, PAD4-InaD, or PAD1'-InaD. **b)** Western blot analysis of cell lysate supernatants from clones expressing PAD1'-InaD using an anti-PA_{83} primary antibody, followed by a HRP-conjugated secondary antibody and chemiluminescent substrate.

samples. To determine if the fusion proteins remained in the soluble fraction or had become insoluble, the particulates were separated from the soluble proteins by centrifugation. Subsequent SDS-PAGE and western blot analysis of both the supernatants and the resuspended pellets revealed that both PAD1-InaD and PAD1'-InaD were partially insoluble, but the majority of the PAD1 fusion protein was present in the pellet (i.e., insoluble) while the PAD1' fusion protein was equally split between the pellet and the supernatant (Figure 31a, b). Although the expected molecular weight of PAD1-InaD was 42 kDa (Figure 29b), when expressed in *E. coli* it ran at two molecular weights, 37 kDa and 45 kDa, with multiple

degradation products in the insoluble fraction (Figure 31b). PAD1'-InaD was present at only moderate concentration and co-purified with various host-cells proteins, but ran at its expected molecular weight, 25 kDa, with minor degradation products (Figure 31a, b). The presence of host-cell proteins and degradation products, as well as the partially insoluble nature of both PAD1-InaD and PAD1'-InaD, made it difficult to determine final yields, but both were estimated to be approximately 0.6 milligrams of protein per liter of cell culture.

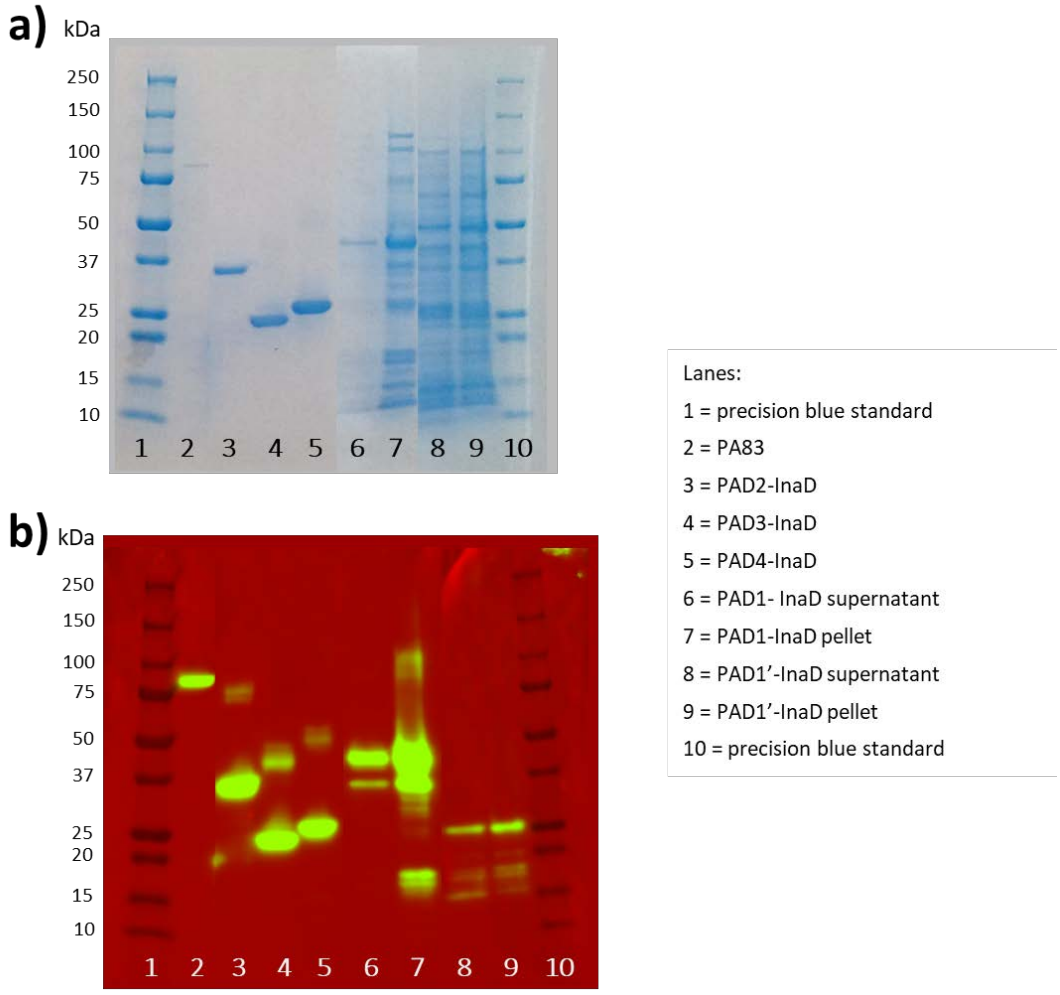

Figure 31. Analysis of purified and concentrated PA domain fusion proteins expressed in *E. coli*. **a)** SDS-PAGE analysis of purified and concentrated PAD2, PAD3, and PAD4 fusion proteins, as well as the insoluble and soluble fractions of the purified and concentrated PAD1 and PAD1' fusion proteins. **b)** Western blot analysis of the same samples using an anti-PA_{83} primary antibody, followed by a HRP-conjugated secondary antibody and chemiluminescent substrate.

Periplasmic expression of PAD fusion proteins using PelB

PelB is a naturally-occurring signal sequence from the secreted PelB protein of the bacterium *Erwinia carotovora* that has been used in *E. coli* expression systems to target proteins to the periplasmic space [674]. Advantages of targeting proteins to the periplasm can include more straightforward purification, less proteolysis, and improved folding [675]. The PelB signal sequence was added to the amino terminus of the PAD1 and PAD1' constructs to target the fusion proteins for secretion into the periplasm. After inducing protein expression with IPTG, the cells were cultured at either 30°C or 37°C overnight. Following centrifugation, the cell pellet was subjected to cellular fractionation to determine the compartment in which the fusion proteins were being expressed. First, the cell pellet was resuspended in a buffer containing EDTA and sucrose to release the periplasmic fraction. After centrifugation, the resuspended spheroplast pellet was subjected to freeze-thaw cycles to lyse the cells, and then centrifuged again to separate the cytoplasmic proteins (supernatant) from the membranes and insoluble proteins (pellet).

Acetone precipitation was used to concentrate process samples that were expected to contain low levels of protein (i.e., the culture supernatant and the sucrose supernatant). Western blotting with an anti-PA_{83} antibody revealed that the PAD1 fusion protein seemed to be expressed at approximately the same level whether induced at 30°C or 37°C and that the addition of a PelB leader sequence did not result in PAD1-InaD being efficiently secreted into the periplasm, as it was present in multiple cellular fractions (Figure 32a). The expression of PAD1'-InaD with the PelB signal sequence also showed inefficient secretion and even lower levels of expression than the PAD1 fusion protein (Figure 32b). The presence of the fusion proteins in the lysis pellets suggests that they may be partially insoluble, which is supported by previous attempts at expression without the PelB leader sequence (Figure 31). Due to the inefficient secretion of both PAD1'-InaD and PAD1-InaD, all cell fractions containing the respective fusion protein were pooled and purified on a Ni-NTA column. After dialysis and concentration, the

estimated yield of PAD1'-InaD was 0.6 mg/L, and PAD1-InaD was 0.75 mg/L. Thus, the addition of the periplasmic secretion signal did not solve the low yield problem and pooling the fractions reintroduced the same co-purifying host-cell proteins seen in the prior expression of the PAD1'-InaD and PAD1-InaD constructs that lacked the PelB signal sequence.

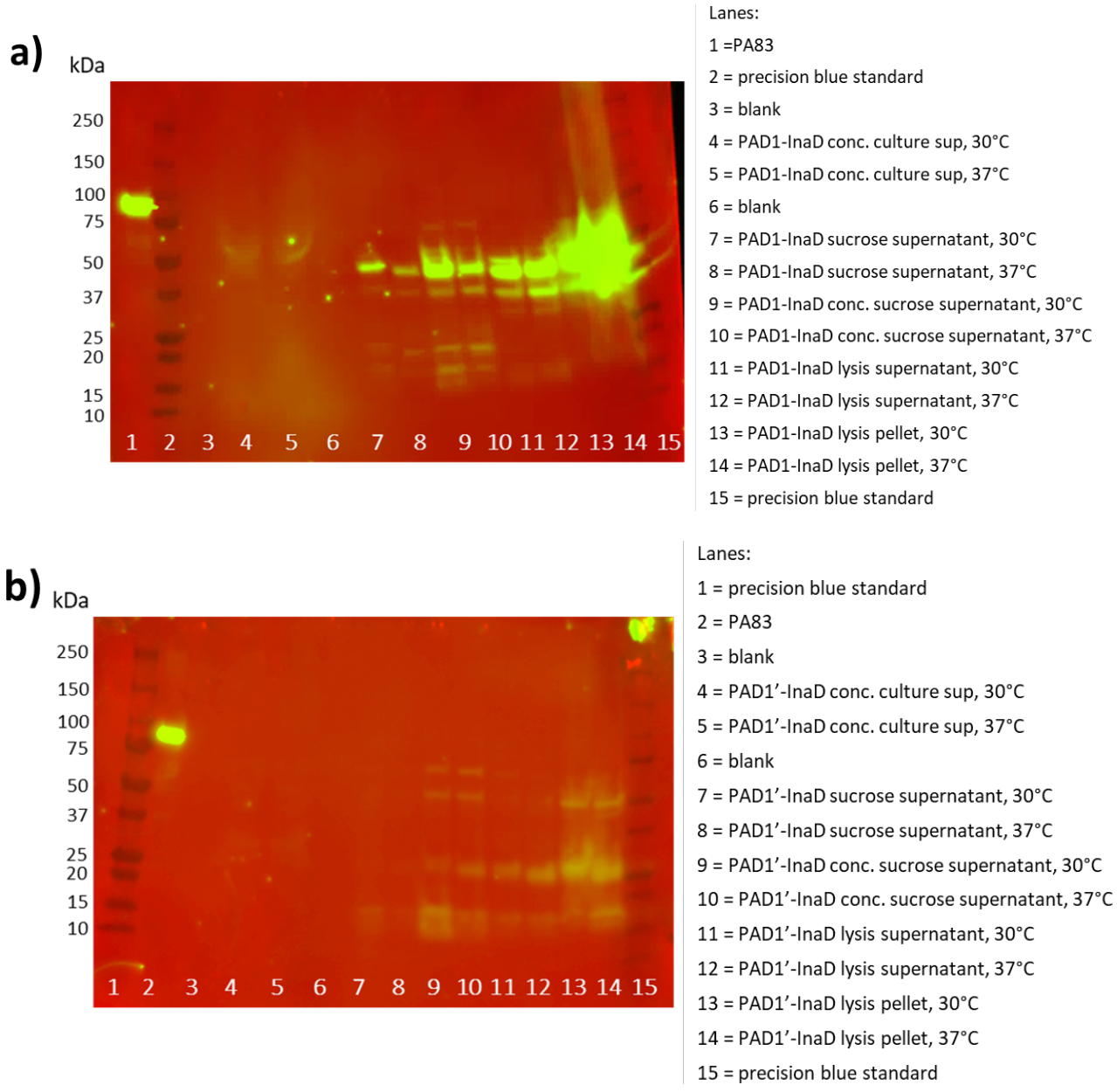

Figure 32. Western blot analysis of the expression of PAD1-InaD and PAD1'-InaD with a PelB periplasmic secretion signal. Cellular fractions from *E. coli* cultures expressing PAD1-InaD **(a)** or PAD1'-InaD **(b)** were grown at 30°C or 37°C and then analyzed by western blot using an anti-PA_{83} primary antibody, followed by a HRP-conjugated secondary antibody, and chemiluminescent substrate. The culture supernatants and sucrose supernatants were concentrated using acetone precipitation.

Expression of MBP fusion proteins

Maltose-binding protein (MBP) is a component of the transport system for malto-oligosaccharides in *E. coli,* and due to its high stability, it is widely used as a fusion protein partner [676,677]. Fusion partner proteins can stabilize proteins that are difficult to express while also conferring high solubility and facilitating protein purification with amylose resin [677]. The codon-optimized sequences for PAD1'-InaD and PAD1-InaD with a C-terminal 6xHis purification were cloned into a pET expression vector containing an IPTG-inducible N-terminal MBP with HRV 3C protease recognition sequence to remove the MBP during purification. After culturing and centrifugation, the resuspended cells were lysed and centrifuged again to separate the insoluble and soluble components. SDS-PAGE analysis demonstrated that MBP-PAD1-InaD ran at a molecular weight of 86 kDa, while MBP-PAD1'-InaD ran at 68 kDa (Figure 33). Reasonable amounts of soluble MBP-PAD1'-InaD and MBP-PAD1-InaD were present in the lysis supernatants, although approximately half of the MBP fusion proteins appeared to be in the lysis pellets, and therefore were presumably insoluble (Figure 33).

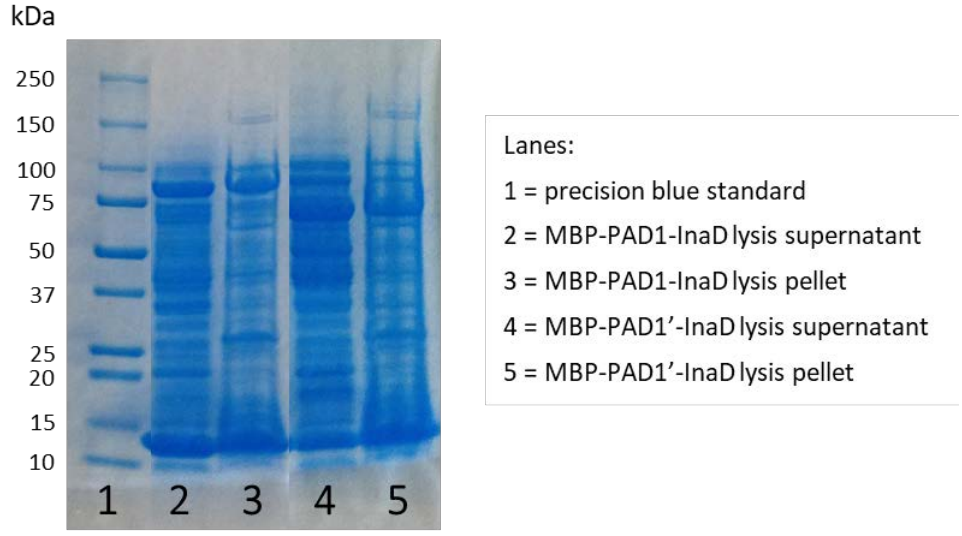

Figure 33. SDS-PAGE analysis of cell lysates from the expression of MBP-PAD1'-InaD and MBP-PAD1-InaD in *E. coli.*

Following cell lysis, the MBP fusion proteins were purified on Ni-NTA resin, and MBP was cleaved off using GST-tagged HRV 3C protease. Cleavage with HRV 3C proved to be reasonably efficient, and following cleavage the GST-tagged HRV3C protease was removed using glutathione agarose (data not shown). Cleaved MBP and any remaining uncleaved MBP fusion proteins were then removed using amylose resin. However, this process was not efficient as western blot analysis using both anti-PA and anti-MBP antibodies revealed that the amylose resin was not efficiently capturing the cleaved MBP and the uncleaved MBP fusion proteins (Figure 34).

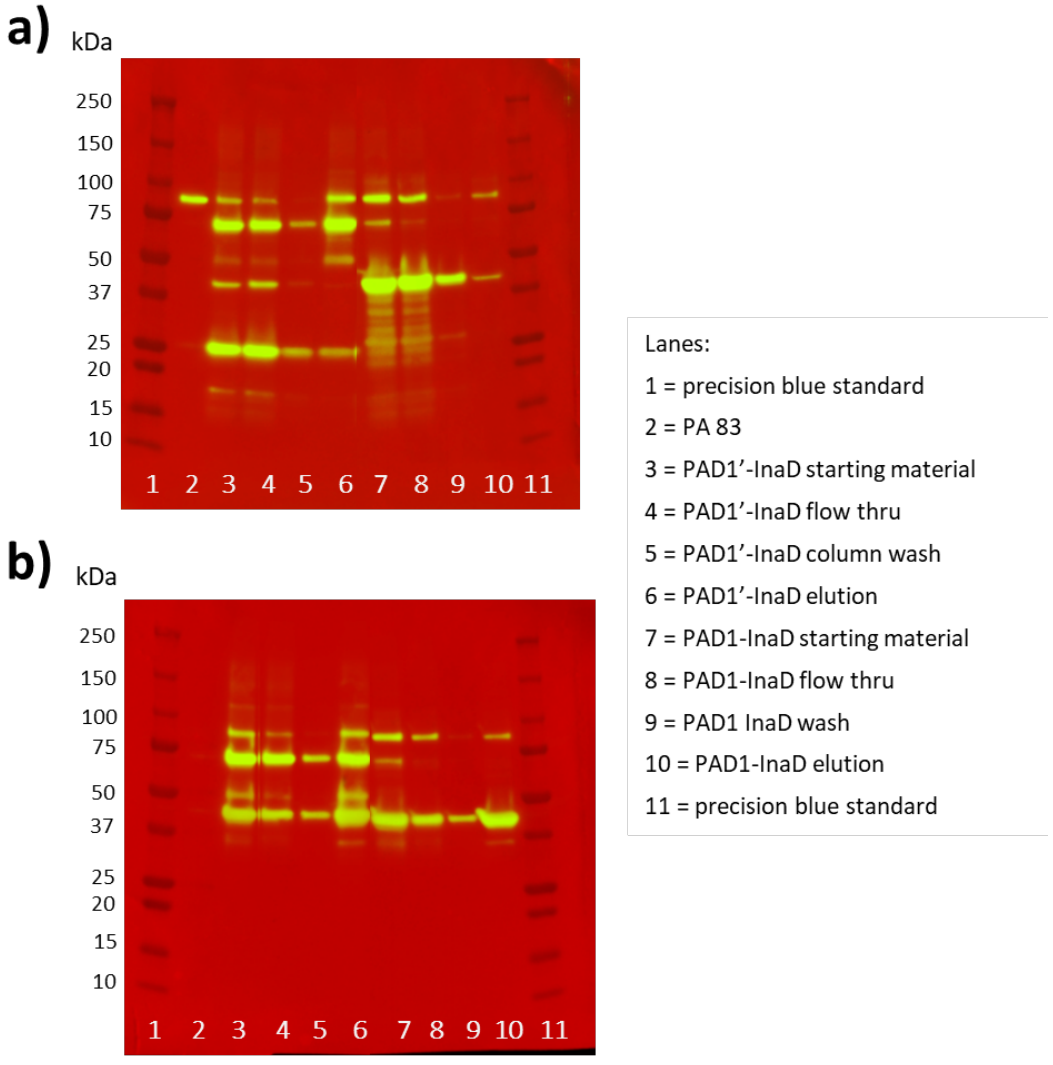

Figure 34. Western blot analysis of the removal of MBP using amylose resin. After HRV 3C cleavage, the proteins were dialyzed into column buffer, and this served as the starting material for MBP removal by on the amylose column. Column fractions were analyzed by western blot using an anti-PA_{83} primary antibody **(a)** or an anti-MBP primary antibody **(b)** followed by HRP-conjugated secondary antibodies, and chemiluminescent substrate.

The amylose column flow-throughs had to be run at least three consecutive times on amylose resin to remove the majority of the MBP. After diafiltration and ultrafiltration (DF/UF), the process samples were analyzed by SDS-PAGE and western blot, which revealed that the purified PAD1'-InaD contained no visible no host-cell proteins (Figure 35a), but did contain residual MBP (Figure 35c). PAD1'-InaD showed signs of degradation (Figure 35a, c), and was not very concentrated (Figure 35a). The purified and concentrated PAD1-InaD contained no visible host-cell proteins (Figure 35a), but still contained quite a bit of residual MBP (Figure 35c). Also, because PAD1'-InaD and MBP had the same apparent molecular weight of 45 kDa (Figure 35b, c), the 45 kDa band, that is supposedly purified and concentrated PAD1-InaD, is really a mixture of the two proteins. The estimated final yields for this method of expression, as well as the previous expression methods, can be seen in Table 11.

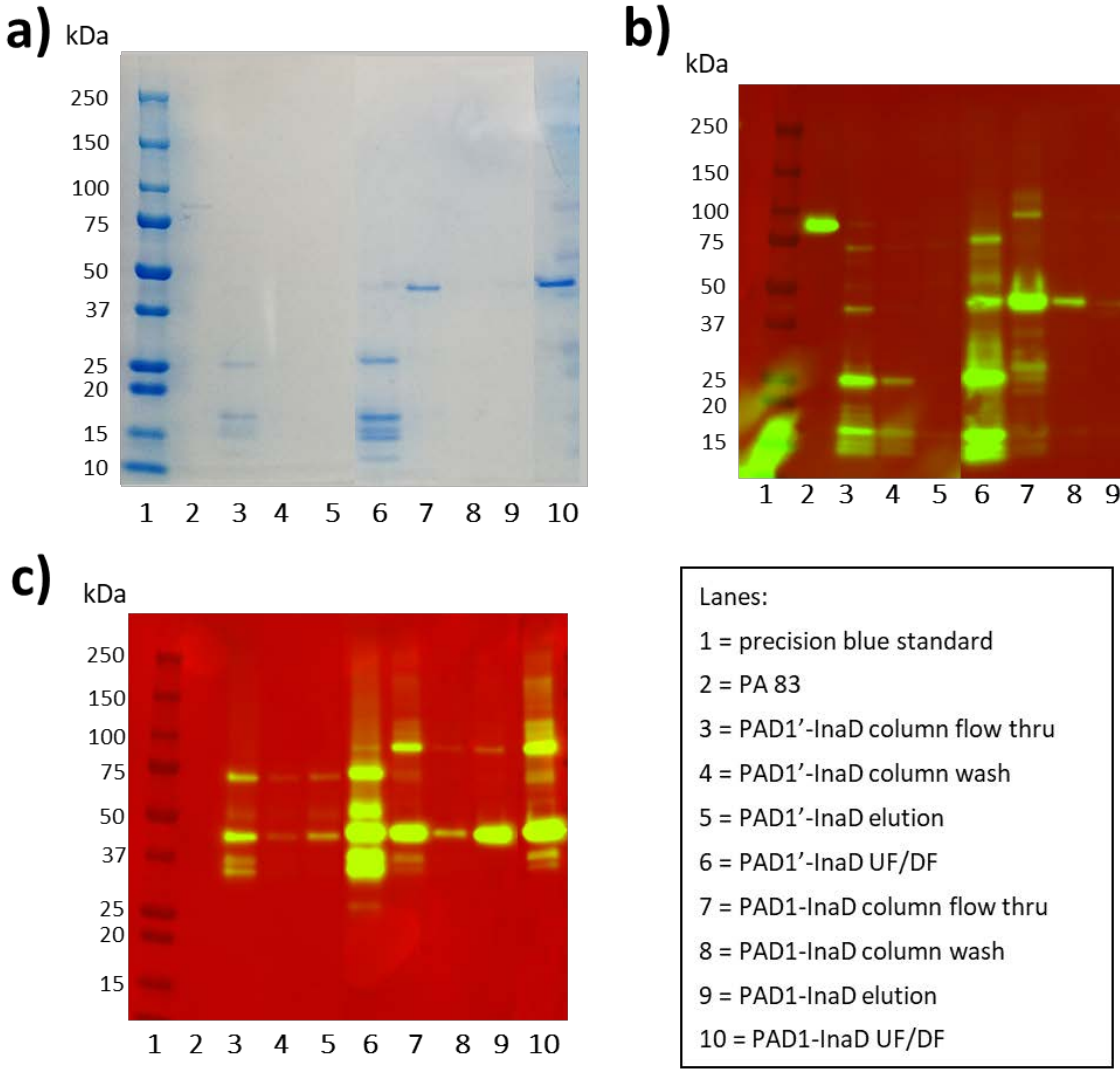

Figure 35. SDS-PAGE and western blot analysis MBP-PAD1-InaD and MBP-PAD1'-InaD purification process samples. **a)** Process samples from the 3rd consecutive amylose column for PAD1-InaD and the 4th column for PAD1'-InaD and a subsequent ultrafiltration and diafiltration (UF/DF) step were analyzed SDS-PAGE. Western blotting of the same samples using an anti-PA_{83} primary antibody **(b)** or an anti-MBP primary antibody **(c)** followed by HRP-conjugated secondary antibodies, and chemiluminescent substrate.

Table 11. Final yields and total amounts of purified PA domain fusion proteins.

Fusion protein	Expression Host	Additional sequence	Estimated yield after purification [a]	Total amount of purified product [b]
PAD1'-InaD	Plant (*N. benthamiana*)	-	24 ng/g*	1.4 ug
	Bacterial (*E. coli*)	-	0.6 mg/L	420 µg
		PelB	0.6 mg/L	250 µg
		MBP	2.6 mg/L	34 µg
PAD1-InaD	Plant (*N. benthamiana*)	-	95 ng/g *	30 µg
	Bacterial (*E. coli*)	-	0.6 mg/L	610 µg
		PelB	0.75 mg/L	375 µg
		MBP	3.3 mg/L	43 µg
PAD2-InaD	Bacterial (*E. coli*)	-	62 mg/L	1,250 µg
PAD3-InaD	Bacterial (*E. coli*)	-	30 mg/L	1,800 µg
PAD4-InaD	Bacterial (*E. coli*)	-	85 mg/L	5,100 µg

*Estimated based on western blot analysis with a known amount of the positive control protein, PA_{83}. However, only a fraction of the anti-PA_{83} antibodies used bind to each domain of PA, so actual yields are likely lower than these estimates.

[a] For plant-based expression, final yields are in units of nanograms of protein per gram of fresh weight leaf tissue. For bacterial expression, final yields are in units of milligrams of protein per liter of cell culture.

[b] Amount of purified product prior to analysis by SDS-PAGE, western blot, and BCA. Thus, less protein was available for subsequent docking reactions.

Functional analysis by ELISA Production and purification of TMV-EFCA

In addition to western blotting, the purified PAD2-InaD, PAD3-InaD, and PAD4-InaD were analyzed by indirect ELISA to check whether they could be recognized by goat anti-PA_{83} polyclonal IgG antibodies. Endpoint titers, defined as the reciprocal of the highest antibody dilution that gave a reading above the cutoff, were determined to provide a semi-quantitative measure of the proportion of the polyclonal anti-PA_{83} antibodies bound to each fusion protein. Figure 36 shows how the signal (i.e., absorbance at 450 nm) decreases with each successive dilution of the anti-PA_{83} primary antibody or, in the case of the cutoffs, normal goat serum. The estimated endpoint dilutions for the PAD2, PAD3, and PAD4 are 1.64×10^6, 8.19×10^5, and 4.10×10^5, respectively (Figure 36). This suggests the PAD2 region of the PA_{83} immunogen may contain more immunogenic epitopes than PAD3 or PAD4 and thus may have

elicited more antibodies. Alternatively, it could indicate that the PA portion of the PAD2-InaD fusion protein retained more of its native structure, and therefore was able to bind more of the anti-PA_{83} antibodies. Although, perhaps the most likely explanation comes from the fact that domain 2 contains more amino acids than domain 3 or domain 4. Nevertheless, along with the western blots, the ability of the anti-PA_{83} serum to bind to all three fusion proteins verifies that the purified fusion proteins contain antigenic PA epitopes.

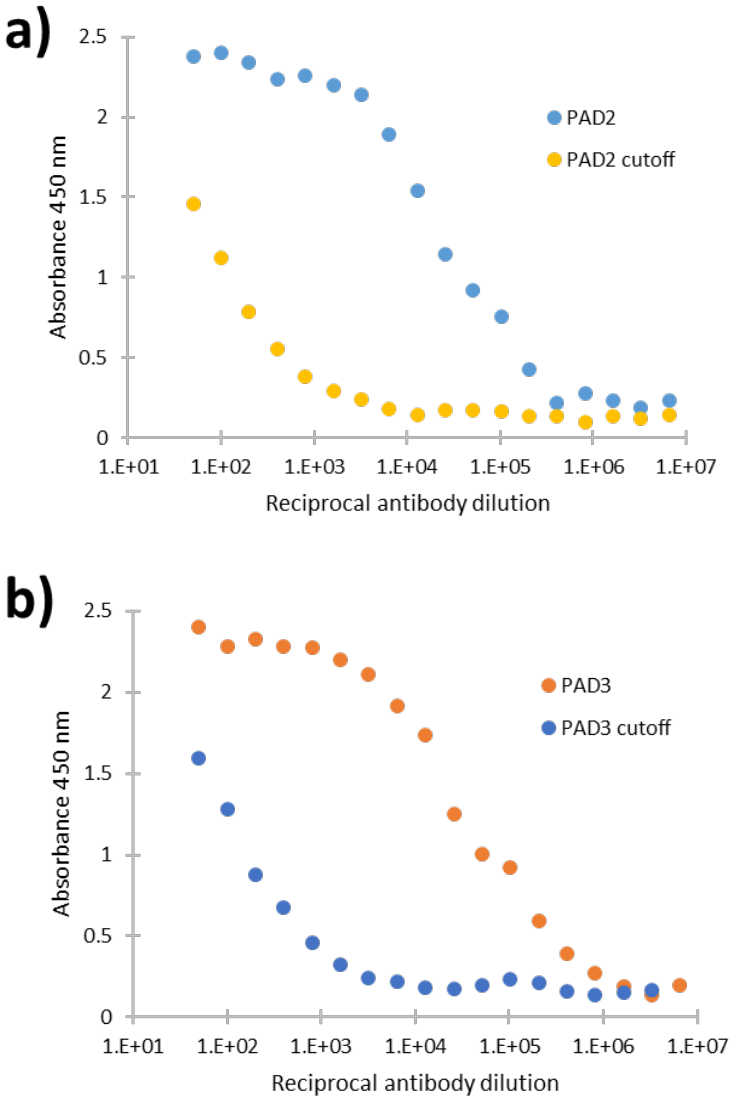

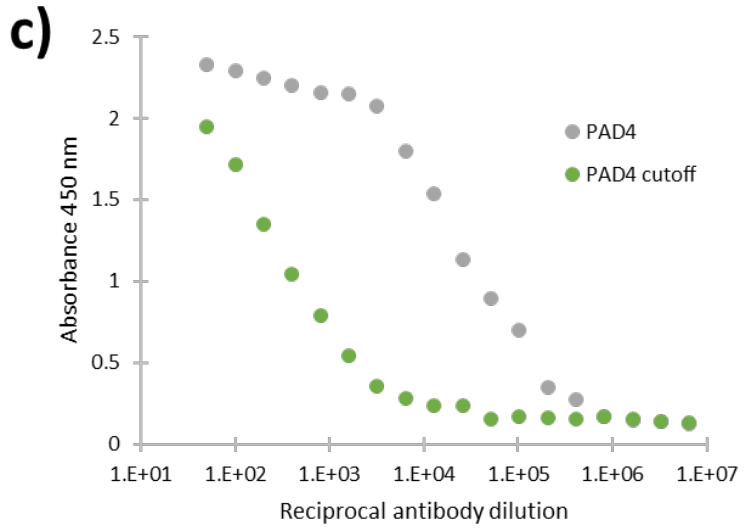

Figure 36. Analysis of purified PAD fusion proteins by ELISA. Purified PAD2-InaD **(a)**, PAD3-InaD **(b)**, or PAD4-InaD **(c)** fusion proteins were used to coat a 96-well plate. Serially diluted anti-PA_{83} serum was added followed by incubation with an HRP-conjugated secondary antibody and the addition of OPD substrate. Cutoff measurements were obtained using serum from an unvaccinated goat in place of the primary antibody. Each data point represents the average of triplicate wells.

Production and purification of TMV-EFCA

To create the PA domain-TMV viral nanoparticles, a large stock of TMV-EFCA was first made by rub-inoculating purified TMV-EFCA onto the leaves of *N. benthamiana* plants. Following PEG precipitation, SDS-PAGE analysis showed that the majority of TMV-EFCA was in the clarification supernatant, although the addition of the EFCA residues did not change the molecular weight of the TMV coat protein enough to show a visible difference between TMV-EFCA and wild-type TMV on a Coomassie-stained gel (Figure 37a). Thus, to confirm the presence of TMV-EFCA, the clarification supernatant was used in docking reaction with GFP-InaD. GFP-InaD was added to TMV-EFCA followed by PEG-precipitation and centrifugation. Any undocked fusion protein remained in the supernatant, while any decorated or undecorated viral particles were found in the pellets. An SDS-PAGE analysis of the non-reduced reaction samples demonstrated that the newly-made TMV-EFCA was able to dock and lock to the GFP-InaD fusion protein (Figure 37b). The docked GFP-InaD band had an apparent molecular weight of approximately 60 kDa, while alone TMV-EFCA ran at 18 kDa and undocked GRP-InaD ran at 35 kDa (Figure 37b).

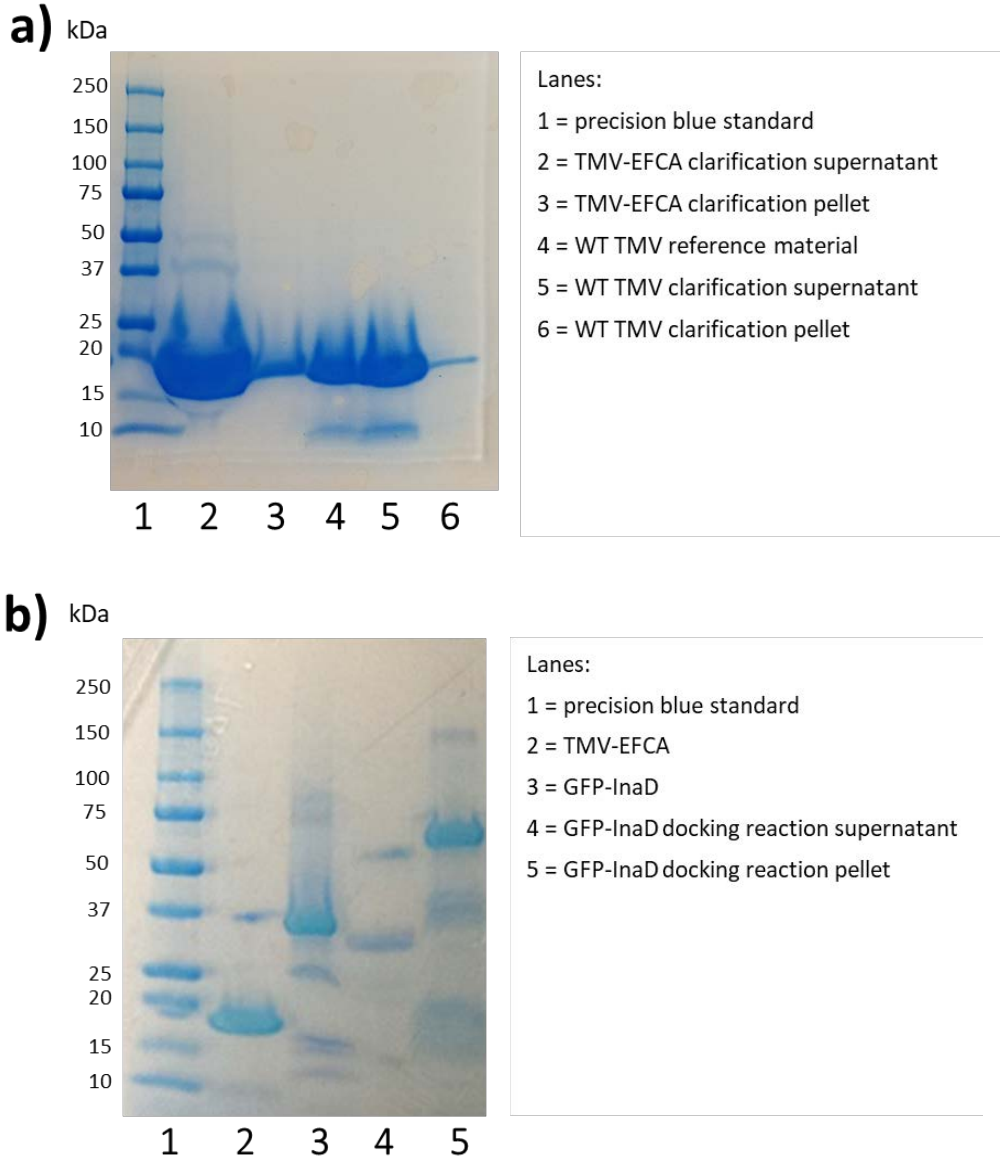

Figure 37. SDS-PAGE analysis of TMV-EFCA. **a)** TMV-EFCA and wild type TMV were extracted from *N. benthamiana* and purified by PEG precipitation, reduced samples from the subsequent clarification process were analyzed by SDS-PAGE. **b)** GFP-InaD was docked onto TMV-EFCA, followed by PEG precipitation and centrifugation to pellet the viral nanoparticles. Non-reduced samples from the docking reaction as well as the individual components of the docking reaction were analyzed by SDS-PAGE.

Dock-and-Lock reactions to create VNPs

To create PAD-TMV viral nanoparticles, dock-and-lock reactions were performed to covalently attach the PAD-InaD fusion proteins expressed in *E. coli* (Table 11) to the TMV-EFCA virus scaffold. Docking tests were performed by adding 10 µg of the virus scaffold to a molar excess of purified PAD fusion protein in reaction buffer. Following a 30 min incubation at room temperature, the viral particles

were precipitated by adding PEG to a final concentration of 4% and NaCl to 0.6 M. After incubating the mixture on ice, centrifugation separated the precipitated viral particles (pellet) from any undocked PAD fusion proteins (supernatant) and SDS-PAGE was used to analyze the results. Figure 38a demonstrates that docking purified PAD1-InaD to TMV-EFCA produced VNPs with coat proteins of approximately 70 kDa and that in the presence of a reducing agent, the PAD1-TMV coat proteins is reduced to its constituent parts. In contrast, the *E. coli* -produced PAD1' fusion protein was not very concentrated and contained high amounts of co-purifying host-cell proteins, and these factors likely prevented PAD1'-InaD from docking to TMV-EFCA (Figure 38b). Interestingly, the co-purifying host-cell proteins were present in the "viral" pellet following PEG precipitation, suggesting that they may have been forming insoluble aggregates. If PAD1'-InaD were part of this insoluble aggregate, it would explain why it was unable to dock. Although the PAD2, PAD3, and PAD4 fusion proteins contained few host-cells proteins and were used at relatively high concentrations in the docking reactions, SDS-PAGE analysis revealed that the docking process was inefficient (Figure 38c, d), even though a concurrent GFP docking reaction worked well (Figure 38d). Additional docking reactions were performed with the PAD2, PAD3, and PAD4 fusion proteins using different ratios of fusion protein to TMV-EFCA produced similar results (data not shown).

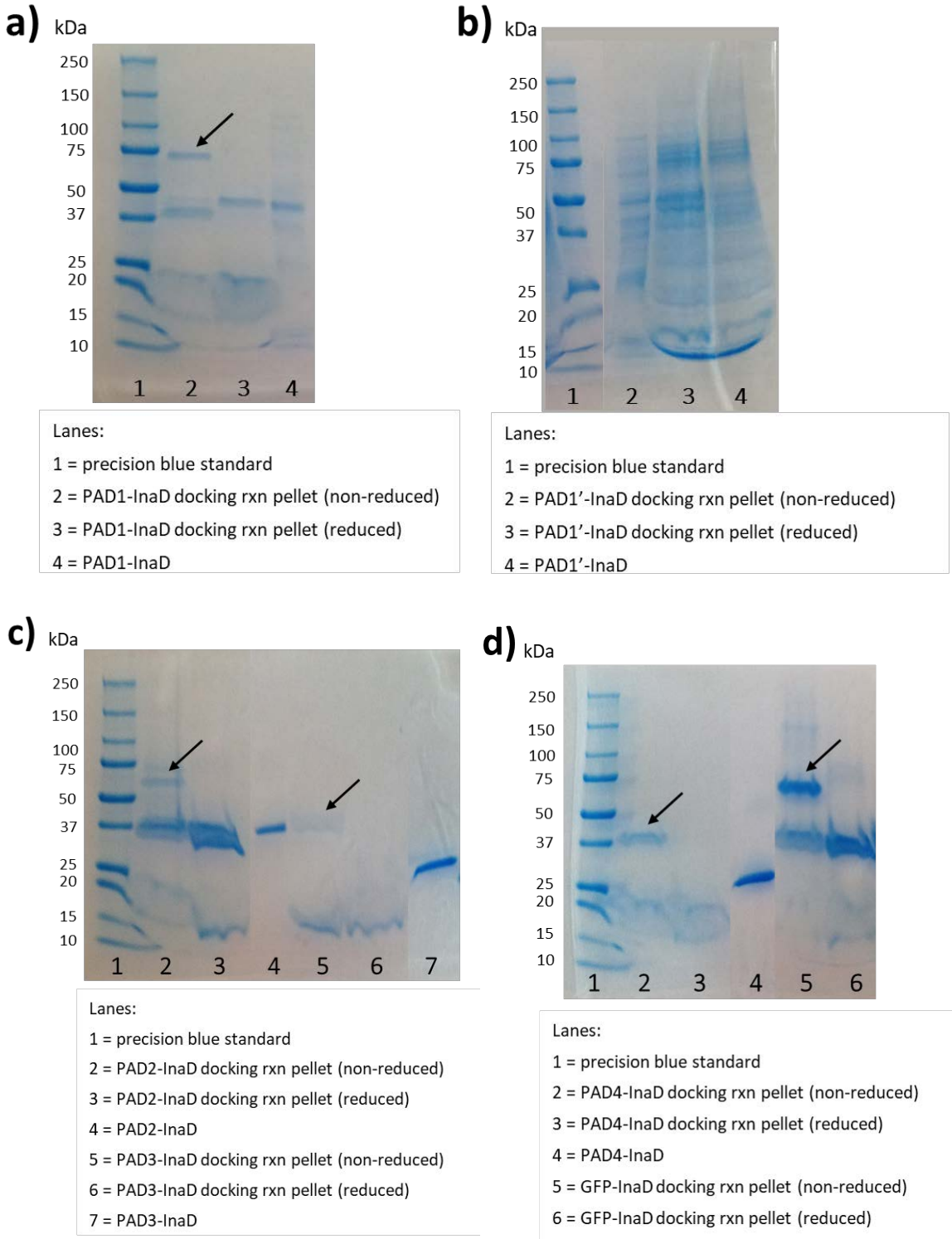

Figure 38. SDS-PAGE of docking reaction for *E. coli*-expressed PAD fusion proteins. Docking reactions were performed using TMV-EFCA and various fusion proteins, followed by PEG precipitation and centrifugation to pellet the viral nanoparticles. The purified fusion proteins, along with non-reduced and reduced samples from the docking reactions were run on SDS-PAGE. **a)** PAD1-InaD. **b)** PAD1'-InaD. **c)** PAD2-InaD and PAD3-InaD. **d)** PAD4-InaD and GFP-InaD. Where applicable, black arrows indicate docked fusion protein.

DISCUSSION

As an alternative to the viral nanoparticles discussed in the previous chapter, in which small linear epitopes were genetically fused to the TMV coat protein, this chapter explored the Dock-and-Lock system. The potential advantages of this method include the ability to display epitopes on TMV that might otherwise cause necrosis or inhibit viral assembly and the capacity to attach large, structurally complex antigens to the surface of TMV. However, this method necessitates the production and purification of fusion proteins in an appropriate expression system. Selecting an expression system for the production of recombinant proteins depends on several factors, including posttranslational modifications, disulfide bonds, and the destination of the expressed protein [678]. The PA domain portion of the fusion protein is prokaryotic, and the InaD portion is eukaryotic, which suggested it could be expressed in either a prokaryotic or eukaryotic expression system. Thus, eukaryotic plant-based expression in *N. benthamiana* and prokaryotic expression in *E. coli* were attempted.

Plant-based Expression of PA Fusion proteins

While protein expression levels in *N. benthamiana* using TMV expression vectors is dependent on the recombinant protein being produced, yields between 100 µg and 5 mg of protein per gram of fresh leaf biomass are common [138,176,679,680]. Smith *et al*. used a TMV vector to produce streptavidin-antigen fusion proteins in *N. benthamiana* and recovered 60–120 µg of functional protein per gram of leaf tissue [681]. The estimated yields for the two PAD fusion proteins expressed in *N. benthamiana*, which were on the order of ng/g (Table 11), proved to be at least an order of magnitude lower than the customary yield from this production system. The low yields for PAD1'-InaD and PAD1-InaD were initially ascribed to either *in planta* degradation or low expression levels, and expression of the PAD2, PAD3, and PAD4 fusion proteins in *N. benthamiana* was not attempted until a solution could be found to the low yield problem. Because harvesting leaf tissue at different DPIs and stabilizing the protein by

adding protease inhibitors to the plant cell extracts did not increase the yields of PAD1'-InaD and PAD1-InaD (data not shown), the addition of signal sequences was considered. For example, adding regulatory elements, such as PR1a and KDEL, has been shown to increase expression levels and improve yields [682,683]. However, adding these signal sequences would have required re-cloning all five constructs and increased yield were not a guarantee. Neither the PA portion nor the InaD portion of the fusion proteins contains post-translational modifications, so a prokaryotic expression host was used as an alternative.

E. coli-based Expression of PA Fusion Proteins

The advantages of using an *E. coli*- based expression system include ease of transformation, rapid growth, straightforward culturing techniques using inexpensive media, and high yields [684]. However, recombinant proteins expressed at high levels in the cytoplasm are prone to aggregation and can form inclusion bodies in which proteins are not properly folded, are insoluble, and/or have incorrect disulfide bonds. While inclusion bodies can protect proteins from proteolysis, the denatured proteins must be extracted using denaturing agents and then refolded into a more native conformation, which can lead to low final yields [669]. The PAD2, PAD3, and PAD4 fusion proteins were found in the insoluble fraction after cell lysis and thus had likely formed inclusion bodies. However, this was not a problem as native PA_{83} contains no cysteine residues (i.e., does not contain disulfide bonds) and the portion of InaD used for dock-and-lock contains only one cysteine residue.

Furthermore, the insoluble PAD fusion proteins were easily denatured with urea and then refolded on the Ni-NTA column with final yields of purified protein in the milligrams per liter range. While yields from *E. coli* are process and protein-dependent, they generally range from 0.1 mg to 1 g of protein per liter of cell culture [680,685-689], and recombinant soluble PA has been expressed in *E. coli* at 1.5 to 125 mg/L [690,691]. Other studies have shown that PA domains can be successfully produced in *E. coli* at yields ranging from 1-43 mg/L [692,693]. Given all this, it is fair to say that the yields of recombinant PAD2-InaD, PAD3-InaD, and PAD4-InaD were moderate.

PelB

A variety of strategies can be employed to overcome low expression problems in *E. coli* including the use of different promoters, the use of different host strains, co-expression of chaperones, reduction of culture temperature, and the use of secretion signals to target the proteins to the periplasm or culture medium [694]. Although the focus of this project was not the optimization of protein production/purification, several different strategies were employed to increase the yield of the PAD1' and PAD1 fusion proteins. Although protease inhibitors were used during the purification processes for PAD1'-InaD and PAD1-InaD, *in vivo* proteolytic degradation may have been at least partially responsible for the low yields that were initially observed. The periplasmic space contains less proteolytic enzymes and other host cells proteins than the cytoplasm [694], and a secretory signal sequence, such as the PelB sequence from *Erwinia carotovora*, can be added to the N-terminus of a recombinant protein to direct it to the periplasmic space in *E. coli*. Following secretion into the periplasm, the secretory signal is cleaved off by a signal peptidase, and the recombinant protein can be harvested by disrupting the outer membrane to and separating the periplasmic proteins from the spheroplasts. While using PelB to target PAD1'-InaD and PAD1-InaD to the periplasmic space did result in less host-cell protein contaminants, only a fraction of the fusion proteins was actually secreted into the periplasmic space. To ensure maximum yields of the problematic fusion proteins, the periplasmic fractions and the insoluble cell pellets were combined before purification. In summary, although the final yields from adding PelB signal sequence ending up being similar to the yields seen before PelB was added, inefficient secretion into the periplasmic space meant that these yields could not be achieved without using other fractions containing the same host cell proteins that were a problem in the first place.

MBP

Adding MBP to the N-terminus of the PAD1' and PAD1 fusion proteins led to increased expression, but only about half of the crude protein was soluble. This was, however, a vast

improvement over the crude yields seen with the previous constructs. In addition, reducing the temperature to 15°C after IPTG induction or optimizing protein folding may have resulted in increased solubility [695]. Purification on Ni-NTA resin was efficient, but the subsequent HRV 3C cleavage, while highly specific, proved to be only partially effective. Adding additional protease may have resulted in more efficient cleavage, but the GST-tagged HRV 3C protease and the glutathione resin required to remove the protease are quite expensive, so this was not attempted. The third step in the purification process, removing cleaved MBP and the remaining uncleaved MBP fusion proteins using amylose resin, proved to be the most inefficient step as the MBP didn't bind well to the resin. This could have been caused by low intrinsic affinity of the MBP fusion proteins to the amylose or the presence of cellular components or buffer reagents that interfered with binding [695], but glucose was added to the culture media to repress amylase expression, and the column buffer did not contain nonionic detergents. Thus, low intrinsic affinity caused by the PAD-InaD fusion proteins blocking or distorting the maltose-binding site may have been the problem. In summation, the MBP fusion protein constructs led to moderate expression of soluble MBP-PAD1'-InaD and MBP-PAD1-InaD, however, the multistep purification process and inefficient binding of residual MBP to the amylose column ultimately resulted in low yields and the presence of both MBP-related contaminants as well as degradation products.

Ultimately, both PAD1'-InaD and PAD1-InaD proved challenging to express. Because the other fusion proteins (i.e., PAD2-InaD, PAD3-InaD, and PAD4-InaD) were efficiently expressed in the pSX2 vector, the vector was not likely the problem. Instead, the low yield may have been due to issues with the stability and translational efficiency of the mRNA, *in vivo* degradation by host cell proteases, or the inherent toxicity of the protein to the host. Strategies such as enhancing mRNA stability, targeting proteins to different cellular compartments, codon optimization, using molecular chaperones or fusion partner proteins, and/or increasing the stability of the protein to minimize proteolysis may have yielded better results [696]. Several of these strategies were employed, but none resulted in final yields sufficient

to create VNPs using the Dock-and-Lock method. Interestingly, other groups have not had the same problems expressing PA domain 1 [646,692,693,697], although one group did note that three of their domain 1-containing constructs were particularly susceptible to degradation [693].

While the development of these PAD viral nanoparticle vaccines could proceed without the PAD1 and PAD1' VNPs, domain 1 accounts for more than a third of the molecular weight of PA_{83} and multiple studies have shown that this domain contains neutralizing epitopes. Abboud *et al*. found PAD1, and particularly the area around the furin cleavage site, to be highly immunogenic in mice and capable of eliciting LT-neutralizing antibodies [646]. This is in line with other studies that have reported similar observations about the ability of PA domain 1 epitopes to elicit LT-neutralizing antibodies [651,693,698,699]. On the other hand, Crowe *et al.* noted that antibodies directed to the furin cleavage site only provided moderate protection to mice, suggesting that furin cleavage and subsequent binding of LF may occur before the PAD1 antibodies can bind to their target [651]. Instead, antibodies targeting epitopes in the receptor-binding portion of PAD4 and the LF-binding region of PAD1' were shown to provide more robust *in vivo* protection against an LT challenge. Results from other *in vivo* challenge studies have suggested that neutralizing epitopes are primarily found in PA domains 1, 2, and 4 [693,700], and the contributions of PAD1 to protective immunity cannot be discounted.

Docking reactions

Chemically conjugating heterologous protein antigens to the surface of TMV avoids the potentially destabilizing effects of genetically fusing antigens to the coat protein [701]. Such chemical conjugation is facilitated by the presence of reactive side chains, like those found in cysteine, lysine, and glutamate; however, none of these reactive side chains are present on the outer surface assembled TMV virions [183]. In the Dock-and-Lock system, a cysteine residue is added to the C-terminus of the TMV coat protein, and recombinant protein antigens that also contain free cysteine residues can then be docked to the to TMV nanoparticles and used as VNP vaccines. As demonstrated in this work, the

production of such VNPs ultimately depends on the efficiency with which the purified fusion proteins could be docked to TMV-EFCA. Issues with process impurities and low final concentration resulted in inefficient docking of PAD1'-InaD, whether it was expressed in *N. benthamiana* or *E. coli.* Given the slightly higher yields and lower levels of impurities, the *E. coli*-produced PAD1-InaD was able to be concentrated more than PAD1'-InaD during the purification process, which resulted in more efficient docking (Figure 38a). Docking proteins to TMV-EFCA seems to work best when the InaD fusion protein is highly concentrated, soluble, and relatively free of process impurities. In our study, GFP-InaD was provided at a concentration of 2.7 μg/μL, was soluble in the docking reaction buffer, and docked well (Figure 37b). In addition, the free cysteine residue on both TMV-EFCA and the InaD fusion protein needs to be available for docking to occur. Using antioxidants or reducing agents during extraction and purification minimizes unwanted crosslinking among fusion proteins or between the fusion proteins and host-cell proteins prior to docking. Although BME was used during extraction/purification of the fusion proteins, BME is volatile and may have evaporated, leading to an oxidizing environment in which these unwanted disulfide bonds could form.

Additionally, if the cysteine-containing region of the InaD fusion protein is sterically hindered, docking efficiency would likely decrease. Such hindrance could be caused by the three-dimensional structure formed by the individual fusion protein or be caused by aggregation (with or without host cells proteins). Li *et al.* also demonstrated that regardless of the location, adding foreign cysteine residues to TMV led to the formation of distorted and unstable viral particles [702], so it may be the TMV-EFCA rather than the fusion proteins that are responsible for inefficient docking. However, if this were the case, one would expect to see inefficient docking with all fusion proteins rather than just a few. In summation, if inefficient docking is not caused by the inherent properties of the fusion protein, then optimizing the concentration and solubility of the fusion protein and ensuring the fusion protein is in a reduced state and relatively free of process impurities may increase docking efficiency.

Dock-and-Lock is not the only means of conjugating antigens to the surface of TMV though. The tyrosine 139 residue on wild-type TMV has been used to facilitate functionalization through diazonium-coupling [703] and copper(I)-catalyzed azide-alkyne cycloaddition [704]. Other groups have genetically modified TMV to contain surface-exposed lysine residues [183,681,705] or cysteine residues [183,186,190] and used *N*-hydroxysuccinimide(NHS) ester, thioether, or hydrazone linkages to conjugate antigens to the surface of TMV. For example, Smith *et al*. produced TMV-lysine virions with an NHS-biotin linkage and then chemically conjugated it to streptavidin fusion proteins containing the papillomavirus L2 epitope [681]. These systems have their own problems as TMV surface modifications tend to reduce the yield of virions, make them more prone to aggregation, and decrease their solubility [681,702,705]. Furthermore, when McCormick *et al.* compared the immune response characteristics to TMV-epitope conjugates and same epitope that had been genetically fused to the TMV coat protein, they found that the genetic fusion was vastly superior [183].

Animal studies

The western blot and ELISA data presented here show that anti-PA_{83} antibodies are able to bind to recombinant PAD fusion proteins, suggesting they may be in their native conformation, or at least close to their native conformation. Once sufficient quantities the PAD-TMV viral nanoparticles are prepared, the next steps would be to test their immunogenicity in mice and then conduct challenge studies. Such studies by other groups have already shown that recombinant PA domains are immunogenic in mice and induce the production of high levels of IgG with a strong bias toward a T_h2 type response (i.e., IgG1)[646,692,693,697], and repeating such experiments might be unnecessary.

Abboud *et al*. demonstrated that PA domain immunogenicity seems to be more a function of the genetic background of the mouse rather than the characteristics of the domains themselves [646]. Indeed, when it comes to post-vaccination challenge studies, the protection provided by PA-based vaccines may depend on the species of animal used because primary virulence factors and pathogenic

mechanisms differ from species to species [571,706,707]. For example, in mice, the PGA capsule of *B. anthracis* is more virulent than the toxins, and AVA immunizations were not able to protect mice from a spore challenge [707-709]. Any future animal studies using these PAD-TMV VNPs would have to take these factors into account. If anything, the primary aim of animal studies using these VNPs would be to provide insight into the increased immunogenicity of the domains when displayed on TMV and their ability to induce a cellular immune response, which is currently lacking in current PA-based vaccines [710].

Alternative *B. anthracis* antigens

AVA and the U.K.-licensed anthrax vaccine precipitated (AVP) both induce PA-specific antibody responses that are presumably the primary mediators of protection. However, while AVA contains only trace amounts of LF and EF [605], AVP contains detectable levels of both LF and EF [711]. LF-specific antibodies induced by immunization with AVP have been shown to predict *in vitro* neutralization of LT [712], and LF-based vaccines conferred complete protection in mice challenged with B. anthracis spores [713]. LF is also the main target of T cell immunity, and researchers have noted strong $CD4^+$ T cell responses to LF following natural cases of cutaneous anthrax infection as well as in AVP vaccinees [537]. However, while natural cases of anthrax lead to abroad T cell response that includes a variety of Th subsets and cytokines, the T cell response in AVP vaccinated individuals is significantly reduced with a skewed cytokines response and helper T cell polarization [614,714-716]. Infected individuals also have a strong $CD4^+$ T cell response to PA, but vaccinees had a very low response [614], which may be why PA-based vaccines do not elicit long-lasting protection. Coupled with data showing that there is a significant correlation between the duration of infection and T cell immunity to PA, these data suggest that T cell immune responses are just as crucial as B cells responses and that LF-specific immune responses should not be discounted. EF-specific antibodies may also contribute to edema toxin neutralization, although their overall contribution to survival has not been determined [717]. In addition, several groups have developed conjugate vaccines containing other *B. anthracis* antigens, including the PGA found on the capsid of *B.*

anthracis [639,718,719] and spore antigens [537,720], which have shown to provide protection in animal models. Overall, these studies suggest that including LF/EF antigens, recombinant spore antigens, peptidoglycan antigens, and T cell antigens in candidate anthrax vaccines may confer an increased level of protection and elicit longer-lasting immune responses than vaccines based solely on PA. Thus, if subsequent animal studies show that the PAD-TMV VNPs do not elicit a protective and long-lasting immune response, including alternative *B. anthracis* antigens may be beneficial. This could be accomplished by creating additional TMV VNPs displaying these alternative antigens and including them in a multivalent vaccine with the PAD-TMV VNPs.

CONCLUSION

The Commission on the Prevention of Weapons of Mass Destruction Proliferation and Terrorism has stated that medical countermeasures, such as vaccines, are critically important to protect civilians in the event of a bioterror attack, and that the United States is "seriously lacking" in this vital capability [721]. Currently, the only U.S.-licensed anthrax vaccine is AVA, which is expensive to produce and has questionable safety and efficacy. AVA is primarily composed of PA, which plays a critical role during anthrax infection as heptameric PA_{63} forms the pore that allows the EF and LF toxins to enter host cells and exert their cytotoxic activities. TMV viral nanoparticles displaying PA domains could potentially provide a safer, more effective, and economical alternative to AVA, and so we employed the Dock-and-Lock system to create these PAD-TMV VNPs. While difficulties were encountered in the expression of PAD1'-InaD and PAD1-Inad, recombinant PA domain 2, 3 and 4 fusion proteins were successfully expressed as inclusion bodies in an *E. coli* host and then refolded on Ni-NTA columns. All three fusion proteins were recognized by an anti-PA_{83} antibody in both western blots and ELISAs, suggesting near-native conformations were maintained. Conjugating these fusion proteins to TMV was accomplished using the Dock-and-Lock system, which utilizes a simple covalent linkage rather than the complicated

bifunctional chemical cross-linking used to create other VNP vaccines. This investigation has laid the groundwork for testing these VNPs *in vivo* to determine their utility as anthrax vaccine candidates. In addition, this method could easily be applied to attach other anthrax antigens, such as those found on LF, to TMV.

REFERENCES

1. Thompson, M. R., Kaminski, J. J., Kurt-Jones, E. A. & Fitzgerald, K. A. Pattern recognition receptors and the innate immune response to viral infection. *Viruses* **3**, 920-940, doi:10.3390/v3060920 (2011).
2. Janeway, C. J., Travers, P. & Walport, M. in *Immunobiology: The Immune System in Health and Disease.* (Garland Science, 2001).
3. Garred, P. *et al.* A journey through the lectin pathway of complement-MBL and beyond. *Immunol Rev* **274**, 74-97, doi:10.1111/imr.12468 (2016).
4. Monie, T. P. Section 1- A Snapshot of the Innate Immune System in *The Innate Immune System*, 1-40 (Academic Press, 2017).
5. Vidya, M. K. *et al.* Toll-like receptors: Significance, ligands, signaling pathways, and functions in mammals. *Int Rev Immunol* **37**, 20-36, doi:10.1080/08830185.2017.1380200 (2018).
6. Kim, Y. K., Shin, J. S. & Nahm, M. H. NOD-Like Receptors in Infection, Immunity, and Diseases. *Yonsei Med J* **57**, 5-14, doi:10.3349/ymj.2016.57.1.5 (2016).
7. Ozaki, K. & Leonard, W. J. Cytokine and cytokine receptor pleiotropy and redundancy. *Journal of Biological Chemistry* **277**, 29355-29358 (2002).
8. Zundler, S. & Neurath, M. F. Interleukin-12: Functional activities and implications for disease. *Cytokine & Growth Factor Reviews* **26**, 559-568, doi:https://doi.org/10.1016/j.cytogfr.2015.07.003 (2015).
9. Uribe-Querol, E. & Rosales, C. Control of Phagocytosis by Microbial Pathogens. *Front Immunol* **8**, 1368, doi:10.3389/fimmu.2017.01368 (2017).
10. Alcami, A., Symons, J. A., Collins, P. D., Williams, T. J. & Smith, G. L. Blockade of chemokine activity by a soluble chemokine binding protein from vaccinia virus. *J Immunol* **160**, 624-633 (1998).

11. Luckheeram, R. V., Zhou, R., Verma, A. D. & Xia, B. $CD4^+$T cells: differentiation and functions. *Clinical & developmental immunology* **2012**, 925135-925135, doi:10.1155/2012/925135 (2012).
12. Liston, A. in *Progress in Molecular Biology and Translational Science* Vol. 92 (ed. Adrian Liston) 1-3 (Academic Press, 2010).
13. Farrar, J. D., Asnagli, H. & Murphy, K. M. T helper subset development: roles of instruction, selection, and transcription. *The Journal of clinical investigation* **109**, 431-435, doi:10.1172/JCI15093 (2002).
14. Zhu, J. T helper 2 (Th2) cell differentiation, type 2 innate lymphoid cell (ILC2) development and regulation of interleukin-4 (IL-4) and IL-13 production. *Cytokine* **75**, 14-24, doi:10.1016/j.cyto.2015.05.010 (2015).
15. Zhu, J. & Paul, W. E. CD4 T cells: fates, functions, and faults. *Blood* **112**, 1557, doi:10.1182/blood-2008-05-078154 (2008).
16. Janeway, C. J., Travers, P. & Walport, M. *Immunobiology: The Immune System in Health and Disease.* 5th edition, (Garland Science, 2001).
17. Kovacsovics-Bankowski, M., Clark, K., Benacerraf, B. & Rock, K. L. Efficient major histocompatibility complex class I presentation of exogenous antigen upon phagocytosis by macrophages. *Proc Natl Acad Sci USA* **90**, 4942-4946, doi:10.1073/pnas.90.11.4942 (1993).
18. Harding, C. V. & Song, R. Phagocytic processing of exogenous particulate antigens by macrophages for presentation by class I MHC molecules. *J Immunol* **153**, 4925-4933 (1994).
19. Joffre, O. P., Segura, E., Savina, A. & Amigorena, S. Cross-presentation by dendritic cells. *Nat Rev Immunol* **12**, 557-569, doi:10.1038/nri3254 (2012).
20. Raff, M., Alberts, B., Lewis, J., Johnson, A. & Roberts, K. *Molecular Biology of the Cell.* 4th edition. (National Center for Biotechnology Information Bookshelf, 2002).

21. Rahimi, R. A. & Luster, A. D. in *Advances in Immunology.* Vol. 138 (ed. Frederick Alt) 71-98 (Academic Press, 2018).
22. Hoffman, W., Lakkis, F. G. & Chalasani, G. B Cells, Antibodies, and More. *Clinical Journal of the American Society of Nephrology* **11**, 137, doi:10.2215/CJN.09430915 (2016).
23. Siemasko, K. & Clark, M. R. The control and facilitation of MHC class II antigen processing by the BCR. *Current Opinion in Immunology* **13**, 32-36, doi:https://doi.org/10.1016/S0952-7915(00)00178-3 (2001).
24. Nutt, S. L., Hodgkin, P. D., Tarlinton, D. M. & Corcoran, L. M. The generation of antibody-secreting plasma cells. *Nature Reviews Immunology* **15**, 160, doi:10.1038/nri3795 (2015).
25. Inoue, T., Moran, I., Shinnakasu, R., Phan, T. G. & Kurosaki, T. Generation of memory B cells and their reactivation. *Immunological Reviews* **283**, 138-149, doi:10.1111/imr.12640 (2018).
26. Yoshida, T. *et al.* Memory B and memory plasma cells. *Immunological Reviews* **237**, 117-139, doi:10.1111/j.1600-065X.2010.00938.x (2010).
27. Lu, L. L., Suscovich, T. J., Fortune, S. M. & Alter, G. Beyond binding: antibody effector functions in infectious diseases. *Nat Rev Immunol* **18**, 46-61, doi:10.1038/nri.2017.106 (2018).
28. Hooper, D. C. Plant vaccines: an immunological perspective. *Curr Top Microbiol Immunol* **332**, 1-11, doi:10.1007/978-3-540-70868-1_1 (2009).
29. Fishman, J. M., Wiles, K. & Wood, K. J. The acquired immune system response to biomaterials, including both naturally occurring and synthetic biomaterials in *Host Response to Biomaterials* (ed. Stephen Badylak) 151-187 (Elsevier, 2015).
30. Micoli, F., Adamo, R. & Costantino, P. Protein Carriers for Glycoconjugate Vaccines: History, Selection Criteria, Characterization and New Trends. *Molecules* **23**, doi:10.3390/molecules23061451 (2018).

31. Bastola, R. *et al.* Vaccine adjuvants: smart components to boost the immune system. *Arch Pharm Res* **40**, 1238-1248, doi:10.1007/s12272-017-0969-z (2017).
32. Monie, T. P. Section 5- Connecting the Innate and Adaptive Immune Responses in *The Innate Immune System* (ed. Tom P. Monie) 171-187 (Academic Press, 2017).
33. Cunningham, A. L. *et al.* Vaccine development: From concept to early clinical testing. *Vaccine* **34**, 6655-6664, doi:10.1016/j.vaccine.2016.10.016 (2016).
34. Wang, D. L. *et al.* Post-exposure prophylaxis vaccination rate and risk factors of human rabies in mainland China: a meta-analysis. *Epidemiol Infect*, 1-6, doi:10.1017/s0950268818003175 (2018).
35. Macartney, K., Heywood, A. & McIntyre, P. Vaccines for post-exposure prophylaxis against varicella (chickenpox) in children and adults. *Cochrane Database of Systematic Reviews*, doi:10.1002/14651858.CD001833.pub3 (2014).
36. Cheever, M. A. & Higano, C. S. PROVENGE (Sipuleucel-T) in prostate cancer: the first FDA-approved therapeutic cancer vaccine. *Clinical Cancer Research* **17**, 3520-3526 (2011).
37. Thomas, S. & Prendergast, G. C. Cancer Vaccines: A Brief Overview. *Methods Mol Biol* **1403**, 755-761, doi:10.1007/978-1-4939-3387-7_43 (2016).
38. Delany, I., Rappuoli, R. & De Gregorio, E. Vaccines for the 21st century. *EMBO Mol Med* **6**, 708-720, doi:10.1002/emmm.201403876 (2014).
39. Bachmann, M. F. & Jennings, G. T. Vaccine delivery: a matter of size, geometry, kinetics and molecular patterns. *Nature Reviews Immunology* **10**, 787, doi:10.1038/nri2868 (2010).
40. Pulendran, B. & Ahmed, R. Immunological mechanisms of vaccination. *Nature immunology* **12**, 509-517, doi:10.1038/ni.2039 (2011).
41. Cohen, J. How long do vaccines last? The surprising answers may help protect people longer. *Science*, doi:10.1126/science.aax7364 (2019).

42. Sallusto, F., Lanzavecchia, A., Araki, K. & Ahmed, R. From vaccines to memory and back. *Immunity* **33**, 451-463, doi:10.1016/j.immuni.2010.10.008 (2010).

43. Penney, C. A., Thomas, D. R., Deen, S. S. & Walmsley, A. M. Plant-made vaccines in support of the Millennium Development Goals. *Plant Cell Rep* **30**, 789-798, doi:10.1007/s00299-010-0995-5 (2011).

44. Smith, P. G. Concepts of herd protection and immunity. *Procedia in Vaccinology* **2**, 134-139 (2010).

45. Oyston, P. & Robinson, K. The current challenges for vaccine development. *J Med Microbiol* **61**, 889-894, doi:10.1099/jmm.0.039180-0 (2012).

46. World Health Organization, Global vaccine action plan 2011-2020. (2013).

47. Ada, G. Overview of vaccines and vaccination. *Mol Biotechnol* **29**, 255-272, doi:10.1385/mb:29:3:255 (2005).

48. Minor, P. D. Live attenuated vaccines: historical successes and current challenges. *Virology* **479**, 379-392 (2015).

49. Vetter, V., Denizer, G., Friedland, L. R., Krishnan, J. & Shapiro, M. Understanding modern-day vaccines: what you need to know. *Ann Med* **50**, 110-120, doi:10.1080/07853890.2017.1407035 (2018).

50. Fernandez, E. & Diamond, M. S. Vaccination strategies against Zika virus. *Current opinion in virology* **23**, 59-67 (2017).

51. Heinz, F. X. & Stiasny, K. Flaviviruses and flavivirus vaccines. *Vaccine* **30**, 4301-4306 (2012).

52. Wu, X., Smith, T. G. & Rupprecht, C. E. From brain passage to cell adaptation: the road of human rabies vaccine development. *Expert Rev Vaccines* **10**, 1597-1608, doi:10.1586/erv.11.140 (2011).

53. Fletcher, H. A. Sleeping Beauty and the Story of the Bacille Calmette-Guerin Vaccine. *MBio* **7**, doi:10.1128/mBio.01370-16 (2016).

54. Detmer, A. & Glenting, J. Live bacterial vaccines--a review and identification of potential hazards. *Microb Cell Fact* **5**, 23, doi:10.1186/1475-2859-5-23 (2006).

55. Bhardwaj, S. in *Pharmaceutical Medicine and Translational Clinical Research* (eds Divya Vohora & Gursharan Singh) 341-353 (Academic Press, 2018).

56. Moyle, P. M. & Toth, I. Modern subunit vaccines: development, components, and research opportunities. *ChemMedChem* **8**, 360-376, doi:10.1002/cmdc.201200487 (2013).

57. Silva, A. L., Soema, P. C., Slütter, B., Ossendorp, F. & Jiskoot, W. PLGA particulate delivery systems for subunit vaccines: Linking particle properties to immunogenicity. *Human vaccines & immunotherapeutics* **12**, 1056-1069, doi:10.1080/21645515.2015.1117714 (2016).

58. Liljeqvist, S. & Ståhl, S. Production of recombinant subunit vaccines: protein immunogens, live delivery systems and nucleic acid vaccines. *Journal of Biotechnology* **73**, 1-33, doi:https://doi.org/10.1016/S0168-1656(99)00107-8 (1999).

59. Malito, E. *et al.* Structural basis for lack of toxicity of the diphtheria toxin mutant CRM197. *Proceedings of the National Academy of Sciences* **109**, 5229, doi:10.1073/pnas.1201964109 (2012).

60. van der Heiden, M., Duizendstra, A., Berbers, G. A. M., Boots, A. M. H. & Buisman, A.-M. Tetanus Toxoid carrier protein induced T-helper cell responses upon vaccination of middle-aged adults. *Vaccine* **35**, 5581-5588, doi:https://doi.org/10.1016/j.vaccine.2017.08.056 (2017).

61. Hutter, J. & Lepenies, B. Carbohydrate-Based Vaccines: An Overview. *Methods Mol Biol* **1331**, 1-10, doi:10.1007/978-1-4939-2874-3_1 (2015).

62. Berti, F. & Adamo, R. Antimicrobial glycoconjugate vaccines: an overview of classic and modern approaches for protein modification. *Chem Soc Rev* **47**, 9015-9025, doi:10.1039/c8cs00495a (2018).

63. Plummer, E. M. & Manchester, M. Viral nanoparticles and virus-like particles: platforms for contemporary vaccine design. *Wiley Interdiscip Rev Nanomed Nanobiotechnol* **3**, 174-196, doi:10.1002/wnan.119 (2011).

64. Fuenmayor, J., Gòdia, F. & Cervera, L. Production of virus-like particles for vaccines. *New Biotechnology* **39**, 174-180, doi:https://doi.org/10.1016/j.nbt.2017.07.010 (2017).

65. Roldao, A., Mellado, M. C., Castilho, L. R., Carrondo, M. J. & Alves, P. M. Virus-like particles in vaccine development. *Expert Rev Vaccines* **9**, 1149-1176, doi:10.1586/erv.10.115 (2010).

66. Morabito, K. M. & Graham, B. S. Zika Virus Vaccine Development. *J Infect Dis* **216**, S957-s963, doi:10.1093/infdis/jix464 (2017).

67. Iurescia, S., Fioretti, D. & Rinaldi, M. Strategies for improving DNA vaccine performance. *Methods Mol Biol* **1143**, 21-31, doi:10.1007/978-1-4939-0410-5_3 (2014).

68. Bodles-Brakhop, A. M., Heller, R. & Draghia-Akli, R. Electroporation for the delivery of DNA-based vaccines and immunotherapeutics: current clinical developments. *Molecular Therapy* **17**, 585-592 (2009).

69. Larocca, R. A. *et al.* Vaccine protection against Zika virus from Brazil. *Nature* **536**, 474-478 (2016).

70. Morrison, C. DNA vaccines against Zika virus speed into clinical trials. *Nature Reviews Drug Discovery* **15**, 521-522 (2016).

71. Hobernik, D. & Bros, M. DNA Vaccines-How Far From Clinical Use? *International journal of molecular sciences* **19**, 3605, doi:10.3390/ijms19113605 (2018).

72. Martin, J. E. *et al.* A DNA Vaccine for Ebola Virus Is Safe and Immunogenic in a Phase I Clinical Trial. *Clinical and Vaccine Immunology* **13**, 1267, doi:10.1128/CVI.00162-06 (2006).

73. Bhardwaj, D. *et al.* Immunogenicity and protective efficacy of three DNA vaccines encoding pre-erythrocytic- and erythrocytic-stage antigens of *Plasmodium cynomolgi* in rhesus monkeys. *Pathogens and Disease* **34**, 33-43, doi:10.1111/j.1574-695X.2002.tb00600.x (2002).

74. Kramps, T. & Probst, J. Messenger RNA-based vaccines: progress, challenges, applications. *Wiley Interdisciplinary Reviews: RNA* **4**, 737-749 (2013).

75. Reichmuth, A. M., Oberli, M. A., Jaklenec, A., Langer, R. & Blankschtein, D. mRNA vaccine delivery using lipid nanoparticles. *Therapeutic delivery* **7**, 319-334 (2016).

76. McNamara, M. A., Nair, S. K. & Holl, E. K. RNA-based vaccines in cancer immunotherapy. *Journal of immunology research* **2015** (2015).

77. Karikó, K. *et al.* Incorporation of pseudouridine into mRNA yields superior nonimmunogenic vector with increased translational capacity and biological stability. *Molecular therapy* **16**, 1833-1840 (2008).

78. Holtkamp, S. *et al.* Modification of antigen-encoding RNA increases stability, translational efficacy, and T-cell stimulatory capacity of dendritic cells. *Blood* **108**, 4009-4017 (2006).

79. Geall, A. J. *et al.* Nonviral delivery of self-amplifying RNA vaccines. *Proc Natl Acad Sci USA* **109**, 14604-14609, doi:10.1073/pnas.1209367109 (2012).

80. Ura, T., Okuda, K. & Shimada, M. Developments in Viral Vector-Based Vaccines. *Vaccines (Basel)* **2**, 624-641, doi:10.3390/vaccines2030624 (2014).

81. Larocca, C. & Schlom, J. Viral vector-based therapeutic cancer vaccines. *Cancer J* **17**, 359-371, doi:10.1097/PPO.0b013e3182325e63 (2011).

82. Gaspar, H. B. *et al.* Gene therapy of X-linked severe combined immunodeficiency by use of a pseudotyped gammaretroviral vector. *Lancet* **364**, 2181-2187, doi:10.1016/s0140-6736(04)17590-9 (2004).

83. Zhao, L. *et al.* Nanoparticle vaccines. *Vaccine* **32**, 327-337, doi:https://doi.org/10.1016/j.vaccine.2013.11.069 (2014).

84. Pachioni-Vasconcelos, Jde, A. *et al.* Nanostructures for protein drug delivery. *Biomater Sci* **4**, 205-218, doi:10.1039/c5bm00360a (2016).

85. Fredriksen, B. N. & Grip, J. PLGA/PLA micro- and nanoparticle formulations serve as antigen depots and induce elevated humoral responses after immunization of Atlantic salmon (*Salmo salar L.*). *Vaccine* **30**, 656-667, doi:10.1016/j.vaccine.2011.10.105 (2012).

86. Al-Halifa, S., Gauthier, L., Arpin, D., Bourgault, S. & Archambault, D. Nanoparticle-Based Vaccines Against Respiratory Viruses. *Frontiers in Immunology* **10**, 22 (2019).

87. Shao, K. *et al.* Nanoparticle-based immunotherapy for cancer. *ACS Nano* **9**, 16-30, doi:10.1021/nn5062029 (2015).

88. ovier, P. A. Epaxal: a virosomal vaccine to prevent hepatitis A infection. *Expert Rev Vaccines* **7**, 1141-1150, doi:10.1586/14760584.7.8.1141 (2008).

89. ilker, C. *et al.* Nanoparticle-based B-cell targeting vaccines: Tailoring of humoral immune responses by functionalization with different TLR-ligands. *Nanomedicine* **13**, 173-182, doi:10.1016/j.nano.2016.08.028 (2017).

90. Tao, C. Antimicrobial activity and toxicity of gold nanoparticles: research progress, challenges and prospects. *Lett Appl Microbiol* **67**, 537-543, doi:10.1111/lam.13082 (2018).

91. Narayanan, K. B. & Han, S. S. Recombinant helical plant virus-based nanoparticles for vaccination and immunotherapy. *Virus Genes* **54**, 623-637, doi:10.1007/s11262-018-1583-y (2018).

92. Stahl, S. J. & Murray, K. Immunogenicity of peptide fusions to hepatitis B virus core antigen. *Proc Natl Acad Sci USA* **86**, 6283-6287, doi:10.1073/pnas.86.16.6283 (1989).

93. Dale, C. J. *et al.* Chimeric human papilloma virus-simian/human immunodeficiency virus virus-like-particle vaccines: immunogenicity and protective efficacy in macaques. *Virology* **301**, 176-187 (2002).

94. Krammer, F. *et al.* Influenza virus-like particles as an antigen-carrier platform for the ESAT-6 epitope of Mycobacterium tuberculosis. *J Virol Methods* **167**, 17-22, doi:10.1016/j.jviromet.2010.03.003 (2010).

95. Damjanovic, D. *et al.* In vitro assessment of biological activity and stability of the ALVAC-HIV vaccine. *Vaccine* **36**, 5636-5644, doi:10.1016/j.vaccine.2018.07.034 (2018).

96. Terry, R. F., Yamey, G., Miyazaki-Krause, R., Gunn, A. & Reeder, J. C. Funding global health product R&D: the Portfolio-To-Impact Model (P2I), a new tool for modelling the impact of different research portfolios. *Gates Open Res* **2**, 24, doi:10.12688/gatesopenres.12816.2 (2018).

97. Han, S. Clinical vaccine development. *Clinical and experimental vaccine research* **4**, 46-53, doi:10.7774/cevr.2015.4.1.46 (2015).

98. Pronker, E. S., Weenen, T. C., Commandeur, H., Claassen, E. H., & Osterhaus, A. D. Risk in vaccine research and development quantified. *PloS one* **8**, e57755-e57755, doi:10.1371/journal.pone.0057755 (2013).

99. Gouglas, D. *et al.* Estimating the cost of vaccine development against epidemic infectious diseases: a cost minimisation study. *Lancet Glob Health* **6**, e1386-e1396, doi:10.1016/s2214-109x(18)30346-2 (2018).

100. World Health Organization. *10 facts on immunization*, <https://www.who.int/features/factfiles/immunization/en/> (2018).

101. World Health Organization. *Global Vaccine Action Plan*, <https://www.who.int/immunization/sage/meetings/2016/october/3_Regional_vaccine_action_plans_2016_progress_reports.pdf> (2016).

102. Kochhar, S. *et al.* Introducing new vaccines in developing countries. *Expert Rev Vaccines* **12**, 1465-1478, doi:10.1586/14760584.2013.855612 (2013).

103. Kumru, O. S. *et al.* Vaccine instability in the cold chain: mechanisms, analysis and formulation strategies. *Biologicals* **42**, 237-259, doi:10.1016/j.biologicals.2014.05.007 (2014).

104. Kis, Z., Shattock, R., Shah, N. & Kontoravdi, C. Emerging Technologies for Low-Cost, Rapid Vaccine Manufacture. *Biotechnology Journal* **14**, 1800376, doi:10.1002/biot.201800376 (2019).

105. Webby, R. J. & Webster, R. G. Are we ready for pandemic influenza? *Science* **302**, 1519-1522, doi:10.1126/science.1090350 (2003).

106. Milian, E. & Kamen, A. A. Current and Emerging Cell Culture Manufacturing Technologies for Influenza Vaccines. *Biomed Research International*, 11, doi:10.1155/2015/504831 (2015).

107. Gerdil, C. The annual production cycle for influenza vaccine. *Vaccine* **21**, 1776-1779 (2003).

108. Gallo-Ramirez, L. E., Nikolay, A., Genzel, Y. & Reichl, U. Bioreactor concepts for cell culture-based viral vaccine production. *Expert Rev Vaccines* **14**, 1181-1195, doi:10.1586/14760584.2015.1067144 (2015).

109. Legastelois, I. *et al.* Non-conventional expression systems for the production of vaccine proteins and immunotherapeutic molecules. *Hum Vaccin Immunother* **13**, 947-961, doi:10.1080/21645515.2016.1260795 (2017).

110. World Health Organization & Global Alliance for Vaccines and Immunizations. *Key Concepts: Economics of Vaccine Production*, <https://www.who.int/immunization/programmes_systems/financing/analyses/en/briefcase_vacproduction.pdf> (2012).

111. Serdobova, I. & Kieny, M.-P. Assembling a global vaccine development pipeline for infectious diseases in the developing world. *American journal of public health* **96**, 1554-1559, doi:10.2105/AJPH.2005.074583 (2006).

112. Régnier, S. A. & Huels, J. Drug versus vaccine investment: a modelled comparison of economic incentives. *Cost effectiveness and resource allocation : C/E* **11**, 23-23, doi:10.1186/1478-7547-11-23 (2013).

113. Fischer, R., Stoger, E., Schillberg, S., Christou, P. & Twyman, R. M. Plant-based production of biopharmaceuticals. *Current Opinion in Plant Biology* **7**, 152-158, doi:https://doi.org/10.1016/j.pbi.2004.01.007 (2004).

114. Chen, Q. Plant-made vaccines against West Nile virus are potent, safe, and economically feasible. *Biotechnol J* **10**, 671-680, doi:10.1002/biot.201400428 (2015).

115. Buyel, J. F. Plant Molecular Farming - Integration and Exploitation of Side Streams to Achieve Sustainable Biomanufacturing. *Frontiers in plant science* **9**, 1893-1893, doi:10.3389/fpls.2018.01893 (2019).

116. Marsian, J. & Lomonossoff, G. P. Molecular pharming - VLPs made in plants. *Curr Opin Biotechnol* **37**, 201-206, doi:10.1016/j.copbio.2015.12.007 (2016).

117. Nandi, S. *et al.* Techno-economic analysis of a transient plant-based platform for monoclonal antibody production. *MAbs* **8**, 1456-1466, doi:10.1080/19420862.2016.1227901 (2016).

118. Montero-Morales, L. & Steinkellner, H. Advanced Plant-Based Glycan Engineering. *Front Bioeng Biotechnol* **6**, 81, doi:10.3389/fbioe.2018.00081 (2018).

119. Giddings, G. Transgenic plants as protein factories. *Curr Opin Biotechnol* **12**, 450-454 (2001).

120. Gomord, V. *et al.* Plant-specific glycosylation patterns in the context of therapeutic protein production. *Plant Biotechnology Journal* **8**, 564-587, doi:10.1111/j.1467-7652.2009.00497.x (2010).

121. Ward, B. J. *et al.* Human antibody response to N-glycans present on plant-made influenza virus-like particle (VLP) vaccines. *Vaccine* **32**, 6098-6106, doi:10.1016/j.vaccine.2014.08.079 (2014).

122. Shaaltiel, Y. & Tekoah, Y. in *Nat Biotechnol* Vol. 34 706-708 (2016).

123. Castilho, A. *et al.* Proteolytic and N-glycan processing of human alpha1-antitrypsin expressed in *Nicotiana benthamiana*. *Plant Physiol* **166**, 1839-1851, doi:10.1104/pp.114.250720 (2014).

124. Dicker, M., Maresch, D. & Strasser, R. Glyco-engineering for the production of recombinant IgA1 with distinct mucin-type O-glycans in plants. *Bioengineered* **7**, 484-489, doi:10.1080/21655979.2016.1201251 (2016).

125. Castilho, A. *et al.* Engineering of sialylated mucin-type O-glycosylation in plants. *J Biol Chem* **287**, 36518-36526, doi:10.1074/jbc.M112.402685 (2012).

126. *Recombinant Human VEGF 165 Protein (NBC1-21359): Novus Biologicals*, <https://www.novusbio.com/products/vegf-165-recombinant-protein_nbc1-21359> (2019).

127. Yao, J., Weng, Y., Dickey, A. & Wang, K. Y. Plants as Factories for Human Pharmaceuticals: Applications and Challenges. *International journal of molecular sciences* **16**, 28549-28565, doi:10.3390/ijms161226122 (2015).

128. Stoger, E., Sack, M., Fischer, R. & Christou, P. Plantibodies: applications, advantages and bottlenecks. *Curr Opin Biotechnol* **13**, 161-166 (2002).

129. Holtz, B. R. *et al.* Commercial-scale biotherapeutics manufacturing facility for plant-made pharmaceuticals. *Plant Biotechnology Journal* **13**, 1180-1190, doi:10.1111/pbi.12469 (2015).

130. Commandeur, U., Twyman, R. M. & Fischer, R. The biosafety of molecular farming in plants. *AgBiotechNet* **5**, 1-9 (2003).

131. Marillonnet, S. *et al.* In planta engineering of viral RNA replicons: efficient assembly by recombination of DNA modules delivered by Agrobacterium. *Proc Natl Acad Sci U S A* **101**, 6852-6857, doi:10.1073/pnas.0400149101 (2004).

132. Sainsbury, F. & Lomonossoff, G. P. Extremely high-level and rapid transient protein production in plants without the use of viral replication. *Plant Physiol* **148**, 1212-1218, doi:10.1104/pp.108.126284 (2008).

133. Tremblay, R., Wang, D., Jevnikar, A. M. & Ma, S. Tobacco, a highly efficient green bioreactor for production of therapeutic proteins. *Biotechnology Advances* **28**, 214-221, doi:https://doi.org/10.1016/j.biotechadv.2009.11.008 (2010).

134. Avesani, L., Bortesi, L., Santi, L., Falorni, A. & Pezzotti, M. Plant-made pharmaceuticals for the prevention and treatment of autoimmune diseases: where are we? *Expert review of vaccines* **9**, 957-969 (2010).

135. Lienard, D., Sourrouille, C., Gomord, V. & Faye, L. Pharming and transgenic plants. *Biotechnol Annu Rev* **13**, 115-147, doi:10.1016/s1387-2656(07)13006-4 (2007).

136. Nochi, T. *et al.* Rice-based mucosal vaccine as a global strategy for cold-chain- and needle-free vaccination. *Proc Natl Acad Sci USA* **104**, 10986-10991, doi:10.1073/pnas.0703766104 (2007).

137. Tokuhara, D. *et al.* Secretory IgA-mediated protection against *V. cholerae* and heat-labile enterotoxin-producing enterotoxigenic *Escherichia col*i by rice-based vaccine. *Proc Natl Acad Sci U S A* **107**, 8794-8799, doi:10.1073/pnas.0914121107 (2010).

138. Gleba, Y. Y., Tuse, D. & Giritch, A. Plant viral vectors for delivery by Agrobacterium. *Curr Top Microbiol Immunol* **375**, 155-192, doi:10.1007/82_2013_352 (2014).

139. Beasley, D. 'Plantibodies' drugs advance as big pharma stands aside. (2014). https://www.reuters.com/article/us-health-ebola-plants-analysis-idUSKBN0GH0DU20140817

140. Buyel, J. F. & Fischer, R. Scale-down models to optimize a filter train for the downstream purification of recombinant pharmaceutical proteins produced in tobacco leaves. *Biotechnol J* **9**, 415-425, doi:10.1002/biot.201300369 (2014).

141. Buyel, J. F. & Fischer, R. Downstream processing of biopharmaceutical proteins produced in plants: the pros and cons of flocculants. *Bioengineered* **5**, 138-142, doi:10.4161/bioe.28061 (2014).

142. Xu, J., Ge, X. & Dolan, M. C. Towards high-yield production of pharmaceutical proteins with plant cell suspension cultures. *Biotechnol Adv* **29**, 278-299, doi:10.1016/j.biotechadv.2011.01.002 (2011).

143. Shama, L. & Peterson, R. K. The benefits and risks of producing pharmaceutical proteins in plants. *Risk Management Matters* **2**, 28-33 (2004).

144. Fischer, R., Schillberg, S., Hellwig, S., Twyman, R. M. & Drossard, J. GMP issues for recombinant plant-derived pharmaceutical proteins. *Biotechnol Adv* **30**, 434-439, doi:10.1016/j.biotechadv.2011.08.007 (2012).

145. Ma, J. K. *et al.* Plant-derived pharmaceuticals--the road forward. *Trends Plant Sci* **10**, 580-585, doi:10.1016/j.tplants.2005.10.009 (2005).

146. Ma, J. K. *et al.* Regulatory approval and a first-in-human phase I clinical trial of a monoclonal antibody produced in transgenic tobacco plants. *Plant Biotechnol J* **13**, 1106-1120, doi:10.1111/pbi.12416 (2015).

147. Kusnadi, A. R., Nikolov, Z. L. & Howard, J. A. Production of recombinant proteins in transgenic plants: Practical considerations. *Biotechnol Bioeng* **56**, 473-484, doi:10.1002/(sici)1097-0290(19971205)56:5<473::aid-bit1>3.0.co;2-f (1997).

148. D'Aoust, M. A. *et al.* The production of hemagglutinin-based virus-like particles in plants: a rapid, efficient and safe response to pandemic influenza. *Plant Biotechnol J* **8**, 607-619, doi:10.1111/j.1467-7652.2009.00496.x (2010).

149. Lomonossoff, G. P. & D'Aoust, M.-A. Plant-produced biopharmaceuticals: A case of technical developments driving clinical deployment. *Science* **353**, 1237, doi:10.1126/science.aaf6638 (2016).

150. McCormick, A. A. *et al.* Plant-produced idiotype vaccines for the treatment of non-Hodgkin's lymphoma: Safety and immunogenicity in a phase I clinical study. *Proceedings of the National Academy of Sciences* **105**, 10131, doi:10.1073/pnas.0803636105 (2008).

151. Shaaltiel, Y. *et al.* Production of glucocerebrosidase with terminal mannose glycans for enzyme replacement therapy of Gaucher's disease using a plant cell system. *Plant Biotechnol J* **5**, 579-590, doi:10.1111/j.1467-7652.2007.00263.x (2007).

152. Wilson, S. A. & Roberts, S. C. Recent advances towards development and commercialization of plant cell culture processes for the synthesis of biomolecules. *Plant Biotechnology Journal* **10**, 249-268, doi:10.1111/j.1467-7652.2011.00664.x (2012).

153. Tekoah, Y. *et al.* Large-scale production of pharmaceutical proteins in plant cell culture—the protalix experience. *Plant Biotechnology Journal* **13**, 1199-1208, doi:10.1111/pbi.12428 (2015).

154. Tuse, D., Tu, T. & McDonald, K. A. Manufacturing economics of plant-made biologics: case studies in therapeutic and industrial enzymes. *Biomed Res Int* **2014**, 256135, doi:10.1155/2014/256135 (2014).

155. Ma, J. K., Drake, P. M. & Christou, P. The production of recombinant pharmaceutical proteins in plants. *Nat Rev Genet* **4**, 794-805, doi:10.1038/nrg1177 (2003).

156. Yang, S. J., Carter, S. A., Cole, A. B., Cheng, N. H. & Nelson, R. S. A natural variant of a host RNA-dependent RNA polymerase is associated with increased susceptibility to viruses by *Nicotiana benthamiana*. *Proc Natl Acad Sci U S A* **101**, 6297-6302, doi:10.1073/pnas.0304346101 (2004).

157. Goodin, M. M., Zaitlin, D., Naidu, R. A. & Lommel, S. A. *Nicotiana benthamiana*: its history and future as a model for plant-pathogen interactions. *Mol Plant Microbe Interact* **21**, 1015-1026, doi:10.1094/mpmi-21-8-1015 (2008).

158. Davey, R. T., Jr. *et al.* A Randomized, Controlled Trial of ZMapp for Ebola Virus Infection. *N Engl J Med* **375**, 1448-1456, doi:10.1056/NEJMoa1604330 (2016).

159. *Investigational Therapeutics for the Treatment of People With Ebola Virus Disease - ClinicalTrials.gov*, <https://clinicaltrials.gov/ct2/show/NCT03719586> (2019).

160. Pillet, S. *et al.* Immunogenicity and safety of a quadrivalent plant-derived virus like particle influenza vaccine candidate-Two randomized Phase II clinical trials in 18 to 49 and >/=50 years old adults. *PLoS One* **14**, e0216533, doi:10.1371/journal.pone.0216533 (2019).

161. Sainsbury, F. Meeting report Virus-Like Particle and Nano-Particle Vaccines: Sessions 1 and 2: Plenary. *Human vaccines & immunotherapeutics* **10**, 3060-3063, doi:10.4161/21645515.2014.988552 (2014).

162. Tuse, D. *et al.* Clinical Safety and Immunogenicity of Tumor-Targeted, Plant-Made Id-KLH Conjugate Vaccines for Follicular Lymphoma. *Biomed Res Int* **2015**, 648143, doi:10.1155/2015/648143 (2015).

163. Lo, C. Blue Angel: DARPA's vaccine manufacturing challenge. *Pharmaceutical Technology* (2014).

164. Gleba, Y., Klimyuk, V. & Marillonnet, S. Magnifection--a new platform for expressing recombinant vaccines in plants. *Vaccine* **23**, 2042-2048, doi:10.1016/j.vaccine.2005.01.006 (2005).

165. *U.S. FDA Licenses Sanofi Pasteur's New Influenza Vaccine Manufacturing Facility*, <http://www.news.sanofi.us/press-releases?item=137045> (2009).

166. Tirell, M. *The $1.6 billion business of flu*, <https://www.cnbc.com/2015/10/19/the-16-billion-business-of-flu.html> (2015).

167. Chilton, M.-D. *et al.* Stable incorporation of plasmid DNA into higher plant cells: the molecular basis of crown gall tumorigenesis. *Cell* **11**, 263-271, doi:https://doi.org/10.1016/0092-8674(77)90043-5 (1977).

168. Yoshioka, Y. *et al.* Transient gene expression in plant cells mediated by *Agrobacterium tumefaciens:* application for the analysis of virulence loci. *Plant and cell physiology* **37**, 782-789 (1996).

169. Peyret, H. & Lomonossoff, G. P. When plant virology met Agrobacterium: the rise of the deconstructed clones. *Plant biotechnology journal* **13**, 1121-1135, doi:10.1111/pbi.12412 (2015).

170. Marton, L., Wullems, G., Molendijk, L. & Schilperoort, R. In vitro transformation of cultured cells from *Nicotiana tabacum* by *Agrobacterium tumefaciens*. *Nature* **277**, 129 (1979).

171. Kapila, J., De Rycke, R., Van Montagu, M. & Angenon, G. An Agrobacterium-mediated transient gene expression system for intact leaves. *Plant Science* **122**, 101-108, doi:https://doi.org/10.1016/S0168-9452(96)04541-4 (1997).

172. Sukenik, S. C. *et al.* Transient Recombinant Protein Production in Glycoengineered *Nicotiana benthamiana* Cell Suspension Culture. *Int J Mol Sci* **19**, doi:10.3390/ijms19041205 (2018).

173. Ibrahim, A., Odon, V. & Kormelink, R. Plant viruses in plant molecular pharming: towards the use of enveloped viruses. *Frontiers in Plant Science* **10**, 803 (2019).

174. Ahlquist, P. & Janda, M. cDNA cloning and in vitro transcription of the complete brome mosaic virus genome. *Mol Cell Biol* **4**, 2876-2882, doi:10.1128/mcb.4.12.2876 (1984).

175. Grimsley, N., Hohn, B., Hohn, T. & Walden, R. "Agroinfection," an alternative route for viral infection of plants by using the Ti plasmid. *Proc Natl Acad Sci USA* **83**, 3282-3286, doi:10.1073/pnas.83.10.3282 (1986).

176. Lindbo, J. A. High-efficiency protein expression in plants from agroinfection-compatible Tobacco mosaic virus expression vectors. *BMC biotechnology* **7**, 52 (2007).

177. Musiychuk, K. *et al.* A launch vector for the production of vaccine antigens in plants. *Influenza Other Respir Viruses* **1**, 19-25, doi:10.1111/j.1750-2659.2006.00005.x (2007).

178. European Medicines Agency. *Quality of biological active substances produced by stable transgene expression in higher plants*, <https://www.ema.europa.eu/en/quality-biological-active-substances-produced-stable-transgene-expression-higher-plants> (2008).

179. Schodel, F. *et al.* The position of heterologous epitopes inserted in hepatitis B virus core particles determines their immunogenicity. *J Virol* **66**, 106-114 (1992).

180. Porta, C. *et al.* Cowpea mosaic virus-based chimaeras. Effects of inserted peptides on the phenotype, host range, and transmissibility of the modified viruses. *Virology* **310**, 50-63 (2003).

181. Kemnade, J. O. *et al.* Tobacco mosaic virus efficiently targets DC uptake, activation and antigen-specific T cell responses in vivo. *Vaccine* **32**, 4228-4233, doi:10.1016/j.vaccine.2014.04.051 (2014).

182. Creager, A. N. H., Scholthof, K.-B. G., Citovsky, V. & Scholthof, H. B. Tobacco Mosaic Virus: Pioneering Research for a Century. *The Plant Cell* **11**, 301, doi:10.1105/tpc.11.3.301 (1999).

183. McCormick, A. A. & Palmer, K. E. Genetically engineered Tobacco mosaic virus as nanoparticle vaccines. *Expert Rev Vaccines* **7**, 33-41, doi:10.1586/14760584.7.1.33 (2008).

184. Steere, R. L. & Williams, R. C. Identification of Crystalline Inclusion Bodies Extracted Intact from Plant Cells Infected with Tobacco Mosaic Virus. *American Journal of Botany* **40**, 81-84, doi:10.2307/2438849 (1953).

185. Liu, R., Vaishnav, R. A., Roberts, A. M. & Friedland, R. P. Humans have antibodies against a plant virus: evidence from tobacco mosaic virus. *PLoS One* **8**, e60621, doi:10.1371/journal.pone.0060621 (2013).

186. Geiger, F. C. *et al.* TMV nanorods with programmed longitudinal domains of differently addressable coat proteins. *Nanoscale* **5**, 3808-3816, doi:10.1039/C3NR33724C (2013).

187. Kegel, W. K. & van der Schoot, P. Physical Regulation of the Self-Assembly of Tobacco Mosaic Virus Coat Protein. *Biophysical Journal* **91**, 1501-1512, doi:https://doi.org/10.1529/biophysj.105.072603 (2006).

188. Love, A. J., Makarov, V., Yaminsky, I., Kalinina, N. O. & Taliansky, M. E. The use of tobacco mosaic virus and cowpea mosaic virus for the production of novel metal nanomaterials. *Virology* **449**, 133-139, doi:https://doi.org/10.1016/j.virol.2013.11.002 (2014).

189. Koch, C. *et al.* Modified TMV Particles as Beneficial Scaffolds to Present Sensor Enzymes. *Frontiers in Plant Science* **6**, 1137 (2015).

190. Lee, S.-Y., Royston, E., Culver, J. N. & Harris, M. T. Improved metal cluster deposition on a genetically engineered tobacco mosaic virus template. *Nanotechnology* **16**, S435-S441, doi:10.1088/0957-4484/16/7/019 (2005).

191. Smith, M. L., Fitzmaurice, W. P., Turpen, T. H. & Palmer, K. E. Display of peptides on the surface of tobacco mosaic virus particles. *Curr Top Microbiol Immunol* **332**, 13-31, doi:10.1007/978-3-540-70868-1_2 (2009).

192. Phelps, J. P., Dang, N. & Rasochova, L. Inactivation and purification of cowpea mosaic virus-like particles displaying peptide antigens from *Bacillus anthracis*. *Journal of virological methods* **141**, 146-153, doi:10.1016/j.jviromet.2006.12.008 (2007).

193. Mallajosyula, J. K. *et al.* Single-dose monomeric HA subunit vaccine generates full protection from influenza challenge. *Human vaccines & immunotherapeutics* **10**, 586-595, doi:10.4161/hv.27567 (2014).

194. Bachmann, M. F. *et al.* The influence of antigen organization on B cell responsiveness. *Science* **262**, 1448, doi:10.1126/science.8248784 (1993).

195. McCormick, A. A. *et al.* TMV-peptide fusion vaccines induce cell-mediated immune responses and tumor protection in two murine models. *Vaccine* **24**, 6414-6423, doi:10.1016/j.vaccine.2006.06.003 (2006).

196. Banik, S. *et al.* Development of a Multivalent Subunit Vaccine against Tularemia Using Tobacco Mosaic Virus (TMV) Based Delivery System. *PLoS One* **10**, e0130858, doi:10.1371/journal.pone.0130858 (2015).

197. Karasev, A. V. *et al.* Plant based HIV-1 vaccine candidate: Tat protein produced in spinach. *Vaccine* **23**, 1875-1880, doi:10.1016/j.vaccine.2004.11.021 (2005).

198. Sugiyama, Y., Hamamoto, H., Takemoto, S., Watanabe, Y. & Okada, Y. Systemic production of foreign peptides on the particle surface of tobacco mosaic virus. *FEBS Lett* **359**, 247-250 (1995).

199. Bendahmane, M., Koo, M., Karrer, E. & Beachy, R. N. Display of epitopes on the surface of tobacco mosaic virus: impact of charge and isoelectric point of the epitope on virus-host interactions. *J Mol Biol* **290**, 9-20, doi:10.1006/jmbi.1999.2860 (1999).

200. Haynes, J. R. *et al.* Development of a Genetically–Engineered, Candidate Polio Vaccine Employing the Self–Assembling Properties of the Tobacco Mosaic Virus Coat Protein. *Bio/Technology* **4**, 637-641, doi:10.1038/nbt0786-637 (1986).

201. Wu, L. *et al.* Expression of foot-and-mouth disease virus epitopes in tobacco by a tobacco mosaic virus-based vector. *Vaccine* **21**, 4390-4398 (2003).

202. Staczek, J., Bendahmane, M., Gilleland, L. B., Beachy, R. N. & Gilleland, H. E., Jr. Immunization with a chimeric tobacco mosaic virus containing an epitope of outer membrane protein F of Pseudomonas aeruginosa provides protection against challenge with P. aeruginosa. *Vaccine* **18**, 2266-2274 (2000).

203. Turpen, T. H. *et al.* Malarial epitopes expressed on the surface of recombinant tobacco mosaic virus. *Biotechnology (N Y)* **13**, 53-57 (1995).

204. McCormick, A. A., Corbo, T. A., Wykoff-Clary, S., Palmer, K. E. & Pogue, G. P. Chemical conjugate TMV-peptide bivalent fusion vaccines improve cellular immunity and tumor protection. *Bioconjug Chem* **17**, 1330-1338, doi:10.1021/bc060124m (2006).

205. Yin, Z. *et al.* Tobacco mosaic virus as a new carrier for tumor associated carbohydrate antigens. *Bioconjug Chem* **23**, 1694-1703, doi:10.1021/bc300244a (2012).

206. Turpen, T. H., Turpen, A. M., Weinzettl, N., Kumagai, M. H. & Dawson, W. O. Transfection of whole plants from wounds inoculated with Agrobacterium tumefaciens containing cDNA of tobacco mosaic virus. *J Virol Methods* **42**, 227-239 (1993).

207. Gleba, Y., Marillonnet, S. & Klimyuk, V. Engineering viral expression vectors for plants: the 'full virus' and the 'deconstructed virus' strategies. *Curr Opin Plant Biol* **7**, 182-188, doi:10.1016/j.pbi.2004.01.003 (2004).

208. Song, B.-H., Yun, S.-I., Woolley, M. & Lee, Y.-M. Zika virus: history, epidemiology, transmission, and clinical presentation. *Journal of neuroimmunology* **308**, 50-64 (2017).

209. Dick, G., Kitchen, S. & Haddow, A. Zika virus (I). Isolations and serological specificity. *Transactions of the Royal Society of Tropical Medicine and Hygiene* **46**, 509-520 (1952).

210. Duffy, M. R. *et al.* Zika virus outbreak on Yap Island, federated states of Micronesia. *New England Journal of Medicine* **360**, 2536-2543 (2009).

211. Campos, G. S., Bandeira, A. C. & Sardi, S. I. Zika virus outbreak, Bahia, Brazil. *Emerging infectious diseases* **21**, 1885 (2015).

212. Hennessey, M., Fischer, M. & Staples, J. E. Zika virus spreads to new areas—region of the Americas, May 2015–January 2016. *American Journal of Transplantation* **16**, 1031-1034 (2016).

213. Parra, B. *et al.* Guillain-Barre Syndrome Associated with Zika Virus Infection in Colombia. *N Engl J Med* **375**, 1513-1523, doi:10.1056/NEJMoa1605564 (2016).

214. Rubin, E. J., Greene, M. F. & Baden, L. R. Zika Virus and Microcephaly. *N Engl J Med* **374**, 984-985, doi:10.1056/NEJMe1601862 (2016).

215. European Centre for Disease Prevention and Control. *Public Health Emergency of International Concern (PHEIC) declared for Zika and clusters of microcephaly and neurological disorders*. (2016). <http://ecdc.europa.eu/en/news-events/public-health-emergency-international-concern-pheic-declared-zika-and-clusters>.

216. Miner, J. J. & Diamond, M. S. Zika virus pathogenesis and tissue tropism. *Cell host & microbe* **21**, 134-142 (2017).

217. Simpson, D. Zika virus infection in man. *Transactions of the Royal Society of Tropical Medicine and Hygiene* **58**, 335-338 (1964).

218. Cao-Lormeau, V.-M. *et al.* Guillain-Barré Syndrome outbreak associated with Zika virus infection in French Polynesia: a case-control study. *The Lancet* **387**, 1531-1539 (2016).

219. Mlakar, J. *et al.* Zika virus associated with microcephaly. *N Engl J Med* **2016**, 951-958 (2016).

220. Hazin, A. N. *et al.* Computed tomographic findings in microcephaly associated with Zika virus. *New England Journal of Medicine* **374**, 2193-2195 (2016).

221. Cuevas, E. L. Preliminary report of microcephaly potentially associated with Zika virus infection during pregnancy—Colombia, January–November 2016. *MMWR. Morbidity and mortality weekly report* **65** (2016).

222. Miranda-Filho Dde, B. *et al.* Initial Description of the Presumed Congenital Zika Syndrome. *Am J Public Health* **106**, 598-600, doi:10.2105/ajph.2016.303115 (2016).

223. Brasil, P. *et al.* Zika virus infection in pregnant women in Rio de Janeiro. *New England Journal of Medicine* **375**, 2321-2334 (2016).

224. Costa, F. *et al.* Emergence of congenital Zika syndrome: viewpoint from the front lines. *Annals of internal medicine* **164**, 689-691 (2016).

225. França, G. V. *et al.* Congenital Zika virus syndrome in Brazil: a case series of the first 1501 livebirths with complete investigation. *The lancet* **388**, 891-897 (2016).

226. Honein, M. A. *et al.* Birth defects among fetuses and infants of US women with evidence of possible Zika virus infection during pregnancy. *Jama* **317**, 59-68 (2017).

227. Yuki, N. Guillain-Barré syndrome and anti-ganglioside antibodies: a clinician-scientist's journey. *Proceedings of the Japan Academy. Series B, Physical and biological sciences* **88**, 299-326, doi:10.2183/pjab.88.299 (2012).

228. Yuki, N. & Hartung, H. P. Guillain-Barre syndrome. *N Engl J Med* **366**, 2294-2304, doi:10.1056/NEJMra1114525 (2012).

229. Oehler, E. *et al.* Zika virus infection complicated by Guillain-Barre syndrome--case report, French Polynesia, December 2013. *Euro Surveill* **19** (2014).

230. Barbi, L., Coelho, A. V. C., Alencar, L. C. A. & Crovella, S. Prevalence of Guillain-Barre syndrome among Zika virus infected cases: a systematic review and meta-analysis. *Braz J Infect Dis* **22**, 137-141, doi:10.1016/j.bjid.2018.02.005 (2018).

231. Zhao, Z. *et al.* Viral retinopathy in experimental models of Zika infection. *Investigative ophthalmology & visual science* **58**, 4355-4365 (2017).

232. Karimi, O. *et al.* Thrombocytopenia and subcutaneous bleedings in a patient with Zika virus infection. *Lancet* **387**, 939-940, doi:10.1016/s0140-6736(16)00502-x (2016).

233. Carteaux, G. *et al.* Zika Virus Associated with Meningoencephalitis. *N Engl J Med* **374**, 1595-1596, doi:10.1056/NEJMc1602964 (2016).

234. Swaminathan, S., Schlaberg, R., Lewis, J., Hanson, K. E. & Couturier, M. R. Fatal Zika Virus Infection with Secondary Nonsexual Transmission. *N Engl J Med* **375**, 1907-1909, doi:10.1056/NEJMc1610613 (2016).

235. Hamel, R. *et al.* Zika virus: epidemiology, clinical features and host-virus interactions. *Microbes and infection* **18**, 441-449 (2016).

236. Boeuf, P., Drummer, H. E., Richards, J. S., Scoullar, M. J. & Beeson, J. G. The global threat of Zika virus to pregnancy: epidemiology, clinical perspectives, mechanisms, and impact. *BMC medicine* **14**, 112 (2016).

237. Messina, J. P. *et al.* Mapping global environmental suitability for Zika virus. *Elife* **5** (2016).

238. Ryan, S. J., Carlson, C. J., Mordecai, E. A. & Johnson, L. R. Global expansion and redistribution of Aedes-borne virus transmission risk with climate change. *PLoS Negl Trop Dis* **13**, e0007213, doi:10.1371/journal.pntd.0007213 (2019).

239. Samarasekera, U. & Triunfol, M. Concern over Zika virus grips the world. *The Lancet* **387**, 521-524 (2016).

240. Augusto, L. G. d. S. *et al.* Aedes aegypti control in Brazil. (2016).

241. Leonardi, W. *et al.* Bithionol blocks pathogenicity of bacterial toxins, ricin, and Zika virus. *Scientific reports* **6**, 34475 (2016).

242. Wang, Q. *et al.* Molecular determinants of human neutralizing antibodies isolated from a patient infected with Zika virus. *Science translational medicine* **8**, 369ra179-369ra179 (2016).

243. Zhao, H. *et al.* Structural basis of Zika virus-specific antibody protection. *Cell* **166**, 1016-1027 (2016).

244. Sapparapu, G. *et al.* Neutralizing human antibodies prevent Zika virus replication and fetal disease in mice. *Nature* **540**, 443 (2016).

245. Kraemer, M. U. *et al.* The global distribution of the arbovirus vectors Aedes aegypti and Ae. albopictus. *elife* **4** (2015).

246. Gotuzzo, E., Yactayo, S. & Córdova, E. Efficacy and duration of immunity after yellow fever vaccination: systematic review on the need for a booster every 10 years. *The American journal of tropical medicine and hygiene* **89**, 434-444, doi:10.4269/ajtmh.13-0264 (2013).

247. Gao, X. *et al.* Vaccine strategies for the control and prevention of Japanese encephalitis in Mainland China, 1951-2011. *PLoS neglected tropical diseases* **8**, e3015-e3015, doi:10.1371/journal.pntd.0003015 (2014).

248. Newman, C., Friedrich, T. C. & O'Connor, D. H. Macaque monkeys in Zika virus research: 1947–present. *Current opinion in virology* **25**, 34-40 (2017).

249. Dejnirattisai, W. *et al.* Dengue virus sero-cross-reactivity drives antibody-dependent enhancement of infection with zika virus. *Nature immunology* **17**, 1102 (2016).

250. Barba-Spaeth, G. *et al.* Structural basis of potent Zika–dengue virus antibody cross-neutralization. *Nature* **536**, 48 (2016).

251. Stettler, K. *et al.* Specificity, cross-reactivity, and function of antibodies elicited by Zika virus infection. *Science* **353**, 823-826 (2016).

252. Tirado, S. M. & Yoon, K. J. Antibody-dependent enhancement of virus infection and disease. *Viral Immunol* **16**, 69-86, doi:10.1089/088282403763635465 (2003).

253. Leta, S. *et al.* Global risk mapping for major diseases transmitted by Aedes aegypti and Aedes albopictus. *Int J Infect Dis* **67**, 25-35, doi:10.1016/j.ijid.2017.11.026 (2018).

254. Capeding, M. R. *et al.* Clinical efficacy and safety of a novel tetravalent dengue vaccine in healthy children in Asia: a phase 3, randomised, observer-masked, placebo-controlled trial. *Lancet* **384**, 1358-1365, doi:10.1016/s0140-6736(14)61060-6 (2014).

255. Aguiar, M., Halstead, S. B. & Stollenwerk, N. Consider stopping dengvaxia administration without immunological screening. *Expert Rev Vaccines* **16**, 301-302, doi:10.1080/14760584.2017.1276831 (2017).

256. Langerak, T. *et al.* The possible role of cross-reactive dengue virus antibodies in Zika virus pathogenesis. *PLoS Pathog* **15**, e1007640, doi:10.1371/journal.ppat.1007640 (2019).

257. Haque, A., Akcesme, F. B. & Pant, A. B. A systematic review of Zika virus: hurdles toward vaccine development and the way forward. *Antivir Ther*, doi:10.3851/imp3215 (2018).

258. Krubiner, C. B. *et al.* Pregnant women & vaccines against emerging epidemic threats: Ethics guidance for preparedness, research, and response. *Vaccine*, doi:10.1016/j.vaccine.2019.01.011 (2019).

259. Rothman, A. L. & Ennis, F. A. Dengue Vaccine: The Need, the Challenges, and Progress. *The Journal of infectious diseases* **214**, 825-827, doi:10.1093/infdis/jiw068 (2016).

260. Houser, K. & Subbarao, K. Influenza vaccines: challenges and solutions. *Cell host & microbe* **17**, 295-300, doi:10.1016/j.chom.2015.02.012 (2015).

261. Calisher, C. H. *et al.* Antigenic relationships between flaviviruses as determined by cross-neutralization tests with polyclonal antisera. *J Gen Virol* **70 (Pt 1)**, 37-43, doi:10.1099/0022-1317-70-1-37 (1989).

262. Anderson, K. B. *et al.* Interference and Facilitation Between Dengue Serotypes in a Tetravalent Live Dengue Virus Vaccine Candidate. *The Journal of Infectious Diseases* **204**, 442-450, doi:10.1093/infdis/jir279 (2011).

263. Mahoney, R. *et al.* Dengue vaccines regulatory pathways: a report on two meetings with regulators of developing countries. *PLoS Med* **8**, e1000418, doi:10.1371/journal.pmed.1000418 (2011).

264. Dowd, K. A. *et al.* Broadly neutralizing activity of Zika virus-immune sera identifies a single viral serotype. *Cell reports* **16**, 1485-1491 (2016).

265. Aliota, M. T. *et al.* Heterologous Protection against Asian Zika Virus Challenge in Rhesus Macaques. *PLoS Negl Trop Dis* **10**, e0005168, doi:10.1371/journal.pntd.0005168 (2016).

266. Xu, X. *et al.* Identifying Candidate Targets of Immune Responses in Zika Virus Based on Homology to Epitopes in Other Flavivirus Species. *PLoS Curr* **8**, doi:10.1371/currents.outbreaks.9aa2e1fb61b0f632f58a098773008c4b (2016).

267. Lanciotti, R. S., Lambert, A. J., Holodniy, M., Saavedra, S. & Signor, L. D. C. C. Phylogeny of Zika Virus in Western Hemisphere, 2015. *Emerging infectious diseases* **22**, 933-935, doi:10.3201/eid2205.160065 (2016).

268. Haddow, A. D. *et al.* Genetic characterization of Zika virus strains: geographic expansion of the Asian lineage. *PLoS neglected tropical diseases* **6**, e1477 (2012).

269. World Health Organization. *Zika Vaccine Development Technology Roadmap*, <https://www.who.int/immunization/research/development/Zika_Vaccine_Development_Technology_Roadmap_after_consultation_April_2019.pdf> (2019).

270. Bartsch, S. M. *et al.* What is the Value of Different Zika Vaccination Strategies to Prevent and Mitigate Zika Outbreaks. *J Infect Dis*, doi:10.1093/infdis/jiy688 (2018).

271. Shoukat, A., Vilches, T. & Moghadas, S. M. Cost-effectiveness of a potential Zika vaccine candidate: a case study for Colombia. *BMC Med* **16**, 100, doi:10.1186/s12916-018-1091-x (2018).

272. Kuno, G. & Chang, G. J. Full-length sequencing and genomic characterization of Bagaza, Kedougou, and Zika viruses. *Arch Virol* **152**, 687-696, doi:10.1007/s00705-006-0903-z (2007).

273. Ngono, A. E. & Shresta, S. Immune Response to Dengue and Zika. *Annual review of immunology* (2018).

274. Lee, I. *et al.* Probing Molecular Insights into Zika Virus(-)Host Interactions. *Viruses* **10**, doi:10.3390/v10050233 (2018).

275. Liu, J. *et al.* Flavivirus NS1 protein in infected host sera enhances viral acquisition by mosquitoes. *Nat Microbiol* **1**, 16087, doi:10.1038/nmicrobiol.2016.87 (2016).

276. Muller, D. A. & Young, P. R. The flavivirus NS1 protein: molecular and structural biology, immunology, role in pathogenesis and application as a diagnostic biomarker. *Antiviral Res* **98**, 192-208, doi:10.1016/j.antiviral.2013.03.008 (2013).

277. Xie, X., Gayen, S., Kang, C., Yuan, Z. & Shi, P. Y. Membrane topology and function of dengue virus NS2A protein. *J Virol* **87**, 4609-4622, doi:10.1128/jvi.02424-12 (2013).

278. UniProt. *Genome polyprotein - Zika virus (ZIKV)*, <https://www.uniprot.org/uniprot/Q32ZE1> (2019).

279. Hamel, R. *et al.* Biology of Zika virus infection in human skin cells. *Journal of virology* **89**, 8880-8896 (2015).

280. Bowen, J. R., Zimmerman, M. G. & Suthar, M. S. Taking the defensive: Immune control of Zika virus infection. *Virus Res* **254**, 21-26, doi:10.1016/j.virusres.2017.08.018 (2018).

281. Sun, X. *et al.* Transcriptional Changes during Naturally Acquired Zika Virus Infection Render Dendritic Cells Highly Conducive to Viral Replication. *Cell Rep* **21**, 3471-3482, doi:10.1016/j.celrep.2017.11.087 (2017).

282. Moller-Tank, S. & Maury, W. Phosphatidylserine receptors: enhancers of enveloped virus entry and infection. *Virology* **468-470**, 565-580, doi:10.1016/j.virol.2014.09.009 (2014).

283. Mercer, J. & Helenius, A. Apoptotic mimicry: phosphatidylserine-mediated macropinocytosis of vaccinia virus. *Ann N Y Acad Sci* **1209**, 49-55, doi:10.1111/j.1749-6632.2010.05772.x (2010).

284. Tabata, T. *et al.* Zika Virus Targets Different Primary Human Placental Cells, Suggesting Two Routes for Vertical Transmission. *Cell Host Microbe* **20**, 155-166, doi:10.1016/j.chom.2016.07.002 (2016).

285. Liu, S., DeLalio, L. J., Isakson, B. E. & Wang, T. T. AXL-Mediated Productive Infection of Human Endothelial Cells by Zika Virus. *Circ Res* **119**, 1183-1189, doi:10.1161/circresaha.116.309866 (2016).

286. Nowakowski, T. J. *et al.* Expression Analysis Highlights AXL as a Candidate Zika Virus Entry Receptor in Neural Stem Cells. *Cell stem cell* **18**, 591-596, doi:10.1016/j.stem.2016.03.012 (2016).

287. Wang, Z. Y. *et al.* Axl is not an indispensable factor for Zika virus infection in mice. *J Gen Virol* **98**, 2061-2068, doi:10.1099/jgv.0.000886 (2017).

288. Prasad, V. M. *et al.* Structure of the immature Zika virus at 9 Å resolution. *Nature Structural and Molecular Biology* **24**, 184 (2017).

289. Sirohi, D. *et al.* The 3.8 Å resolution cryo-EM structure of Zika virus. *Science* **352**, 467-470 (2016).

290. Kostyuchenko, V. A. *et al.* Structure of the thermally stable Zika virus. *Nature* **533**, 425 (2016).

291. Plevka, P. *et al.* Maturation of flaviviruses starts from one or more icosahedrally independent nucleation centres. *EMBO reports* **12**, 602-606, doi:10.1038/embor.2011.75 (2011).

292. Pierson, T. C. & Diamond, M. S. Degrees of maturity: the complex structure and biology of flaviviruses. *Curr Opin Virol* **2**, 168-175, doi:10.1016/j.coviro.2012.02.011 (2012).

293. Dowd, K. A. & Pierson, T. C. The Many Faces of a Dynamic Virion: Implications of Viral Breathing on Flavivirus Biology and Immunogenicity. *Annu Rev Virol* **5**, 185-207, doi:10.1146/annurev-virology-092917-043300 (2018).

294. Dowd, K. A., Mukherjee, S., Kuhn, R. J. & Pierson, T. C. Combined effects of the structural heterogeneity and dynamics of flaviviruses on antibody recognition. *J Virol* **88**, 11726-11737, doi:10.1128/jvi.01140-14 (2014).

295. Yockey, L. J. *et al.* Vaginal Exposure to Zika Virus during Pregnancy Leads to Fetal Brain Infection. *Cell* **166**, 1247-1256.e1244, doi:10.1016/j.cell.2016.08.004 (2016).

296. Lazear, H. M. *et al.* A Mouse Model of Zika Virus Pathogenesis. *Cell host & microbe* **19**, 720-730, doi:10.1016/j.chom.2016.03.010 (2016).

297. Rossi, S. L. *et al.* Characterization of a Novel Murine Model to Study Zika Virus. *Am J Trop Med Hyg* **94**, 1362-1369, doi:10.4269/ajtmh.16-0111 (2016).

298. Bayer, A. *et al.* Type III Interferons Produced by Human Placental Trophoblasts Confer Protection against Zika Virus Infection. *Cell Host Microbe* **19**, 705-712, doi:10.1016/j.chom.2016.03.008 (2016).

299. Ojha, C. R. *et al.* Toll-like receptor 3 regulates Zika virus infection and associated host inflammatory response in primary human astrocytes. *PLoS One* **14**, e0208543, doi:10.1371/journal.pone.0208543 (2019).

300. Wang, J. P. *et al.* Flavivirus activation of plasmacytoid dendritic cells delineates key elements of TLR7 signaling beyond endosomal recognition. *J Immunol* **177**, 7114-7121 (2006).

301. Nasirudeen, A. M. *et al.* RIG-I, MDA5 and TLR3 synergistically play an important role in restriction of dengue virus infection. *PLoS Negl Trop Dis* **5**, e926, doi:10.1371/journal.pntd.0000926 (2011).

302. Savidis, G. *et al.* The IFITMs Inhibit Zika Virus Replication. *Cell Rep* **15**, 2323-2330, doi:10.1016/j.celrep.2016.05.074 (2016).

303. Khaiboullina, S. F. *et al.* ZIKV infection regulates inflammasomes pathway for replication in monocytes. *Sci Rep* **7**, 16050, doi:10.1038/s41598-017-16072-3 (2017).

304. Hanners, N. W. *et al.* Western Zika Virus in Human Fetal Neural Progenitors Persists Long Term with Partial Cytopathic and Limited Immunogenic Effects. *Cell Rep* **15**, 2315-2322, doi:10.1016/j.celrep.2016.05.075 (2016).

305. Bowen, J. R. *et al.* Zika Virus Antagonizes Type I Interferon Responses during Infection of Human Dendritic Cells. *PLoS Pathog* **13**, e1006164, doi:10.1371/journal.ppat.1006164 (2017).

306. Bayless, N. L., Greenberg, R. S., Swigut, T., Wysocka, J. & Blish, C. A. Zika Virus Infection Induces Cranial Neural Crest Cells to Produce Cytokines at Levels Detrimental for Neurogenesis. *Cell Host Microbe* **20**, 423-428, doi:10.1016/j.chom.2016.09.006 (2016).

307. Kam, Y. W. *et al.* Specific Biomarkers Associated With Neurological Complications and Congenital Central Nervous System Abnormalities From Zika Virus-Infected Patients in Brazil. *J Infect Dis* **216**, 172-181, doi:10.1093/infdis/jix261 (2017).

308. Lum, F.-M. *et al.* Zika Virus Infection Preferentially Counterbalances Human Peripheral Monocyte and/or NK Cell Activity. *mSphere* **3**, e00120-00118, doi:10.1128/mSphereDirect.00120-18 (2018).

309. Delgado, M. A., Elmaoued, R. A., Davis, A. S., Kyei, G. & Deretic, V. Toll-like receptors control autophagy. *Embo j* **27**, 1110-1121, doi:10.1038/emboj.2008.31 (2008).

310. Wu, Y. *et al.* Zika virus evades interferon-mediated antiviral response through the co-operation of multiple nonstructural proteins in vitro. *Cell Discov* **3**, 17006, doi:10.1038/celldisc.2017.6 (2017).

311. Xia, H. *et al.* An evolutionary NS1 mutation enhances Zika virus evasion of host interferon induction. *Nat Commun* **9**, 414, doi:10.1038/s41467-017-02816-2 (2018).

312. Kumar, A. *et al.* Zika virus inhibits type-I interferon production and downstream signaling. *EMBO Rep* **17**, 1766-1775, doi:10.15252/embr.201642627 (2016).

313. Grant, A. *et al.* Zika Virus Targets Human STAT2 to Inhibit Type I Interferon Signaling. *Cell Host Microbe* **19**, 882-890, doi:10.1016/j.chom.2016.05.009 (2016).

314. Daffis, S. *et al.* 2'-O methylation of the viral mRNA cap evades host restriction by IFIT family members. *Nature* **468**, 452-456, doi:10.1038/nature09489 (2010).

315. Heaton, N. S. & Randall, G. Dengue virus-induced autophagy regulates lipid metabolism. *Cell Host Microbe* **8**, 422-432, doi:10.1016/j.chom.2010.10.006 (2010).

316. Cao, B., Parnell, L. A., Diamond, M. S. & Mysorekar, I. U. Inhibition of autophagy limits vertical transmission of Zika virus in pregnant mice. *J Exp Med* **214**, 2303-2313, doi:10.1084/jem.20170957 (2017).

317. Lennemann, N. J. & Coyne, C. B. Dengue and Zika viruses subvert reticulophagy by NS2B3-mediated cleavage of FAM134B. *Autophagy* **13**, 322-332, doi:10.1080/15548627.2016.1265192 (2017).

318. Monel, B. *et al.* Zika virus induces massive cytoplasmic vacuolization and paraptosis-like death in infected cells. *Embo j* **36**, 1653-1668, doi:10.15252/embj.201695597 (2017).

319. Shrestha, B. & Diamond, M. S. Role of CD8+ T Cells in Control of West Nile Virus Infection. *Journal of Virology* **78**, 8312, doi:10.1128/JVI.78.15.8312-8321.2004 (2004).

320. Larena, M., Regner, M., Lee, E. & Lobigs, M. Pivotal Role of Antibody and Subsidiary Contribution of CD8+ T Cells to Recovery from Infection in a Murine Model of Japanese Encephalitis. *Journal of Virology* **85**, 5446, doi:10.1128/JVI.02611-10 (2011).

321. Pardy, R. D. *et al.* Analysis of the T Cell Response to Zika Virus and Identification of a Novel CD8+ T Cell Epitope in Immunocompetent Mice. *PLoS Pathog* **13**, e1006184, doi:10.1371/journal.ppat.1006184 (2017).

322. Elong Ngono, A. *et al.* Mapping and Role of the CD8+ T Cell Response During Primary Zika Virus Infection in Mice. *Cell Host Microbe* **21**, 35-46, doi:10.1016/j.chom.2016.12.010 (2017).

323. Hickman, H. D. & Pierson, T. C. T Cells Take on Zika Virus. *Immunity* **46**, 13-14, doi:https://doi.org/10.1016/j.immuni.2016.12.020 (2017).

324. Wen, J. *et al.* Dengue virus-reactive CD8+ T cells mediate cross-protection against subsequent Zika virus challenge. *Nature communications* **8**, 1459 (2017).

325. Tappe, D. *et al.* Cytokine kinetics of Zika virus-infected patients from acute to reconvalescent phase. *Med Microbiol Immunol* **205**, 269-273, doi:10.1007/s00430-015-0445-7 (2016).

326. Grifoni, A. *et al.* Prior Dengue Virus Exposure Shapes T Cell Immunity to Zika Virus in Humans. *J Virol* **91**, doi:10.1128/jvi.01469-17 (2017).

327. Yauch, L. E. *et al.* CD4+ T Cells Are Not Required for the Induction of Dengue Virus-Specific CD8+ T Cell or Antibody Responses but Contribute to Protection after Vaccination. *The Journal of Immunology* **185**, 5405, doi:10.4049/jimmunol.1001709 (2010).

328. Elong Ngono, A. *et al.* CD4+ T cells promote humoral immunity and viral control during Zika virus infection. *PLoS Pathog* **15**, e1007474, doi:10.1371/journal.ppat.1007474 (2019).

329. Nybakken, G. E. *et al.* Structural basis of West Nile virus neutralization by a therapeutic antibody. *Nature* **437**, 764-769, doi:10.1038/nature03956 (2005).

330. He, R. T. *et al.* Antibodies that block virus attachment to Vero cells are a major component of the human neutralizing antibody response against dengue virus type 2. *J Med Virol* **45**, 451-461 (1995).
331. Shi, X. *et al.* A bispecific antibody effectively neutralizes all four serotypes of dengue virus by simultaneous blocking virus attachment and fusion. *MAbs* **8**, 574-584, doi:10.1080/19420862.2016.1148850 (2016).
332. Robbiani, D. F. *et al.* Recurrent potent human neutralizing antibodies to Zika virus in Brazil and Mexico. *Cell* **169**, 597-609. e511 (2017).
333. Magnani, D. M. *et al.* Neutralizing human monoclonal antibodies prevent Zika virus infection in macaques. *Science translational medicine* **9**, eaan8184 (2017).
334. Pierson, T. C., Fremont, D. H., Kuhn, R. J. & Diamond, M. S. Structural insights into the mechanisms of antibody-mediated neutralization of flavivirus infection: implications for vaccine development. *Cell Host Microbe* **4**, 229-238, doi:10.1016/j.chom.2008.08.004 (2008).
335. Dowd, K. A. & Pierson, T. C. Antibody-mediated neutralization of flaviviruses: a reductionist view. *Virology* **411**, 306-315, doi:10.1016/j.virol.2010.12.020 (2011).
336. Della-Porta, A. J. & Westaway, E. G. A multi-hit model for the neutralization of animal viruses. *J Gen Virol* **38**, 1-19, doi:10.1099/0022-1317-38-1-1 (1978).
337. Pierson, T. C. *et al.* The stoichiometry of antibody-mediated neutralization and enhancement of West Nile virus infection. *Cell Host Microbe* **1**, 135-145, doi:10.1016/j.chom.2007.03.002 (2007).
338. Conde, J. N., Silva, E. M., Barbosa, A. S. & Mohana-Borges, R. The Complement System in Flavivirus Infections. *Front Microbiol* **8**, 213, doi:10.3389/fmicb.2017.00213 (2017).
339. Fuchs, A. *et al.* Direct complement restriction of flavivirus infection requires glycan recognition by mannose-binding lectin. *Cell Host Microbe* **8**, 186-195, doi:10.1016/j.chom.2010.07.007 (2010).
340. Avirutnan, P. *et al.* Complement-mediated neutralization of dengue virus requires mannose-binding lectin. *MBio* **2**, doi:10.1128/mBio.00276-11 (2011).

341. Schiela, B. *et al.* Active Human Complement Reduces the Zika Virus Load via Formation of the Membrane-Attack Complex. *Front Immunol* **9**, 2177, doi:10.3389/fimmu.2018.02177 (2018).

342. Avirutnan, P. *et al.* Antagonism of the complement component C4 by flavivirus nonstructural protein NS1. *J Exp Med* **207**, 793-806, doi:10.1084/jem.20092545 (2010).

343. Goncalvez, A. P., Engle, R. E., St Claire, M., Purcell, R. H. & Lai, C. J. Monoclonal antibody-mediated enhancement of dengue virus infection in vitro and in vivo and strategies for prevention. *Proc Natl Acad Sci USA* **104**, 9422-9427, doi:10.1073/pnas.0703498104 (2007).

344. Beltramello, M. *et al.* The human immune response to Dengue virus is dominated by highly cross-reactive antibodies endowed with neutralizing and enhancing activity. *Cell host & microbe* **8**, 271-283, doi:10.1016/j.chom.2010.08.007 (2010).

345. Rodenhuis-Zybert, I. A. *et al.* Immature dengue virus: a veiled pathogen? *PLoS pathogens* **6**, e1000718 (2010).

346. Zhang, Y. *et al.* Structures of immature flavivirus particles. *Embo j* **22**, 2604-2613, doi:10.1093/emboj/cdg270 (2003).

347. Yu, I. M. *et al.* Structure of the immature dengue virus at low pH primes proteolytic maturation. *Science* **319**, 1834-1837, doi:10.1126/science.1153264 (2008).

348. Rodenhuis-Zybert, I. A. *et al.* Immature dengue virus: a veiled pathogen? *PLoS Pathog* **6**, e1000718, doi:10.1371/journal.ppat.1000718 (2010).

349. Ubol, S. & Halstead, S. B. How innate immune mechanisms contribute to antibody-enhanced viral infections. *Clin Vaccine Immunol* **17**, 1829-1835, doi:10.1128/cvi.00316-10 (2010).

350. Deng, Y.-Q. *et al.* A broadly flavivirus cross-neutralizing monoclonal antibody that recognizes a novel epitope within the fusion loop of E protein. *PloS one* **6**, e16059 (2011).

351. Rey, F. A., Stiasny, K., Vaney, M. C., Dellarole, M. & Heinz, F. X. The bright and the dark side of human antibody responses to flaviviruses: lessons for vaccine design. *EMBO Rep* **19**, 206-224, doi:10.15252/embr.201745302 (2018).

352. Bardina, S. V. *et al.* Enhancement of Zika virus pathogenesis by preexisting antiflavivirus immunity. *Science* **356**, 175-180, doi:10.1126/science.aal4365 (2017).

353. Brown, J. A. *et al.* Dengue Virus Immunity Increases Zika Virus-Induced Damage during Pregnancy. *Immunity* **50**, 751-762.e755, doi:10.1016/j.immuni.2019.01.005 (2019).

354. Rathore, A. P. S., Saron, W. A. A., Lim, T., Jahan, N. & St John, A. L. Maternal immunity and antibodies to dengue virus promote infection and Zika virus-induced microcephaly in fetuses. *Sci Adv* **5**, eaav3208, doi:10.1126/sciadv.aav3208 (2019).

355. Rodriguez-Barraquer, I. *et al.* Impact of preexisting dengue immunity on Zika virus emergence in a dengue endemic region. *Science* **363**, 607-610, doi:10.1126/science.aav6618 (2019).

356. Pedroso, C. *et al.* Cross-Protection of Dengue Virus Infection against Congenital Zika Syndrome, Northeastern Brazil. *Emerg Infect Dis* **25**, doi:10.3201/eid2508.190113 (2019).

357. Halstead, S. B., Mahalingam, S., Marovich, M. A., Ubol, S. & Mosser, D. M. Intrinsic antibody-dependent enhancement of microbial infection in macrophages: disease regulation by immune complexes. *Lancet Infect Dis* **10**, 712-722, doi:10.1016/s1473-3099(10)70166-3 (2010).

358. Polack, F. P. *et al.* A role for immune complexes in enhanced respiratory syncytial virus disease. *J Exp Med* **196**, 859-865, doi:10.1084/jem.20020781 (2002).

359. Quinn, M. *Investigation of the Intrinsic Antibody Dependent Enhancement Hypothesis* PhD thesis, University of Rochester, (2011).

360. Oduyebo, T. *et al.* Update: Interim Guidance for Health Care Providers Caring for Pregnant Women with Possible Zika Virus Exposure - United States (Including U.S. Territories), July 2017. *MMWR Morb Mortal Wkly Rep* **66**, 781-793, doi:10.15585/mmwr.mm6629e1 (2017).

361. Zhao, L. Z. *et al.* Kinetics of antigen-specific IgM/IgG/IgA antibody responses during Zika virus natural infection in two patients. *J Med Virol* **91**, 872-876, doi:10.1002/jmv.25366 (2019).

362. Hansen, S. *et al.* Diagnosing Zika virus infection against a background of other flaviviruses: Studies in high resolution serological analysis. *Sci Rep* **9**, 3648, doi:10.1038/s41598-019-40224-2 (2019).

363. Keasey, S. L. *et al.* Antibody Responses to Zika Virus Infections in Environments of Flavivirus Endemicity. *Clin Vaccine Immunol* **24**, doi:10.1128/cvi.00036-17 (2017).

364. Fibriansah, G. *et al.* DENGUE VIRUS. Cryo-EM structure of an antibody that neutralizes dengue virus type 2 by locking E protein dimers. *Science* **349**, 88-91, doi:10.1126/science.aaa8651 (2015).

365. de Alwis, R. *et al.* Identification of human neutralizing antibodies that bind to complex epitopes on dengue virions. *Proc Natl Acad Sci USA* **109**, 7439-7444, doi:10.1073/pnas.1200566109 (2012).

366. Heinz, F. X. & Stiasny, K. The antigenic structure of Zika virus and its relation to other flaviviruses: implications for infection and immunoprophylaxis. *Microbiol. Mol. Biol. Rev.* **81**, e00055-00016 (2017).

367. Ojha, C. R. *et al.* Complementary Mechanisms Potentially Involved in the Pathology of Zika Virus. *Front Immunol* **9**, 2340, doi:10.3389/fimmu.2018.02340 (2018).

368. Dai, L. *et al.* Structures of the Zika Virus Envelope Protein and Its Complex with a Flavivirus Broadly Protective Antibody. *Cell Host & Microbe* **19**, 696-704, doi:10.1016/j.chom.2016.04.013 (2016).

369. Fibriansah, G. *et al.* A potent anti-dengue human antibody preferentially recognizes the conformation of E protein monomers assembled on the virus surface. *EMBO Mol Med* **6**, 358-371, doi:10.1002/emmm.201303404 (2014).

370. Rouvinski, A. *et al.* Recognition determinants of broadly neutralizing human antibodies against dengue viruses. *Nature* **520**, 109 (2015).

371. Zhang, S. *et al.* Neutralization mechanism of a highly potent antibody against Zika virus. *Nat Commun* **7**, 13679, doi:10.1038/ncomms13679 (2016).

372. Hasan, S. S. *et al.* A human antibody against Zika virus crosslinks the E protein to prevent infection. *Nature communications* **8**, 14722 (2017).

373. Wang, J. *et al.* A Human Bi-specific Antibody against Zika Virus with High Therapeutic Potential. *Cell* **171**, 229-241.e215, doi:10.1016/j.cell.2017.09.002 (2017).

374. Long, F. *et al.* Structural basis of a potent human monoclonal antibody against Zika virus targeting a quaternary epitope. *Proceedings of the National Academy of Sciences* **116**, 1591-1596 (2019).

375. Swanstrom, J. *et al.* Dengue virus envelope dimer epitope monoclonal antibodies isolated from dengue patients are protective against Zika virus. *MBio* **7**, e01123-01116 (2016).

376. Collins, M. H. *et al.* Human antibody response to Zika targets type-specific quaternary structure epitopes. *JCI Insight* **4**, doi:10.1172/jci.insight.124588 (2019).

377. Recher, M., Hunziker, L., Ciurea, A., Harris, N. & Lang, K. S. Public, private and non-specific antibodies induced by non-cytopathic viral infections. *Curr Opin Microbiol* **7**, 426-433, doi:10.1016/j.mib.2004.06.008 (2004).

378. Ahmad, S. S., Amin, T. N. & Ustianowski, A. Zika virus: management of infection and risk. *Bmj* **352**, i1062, doi:10.1136/bmj.i1062 (2016).

379. Li, G. *et al.* Characterization of cytopathic factors through genome-wide analysis of the Zika viral proteins in fission yeast. *Proceedings of the National Academy of Sciences* **114**, E376-E385 (2017).

380. Sherman, K. E. *et al.* Zika virus replication and cytopathic effects in liver cells. *PLoS One* **14**, e0214016, doi:10.1371/journal.pone.0214016 (2019).

381. Alpuche-Lazcano, S. P. *et al.* Higher Cytopathic Effects of a Zika Virus Brazilian Isolate from Bahia Compared to a Canadian-Imported Thai Strain. *Viruses* **10**, doi:10.3390/v10020053 (2018).

382. Ketkar, H., Herman, D. & Wang, P. Genetic Determinants of the Re-Emergence of Arboviral Diseases. *Viruses* **11**, doi:10.3390/v11020150 (2019).

383. Quicke, K. M. *et al.* Zika Virus Infects Human Placental Macrophages. *Cell Host Microbe* **20**, 83-90, doi:10.1016/j.chom.2016.05.015 (2016).

384. Meertens, L. *et al.* Axl mediates ZIKA virus entry in human glial cells and modulates innate immune responses. *Cell reports* **18**, 324-333 (2017).

385. Hamel, R. *et al.* African and Asian Zika virus strains differentially induce early antiviral responses in primary human astrocytes. *Infect Genet Evol* **49**, 134-137, doi:10.1016/j.meegid.2017.01.015 (2017).

386. Roach, T. & Alcendor, D. J. Zika virus infection of cellular components of the blood-retinal barriers: implications for viral associated congenital ocular disease. *J Neuroinflammation* **14**, 43, doi:10.1186/s12974-017-0824-7 (2017).

387. Li, C. *et al.* Zika virus disrupts neural progenitor development and leads to microcephaly in mice. *Cell stem cell* **19**, 120-126 (2016).

388. Tang, H. *et al.* Zika Virus Infects Human Cortical Neural Progenitors and Attenuates Their Growth. *Cell Stem Cell* **18**, 587-590, doi:10.1016/j.stem.2016.02.016 (2016).

389. Maestre, A. M. & Fernandez-Sesma, A. Finding Clues for Congenital Zika Syndrome: Zika Virus Selective Infection of Immature Neurons. *EBioMedicine* **10**, 7-8, doi:10.1016/j.ebiom.2016.07.026 (2016).

390. Dang, J. *et al.* Zika Virus Depletes Neural Progenitors in Human Cerebral Organoids through Activation of the Innate Immune Receptor TLR3. *Cell Stem Cell* **19**, 258-265, doi:10.1016/j.stem.2016.04.014 (2016).

391. Zhang, F. *et al.* American Strain of Zika Virus Causes More Severe Microcephaly Than an Old Asian Strain in Neonatal Mice. *EBioMedicine* **25**, 95-105, doi:10.1016/j.ebiom.2017.10.019 (2017).

392. Cugola, F. R. *et al.* The Brazilian Zika virus strain causes birth defects in experimental models. *Nature* **534**, 267-271, doi:10.1038/nature18296 (2016).

393. Garcez, P. P. *et al.* Zika virus impairs growth in human neurospheres and brain organoids. *Science* **352**, 816-818, doi:10.1126/science.aaf6116 (2016).

394. Yoon, K. J. *et al.* Zika-Virus-Encoded NS2A Disrupts Mammalian Cortical Neurogenesis by Degrading Adherens Junction Proteins. *Cell Stem Cell* **21**, 349-358.e346, doi:10.1016/j.stem.2017.07.014 (2017).

395. Uncini, A., Shahrizaila, N. & Kuwabara, S. Zika virus infection and Guillain-Barre syndrome: a review focused on clinical and electrophysiological subtypes. *J Neurol Neurosurg Psychiatry* **88**, 266-271, doi:10.1136/jnnp-2016-314310 (2017).

396. Cumberworth, S. L. *et al.* Zika virus tropism and interactions in myelinating neural cell cultures: CNS cells and myelin are preferentially affected. *Acta Neuropathol Commun* **5**, 50, doi:10.1186/s40478-017-0450-8 (2017).

397. Chimelli, L. *et al.* The spectrum of neuropathological changes associated with congenital Zika virus infection. *Acta Neuropathol* **133**, 983-999, doi:10.1007/s00401-017-1699-5 (2017).

398. Cusick, M. F., Libbey, J. E. & Fujinami, R. S. Molecular mimicry as a mechanism of autoimmune disease. *Clin Rev Allergy Immunol* **42**, 102-111, doi:10.1007/s12016-011-8293-8 10.1007/s12016-011-8294-7 (2012).

399. Koma, T. *et al.* Zika virus infection elicits auto-antibodies to C1q. *Scientific Reports* **8**, 1882 (2018).

400. Homan, J., Malone, R. W., Darnell, S. J. & Bremel, R. D. Antibody mediated epitope mimicry in the pathogenesis of Zika virus related disease. *bioRxiv*, 044834 (2016).

401. Sekiguchi, Y. *et al.* Antiganglioside antibodies are associated with axonal Guillain-Barre syndrome: a Japanese-Italian collaborative study. *J Neurol Neurosurg Psychiatry* **83**, 23-28, doi:10.1136/jnnp-2011-300309 (2012).

402. Dai, L. *et al.* Molecular basis of antibody-mediated neutralization and protection against flavivirus. *IUBMB life* **68**, 783-791 (2016).

403. Zhu, Z. *et al.* Comparative genomic analysis of pre-epidemic and epidemic Zika virus strains for virological factors potentially associated with the rapidly expanding epidemic. *Emerging microbes & infections* **5**, e22-e22, doi:10.1038/emi.2016.48 (2016).

404. Harrison, S. C. Immunogenic cross-talk between dengue and Zika viruses. *Nature immunology* **17**, 1010 (2016).

405. Allison, S. L. *et al.* Oligomeric rearrangement of tick-borne encephalitis virus envelope proteins induced by an acidic pH. *Journal of Virology* **69**, 695 (1995).

406. Stiasny, K., Kiermayr, S., Holzmann, H. & Heinz, F. X. Cryptic properties of a cluster of dominant flavivirus cross-reactive antigenic sites. *Journal of virology* **80**, 9557-9568 (2006).

407. Dejnirattisai, W. *et al.* A new class of highly potent, broadly neutralizing antibodies isolated from viremic patients infected with dengue virus. *Nature immunology* **16**, 170 (2015).

408. Oliphant, T. *et al.* Antibody Recognition and Neutralization Determinants on Domains I and II of West Nile Virus Envelope Protein. *Journal of Virology* **80**, 12149, doi:10.1128/JVI.01732-06 (2006).

409. Dejnirattisai, W. *et al.* Cross-Reacting Antibodies Enhance Dengue Virus Infection in Humans. *Science* **328**, 745, doi:10.1126/science.1185181 (2010).

410. Lai, C.-Y. *et al.* Analysis of cross-reactive antibodies recognizing the fusion loop of envelope protein and correlation with neutralizing antibody titers in Nicaraguan dengue cases. *PLoS neglected tropical diseases* **7**, e2451-e2451, doi:10.1371/journal.pntd.0002451 (2013).

411. Sultana, H. *et al.* Fusion loop peptide of the West Nile virus envelope protein is essential for pathogenesis and is recognized by a therapeutic cross-reactive human monoclonal antibody. *Journal of immunology (Baltimore, Md. : 1950)* **183**, 650-660, doi:10.4049/jimmunol.0900093 (2009).

412. Dowd, K. A. *et al.* Rapid development of a DNA vaccine for Zika virus. *Science*, aai9137 (2016).

413. Abbink, P. *et al.* Protective efficacy of multiple vaccine platforms against Zika virus challenge in rhesus monkeys. *Science* **353**, 1129-1132 (2016).

414. Collins, M. H. & Metz, S. W. Progress and Works in Progress: Update on Flavivirus Vaccine Development. *Clinical Therapeutics* **39**, 1519-1536, doi:10.1016/j.clinthera.2017.07.001 (2017).

415. Hanna, S. L. *et al.* N-linked glycosylation of West Nile virus envelope proteins influences particle assembly and infectivity. *Journal of virology* **79**, 13262-13274 (2005).

416. Li, J., Bhuvanakantham, R., Howe, J. & Ng, M.-L. The glycosylation site in the envelope protein of West Nile virus (Sarafend) plays an important role in replication and maturation processes. *Journal of general virology* **87**, 613-622 (2006).

417. Moudy, R. M., Zhang, B., Shi, P. Y. & Kramer, L. D. West Nile virus envelope protein glycosylation is required for efficient viral transmission by Culex vectors. *Virology* **387**, 222-228, doi:10.1016/j.virol.2009.01.038 (2009).

418. Yoshii, K., Yanagihara, N., Ishizuka, M., Sakai, M. & Kariwa, H. N-linked glycan in tick-borne encephalitis virus envelope protein affects viral secretion in mammalian cells, but not in tick cells. *J Gen Virol* **94**, 2249-2258, doi:10.1099/vir.0.055269-0 (2013).

419. Beasley, D. W. *et al.* Envelope protein glycosylation status influences mouse neuroinvasion phenotype of genetic lineage 1 West Nile virus strains. *Journal of virology* **79**, 8339-8347 (2005).

420. Shirato, K. *et al.* Viral envelope protein glycosylation is a molecular determinant of the neuroinvasiveness of the New York strain of West Nile virus. *J Gen Virol* **85**, 3637-3645, doi:10.1099/vir.0.80247-0 (2004).

421. Kawano, H., Rostapshov, V., Rosen, L. & Lai, C. J. Genetic determinants of dengue type 4 virus neurovirulence for mice. *J Virol* **67**, 6567-6575 (1993).

422. Lee, E., Leang, S. K., Davidson, A. & Lobigs, M. Both E protein glycans adversely affect dengue virus infectivity but are beneficial for virion release. *J Virol* **84**, 5171-5180, doi:10.1128/jvi.01900-09 (2010).

423. Rey, F. A., Heinz, F. X., Mandl, C., Kunz, C. & Harrison, S. C. The envelope glycoprotein from tick-borne encephalitis virus at 2 A resolution. *Nature* **375**, 291-298, doi:10.1038/375291a0 (1995).

424. Goo, L. *et al.* The Zika virus envelope protein glycan loop regulates virion antigenicity. *Virology* **515**, 191-202 (2018).

425. Fontes-Garfias, C. R. *et al.* Functional analysis of glycosylation of Zika virus envelope protein. *Cell reports* **21**, 1180-1190 (2017).

426. Annamalai, A. S. *et al.* Zika virus encoding nonglycosylated envelope protein is attenuated and defective in neuroinvasion. *Journal of virology* **91**, e01348-01317 (2017).

427. Wen, D. *et al.* N-glycosylation of Viral E Protein Is the Determinant for Vector Midgut Invasion by Flaviviruses. *mBio* **9**, e00046-00018 (2018).

428. Mossenta, M., Marchese, S., Poggianella, M., Slon Campos, J. L. & Burrone, O. R. Role of N-glycosylation on Zika virus E protein secretion, viral assembly and infectivity. *Biochem Biophys Res Commun* **492**, 579-586, doi:10.1016/j.bbrc.2017.01.022 (2017).

429. Hayes, E. B. Zika virus outside Africa. *Emerg Infect Dis* **15**, 1347-1350, doi:10.3201/eid1509.090442 (2009).

430. Faye, O. *et al.* Molecular evolution of Zika virus during its emergence in the 20th century. *PLoS neglected tropical diseases* **8**, e2636 (2014).

431. Lanciotti, R. S. *et al.* Genetic and serologic properties of Zika virus associated with an epidemic, Yap State, Micronesia, 2007. *Emerging infectious diseases* **14**, 1232 (2008).

432. Faria, N. R. *et al.* Zika virus in the Americas: Early epidemiological and genetic findings. *Science* **352**, 345-349, doi:10.1126/science.aaf5036 (2016).

433. Simón, D., Fajardo, A., Moreno, P., Moratorio, G. & Cristina, J. An Evolutionary Insight into Zika Virus Strains Isolated in the Latin American Region. *Viruses* **10**, 698 (2018).

434. Pettersson, J. H. *et al.* How Did Zika Virus Emerge in the Pacific Islands and Latin America? *MBio* **7**, doi:10.1128/mBio.01239-16 (2016).

435. Tripathi, S. *et al.* A novel Zika virus mouse model reveals strain specific differences in virus pathogenesis and host inflammatory immune responses. *PLoS Pathog* **13**, e1006258, doi:10.1371/journal.ppat.1006258 (2017).

436. Gubler, D. J., Vasilakis, N. & Musso, D. History and Emergence of Zika Virus. *J Infect Dis* **216**, S860-s867, doi:10.1093/infdis/jix451 (2017).

437. Wang, L. *et al.* From mosquitos to humans: genetic evolution of Zika virus. *Cell host & microbe* **19**, 561-565 (2016).

438. Anfasa, F. *et al.* Phenotypic differences between Asian and African lineage Zika viruses in human neural progenitor cells. *MSphere* **2**, e00292-00217 (2017).

439. Ramaiah, A. *et al.* Comparative analysis of protein evolution in the genome of pre-epidemic and epidemic Zika virus. *Infect Genet Evol* **51**, 74-85, doi:10.1016/j.meegid.2017.03.012 (2017).

440. Musso, D. & Gubler, D. J. Zika Virus. *Clin Microbiol Rev* **29**, 487-524, doi:10.1128/cmr.00072-15 (2016).

441. Rossi, S. L., Ebel, G. D., Shan, C., Shi, P. Y. & Vasilakis, N. Did Zika Virus Mutate to Cause Severe Outbreaks? *Trends Microbiol* **26**, 877-885, doi:10.1016/j.tim.2018.05.007 (2018).

442. Simonin, Y., van Riel, D., Van de Perre, P., Rockx, B. & Salinas, S. Differential virulence between Asian and African lineages of Zika virus. *PLoS Negl Trop Dis* **11**, e0005821, doi:10.1371/journal.pntd.0005821 (2017).

443. Simonin, Y. *et al.* Zika Virus Strains Potentially Display Different Infectious Profiles in Human Neural Cells. *EBioMedicine* **12**, 161-169, doi:10.1016/j.ebiom.2016.09.020 (2016).

444. Dowall, S. D. *et al.* Lineage-dependent differences in the disease progression of Zika virus infection in type-I interferon receptor knockout (A129) mice. *PLoS Negl Trop Dis* **11**, e0005704, doi:10.1371/journal.pntd.0005704 (2017).

445. Smith, D. R. *et al.* African and Asian Zika Virus Isolates Display Phenotypic Differences Both In Vitro and In Vivo. *Am J Trop Med Hyg* **98**, 432-444, doi:10.4269/ajtmh.17-0685 (2018).

446. Duggal, N. K. *et al.* Differential Neurovirulence of African and Asian Genotype Zika Virus Isolates in Outbred Immunocompetent Mice. *Am J Trop Med Hyg* **97**, 1410-1417, doi:10.4269/ajtmh.17-0263 (2017).

447. Foy, B. D. *et al.* Probable non-vector-borne transmission of Zika virus, Colorado, USA. *Emerg Infect Dis* **17**, 880-882, doi:10.3201/eid1705.101939 (2011).

448. Fagbami, A. H. Zika virus infections in Nigeria: virological and seroepidemiological investigations in Oyo State. *J Hyg (Lond)* **83**, 213-219 (1979).

449. Herrera, B. B. *et al.* Continued Transmission of Zika Virus in Humans in West Africa, 1992-2016. *J Infect Dis* **215**, 1546-1550, doi:10.1093/infdis/jix182 (2017).

450. Vielle, N. J. *et al.* Silent infection of human dendritic cells by African and Asian strains of Zika virus. *Sci Rep* **8**, 5440, doi:10.1038/s41598-018-23734-3 (2018).

451. Liu, Y. *et al.* Evolutionary enhancement of Zika virus infectivity in Aedes aegypti mosquitoes. *Nature* **545**, 482-486, doi:10.1038/nature22365 (2017).

452. Yuan, L. *et al.* A single mutation in the prM protein of Zika virus contributes to fetal microcephaly. *Science* **358**, 933-936, doi:10.1126/science.aam7120 (2017).

453. Beaver, J. T., Lelutiu, N., Habib, R. & Skountzou, I. Evolution of Two Major Zika Virus Lineages: Implications for Pathology, Immune Response, and Vaccine Development. *Front Immunol* **9**, 1640, doi:10.3389/fimmu.2018.01640 (2018).

454. Sabin, A. B. & Schlesinger, R. W. Production of immunity to dengue with virus modified by propagation in mice. *Science* **101**, 640-642, doi:10.1126/science.101.2634.640 (1945).

455. Hahn, C. S., Dalrymple, J. M., Strauss, J. H. & Rice, C. M. Comparison of the virulent Asibi strain of yellow fever virus with the 17D vaccine strain derived from it. *Proc Natl Acad Sci U S A* **84**, 2019-2023, doi:10.1073/pnas.84.7.2019 (1987).

456. Enfissi, A., Codrington, J., Roosblad, J., Kazanji, M. & Rousset, D. Zika virus genome from the Americas. *Lancet* **387**, 227-228, doi:10.1016/s0140-6736(16)00003-9 (2016).

457. Chavez, J. H., Silva, J. R., Amarilla, A. A. & Moraes Figueiredo, L. T. Domain III peptides from flavivirus envelope protein are useful antigens for serologic diagnosis and targets for immunization. *Biologicals* **38**, 613-618, doi:10.1016/j.biologicals.2010.07.004 (2010).

458. Basu, R., Zhai, L., Contreras, A. & Tumban, E. Immunization with phage virus-like particles displaying Zika virus potential B-cell epitopes neutralizes Zika virus infection of monkey kidney cells. *Vaccine* **36**, 1256-1264, doi:10.1016/j.vaccine.2018.01.056 (2018).

459. Dai, S., Zhang, T., Zhang, Y., Wang, H. & Deng, F. Zika Virus Baculovirus-Expressed Virus-Like Particles Induce Neutralizing Antibodies in Mice. *Virol Sin* **33**, 213-226, doi:10.1007/s12250-018-0030-5 (2018).

460. Yang, M., Sun, H., Lai, H., Hurtado, J. & Chen, Q. Plant-produced Zika virus envelope protein elicits neutralizing immune responses that correlate with protective immunity against Zika virus in mice. *Plant biotechnology journal* **16**, 572-580 (2018).

461. Themis Bioscience: Zika Vaccine Development Receives Big Boost *by Innovate UK Public Relations Agency for Research & Education GmbH*, <http://prd.at/en/newsroom-clients/themis-bioscience-zika-vaccine-development-receives-big-boost-by-innovate-uk/> (2016).

462. National Institutes of Health. *NIH begins clinical trial of live, attenuated Zika vaccine*, <https://www.ncbi.nlm.nih.gov/pubmed/> (2018).

463. National Institute of Allergy and Infectious Diseases. *Zika Virus Vaccines*, <https://www.niaid.nih.gov/diseases-conditions/zika-vaccines> (

464. World Health Organization. *Vaccine pipeline tracker*, <http://www.who.int/immunization/research/vaccine_pipeline_tracker_spreadsheet/en/> (2018).

465. Modjarrad, K. *et al.* Preliminary aggregate safety and immunogenicity results from three trials of a purified inactivated Zika virus vaccine candidate: phase 1, randomised, double-blind, placebo-controlled clinical trials. *Lancet* **391**, 563-571, doi:10.1016/s0140-6736(17)33106-9 (2018).

466. *Randomized, Placebo-controlled, Observer-blinded Phase 1 Safety and Immunogenicity Study of Inactivated Zika Virus Vaccine Candidate in Healthy Adults -ClinicalTrials.gov*, <https://clinicaltrials.gov/ct2/show/NCT03425149> (2018).

467. World Health Organization. *Vaccine Pipeline Tracker*, <http://www.who.int/immunization/research/vaccine_pipeline_tracker_spreadsheet/en/> (2019).

468. Gaudinski, M. R. *et al.* Safety, tolerability, and immunogenicity of two Zika virus DNA vaccine candidates in healthy adults: randomised, open-label, phase 1 clinical trials. *Lancet* **391**, 552-562, doi:10.1016/s0140-6736(17)33105-7 (2018).

469. Tebas, P. *et al.* Safety and Immunogenicity of an Anti-Zika Virus DNA Vaccine - Preliminary Report. *N Engl J Med*, doi:10.1056/NEJMoa1708120 (2017).

470. Pardi, N. *et al.* Zika virus protection by a single low-dose nucleoside-modified mRNA vaccination. *Nature* **543**, 248 (2017).

471. Ramsauer, K. *et al.* Immunogenicity, safety, and tolerability of a recombinant measles-virus-based chikungunya vaccine: a randomised, double-blind, placebo-controlled, active-comparator, first-in-man trial. *Lancet Infectious Diseases* **15**, 519-527, doi:10.1016/S1473-3099(15)70043-5 (2015).

472. *Zika-Vaccine Dose Finding Study Regarding Safety, Immunogenicity and Tolerability - ClinicalTrials.gov*, <https://clinicaltrials.gov/ct2/show/NCT02996890> (2018).

473. *Themis Bioscience: Zika Vaccine Development Receives Big Boost by Innovate UK*, <http://prd.at/en/newsroom-clients/themis-bioscience-zika-vaccine-development-receives-big-boost-by-innovate-uk/> (September 6, 2016).

474. *ExPASy - Compute pI/Mw tool*, <https://web.expasy.org/compute_pi/> (2018).

475. New England Biolabs. PCR Using Q5® High-Fidelity DNA Polymerase. (2018).

476. New England Biolabs. *NEBuilder*, <https://nebuilder.neb.com/> (2018).

477. Bruckman, M. A. & Steinmetz, N. F. Chemical modification of the inner and outer surface of Tobacco Mosaic Virus in *Virus Hybrids as Nanomaterials* 173-185 (Springer, 2014).

478. Shamloul, M., Trusa, J., Mett, V. & Yusibov, V. Optimization and utilization of Agrobacterium-mediated transient protein production in Nicotiana. *Journal of visualized experiments: JoVE* (2014).

479. Sugasawara, R. J., Cahoon, B. E. & Karu, A. E. The influence of murine macrophage-conditioned medium on cloning efficiency, antibody synthesis, and growth rate of hybridomas. *J Immunol Methods* **79**, 263-275 (1985).

480. Stanker, L. H., Merrill, P., Scotcher, M. C. & Cheng, L. W. Development and partial characterization of high-affinity monoclonal antibodies for botulinum toxin type A and their use in analysis of milk by sandwich ELISA. *Journal of Immunological Methods* **336**, 1-8, doi:https://doi.org/10.1016/j.jim.2008.03.003 (2008).

481. Bigbee, W. L., Vanderlaan, M., Fong, S. S. & Jensen, R. H. Monoclonal antibodies specific for the M- and N-forms of human glycophorin A. *Mol Immunol* **20**, 1353-1362 (1983).

482. Frey, A., Di Canzio, J. & Zurakowski, D. A statistically defined endpoint titer determination method for immunoassays. *Journal of immunological methods* **221**, 35-41 (1998).

483. de Alwis, R. & de Silva, A. M. Measuring antibody neutralization of dengue virus (DENV) using a flow cytometry-based technique in *Dengue*. 27-39 (Springer, 2014).

484. Lynch, R. M. *et al.* Augmented Zika and Dengue Neutralizing Antibodies Are Associated With Guillain-Barré Syndrome. *The Journal of infectious diseases* **219**, 26-30, doi:10.1093/infdis/jiy466 (2019).

485. Harrison, S. C. Viral membrane fusion. *Virology* **479-480**, 498-507, doi:10.1016/j.virol.2015.03.043 (2015).

486. Mendes, Y. S. *et al.* The structural dynamics of the flavivirus fusion peptide-membrane interaction. *PLoS One* **7**, e47596, doi:10.1371/journal.pone.0047596 (2012).

487. Lynch, R. M. *et al.* Augmented Zika and Dengue Neutralizing Antibodies Are Associated With Guillain-Barre Syndrome. *J Infect Dis* **219**, 26-30, doi:10.1093/infdis/jiy466 (2019).

488. Oduyebo, T. Update: interim guidelines for health care providers caring for pregnant women and women of reproductive age with possible Zika virus exposure—United States, 2016. *MMWR. Morbidity and mortality weekly report* **65** (2016).

489. Hraber, P., Bradfute, S., Clarke, E., Ye, C. & Pitard, B. Amphiphilic block copolymer delivery of a DNA vaccine against Zika virus. *Vaccine* **36**, 6911-6917, doi:https://doi.org/10.1016/j.vaccine.2018.10.022 (2018).

490. Carlin, A. F. *et al.* Deconvolution of pro- and antiviral genomic responses in Zika virus-infected and bystander macrophages. *Proceedings of the National Academy of Sciences of the United States of America* **115**, E9172-E9181, doi:10.1073/pnas.1807690115 (2018).

491. Li, Q. *et al.* TMV recombinants encoding fused foreign transmembrane domains to the CP subunit caused local necrotic response on susceptible tobacco. *Virology* **348**, 253-259, doi:https://doi.org/10.1016/j.virol.2005.11.013 (2006).

492. Les Erickson, F. *et al.* The helicase domain of the TMV replicase proteins induces the N-mediated defence response in tobacco. *The Plant Journal* **18**, 67-75, doi:10.1046/j.1365-313X.1999.00426.x (1999).

493. Wroblewski, T., Tomczak, A. & Michelmore, R. Optimization of Agrobacterium-mediated transient assays of gene expression in lettuce, tomato and Arabidopsis. *Plant Biotechnol J* **3**, 259-273, doi:10.1111/j.1467-7652.2005.00123.x (2005).

494. Balsitis, S. J. *et al.* Lethal antibody enhancement of dengue disease in mice is prevented by Fc modification. *PLoS pathogens* **6**, e1000790 (2010).

495. Mason, R. A., Tauraso, N. M., Spertzel, R. O. & Ginn, R. K. Yellow fever vaccine: direct challenge of monkeys given graded doses of 17D vaccine. *Appl Microbiol* **25**, 539-544 (1973).

496. Goncalvez, A. P. *et al.* Humanized monoclonal antibodies derived from chimpanzee Fabs protect against Japanese encephalitis virus in vitro and in vivo. *J Virol* **82**, 7009-7021, doi:10.1128/jvi.00291-08 (2008).

497. Ishikawa, T., Yamanaka, A. & Konishi, E. A review of successful flavivirus vaccines and the problems with those flaviviruses for which vaccines are not yet available. *Vaccine* **32**, 1326-1337, doi:https://doi.org/10.1016/j.vaccine.2014.01.040 (2014).

498. Plotkin, S. A. Correlates of protection induced by vaccination. *Clin Vaccine Immunol* **17**, 1055-1065, doi:10.1128/cvi.00131-10 (2010).

499. Muthumani, K. *et al.* In vivo protection against ZIKV infection and pathogenesis through passive antibody transfer and active immunisation with a prMEnv DNA vaccine. *NPJ Vaccines* **1**, 16021, doi:10.1038/npjvaccines.2016.21 (2016).

500. Espinosa, D. *et al.* Passive Transfer of Immune Sera Induced by a Zika Virus-Like Particle Vaccine Protects AG129 Mice Against Lethal Zika Virus Challenge. *EBioMedicine* (2017).

501. Shan, C. *et al.* A live-attenuated Zika virus vaccine candidate induces sterilizing immunity in mouse models. *Nat Med* **23**, 763-767, doi:10.1038/nm.4322 (2017).

502. Kraus, A. A., Messer, W., Haymore, L. B. & De Silva, A. M. Comparison of plaque-and flow cytometry-based methods for measuring dengue virus neutralization. *Journal of clinical microbiology* **45**, 3777-3780 (2007).

503. Libraty, D. H. *et al.* Clinical and immunological risk factors for severe disease in Japanese encephalitis. *Trans R Soc Trop Med Hyg* **96**, 173-178, doi:10.1016/s0035-9203(02)90294-4 (2002).

504. Amor, S., Scallan, M. F., Morris, M. M., Dyson, H. & Fazakerley, J. K. Role of immune responses in protection and pathogenesis during Semliki Forest virus encephalitis. *J Gen Virol* **77 (Pt 2)**, 281-291, doi:10.1099/0022-1317-77-2-281 (1996).

505. Skountzou, I. *et al.* Influenza virus-specific neutralizing IgM antibodies persist for a lifetime. *Clin Vaccine Immunol* **21**, 1481-1489, doi:10.1128/cvi.00374-14 (2014).

506. Diamond, M. S. *et al.* A critical role for induced IgM in the protection against West Nile virus infection. *J Exp Med* **198**, 1853-1862, doi:10.1084/jem.20031223 (2003).

507. Chua, C. L., Sam, I. C., Chiam, C. W. & Chan, Y. F. The neutralizing role of IgM during early Chikungunya virus infection. *PLoS One* **12**, e0171989, doi:10.1371/journal.pone.0171989 (2017).

508. Dorfmeier, C. L., Shen, S., Tzvetkov, E. P. & McGettigan, J. P. Reinvestigating the role of IgM in rabies virus postexposure vaccination. *J Virol* **87**, 9217-9222, doi:10.1128/jvi.00995-13 (2013).

509. Ravichandran, S. *et al.* Differential human antibody repertoires following Zika infection and the implications for serodiagnostics and disease outcome. *Nat Commun* **10**, 1943, doi:10.1038/s41467-019-09914-3 (2019).

510. Tongren, J. E., Corran, P. H., Jarra, W., Langhorne, J. & Riley, E. M. Epitope-specific regulation of immunoglobulin class switching in mice immunized with malarial merozoite surface proteins. *Infect Immun* **73**, 8119-8129, doi:10.1128/iai.73.12.8119-8129.2005 (2005).

511. Lange, H. *et al.* Immunoglobulin class switching appears to be regulated by B-cell antigen receptor-specific T-cell action. *Eur J Immunol* **42**, 1016-1029, doi:10.1002/eji.201141857 (2012).

512. Berek, C. & Ziegner, M. The maturation of the immune response. *Immunol Today* **14**, 400-404, doi:10.1016/0167-5699(93)90143-9 (1993).

513. Koblischke, M. *et al.* Structural Influence on the Dominance of Virus-Specific CD4 T Cell Epitopes in Zika Virus Infection. *Front Immunol* **9**, 1196, doi:10.3389/fimmu.2018.01196 (2018).

514. Ngono, A. E. & Shresta, S. Immune Response to Dengue and Zika. *Annu Rev Immunol* **36**, 279-308, doi:10.1146/annurev-immunol-042617-053142 (2018).

515. Huang, H. *et al.* CD8(+) T Cell Immune Response in Immunocompetent Mice during Zika Virus Infection. *J Virol* **91**, doi:10.1128/jvi.00900-17 (2017).

516. Wen, J. *et al.* Identification of Zika virus epitopes reveals immunodominant and protective roles for dengue virus cross-reactive CD8(+) T cells. *Nat Microbiol* **2**, 17036, doi:10.1038/nmicrobiol.2017.36 (2017).

517. Reynolds, C. *et al.* T cell immunity to Zika virus targets immunodominant epitopes that show cross-reactivity with other Flaviviruses. *Scientific reports* **8**, 672 (2018).

518. Delgado, F. G. *et al.* Improved Immune Responses Against Zika Virus After Sequential Dengue and Zika Virus Infection in Humans. *Viruses* **10**, doi:10.3390/v10090480 (2018).

519. Chahal, J. S. *et al.* An RNA nanoparticle vaccine against Zika virus elicits antibody and CD8+ T cell responses in a mouse model. *Sci Rep* **7**, 252, doi:10.1038/s41598-017-00193-w (2017).

520. Scherwitzl, I., Mongkolsapaja, J. & Screaton, G. Recent advances in human flavivirus vaccines. *Current Opinion in Virology* **23**, 95-101, doi:https://doi.org/10.1016/j.coviro.2017.04.002 (2017).

521. Hanna, S. L. *et al.* N-linked glycosylation of west nile virus envelope proteins influences particle assembly and infectivity. *J Virol* **79**, 13262-13274, doi:10.1128/JVI.79.21.13262-13274.2005 (2005).

522. Mondotte, J. A., Lozach, P. Y., Amara, A. & Gamarnik, A. V. Essential role of dengue virus envelope protein N glycosylation at asparagine-67 during viral propagation. *J Virol* **81**, 7136-7148, doi:10.1128/JVI.00116-07 (2007).

523. Xu, X., Sette, A. & Peters, B. Computational analysis of Zika virus: Flavivirus antibody epitope data mapped onto the Zika virus proteome suggest potential shared and unique epitopes. *URL www. iedb. org/downloader. php* (2016).

524. Tharakaraman, K. *et al.* Rational engineering and characterization of an mAb that neutralizes Zika virus by targeting a mutationally constrained quaternary epitope. *Cell host & microbe* **23**, 618-627. e616 (2018).

525. Teoh, E. P. *et al.* The structural basis for serotype-specific neutralization of dengue virus by a human antibody. *Sci Transl Med* **4**, 139ra183, doi:10.1126/scitranslmed.3003888 (2012).

526. Gallichotte, E. N. *et al.* A new quaternary structure epitope on dengue virus serotype 2 is the target of durable type-specific neutralizing antibodies. *MBio* **6**, e01461-01415, doi:10.1128/mBio.01461-15 (2015).

527. Yu, L. *et al.* Delineating antibody recognition against Zika virus during natural infection. *JCI Insight* **2**, doi:10.1172/jci.insight.93042 (2017).

528. Graham, B. S. Advances in antiviral vaccine development. *Immunol Rev* **255**, 230-242, doi:10.1111/imr.12098 (2013).

529. Jückstock, J., Rothenburger, M., Friese, K. & Traunmüller, F. Passive Immunization against Congenital Cytomegalovirus Infection: Current State of Knowledge. *Pharmacology* **95**, 209-217, doi:10.1159/000381626 (2015).

530. Young, M. K., Cripps, A. W., Nimmo, G. R. & van Driel, M. L. Post-exposure passive immunisation for preventing rubella and congenital rubella syndrome. *Cochrane Database of Systematic Reviews*, doi:10.1002/14651858.CD010586.pub2 (2015).

531. Hessell, A. J. *et al.* Fc receptor but not complement binding is important in antibody protection against HIV. *Nature* **449**, 101-104, doi:10.1038/nature06106 (2007).

532. Irani, V. *et al.* Molecular properties of human IgG subclasses and their implications for designing therapeutic monoclonal antibodies against infectious diseases. *Molecular Immunology* **67**, 171-182, doi:https://doi.org/10.1016/j.molimm.2015.03.255 (2015).

533. Friede, M. *Monoclonal antibodies for infectious diseases*, <https://www.who.int/immunization/research/forums_and_initiatives/1_MFriede_mAbs_infectious_diseases_gvirf16.pdf?ua=1> (

534. Chitlaru, T. *et al.* Next-Generation Bacillus anthracis Live Attenuated Spore Vaccine Based on the htrA-(High Temperature Requirement A) Sterne Strain. *Scientific reports* **6**, 18908 (2016).

535. World Health Organization & International Office of Epizootics. *Anthrax in humans and animals*. (World Health Organization, 2008).

536. Dembek, Z. F. *Medical aspects of biological warfare*. (Department of the Army, 2008).

537. Altmann, D. M. Host immunity to Bacillus anthracis lethal factor and other immunogens: implications for vaccine design. *Expert Rev Vaccines* **14**, 429-434, doi:10.1586/14760584.2015.981533 (2015).

538. Centers for Disease Control and Prevention. Bioterrorism Agents/Diseases. (Updated August 17, 2017).

539. Bower, W. A., Hendricks, K. A., Pillai, S. K., Guarnizo, J. T. & Meaney-Delman, D. Clinical framework and medical countermeasure use during an anthrax mass-casualty incident. (2015).

540. Goel, A. K. Anthrax: a disease of biowarfare and public health importance. *World Journal of Clinical Cases: WJCC* **3**, 20 (2015).

541. Sweeney, D. A., Hicks, C. W., Cui, X., Li, Y. & Eichacker, P. Q. Anthrax infection. *Am J Respir Crit Care Med* **184**, 1333-1341, doi:10.1164/rccm.201102-0209CI (2011).

542. Minang, J. T. *et al.* Enhanced early innate and T cell-mediated responses in subjects immunized with Anthrax Vaccine Adsorbed Plus CPG 7909 (AV7909). *Vaccine* **32**, 6847-6854 (2014).

543. Committee on Prepositioned Medical Countermeasures for the Public. *Prepositioning Antibiotics for Anthrax*. (National Academies Press, 2012).

544. Athamna, A. *et al.* Selection of Bacillus anthracis isolates resistant to antibiotics. *Journal of Antimicrobial Chemotherapy* **54**, 424-428 (2004).

545. Brouillard, J. E., Terriff, C. M., Tofan, A. & Garrison, M. W. Antibiotic selection and resistance issues with fluoroquinolones and doxycycline against bioterrorism agents. *Pharmacotherapy: The Journal of Human Pharmacology and Drug Therapy* **26**, 3-14 (2006).

546. Price, L. B. *et al.* In vitro selection and characterization of Bacillus anthracis mutants with high-level resistance to ciprofloxacin. *Antimicrobial agents and chemotherapy* **47**, 2362-2365 (2003).

547. Sharma, S., Thomas, D., Marlett, J., Manchester, M. & Young, J. A. Efficient neutralization of antibody-resistant forms of anthrax toxin by a soluble receptor decoy inhibitor. *Antimicrobial agents and chemotherapy* **53**, 1210-1212 (2009).

548. Heine, H. *et al.* Evaluation of Combination Drug Therapy for Treatment of Antibiotic-Resistant Inhalation Anthrax in a Murine Model. *Antimicrobial agents and chemotherapy* **61**, e00788-00717 (2017).

549. Friebe, S., van der Goot, F. G. & Bürgi, J. The Ins and Outs of Anthrax Toxin. *Toxins* **8**, 69, doi:10.3390/toxins8030069 (2016).

550. Abrami, L., Reig, N. & van der Goot, F. G. Anthrax toxin: the long and winding road that leads to the kill. *Trends in microbiology* **13**, 72-78 (2005).

551. Abrami, L., Liu, S., Cosson, P., Leppla, S. H. & van der Goot, F. G. Anthrax toxin triggers endocytosis of its receptor via a lipid raft-mediated clathrin-dependent process. *J Cell Biol* **160**, 321-328, doi:10.1083/jcb.200211018 (2003).

552. McComb, R. C. & Martchenko, M. Neutralizing antibody and functional mapping of Bacillus anthracis protective antigen—The first step toward a rationally designed anthrax vaccine. *Vaccine* **34**, 13-19, doi:https://doi.org/10.1016/j.vaccine.2015.11.025 (2016).

553. Milne, J. C., Furlong, D., Hanna, P. C., Wall, J. S. & Collier, R. J. Anthrax protective antigen forms oligomers during intoxication of mammalian cells. *J Biol Chem* **269**, 20607-20612 (1994).

554. Duesbery, N. S. *et al.* Proteolytic inactivation of MAP-kinase-kinase by anthrax lethal factor. *Science* **280**, 734-737 (1998).

555. Levinsohn, J. L. *et al.* Anthrax lethal factor cleavage of Nlrp1 is required for activation of the inflammasome. *PLoS Pathog* **8**, e1002638, doi:10.1371/journal.ppat.1002638 (2012).

556. Moayeri, M., Haines, D., Young, H. A. & Leppla, S. H. Bacillus anthracis lethal toxin induces TNF-alpha-independent hypoxia-mediated toxicity in mice. *J Clin Invest* **112**, 670-682, doi:10.1172/jci17991 (2003).

557. Cui, X. *et al.* Lethality during continuous anthrax lethal toxin infusion is associated with circulatory shock but not inflammatory cytokine or nitric oxide release in rats. *Am J Physiol Regul Integr Comp Physiol* **286**, R699-709, doi:10.1152/ajpregu.00593.2003 (2004).

558. Smith, H. & Keppie, J. Observations on experimental anthrax; demonstration of a specific lethal factor produced in vivo by Bacillus anthracis. *Nature* **173**, 869-870, doi:10.1038/173869a0 (1954).

559. Leppla, S. H. Anthrax toxin edema factor: a bacterial adenylate cyclase that increases cyclic AMP concentrations of eukaryotic cells. *Proceedings of the National Academy of Sciences* **79**, 3162-3166 (1982).

560. Doganay, M. in *Infectious Diseases (Fourth Edition)* (eds Jonathan Cohen, William G. Powderly, & Steven M. Opal) 1123-1128.e1121 (Elsevier, 2017).

561. Popov, S. G. *et al.* Effective antiprotease-antibiotic treatment of experimental anthrax. *BMC infectious diseases* **5**, 25-25, doi:10.1186/1471-2334-5-25 (2005).

562. Chung, M. C. *et al.* Secreted neutral metalloproteases of Bacillus anthracis as candidate pathogenic factors. *J Biol Chem* **281**, 31408-31418, doi:10.1074/jbc.M605526200 (2006).

563. Popova, T. G. *et al.* Acceleration of epithelial cell syndecan-1 shedding by anthrax hemolytic virulence factors. *BMC microbiology* **6**, 8-8, doi:10.1186/1471-2180-6-8 (2006).

564. Shannon, J. G., Ross, C. L., Koehler, T. M. & Rest, R. F. Characterization of anthrolysin O, the Bacillus anthracis cholesterol-dependent cytolysin. *Infection and immunity* **71**, 3183-3189, doi:10.1128/iai.71.6.3183-3189.2003 (2003).

565. Spencer, R. C. Bacillus anthracis. *Journal of clinical pathology* **56**, 182-187, doi:10.1136/jcp.56.3.182 (2003).

566. Abrami, L. *et al.* Hijacking multivesicular bodies enables long-term and exosome-mediated long-distance action of anthrax toxin. *Cell Rep* **5**, 986-996, doi:10.1016/j.celrep.2013.10.019 (2013).

567. Guichard, A., Nizet, V. & Bier, E. New insights into the biological effects of anthrax toxins: linking cellular to organismal responses. *Microbes and infection* **14**, 97-118, doi:10.1016/j.micinf.2011.08.016 (2012).

568. Quinn, C. P. *et al.* Immune Responses to Bacillus anthracis Protective Antigen in Patients with Bioterrorism-Related Cutaneous or Inhalation Anthrax. *The Journal of Infectious Diseases* **190**, 1228-1236, doi:10.1086/423937 (2004).

569. Oliva, C. R. *et al.* The integrin Mac-1 (CR3) mediates internalization and directs Bacillus anthracis spores into professional phagocytes. *Proc Natl Acad Sci U S A* **105**, 1261-1266, doi:10.1073/pnas.0709321105 (2008).

570. Gu, C., Jenkins, S. A., Xue, Q. & Xu, Y. Activation of the classical complement pathway by Bacillus anthracis is the primary mechanism for spore phagocytosis and involves the spore surface protein BclA. *Journal of immunology (Baltimore, Md. : 1950)* **188**, 4421-4431, doi:10.4049/jimmunol.1102092 (2012).

571. Tournier, J. N. & Mohamadzadeh, M. Key roles of dendritic cells in lung infection and improving anthrax vaccines. *Trends Mol Med* **16**, 303-312, doi:10.1016/j.molmed.2010.04.006 (2010).

572. Hu, H., Sa, Q., Koehler, T. M., Aronson, A. I. & Zhou, D. Inactivation of Bacillus anthracis spores in murine primary macrophages. *Cell Microbiol* **8**, 1634-1642, doi:10.1111/j.1462-5822.2006.00738.x (2006).

573. Cote, C. K., Rea, K. M., Norris, S. L., van Rooijen, N. & Welkos, S. L. The use of a model of in vivo macrophage depletion to study the role of macrophages during infection with Bacillus anthracis spores. *Microbial Pathogenesis* **37**, 169-175, doi:https://doi.org/10.1016/j.micpath.2004.06.013 (2004).

574. Kang, T. J. *et al.* Murine macrophages kill the vegetative form of Bacillus anthracis. *Infect Immun* **73**, 7495-7501, doi:10.1128/iai.73.11.7495-7501.2005 (2005).

575. Guidi-Rontani, C., Levy, M., Ohayon, H. & Mock, M. Fate of germinated Bacillus anthracis spores in primary murine macrophages. *Mol Microbiol* **42**, 931-938 (2001).

576. Dixon, T. C., Fadl, A. A., Koehler, T. M., Swanson, J. A. & Hanna, P. C. Early Bacillus anthracis-macrophage interactions: intracellular survival survival and escape. *Cell Microbiol* **2**, 453-463 (2000).

577. Welkos, S., Friedlander, A., Weeks, S., Little, S. & Mendelson, I. In-vitro characterisation of the phagocytosis and fate of anthrax spores in macrophages and the effects of anti-PA antibody. *J Med Microbiol* **51**, 821-831, doi:10.1099/0022-1317-51-10-821 (2002).

578. Ross, J. M. The pathogenesis of anthrax following the administration of spores by the respiratory route. *The Journal of Pathology and Bacteriology* **73**, 485-494, doi:10.1002/path.1700730219 (1957).

579. Shetron-Rama, L. M., Herring-Palmer, A. C., Huffnagle, G. B. & Hanna, P. Transport of Bacillus anthracis from the lungs to the draining lymph nodes is a rapid process facilitated by CD11c+ cells. *Microbial Pathogenesis* **49**, 38-46, doi:https://doi.org/10.1016/j.micpath.2010.02.004 (2010).

580. Cleret, A. *et al.* Lung Dendritic Cells Rapidly Mediate Anthrax Spore Entry through the Pulmonary Route. *The Journal of Immunology* **178**, 7994, doi:10.4049/jimmunol.178.12.7994 (2007).

581. Tonello, F. & Zornetta, I. Bacillus anthracis factors for phagosomal escape. *Toxins (Basel)* **4**, 536-553, doi:10.3390/toxins4070536 (2012).

582. Glomski, I. J. *et al.* Murine splenocytes produce inflammatory cytokines in a MyD88-dependent response to Bacillus anthracis spores. *Cell Microbiol* **9**, 502-513, doi:10.1111/j.1462-5822.2006.00806.x (2007).

583. Basu, S. *et al.* Role of Bacillus anthracis spore structures in macrophage cytokine responses. *Infect Immun* **75**, 2351-2358, doi:10.1128/iai.01982-06 (2007).

584. Gonzales, C. M. *et al.* Antibacterial role for natural killer cells in host defense to Bacillus anthracis. *Infection and immunity* **80**, 234-242, doi:10.1128/IAI.05439-11 (2012).

585. Moayeri, M. *et al.* Inflammasome sensor Nlrp1b-dependent resistance to anthrax is mediated by caspase-1, IL-1 signaling and neutrophil recruitment. *PLoS Pathog* **6**, e1001222, doi:10.1371/journal.ppat.1001222 (2010).

586. Hahn, B. L., Bischof, T. S. & Sohnle, P. G. Superficial exudates of neutrophils prevent invasion of Bacillus anthracis bacilli into abraded skin of resistant mice. *International Journal of Experimental Pathology* **89**, 180-187, doi:10.1111/j.1365-2613.2008.00584.x (2008).

587. Mayer-Scholl, A. *et al.* Human neutrophils kill Bacillus anthracis. *PLoS Pathog* **1**, e23, doi:10.1371/journal.ppat.0010023 (2005).

588. Albrink, W. S., Brooks, S. M., Biron, R. E. & Kopel, M. Human inhalation anthrax. A report of three fatal cases. *Am J Pathol* **36**, 457-471 (1960).

589. Fouet, A. & Mesnage, S. Bacillus anthracis cell envelope components. *Curr Top Microbiol Immunol* **271**, 87-113 (2002).

590. Iyer, J. K. *et al.* Inflammatory cytokine response to Bacillus anthracis peptidoglycan requires phagocytosis and lysosomal trafficking. *Infection and immunity* **78**, 2418-2428, doi:10.1128/IAI.00170-10 (2010).

591. Mauck, J. & Glaser, L. Turnover of the cell wall of Bacillus subtilis W-23 during logarithmic growth. *Biochem Biophys Res Commun* **39**, 699-706, doi:10.1016/0006-291x(70)90261-5 (1970).

592. Hsu, L. C. *et al.* A NOD2-NALP1 complex mediates caspase-1-dependent IL-1beta secretion in response to Bacillus anthracis infection and muramyl dipeptide. *Proc Natl Acad Sci U S A* **105**, 7803-7808, doi:10.1073/pnas.0802726105 (2008).

593. Ali, S. R. *et al.* Anthrax toxin induces macrophage death by p38 MAPK inhibition but leads to inflammasome activation via ATP leakage. *Immunity* **35**, 34-44, doi:10.1016/j.immuni.2011.04.015 (2011).

594. Kengatharan, K. M., De Kimpe, S., Robson, C., Foster, S. J. & Thiemermann, C. Mechanism of gram-positive shock: identification of peptidoglycan and lipoteichoic acid moieties essential in the induction of nitric oxide synthase, shock, and multiple organ failure. *J Exp Med* **188**, 305-315, doi:10.1084/jem.188.2.305 (1998).

595. Popescu, N. I. *et al.* Peptidoglycan induces disseminated intravascular coagulation in baboons through activation of both coagulation pathways. *Blood* **132**, 849-860, doi:10.1182/blood-2017-10-813618 (2018).

596. Calzas, C. *et al.* Antibody Response Specific to the Capsular Polysaccharide Is Impaired in *Streptococcus suis* Serotype 2-Infected Animals. *Infection and Immunity* **83**, 441, doi:10.1128/IAI.02427-14 (2015).

597. Jones, C. Vaccines based on the cell surface carbohydrates of pathogenic bacteria. *An Acad Bras Cienc* **77**, 293-324, doi:/S0001-37652005000200009 (2005).

598. Goodman, J. W. & Nitecki, D. E. Immunochemical studies on the poly-gamma-D-glutamyl capsule of Bacillus anthracis. I. Characterization of the polypeptide and of the specificity of its reaction with rabbit antisera. *Biochemistry* **5**, 657-665, doi:10.1021/bi00866a036 (1966).

599. Laws, T. R. *et al.* A Comparison of the Adaptive Immune Response between Recovered Anthrax Patients and Individuals Receiving Three Different Anthrax Vaccines. *PLoS One* **11**, e0148713, doi:10.1371/journal.pone.0148713 (2016).

600. Price, B. M. *et al.* Protection against anthrax lethal toxin challenge by genetic immunization with a plasmid encoding the lethal factor protein. *Infect Immun* **69**, 4509-4515, doi:10.1128/iai.69.7.4509-4515.2001 (2001).

601. Beedham, R. J., Turnbull, P. C. & Williamson, E. D. Passive transfer of protection against Bacillus anthracis infection in a murine model. *Vaccine* **19**, 4409-4416 (2001).

602. Enkhtuya, J. *et al.* Significant passive protective effect against anthrax by antibody to Bacillus anthracis inactivated spores that lack two virulence plasmids. *Microbiology* **152**, 3103-3110, doi:10.1099/mic.0.28788-0 (2006).

603. Little, S., Ivins, B., Fellows, P. & Friedlander, A. Passive protection by polyclonal antibodies against Bacillus anthracis infection in guinea pigs. *Infection and Immunity* **65**, 5171-5175 (1997).

604. Weiss, S. *et al.* Immunological Correlates for Protection against Intranasal Challenge of *Bacillus anthracis* Spores Conferred by a Protective Antigen-Based Vaccine in Rabbits. *Infection and Immunity* **74**, 394, doi:10.1128/IAI.74.1.394-398.2006 (2006).

605. Leppla, S. H., Robbins, J. B., Schneerson, R. & Shiloach, J. Development of an improved vaccine for anthrax. *The Journal of clinical investigation* **110**, 141-144 (2002).

606. Friedlander, A. M., Bhatnagar, R., Leppla, S. H., Johnson, L. & Singh, Y. Characterization of macrophage sensitivity and resistance to anthrax lethal toxin. *Infection and Immunity* **61**, 245 (1993).

607. Tournier, J.-N., Rossi Paccani, S., Quesnel-Hellmann, A. & Baldari, C. T. Anthrax toxins: A weapon to systematically dismantle the host immune defenses. *Molecular Aspects of Medicine* **30**, 456-466, doi:https://doi.org/10.1016/j.mam.2009.06.002 (2009).

608. O'Brien, J., Friedlander, A., Dreier, T., Ezzell, J. & Leppla, S. Effects of anthrax toxin components on human neutrophils. *Infect Immun* **47**, 306-310 (1985).

609. Hoover, D. L. *et al.* Anthrax edema toxin differentially regulates lipopolysaccharide-induced monocyte production of tumor necrosis factor alpha and interleukin-6 by increasing intracellular cyclic AMP. *Infect Immun* **62**, 4432-4439 (1994).

610. Comer, J. E., Chopra, A. K., Peterson, J. W. & Konig, R. Direct inhibition of T-lymphocyte activation by anthrax toxins in vivo. *Infect Immun* **73**, 8275-8281, doi:10.1128/iai.73.12.8275-8281.2005 (2005).

611. Paccani, S. R. *et al.* Anthrax toxins suppress T lymphocyte activation by disrupting antigen receptor signaling. *J Exp Med* **201**, 325-331, doi:10.1084/jem.20041557 (2005).

612. Fang, H., Xu, L., Chen, T. Y., Cyr, J. M. & Frucht, D. M. Anthrax Lethal Toxin Has Direct and Potent Inhibitory Effects on B Cell Proliferation and Immunoglobulin Production. *The Journal of Immunology* **176**, 6155, doi:10.4049/jimmunol.176.10.6155 (2006).

613. Pickering, A. K. *et al.* Cytokine response to infection with Bacillus anthracis spores. *Infection and immunity* **72**, 6382-6389, doi:10.1128/IAI.72.11.6382-6389.2004 (2004).

614. Ingram, R. J. *et al.* Natural Exposure to Cutaneous Anthrax Gives Long-Lasting T Cell Immunity Encompassing Infection-Specific Epitopes. *The Journal of Immunology* **184**, 3814, doi:10.4049/jimmunol.0901581 (2010).

615. Moayeri, M., Leppla, S. H., Vrentas, C., Pomerantsev, A. P. & Liu, S. Anthrax Pathogenesis. *Annu Rev Microbiol* **69**, 185-208, doi:10.1146/annurev-micro-091014-104523 (2015).

616. Day, J., Friedman, A. & Schlesinger, L. S. Modeling the host response to inhalation anthrax. *Journal of theoretical biology* **276**, 199-208, doi:10.1016/j.jtbi.2011.01.054 (2011).

617. Wilkening, D. A. Modeling the incubation period of inhalational anthrax. *Med Decis Making* **28**, 593-605, doi:10.1177/0272989x08315245 (2008).

618. Mamedov, T. *et al.* Production of Functionally Active and Immunogenic Non-Glycosylated Protective Antigen from Bacillus anthracis in Nicotiana benthamiana by Co-Expression with Peptide-N-Glycosidase F (PNGase F) of Flavobacterium meningosepticum. *PloS one* **11**, e0153956-e0153956, doi:10.1371/journal.pone.0153956 (2016).

619. Cybulski Jr, R. J., Sanz, P. & O'Brien, A. D. Anthrax vaccination strategies. *Molecular aspects of medicine* **30**, 490-502 (2009).

620. Solomon, I. H. & Milner Jr, D. A. Histopathology of vaccine-preventable diseases. *Histopathology* **70**, 109-122 (2017).

621. Brey, R. N. Molecular basis for improved anthrax vaccines. *Adv Drug Deliv Rev* **57**, 1266-1292, doi:10.1016/j.addr.2005.01.028 (2005).

622. Turnbull, P. C. Current status of immunization against anthrax: old vaccines may be here to stay for a while. *Curr Opin Infect Dis* **13**, 113-120 (2000).

623. Plotkin, S. & Grabenstein, J. D. Countering Anthrax: Vaccines and Immunoglobulins. *Clinical Infectious Diseases* **46**, 129-136, doi:10.1086/523578 (2008).

624. Food and Drug Administration. *BioThrax (Anthrax Vaccine Adsorbed) Prescribing Information*, <https://www.fda.gov/media/71954/download> (2019).

625. Bush, L. M. & Perez, M. T. The anthrax attacks 10 years later. *Annals of internal medicine* **156**, 41-44 (2012).

626. Keim, P. S., Walker, D. H. & Zilinskas, R. A. Time to Worry about Anthrax Again. *Sci Am* **316**, 70-75, doi:10.1038/scientificamerican0417-70 (2017).

627. Zilinskas, R. A. Iraq's biological weapons. The past as future? *Jama* **278**, 418-424 (1997).

628. Gilligan, P. H. Therapeutic challenges posed by bacterial bioterrorism threats. *Curr Opin Microbiol* **5**, 489-495 (2002).

629. Use of anthrax vaccine in response to terrorism: supplemental recommendations of the Advisory Committee on Immunization Practices. *MMWR Morb Mortal Wkly Rep* **51**, 1024-1026 (2002).

630. Fowler, K., McBride, B. W., Turnbull, P. C. & Baillie, L. W. Immune correlates of protection against anthrax. *J Appl Microbiol* **87**, 305 (1999).

631. Iacono-Connors, L. C., Welkos, S. L., Ivins, B. E. & Dalrymple, J. M. Protection against anthrax with recombinant virus-expressed protective antigen in experimental animals. *Infect Immun* **59**, 1961-1965 (1991).

632. Little, S. F., Leppla, S. H. & Cora, E. Production and characterization of monoclonal antibodies to the protective antigen component of Bacillus anthracis toxin. *Infect Immun* **56**, 1807-1813 (1988).

633. Hepler, R. W. *et al.* A recombinant 63-kDa form of Bacillus anthracis protective antigen produced in the yeast Saccharomyces cerevisiae provides protection in rabbit and primate inhalational challenge models of anthrax infection. *Vaccine* **24**, 1501-1514, doi:10.1016/j.vaccine.2005.10.018 (2006).

634. McBride, B. W. *et al.* Protective efficacy of a recombinant protective antigen against Bacillus anthracis challenge and assessment of immunological markers. *Vaccine* **16**, 810-817 (1998).

635. Little, S. F. *et al.* Duration of protection of rabbits after vaccination with Bacillus anthracis recombinant protective antigen vaccine. *Vaccine* **24**, 2530-2536, doi:10.1016/j.vaccine.2005.12.028 (2006).

636. Pittman, P. R. *et al.* Anthrax vaccine: immunogenicity and safety of a dose-reduction, route-change comparison study in humans. *Vaccine* **20**, 1412-1420 (2002).

637. *Emergent BioSolutions Prepares for Initial Shipments of AV7909 Anthrax Vaccine Candidate into the Strategic National Stockpile | Emergent BioSolutions Inc.*, <https://investors.emergentbiosolutions.com/news-releases/news-release-details/emergent-biosolutions-prepares-initial-shipments-av7909-anthrax> (

638. Klinman, D. M., Xie, H., Little, S. F., Currie, D. & Ivins, B. E. CpG oligonucleotides improve the protective immune response induced by the anthrax vaccination of rhesus macaques. *Vaccine* **22**, 2881-2886, doi:10.1016/j.vaccine.2003.12.020 (2004).

639. Rhie, G. E. *et al.* A dually active anthrax vaccine that confers protection against both bacilli and toxins. *Proc Natl Acad Sci U S A* **100**, 10925-10930, doi:10.1073/pnas.1834478100 (2003).

640. Feinen, B., Petrovsky, N., Verma, A. & Merkel, T. J. Advax-adjuvanted recombinant protective antigen provides protection against inhalational anthrax that is further enhanced by addition of murabutide adjuvant. *Clin Vaccine Immunol* **21**, 580-586, doi:10.1128/cvi.00019-14 (2014).

641. Bellanti, J. A. *et al.* Phase 1 study of a recombinant mutant protective antigen of Bacillus anthracis. *Clin Vaccine Immunol* **19**, 140-145, doi:10.1128/cvi.05556-11 (2012).

642. Campbell, J. D. *et al.* Safety, reactogenicity and immunogenicity of a recombinant protective antigen anthrax vaccine given to healthy adults. *Hum Vaccin* **3**, 205-211, doi:10.4161/hv.3.5.4459 (2007).

643. Gorse, G. J. *et al.* Immunogenicity and tolerance of ascending doses of a recombinant protective antigen (rPA102) anthrax vaccine: a randomized, double-blinded, controlled, multicenter trial. *Vaccine* **24**, 5950-5959, doi:10.1016/j.vaccine.2006.05.044 (2006).

644. Brown, B. K. *et al.* Phase I study of safety and immunogenicity of an Escherichia coli-derived recombinant protective antigen (rPA) vaccine to prevent anthrax in adults. *PLoS One* **5**, e13849, doi:10.1371/journal.pone.0013849 (2010).

645. Keitel, W. A. *et al.* Evaluation of a plasmid DNA-based anthrax vaccine in rabbits, nonhuman primates and healthy adults. *Hum Vaccin* **5**, 536-544, doi:10.4161/hv.5.8.8725 (2009).

646. Abboud, N. & Casadevall, A. Immunogenicity of Bacillus anthracis protective antigen domains and efficacy of elicited antibody responses depend on host genetic background. *Clinical and Vaccine Immunology* **15**, 1115-1123 (2008).

647. Kelly-Cirino, C. D. & Mantis, N. J. Neutralizing monoclonal antibodies directed against defined linear epitopes on domain 4 of anthrax protective antigen. *Infection and immunity* **77**, 4859-4867 (2009).

648. McComb, R. C., Ho, C.-L., Bradley, K. A., Grill, L. K. & Martchenko, M. Presentation of peptides from Bacillus anthracis protective antigen on Tobacco Mosaic Virus as an epitope targeted anthrax vaccine. *Vaccine* **33**, 6745-6751 (2015).

649. Miller, C. J., Elliott, J. L. & Collier, R. J. Anthrax protective antigen: prepore-to-pore conversion. *Biochemistry* **38**, 10432-10441, doi:10.1021/bi990792d (1999).

650. Sellman, B. R., Mourez, M. & Collier, R. J. Dominant-negative mutants of a toxin subunit: an approach to therapy of anthrax. *Science* **292**, 695-697, doi:10.1126/science.109563 (2001).

651. Crowe, S. R. *et al.* Select human anthrax protective antigen epitope-specific antibodies provide protection from lethal toxin challenge. *J Infect Dis* **202**, 251-260, doi:10.1086/653495 (2010).

652. Petosa, C., Collier, R. J., Klimpel, K. R., Leppla, S. H. & Liddington, R. C. Crystal structure of the anthrax toxin protective antigen. *Nature* **385**, 833 (1997).

653. Klimpel, K. R., Molloy, S. S., Thomas, G. & Leppla, S. H. Anthrax toxin protective antigen is activated by a cell surface protease with the sequence specificity and catalytic properties of furin. *Proceedings of the National Academy of Sciences* **89**, 10277-10281 (1992).

654. Molloy, S., Bresnahan, P., Leppla, S. H., Klimpel, K. & Thomas, G. Human furin is a calcium-dependent serine endoprotease that recognizes the sequence Arg-XX-Arg and efficiently cleaves anthrax toxin protective antigen. *Journal of Biological Chemistry* **267**, 16396-16402 (1992).

655. Chauhan, V. & Bhatnagar, R. Identification of amino acid residues of anthrax protective antigen involved in binding with lethal factor. *Infect Immun* **70**, 4477-4484, doi:10.1128/iai.70.8.4477-4484.2002 (2002).

656. Benson, E. L., Huynh, P. D., Finkelstein, A. & Collier, R. J. Identification of residues lining the anthrax protective antigen channel. *Biochemistry* **37**, 3941-3948 (1998).

657. Miller, C. J., Elliott, J. L. & Collier, R. J. Anthrax protective antigen: prepore-to-pore conversion. *Biochemistry* **38**, 10432-10441 (1999).

658. Batra, S., Gupta, P., Chauhan, V., Singh, A. & Bhatnagar, R. Trp 346 and Leu 352 residues in protective antigen are required for the expression of anthrax lethal toxin activity. *Biochem Biophys Res Commun* **281**, 186-192, doi:10.1006/bbrc.2001.4320 (2001).

659. Mogridge, J., Mourez, M. & Collier, R. J. Involvement of domain 3 in oligomerization by the protective antigen moiety of anthrax toxin. *Journal of bacteriology* **183**, 2111-2116 (2001).

660. Bradley, K. A., Mogridge, J., Mourez, M., Collier, R. J. & Young, J. A. Identification of the cellular receptor for anthrax toxin. *Nature* **414**, 225 (2001).

661. Brossier, F., Sirard, J.-C., Guidi-Rontani, C., Duflot, E. & Mock, M. Functional analysis of the carboxy-terminal domain of Bacillus anthracis protective antigen. *Infection and immunity* **67**, 964-967 (1999).

662. Singh, Y., Klimpel, K., Quinn, C. P., Chaudhary, V. & Leppla, S. The carboxyl-terminal end of protective antigen is required for receptor binding and anthrax toxin activity. *Journal of Biological Chemistry* **266**, 15493-15497 (1991).

663. Werner, S., Marillonnet, S., Hause, G., Klimyuk, V. & Gleba, Y. Immunoabsorbent nanoparticles based on a tobamovirus displaying protein A. *Proc Natl Acad Sci U S A* **103**, 17678-17683, doi:10.1073/pnas.0608869103 (2006).

664. Padgett, H. S. Generation of antigenic virus-like particles through protein-protein linkages. (Google Patents, 2013).

665. Kimple, M. E., Siderovski, D. P. & Sondek, J. Functional relevance of the disulfide-linked complex of the N-terminal PDZ domain of InaD with NorpA. *Embo j* **20**, 4414-4422, doi:10.1093/emboj/20.16.4414 (2001).

666. GE Life Sciences. Rapid and efficient purification and refolding of a (histidine)6-tagged recombinant protein produced in E. coli as inclusion bodies - 18113437ac.pdf. (2019). <https://www.gelifesciences.co.jp/catalog/pdf/18113437ac.pdf>.

667. GE Life Sciences. *Instructions: HisTrap HP, 1 ml and 5 mL*, <http://webhome.auburn.edu/~duinedu/manuals/HisTrapHP.pdf> (

668. Qiagen. *The QIAexpressionist*, <https://www.qiagen.com/us/resources/resourcedetail?id=79ca2f7d-42fe-4d62-8676-4cfa948c9435(=en> (2019).

669. Wingfield, P. T. Overview of the purification of recombinant proteins. *Curr Protoc Protein Sci* **80**, 6.1.1-35, doi:10.1002/0471140864.ps0601s80 (2015).

670. Thermo Fisher. *User Guide: Pierce HRV 3C Protease*, <https://www.thermofisher.com/document-connect/document-connect.html?url=https%3A%2F%2Fassets.thermofisher.com%2FTFS-Assets%2FLSG%2FPackage-Inserts%2FMAN0011861_Pierce_HRV_3C_Protease_UG.pdf&title=VXNlciBHdWlkZTogIFBpZXJjZSBIUlYgM0MgUHJvdGVhc2U=> (2019).

671. Thermo Fisher. *User Guide: Pierce Glutathione Agarose*, <https://www.thermofisher.com/document-connect/document-connect.html?url=https%3A%2F%2Fassets.thermofisher.com%2FTFS-Assets%2FLSG%2Fmanuals%2FMAN0011719_Pierce_Glutathione_Agarose_UG.pdf&title=VXNlciBHdWlkZTogIFBpZXJjZSBHbHV0YXRoaW9uZSBBZ2Fyb3Nl> (2019).

672. New England Biolabs. *Purification of a Fusion Protein generated by The pMAL Protein Fusion and Purification System (E8200) | NEB*, <https://www.neb.com/protocols/0001/01/01/purification-of-a-fusion-protein-generated-by-the-pmal-protein-fusion-and-purification-system-e8200> (

673. Fic, E., Kedracka-Krok, S., Jankowska, U., Pirog, A. & Dziedzicka-Wasylewska, M. Comparison of protein precipitation methods for various rat brain structures prior to proteomic analysis. *Electrophoresis* **31**, 3573-3579, doi:10.1002/elps.201000197 (2010).

674. Singh, P. *et al.* Effect of signal peptide on stability and folding of Escherichia coli thioredoxin. *PloS one* **8**, e63442-e63442, doi:10.1371/journal.pone.0063442 (2013).

675. Makrides, S. C. Strategies for achieving high-level expression of genes in Escherichia coli. *Microbiological reviews* **60**, 512-538 (1996).

676. Novokhatny, V. & Ingham, K. Thermodynamics of maltose binding protein unfolding. *Protein science : a publication of the Protein Society* **6**, 141-146, doi:10.1002/pro.5560060116 (1997).

677. Costa, S., Almeida, A., Castro, A. & Domingues, L. Fusion tags for protein solubility, purification and immunogenicity in Escherichia coli: the novel Fh8 system. *Frontiers in microbiology* **5**, 63-63, doi:10.3389/fmicb.2014.00063 (2014).

678. Brondyk, W. H. in *Methods in Enzymology* Vol. 463 (eds Richard R. Burgess & Murray P. Deutscher) 131-147 (Academic Press, 2009).

679. Marusic, C. *et al.* Production of an active anti-CD20-hIL-2 immunocytokine in Nicotiana benthamiana. *Plant Biotechnol J* **14**, 240-251, doi:10.1111/pbi.12378 (2016).

680. Merlin, M., Gecchele, E., Capaldi, S., Pezzotti, M. & Avesani, L. Comparative evaluation of recombinant protein production in different biofactories: the green perspective. *Biomed Res Int* **2014**, 136419, doi:10.1155/2014/136419 (2014).

681. Smith, M. L. *et al.* Modified tobacco mosaic virus particles as scaffolds for display of protein antigens for vaccine applications. *Virology* **348**, 475-488 (2006).

682. Xu, H. *et al.* Combined use of regulatory elements within the cDNA to increase the production of a soluble mouse single-chain antibody, scFv, from tobacco cell suspension cultures. *Protein Expr Purif* **24**, 384-394, doi:10.1006/prep.2001.1580 (2002).

683. Ziegler, M. T., Thomas, S. R. & Danna, K. J. Accumulation of a thermostable endo-1,4-β-D-glucanase in the apoplast of Arabidopsis thaliana leaves. *Molecular Breeding* **6**, 37-46, doi:10.1023/A:1009667524690 (2000).

684. Rosano, G. L. & Ceccarelli, E. A. Recombinant protein expression in Escherichia coli: advances and challenges. *Frontiers in microbiology* **5**, 172-172, doi:10.3389/fmicb.2014.00172 (2014).

685. Craig, S. P., 3rd, Yuan, L., Kuntz, D. A., McKerrow, J. H. & Wang, C. C. High level expression in Escherichia coli of soluble, enzymatically active schistosomal hypoxanthine/guanine phosphoribosyltransferase and trypanosomal ornithine decarboxylase. *Proc Natl Acad Sci U S A* **88**, 2500-2504, doi:10.1073/pnas.88.6.2500 (1991).

686. Kleiner-Grote, G. R. M., Risse, J. M. & Friehs, K. Secretion of recombinant proteins from E. coli. *Engineering in Life Sciences* **18**, 532-550, doi:10.1002/elsc.201700200 (2018).

687. Sivashanmugam, A. *et al.* Practical protocols for production of very high yields of recombinant proteins using Escherichia coli. *Protein science : a publication of the Protein Society* **18**, 936-948, doi:10.1002/pro.102 (2009).

688. Bhoir, S., Shaik, A., Thiruvenkatam, V. & Kirubakaran, S. High yield bacterial expression, purification and characterisation of bioactive Human Tousled-like Kinase 1B involved in cancer. *Scientific Reports* **8**, 4796, doi:10.1038/s41598-018-22744-5 (2018).

689. Goulas, T. *et al.* The pCri System: a vector collection for recombinant protein expression and purification. *PLoS One* **9**, e112643, doi:10.1371/journal.pone.0112643 (2014).

690. Suryanarayana, N. *et al.* Soluble Expression and Characterization of Biologically Active Bacillus anthracis Protective Antigen in Escherichia coli. *Mol Biol Int* **2016**, 4732791, doi:10.1155/2016/4732791 (2016).

691. Chauhan, V., Singh, A., Waheed, S. M., Singh, S. & Bhatnagar, R. Constitutive expression of protective antigen gene of Bacillus anthracis in Escherichia coli. *Biochem Biophys Res Commun* **283**, 308-315, doi:10.1006/bbrc.2001.4777 (2001).

692. Sarkes, D. A., Kogot, J. M., Val-Addo, I., Stratis-Cullum, D. N. & Pellegrino, P. M. Cloning and Expressing Recombinant Protective Antigen Domains of B. anthracis. (ARMY RESEARCH LAB ADELPHI MD SENSORS AND ELECTRON DEVICES DIRECTORATE, 2011).

693. Flick-Smith, H. C. *et al.* A recombinant carboxy-terminal domain of the protective antigen of Bacillus anthracis protects mice against anthrax infection. *Infection and immunity* **70**, 1653-1656, doi:10.1128/iai.70.3.1653-1656.2002 (2002).

694. Choi, J. H. & Lee, S. Y. Secretory and extracellular production of recombinant proteins using Escherichia coli. *Appl Microbiol Biotechnol* **64**, 625-635, doi:10.1007/s00253-004-1559-9 (2004).

695. New England Biolabs. P*urification of a Fusion Protein generated by The pMAL Protein Fusion and Purification System. Vol. NEB #E8200S.*

696. Makrides, S. C. Strategies for achieving high-level expression of genes in Escherichia coli. *Microbiol Rev* **60**, 512-538 (1996).

697. Varshney, A. & Goel, A. Development of recombinant domains of protective antigen of Bacillus anthracis and evaluation of their immune response in mouse model for use as vaccine candidates for anthrax. *J Bioterror Biodef* **7**, 10.4172 (2016).

698. Rivera, J. *et al.* A monoclonal antibody to Bacillus anthracis protective antigen defines a neutralizing epitope in domain 1. *Infect Immun* **74**, 4149-4156, doi:10.1128/iai.00150-06 (2006).

699. Stokes, M. G. *et al.* Oral administration of a Salmonella enterica-based vaccine expressing Bacillus anthracis protective antigen confers protection against aerosolized B. anthracis. *Infect Immun* **75**, 1827-1834, doi:10.1128/iai.01242-06 (2007).

700. Oscherwitz, J., Yu, F., Jacobs, J. L. & Cease, K. B. Recombinant Vaccine Displaying the Loop-Neutralizing Determinant from Protective Antigen Completely Protects Rabbits from Experimental Inhalation Anthrax. *Clinical and Vaccine Immunology* **20**, 341, doi:10.1128/CVI.00612-12 (2013).

701. Steele, J. F. C. *et al.* Synthetic plant virology for nanobiotechnology and nanomedicine. *Wiley Interdiscip Rev Nanomed Nanobiotechnol* **9**, doi:10.1002/wnan.1447 (2017).

702. Li, Q. *et al.* Morphology and stability changes of recombinant TMV particles caused by a cysteine residue in the foreign peptide fused to the coat protein. *Journal of Virological Methods* **140**, 212-217, doi:https://doi.org/10.1016/j.jviromet.2006.10.011 (2007).

703. Schlick, T. L., Ding, Z., Kovacs, E. W. & Francis, M. B. Dual-surface modification of the tobacco mosaic virus. *J Am Chem Soc* **127**, 3718-3723, doi:10.1021/ja046239n (2005).

704. Bruckman, M. A. *et al.* Surface Modification of Tobacco Mosaic Virus with “Click” Chemistry. *ChemBioChem* **9**, 519-523, doi:10.1002/cbic.200700559 (2008).

705. Demir, M. & Stowell, M. H. B. A chemoselective biomolecular template for assembling diverse nanotubular materials. *Nanotechnology* **13**, 541-544, doi:10.1088/0957-4484/13/4/318 (2002).

706. wenhafel, N. A. Pathology of Inhalational Anthrax Animal Models. *Veterinary Pathology* **47**, 819-830, doi:10.1177/0300985810378112 (2010).

707. Welkos, S., Bozue, J., Twenhafel, N. & Cote, C. Animal Models for the Pathogenesis, Treatment, and Prevention of Infection by Bacillus anthracis. *Microbiol Spectr* **3**, Tbs-0001-2012, doi:10.1128/microbiolspec.TBS-0001-2012 (2015).

708. Welkos, S. L. Plasmid-associated virulence factors of non-toxigenic (pX01-) Bacillus anthracis. *Microb Pathog* **10**, 183-198 (1991).

709. Welkos, S. L. & Friedlander, A. M. Comparative safety and efficacy against Bacillus anthracis of protective antigen and live vaccines in mice. *Microb Pathog* **5**, 127-139 (1988).

710. Ingram, R. J. *et al.* Natural cutaneous anthrax infection, but not vaccination, induces a CD4+ T cell response involving diverse cytokines. *Cell & Bioscience* **5**, 20, doi:10.1186/s13578-015-0011-4 (2015).

711. Charlton, S. *et al.* A study of the physiology of Bacillus anthracis Sterne during manufacture of the UK acellular anthrax vaccine. *J Appl Microbiol* **103**, 1453-1460, doi:10.1111/j.1365-2672.2007.03391.x (2007).

712. Dumas, E. K. *et al.* Lethal factor antibodies contribute to lethal toxin neutralization in recipients of anthrax vaccine precipitated. *Vaccine* **35**, 3416-3422, doi:10.1016/j.vaccine.2017.05.006 (2017).

713. Baillie, L. W. *et al.* An anthrax subunit vaccine candidate based on protective regions of Bacillus anthracis protective antigen and lethal factor. *Vaccine* **28**, 6740-6748, doi:10.1016/j.vaccine.2010.07.075 (2010).

714. Rossi Paccani, S. *et al.* The adenylate cyclase toxins of Bacillus anthracis and Bordetella pertussis promote Th2 cell development by shaping T cell antigen receptor signaling. *PLoS Pathog* **5**, e1000325, doi:10.1371/journal.ppat.1000325 (2009).

715. Paccani, S. R. *et al.* The adenylate cyclase toxin of Bacillus anthracis is a potent promoter of T(H)17 cell development in *J Allergy Clin Immunol* Vol. 127 1635-1637 (2011).

716. Ingram, R. J. *et al.* Natural exposure to cutaneous anthrax gives long-lasting T cell immunity encompassing infection-specific epitopes. *J Immunol* **184**, 3814-3821, doi:10.4049/jimmunol.0901581 (2010).

717. Dumas, E. K. *et al.* Anthrax Vaccine Precipitated Induces Edema Toxin-Neutralizing, Edema Factor-Specific Antibodies in Human Recipients. *Clin Vaccine Immunol* **24**, doi:10.1128/cvi.00165-17 (2017).

718. Joyce, J. *et al.* Immunogenicity and protective efficacy of Bacillus anthracis poly-gamma-D-glutamic acid capsule covalently coupled to a protein carrier using a novel triazine-based conjugation strategy. *J Biol Chem* **281**, 4831-4843, doi:10.1074/jbc.M509432200 (2006).

719. Chabot, D. J. *et al.* Anthrax capsule vaccine protects against experimental infection. *Vaccine* **23**, 43-47, doi:10.1016/j.vaccine.2004.05.029 (2004).

720. Cote, C. K. *et al.* Characterization of a multi-component anthrax vaccine designed to target the initial stages of infection as well as toxaemia. *J Med Microbiol* **61**, 1380-1392, doi:10.1099/jmm.0.045393-0 (2012).

721. De Groot, A. S. *et al.* Making vaccines "on demand": a potential solution for emerging pathogens and biodefense? *Hum Vaccin Immunother* **9**, 1877-1884, doi:10.4161/hv.25611 (2013).